www.haleyaldrich.com

REPORT ON

ENHANCED SEISMIC DESIGN CONSIDERATIONS
PDX FUEL TANK PROJECT
PORTLAND INTERNATIONAL AIRPORT
PORTLAND, OREGON

by
Haley & Aldrich, Inc.
Portland, Oregon

for
Burns & McDonnell
Bloomington, Minnesota

File No. 0203009-101
29 September 2023

HALEY ALDRICH

HALEY & ALDRICH, INC.
6420 S MACADAM AVENUE
SUITE 100
PORTLAND, OR 97239
503.620.7284

SIGNATURE PAGE FOR

REPORT ON
ENHANCED SEISMIC DESIGN CONSIDERATIONS
PDX FUEL TANK PROJECT
PORTLAND INTERNATIONAL AIRPORT
PORTLAND, OREGON

PREPARED FOR
BURNS & MCDONNELL
BLOOMINGTON, MINNESOTA

PREPARED BY:

Daniel Hutabarat, Ph.D., P.E.
Project Geotechnical Engineer
Haley & Aldrich, Inc.

REVIEWED AND APPROVED BY:

Michael Chamberlain, P.E.
Project Manager
Haley & Aldrich, Inc.

REGISTERED PROFESSIONAL ENGINEER
69452PE
Allison Pyrch Digitally signed by Allison Pyrch Date: 2023.09.29 10:51:12 -07'00'
OREGON
Nov. 14, 2006
ALLISON MARIE PYRCH
RENEWAL DATE: 12/31/24

Allison Pyrch, P.E., G.E.
Principal Geotechnical Engineer
Haley & Aldrich, Inc.

Brice Exley

Brice Exley, P.E.
Principal Geotechnical Engineer
Haley & Aldrich, Inc.

Table of Contents

Table of Contents

List of Tables

List of Figures

List of Appendices

1. Introduction

This report provides a comprehensive overview of our enhanced seismic design analyses, performed to support the geotechnical seismic vulnerability assessment (SVA) and design for the proposed new fuel tanks at Portland International Airport (PDX) in Portland, Oregon (Project Site). The geotechnical seismic analyses documented within this report are also intended to apply to the existing tanks at the site. The report has been prepared exclusively for Burns & McDonnell (B&M), based on the current project conceptualization and discussions with B&M. Our understanding of the subsurface soil conditions is based on explorations at discrete locations at the site. Soil properties inferred from the field and laboratory tests formed the basis for developing the geotechnical recommendations contained in this report. Soil conditions may vary in the areas between the explorations, and the nature and extent of the variations may not be evident until construction. If variations appear, it may be necessary to reevaluate the recommendations in this report.

We understand, based on review of the draft Oregon Department of Environmental Quality (DEQ) 2023 for Fuel Tank Seismic Stability (dated 31 May 2023 for public comment), that the current Oregon Structural Specialty Code (OSSC, 2022) represents the general basis of design for evaluation and design of the new and existing fuel tanks described in this report. The current building code references American Society of Civil Engineers (ASCE) 7-16 for seismic design considerations. Considering this, the seismic hazard and ground motion time history analyses documented within this report were developed in general accordance with the requirements of ASCE 7-16.

The report is structured into the following sections:

1. Introduction
2. Purpose, Scope, and Use of This Report
3. Site and Project Understanding
4. Subsurface Conditions
5. Engineering Analysis & Seismic Vulnerability Evaluation
6. Limitations
7. Closure
8. References

Tables and figures are included or referenced throughout the report to illustrate the project area, exploration locations, and seismic vulnerability assessment results. The appendices provide detailed information, including the logs of deep boring explorations (Appendix A), the summary of subsurface engineering properties interpreted from Cone Penetrometer Testing (CPT) tests (Appendix B), constant rate of strain (CRS) consolidation and cyclic and monotonic direct simple shear (DSS) performed by Haley & Aldrich, Inc. (Haley & Aldrich) (Appendix C), probabilistic and deterministic seismic hazard analysis and design ground motion characterization (Appendix D), advanced two-dimensional (2D) nonlinear deformation analysis using FLAC (Appendix E), and a summary of the geophysical survey (Appendix F).

2. Purpose, Scope, and Use of This Report

Our primary objective is to provide B&M with a sitewide geotechnical seismic hazard evaluation to support the SVA and eventual design and construction of the proposed fuel tank facilities at the PDX Project Site. Figure 1 shows the vicinity map of the Project Site.

The scope of our services encompasses the following tasks:

1. ***In situ* geotechnical explorations**

   We conducted various field tests, including borings, CPTs with seismic and pore pressure measurement, and a geophysical survey. These explorations aimed to characterize the subsurface conditions and soil engineering properties at the Project Site. Full documentation of these geotechnical explorations is presented in the project geotechnical data report (Haley & Aldrich, 2023).

2. **Advanced laboratory testing**

   To further understand the dynamic strength and cyclic behavior of the Project Site, we performed advanced laboratory tests including index testing, constant rate of strain consolidation testing (CRS), and cyclic and monotonic direct simple shear testing (CDSS and DSS).

3. **Geotechnical engineering analyses, evaluations, and recommendations**

   Our work involved conducting several analyses to inform the design and construction process, including:

   - Seismic hazard analysis and design ground motion characterization: This analysis estimated the ground motion parameters at the Project Site for an MCE_R (approximately 2475-year return period) hazard level.
   - 2D nonlinear deformation analysis (NDA): This analysis estimated the amount of permanent lateral and vertical displacement expected during an MCE_R level earthquake event.
   - One-dimensional (1D) nonlinear site response analysis (SRA): This analysis estimated the site-specific Design MCE_R (Maximum Considered Earthquake Response) spectrum.
   - Production of this enhanced seismic design report.

It is important to note that, while our study includes the levee zone located north of the project site on NE Marine Drive, a detailed analysis of the existing levee is beyond the scope of this study. Due to the limited availability of geotechnical information related to the levee, reasonable geotechnical properties were assumed, as discussed in Section 5 of this report. The geometry of the levee was modeled using publicly available topography and bathymetry data depicted in Figure 2.

This report is intended exclusively for the use of B&M. Our work was conducted in accordance with generally accepted geotechnical engineering practices applicable to projects of similar nature and locality at the time the services were performed. No other warranty, expressed or implied, is made. Our scope of services does not cover any environmental aspects related to the project.

3. Site and Project Understanding

The existing fuel facility is located near the northwest end of the PDX property. The current facility is roughly rectangular and encompasses approximately 3.3 acres with three aboveground fuel storage tanks and surrounding support equipment. The proposed development will include portions of the existing property and will extend to the north and east of the existing storage tank area. The site is relatively flat, with a slight gradient of less than 2 feet across the project area. Elevations range from approximately 20 to 22 feet above mean sea level (MSL). The gradient increases gradually toward the Columbia River (north of the existing facility) where the slope ranges from approximately 0.5 to 1.0 percent.

We previously performed work at the site and provided a geotechnical report (dated 17 September 2020) with design and construction recommendations for prior facility improvements including a new electrical building, upgrades to the existing substation, addition of a buried bulk spill containment unit, a new fueling canopy, and installation of light poles at various points across the site.

We understand the proposed improvements include two new 120-foot-diameter by 32-foot-high aboveground fuel storage tanks and a new operations and fire protection building. Other ancillary improvements will include new light poles and pavements for access roads. One of the three existing fuel tanks as well as much of the ancillary infrastructure will remain in service.

Based on our previous work, the upper soil layer (e.g., fill and alluvium) are susceptible to consolidation settlement due to building and tank loads, and to post-seismic settlement and strength reduction in the event of an earthquake. The site is also expected to be susceptible to lateral spreading due to the site's proximity (within 1500 feet away) to the Columbia River. These conditions are likely to prevent the use of a conventional spread-footing foundation system for most improvements without ground improvements. Based on our previous work and the provided information, the current anticipated foundation types are shallow drilled or formed shafts for light poles, either interlocking spread footings or deep foundations for the operations and fire protection building, and deep foundations (piles or drilled shafts) for the fuel tanks. Ground improvement may also be considered.

Specific to the scope of services included within this report, we understand that new regulatory rules will require seismic evaluation and potential stabilization of existing fuel tanks at the site. The new tanks will potentially require greater than normal seismic stabilization measures. As seismic evaluation of the existing tanks was not required previously, our 2020 geotechnical report for the site only included simplified assessments of various seismic considerations (e.g., liquefaction susceptibility, liquefaction-induced settlement, lateral spreading concerns, etc.) and did not include recommendations for mitigation of these concerns. The scope of services included within this report was developed to include advanced laboratory testing results and site-specific seismic modeling that will be used to produce better estimates of the seismic hazards important to the existing and new fuel tanks at the site. Potential mitigation strategies and foundation recommendations will be included in a new geotechnical report for the site and the seismic mitigation plan developed to meet the new DEQ requirements for the new structures.

3.1 SEISMICALLY INDUCED GEOTECHNICAL HAZARDS

Based on our evaluation, the major potential seismically induced geotechnical hazards at the project sites include lateral spreading (possibly flow failure), liquefaction-induced ground failure, and ejecta-induced settlement. Our review of these hazards is based on the soils encountered in explorations at the site, regional experience, and our knowledge of local seismicity.

3.1.1 Lateral Spreading

Lateral spreading commonly occurs on mildly sloping ground and involves lateral displacement caused by the accumulation of cyclic shear strain during earthquake. As the soil undergoes cyclic loading, excess pore pressure builds up, reducing the effective stress and gradually leading to a reduction in shear strength. This accumulation of shear strain ultimately results in permanent lateral deformation. Excessive lateral displacement resulting from lateral spreading can impact the fuel tank facility area by increasing the lateral force and displacement exerted on the tank foundation. Given the proximity of the project site to the Columbia River and the presence of liquefiable soil, we conducted an evaluation of the potential geotechnical impact on fuel tank facilities due to lateral deformation caused by liquefaction-induced lateral spreading during a design-level event. However, it is possible that the upslope geometry from the project site toward the levee may help reduce lateral displacement.

3.1.2 Flow failure

Flow failure typically occurs at sites with sloping ground (>2.0 percent) and/or a significant free-face condition nearby, underlain by very loose, contractive soil deposits (e.g., loose granular soil or non-plastic fine-grained soil). In such cases, the soil experiences a more significant reduction in shear strength caused by soil liquefaction within or beneath the slope. If the post-earthquake shear strength is lower than the gravitational forces acting along a critical failure surface, flow failure instability can be initiated. Moreover, once the earthquake shaking ceases, the presence of a low-permeability soil layer on top of a liquefied, high-permeability clean sand layer may produce a water-film layer that becomes a critical failure surface (i.e., described as void redistribution mechanisms by Idriss & Boulanger, 2008). To assess this condition (and the potential for flow failure affecting our site), we performed limit equilibrium slope stability analyses utilizing liquefied strengths for soils expected to be susceptible to liquefaction. These liquefied strengths were developed considering void redistribution effects. This analysis is documented in Section 5.5.1 of this report and indicates that flow failure is unlikely to impact the structures at our site.

3.1.3 Liquefaction-Induced Free Field Settlement and Ground Failure

Liquefaction is caused by rapid increase of excess pore water pressure that reduces the effective stress between soil particles to a low value, loosening the frictional contact of soil particles, resulting in sudden loss of shear strength and stiffness of the soil. In general, loose, saturated sandy soils with low silt and clay content are most susceptible to experience strength loss. Silty soils with low plasticity are also susceptible. For any soil type, the soil must be saturated for liquefaction to occur. The consequences of soil liquefaction may include excessive ground settlement and lateral deformation. Post-liquefaction (or reconsolidation) settlement occurs because liquefiable soils tend to get redistributed and become denser after the earthquake and after excess porewater pressure dissipates. Ground surface settlement is not typically uniform across the area and can result in significant differential settlement.

To preliminarily evaluate the extent of liquefaction triggering on the clean sand deposit at the project site, we performed a CPT-based liquefaction triggering simplified analysis using the procedure proposed by Boulanger & Idriss (2016) up to a depth of 150 feet. The preliminary CPT-based liquefaction analysis considered an earthquake magnitude (M_w) of 9.0 and a surface peak horizontal ground acceleration (PGA_M) of 0.55 g. The PGA_M of 0.55g is consistent with the ASCE 7-16 with a 2 percent probability of exceedance in 50 years and Site Class E. Based on our analysis, the CPT-based simplified procedure estimates that liquefaction is triggered within a depth range of 40 feet to 150 feet. The estimated post-liquefaction reconsolidation vertical settlement from the CPT-based simplified method (with depth correction factor) using the same M_w and PGA_M values ranges from 15 to 25 inches. Although the simplified procedure is useful for performing a preliminary assessment and estimating the resulting effect, it can sometimes introduce unnecessary conservatism. The simplified procedure is derived from empirical case histories collected from soil samples above 50 feet, which might be inappropriate for estimating liquefaction triggering of soils deeper than that threshold. The SVA study presented in this report performed a more advanced 2D nonlinear deformation analysis using advanced soil constitutive models created to simulate the behavior of sands and silts under seismic loading. This approach offers the advantage of simulating the dynamic response of the site and using a more mechanistically defensible methodology to estimate the extent of liquefaction triggering.

3.1.4 Ejecta-induced Settlement and Ground Failure

During earthquake shaking, excess pore water pressure is generated and, if it reaches a sufficient pressure, it can trigger high-gradient upward seepage during the earthquake or even after the shaking stops. The resulting effects from the dissipation process of excess pore water pressure could be significant for lightweight structures below the groundwater table in shallow ground such as manholes, pipelines, etc. We used the recent methodology proposed by Hutabarat & Bray (2022) to evaluate the severity of liquefaction-induced ground failure caused by upward seepage pressure and sediment ejecta. This method considers the dynamic response of the site and the counterbalancing forces between upward seepage pressure (liquefaction demand, L_D) and the crust material (crust resistance factor, C_R).

The thickness of low-permeability layers of soil and the non-liquefiable crust layer at the project site ranging from 40 to 60 feet thick contributes to a high crust resistance factor. From the liquefaction demand side, the liquefiable layer at depth >50 feet is unlikely to produce sufficient artesian pressure to produce sand ejecta (sand boil) at the ground surface. Based on our analysis using the design-level earthquake and available CPT data of the project site, we anticipated the ejecta-induced ground failure severity falls in the “None” category of the Hutabarat & Bray (2022) L_D-C_R chart. Therefore, the estimated ejecta-induced settlement is negligible.

4. Subsurface Conditions

4.1 PROJECT GEOTECHNICAL EXPLORATION

We developed our conceptual geotechnical recommendations based on our interpretations on subsurface information obtained from *in situ* and laboratory testing presented in this report. We completed:

- one onshore geotechnical boring in 2019,
- two onshore geotechnical borings in 2023,
- two CPTs with pore pressure dissipation testing in 2019,
- one seismic CPT (SCPTu) with pore pressure dissipation testing in 2019, and
- three SCPTu soundings with pore pressure dissipation testing in 2023.

The deepest geotechnical borings were advanced to a depth of 151.5 feet (see Appendix A for boring log). The CPT soundings were advanced to a depth 150.2 feet (see Appendix B) to complement the boring log interpretation and to determine engineering properties of soil in our analysis. The locations of geotechnical borings and CPTs are shown in Figure 2.

4.2 SUBSURFACE SOIL CONDITIONS

Our understanding of the subsurface conditions is based on our review of available geotechnical data, including our borings (Appendix A) and CPT sounding data (Appendix B). A cross-section across the fuel tanks immediate vicinity is shown on Figure 3. An additional cross-section profile of generalized subsurface conditions (for 2D modeling purpose) from the fuel tank perimeter to Columbia River is shown in Figure 4. As shown in Figure 3 and Figure 4, we classified the project site into three engineering soil units (ESUs), as interpreted from existing borings and CPTs, as discussed below:

ESU-1 (Top Soil / Fill) – This ESU consists of silty, poorly graded sand (SM to SP-SM) sand to a depth of approximately 7 to 15 feet below ground surface (bgs). The soils appeared to be brown, fine to medium grained, and poorly graded sand with a variable amount of silt. This unit is unsaturated most of the time as the ground water table fluctuations are rarely expected to rise above the base of this ESU.

ESU-2 (Overbank Deposit) – This ESU underlies the ESU-1 layer. This ESU consists of interbedded low plasticity clay (CL), silt (ML), and sandy silt to silty sand (SM) extended to depths varying between approximately 40 and 50 feet bgs. We performed soil index testing from undisturbed soil samples taken between depths of 15 feet to 42 feet. The plasticity index (PI) of this ESU ranges from 12 to 23 with an average value of 16 and a standard deviation of 4. The water content (w_c) ranges from 33 to 60 percent with an average value of 46 percent and standard deviation of 10 percent. The liquid limit (LL) of the soil samples ranges from 33 to 55 (average value of 46) resulting w_c/LL value from 0.7 to 1.3 (average value 1.0). According to the Bray & Sancio (2006) criteria, 50 percent of the tested soil sample is classified as moderately susceptible to strength loss during cyclic loading and the other 50 percent of the tested soil sample is classified as non-susceptible. Figure B-1 of Appendix B showed more detail of engineering properties of this ESU. The advanced laboratory testing results, performed on samples taken from this ESU, are summarized in Appendix C of this report.

ESU-3 (Columbia River Sand) – Underlying ESU-2, this ESU consists of fully saturated, poorly graded, loose to medium-dense, micaceous, clean-sand with traces of silt (SP to SP-SM) with fines content ranging from 5 to 13 percent. Based on the normalized penetration resistance value (q_{c1N}) the clean-sand deposit is liquefiable (q_{c1N} <150) from a depth of 40 feet to a depth of 135 feet bgs. We estimate the *in situ* relative density (D_R) of this ESU ranges from 40 to 58 percent (loose to medium dense sand). For modeling purposes, we distinguish this ESU into three subgroups namely ESU-3a (40 to 60 feet bgs), ESU-3b (60 to 120 feet bgs), and ESU-3c (120 to 160 feet bgs) to account for increasing relative density with depth. Figure B-2 of Appendix B shows more details related to the engineering properties of this ESU.

4.3 GROUNDWATER CONDITIONS

Based on the interpretation of the boring log explorations (Appendix A) and pore pressure measurements from six CPTs (Appendix B), the groundwater table within the fuel tank perimeter is estimated to be approximately 12 to 17 feet bgs. For modeling purposes, the groundwater table was taken at a depth of approximately 15 feet bgs, as shown in Figure 3. In Figure 4, the phreatic line (groundwater table) is depicted, which decreases from 15 feet bgs (El. +7.0) at the fuel tank area to El. +0.0, matching the groundwater elevation of the Columbia River. Soil elements below the groundwater table shown in Figure 4 are assumed to be fully saturated.

5. Engineering Analyses and Seismic Vulnerability Evaluation

5.1 SEISMIC SETTING

Oregon is located near the contact between two large crustal tectonic plates. The Juan de Fuca Plate constitutes the floor of the Pacific Ocean off the northwestern coast of the United States and moves northeastward from its spreading ridge boundary with the Pacific Plate at an average rate of approximately 1.5 inches per year. As the Juan de Fuca Plate converges with continental North America, it subducts or dips below the North American Plate, forming a shallow, eastward-dipping contact interface. This boundary is referred to as the Cascadia Subduction Zone (CSZ) and is responsible for seismic activity in the western regions of Washington and Oregon. The CSZ gives rise to earthquakes associated with three types of source zones: subduction interface, subduction intraslab, and shallow crustal earthquakes.

Figure 5 illustrates that the seismicity of the Pacific Northwest (PNW) region is predominantly influenced by the Cascadia Subduction Zone. In this zone, the offshore Juan de Fuca Plate subducts beneath the continental North American Plate. Subduction zones typically exhibit three main types of earthquakes: crustal earthquakes, interface subduction earthquakes, and intraslab subduction earthquakes.

Intraslab and Interface Sources. A subduction zone is characterized by the interaction of a down-going oceanic plate, such as the Juan de Fuca Plate, and an overriding continental plate, such as the North American Plate. The displacement caused by the subduction of the Juan de Fuca Plate below the North American Plate does not generally manifest as slip between the two plates; rather, it is absorbed by compression of the North American Plate at the interface at relatively shallow depths. When the magnitude of the compression becomes large enough to overcome the stresses locking the plates together, the plates will suddenly rupture, causing an interface earthquake. Based on geologic and historical evidence, this compression is released about every 350 to 600 years on average in the form of magnitude 8.0 to 9.0 earthquakes. The most recent CSZ interface event is thought to have occurred around 9 p.m. local time on 26 January 1700, based on paleoseismic evidence and historical records of an orphan tsunami along the Japanese coast (Atwater et al. 2005). Interface earthquakes (such as the 2011 magnitude 9.0 Tohoku earthquake in northern Japan) are some of the largest magnitude earthquakes on record. Characteristics of this type of earthquake may include very large ground accelerations, shaking durations in excess of 3 minutes, and particularly strong long-period ground motions, which may affect tall or long-period structures.

Intraslab earthquakes originate from a deeper zone of seismicity that is associated with bending and breaking of the subducting Juan de Fuca Plate. Intraslab earthquakes (such as the 2001 magnitude 7.0 Nisqually earthquake in west central Washington) occur at depths of 40 to 70 kilometers (km) (130,000 to 230,000 feet) and can produce earthquakes with magnitudes greater than magnitude 7.0. Deep intraslab earthquakes tend to be felt over larger areas than shallower crustal events, and generally lack significant aftershocks.

Crustal Sources. Shallow crustal faults are caused by cracking of the continental crust resulting from the stress that builds as the subduction zone plates remain locked together. Few surficial geologic traces exist of the shallow crustal faults in the Portland, Oregon area. The nearest series of known shallow crustal faults, including the Portland Hills Fault, East Bank Fault, Oatfield Fault, Lacamas Lake, and the Beaverton Fault Zone, have had their surface traces either eroded away or buried by ancient flood deposits, but have been mapped by seismic reflection and refraction studies and other geophysical methods. Therefore, less information is known about these faults than faults with distinct surface traces.

Crustal seismicity from known faults near the project site is generally dominated by the Portland Hills Fault, located approximately 6 miles from the project site. The Portland Hills, Oatfield, and East Bank faults run in a generally northwest-southeast direction through downtown Portland, and the Portland Hills Fault is generally believed to be capable of producing earthquake events with magnitude 7.0 or greater with a return period from 10,000 years to 20,000 years (Petersen et. al., 2014). No estimates for the maximum expected earthquake magnitudes are available for the Beaverton Fault Zone and the Oatfield Fault (Peterson et. al., 2014); however, the East Bank Fault has a lower estimated slip rate and an expected maximum earthquake magnitude of 6.2. These faults and other crustal sources contribute significantly to the seismic hazard at all periods.

5.2 SITE CLASS FOR SEISMIC DESIGN

We determined the soil site class based on the foundation soil information following the guidelines of ASCE 7-16, as referenced by the current OSSC. The soil site class is determined by considering the soil characteristics and measured shear wave velocity data at the site up to a depth of 100 feet bgs. Table 1 provides a summary of the measured shear wave velocity data obtained from SCPTu soundings, refraction microtremor (ReMi) tests and multichannel analysis of surface waves (MASW) testing. Based on our calculations, the site is classified as seismic Site Class E, without accounting for the presence of liquefiable soils at the Project Site. **As a liquefaction hazard is determined to be present at the site, the site is classified as Site Class F and a site response analysis is required to determine the site-specific response spectrum.**

Table 1. Summary of Geophysical Measurement Results and Site Class

Measurement	Elevation (feet) NAVD88	Latitude	Longitude	V_{S30} (ft/s)[a]
ReMi-1	23.1	45.597666	–122.614894	607 (Site D)
ReMi-2	24.0	45.598167	–122.614895	608 (Site D)
ReMi-3	24.5	45.598619	–122.614903	614 (Site D)
ReMi-4	36.0	45.600218	–122.613956	531 (Site E)
SCPT-1	22.5	45.59739	–122.61306	650 (Site D)
SCPT-4	23.0	45.597566	–122.614008	602 (Site D)
SCPT-5	20.4	45.596392	–122.613845	517 (Site E)
SCPT-6	22.4	45.597485	–122.612872	583 (Site E)

Notes:
a. feet per second = ft/s; Site Classifications are based on ASCE 7-16

5.3 SITE-SPECIFIC GROUND MOTION HAZARD ANALYSIS

Site-specific probabilistic seismic hazard analysis (PSHA) and deterministic seismic hazard analysis (DSHA) were performed to obtain a target MCE_R response spectrum for the project. This MCE_R spectrum is used as the target response spectrum for selection of ground motion time histories for use in our 1D nonlinear site response analyses (SRA) and 2D nonlinear deformation analyses (NDA). The PSHA/DSHA framework and results are presented in the following sections.

The overall procedure involved the following steps:

1. Development of a probabilistic, risk-adjusted MCE_R response spectrum for the site considering elastic half-space conditions. This spectrum is based on a comprehensive evaluation of the probabilistic seismic hazard.
2. Development of a deterministic MCE_R response spectrum for the site. This spectrum is derived from a deterministic analysis that considers specific earthquake scenarios and corresponding ground motions.
3. Calculation of the recommended target MCE_R response spectrum, which is determined as the lesser of the probabilistic and deterministic spectra. This ensures a conservative approach in selecting the design response spectrum.
4. Verification that the recommended target MCE_R spectrum meets or exceeds the minimum requirements defined by the ASCE 7-16 code for seismic design. This step ensures compliance with the relevant design standards and regulations.

5.3.1 Half-Space V_{S30} and Site Period

Seismic CPT (SCPTu) soundings were conducted at the site, measuring shear wave velocity (Vs) at 1-meter intervals to a maximum depth of approximately 150 feet bgs. In addition, four 1D ReMi tests and one 2D MASW test were performed to provide information about the deep Vs profile at the project site. These tests used arrays spanning up to about 600 to 650 feet in length (see Appendix F). Both active and passive measurements were taken, and 1D Vs profiles were obtained down to a maximum depth of 200 feet. The geophysical measurement report along with their corresponding locations are included in Appendix F.

Figure 6 displays the V_s data measured at the Project Site, reaching a depth of 180 feet bgs. The SCPTu data shows good agreement with the ReMi data in the upper 60 feet of the site. Below 60 feet, the SCPTu data is relied upon more heavily to determine the baseline Vs value. The baseline Vs profile, incorporating all the measurements, is depicted in Figure 6. Using this baseline Vs profile, the fundamental period of the soil profile is calculated to be approximately 1.2 seconds.

Figure 6 also reveals a significant impedance contrast at a depth of 180 feet bgs, as indicated by the ReMi 4 measurement. This measurement, being the only one available at that depth, estimates a shear wave velocity (V_s) of 1,271 feet per second (fps). It is worth noting that this impedance contrast exists below the deepest boring, introducing uncertainty regarding a notable geologic contact.

For the purposes of this study, we consider it reasonable to assume a half-space condition at 180 feet bgs, with a V_{S30} of 1,271 fps, corresponding to a Site Class C (rock outcrop) classification. Based on this assumption, an MCE_R spectrum for "rock outcrop" conditions will be developed, which will be thoroughly discussed in the following section. The developed MCE_R spectrum will serve as the target spectrum for selecting and scaling input ground motion time histories used in our analyses.

5.3.2 Site-Specific Probabilistic Seismic Hazard Analysis (PSHA)

A site-specific PSHA was performed for the site to obtain the probabilistic response spectra for the maximum considered earthquake (MCE) hazard level at half-space condition. The PSHA framework and results are presented in the following sections.

5.3.2.1 Seismic Source Characterization

Our site-specific PSHA was performed using the HAZ45 software. The seismic source characterization (SSC) contains seismic source geometries and recurrence models developed based on the 2014 United States Geological Survey (USGS) National Seismic Hazard Model (NSHM), as documented in USGS Open-File report 2014-1091 and further clarified in correspondence with USGS. Inputs to the PSHA include the earthquake source file, site properties, and ground motion model (GMM) weights.

The earthquake source file used for the analyses includes source models for known faults (such as the Portland Hills Fault), gridded crustal seismicity, and the CSZ. Our HAZ45 earthquake source model was validated against the USGS 2014 National Hazard Maps for grid points in the PNW, including Portland. This validation study was previously presented to a geotechnical peer reviewer on a past peer-reviewed project.

Based on review of the 2018 update to the 2014 NSHM (Petersen et. al., 2020) and communications with the expert consultant who developed the HAZ45 implementation of our seismic source model, we understand the PNW portion of the source model did not change in the 2018 update to the 2014 NSHM. We understand the USGS did look at updating the seismicity catalog extending into 2018, which could slightly impact seismic source rates for the crustal background source as well as the slab sources, which are based on the seismicity catalog. Upon review of this updated seismicity catalog, no new events with a magnitude greater than 4.0 were identified, which is the cut-off magnitude used by the USGS for their gridded calculations. Following this examination, we consider our current PNW seismic source model to be generally consistent with the latest widely accepted and implemented science.

5.3.2.2 Ground Motion Models

The GMM weighting scheme used to compute probabilistic ground motions for each source type are presented below in Tables 2 through 4. The selected GMMs and their associated weights generally represent the practicing state-of-the-art in ground motion hazard evaluation in the PNW, in our opinion.

The Next-Generation Attenuation - West 2 (NGA-West2) crustal GMMs were developed in 2014 and are the latest and most comprehensive GMMs published for crustal sources. Additional epistemic uncertainty per Atik and Youngs (2014) is included with the NGA-West2 crustal GMMs to capture an appropriate level of epistemic uncertainty about the median and sigma models.

The NGA-Subduction GMMs (Parker et al., 2022 [PSHAB], Kuehn et. al., 2020 [KBCG], and Abrahamson and Gulerce, 2020 [AG]) were released to the public for use in 2020 and are applicable to both subduction interface and subduction intraslab source-types. They are based on a more comprehensive and up-to-date subduction zone ground motion database than preceding GMMs. Each of these GMMs includes regionalized terms specifically for use with the Cascadia region. As each of these GMMs represents an equally modern, independently developed model, we assigned equal weights to each of these three GMMs.

Each of the three NGA-Subduction GMMs includes a global version of the model in addition to the Cascadia regionalized version, and each GMM modeling team made different modeling decisions when developing their Cascadia regionalized GMM. These modeling differences are especially noticeable as they relate to each GMMs predictions of subduction interface ground motions due to the lack of large recorded CSZ interface events. We understand that PSHAB chose to anchor their CSZ interface model quite tightly to the global model, KBCG allowed for significant differences between the two, and the AG with adjustments model represents a compromise between these two approaches. We understand that the model authors recommend use of the Cascadia regionalized versions of each GMM at CSZ sites due to differences in the distance and V_{S30} scaling models (among other regional modeling differences).

In our opinion, these differences in modeling decisions between the three Cascadia regionalized models represent an appropriate range of epistemic uncertainty for application to this project.

Other GMMs that were considered for this study, but were not used, include:

1. **Idriss (2014) NGA-West2 GMM**. The Idriss GMM includes significantly fewer input parameters and is less sophisticated than the other NGA-West2 GMMs. The USGS gave this GMM only a 12 percent weight compared to 22 percent to the other NGA-West2 equations in the 2014 NSHM. We omitted the Idriss model from our logic tree weighting scheme.
2. **Atkinson and Macias (2009) GMM.** This equation was derived entirely from earthquake simulations rather than from observed ground motions and lacks a term corresponding to the site-specific V_{S30}. This GMM is also noted to have a potentially unrealistic flatter spectral decay at long periods when compared to recorded ground motions and other subduction interface GMMs.
3. **BCHydro (2018) GMM**. Prior to release of the NGA-Subduction expressions, the 2018 BCHydro GMM (Abrahamson et al., 2018) was considered the state-of-the-art subduction GMM. As the AG model contains borrowed terms from the BCHydro GMM and represents a regionalized version of the 2018 model, the 2018 BCHydro GMM was excluded from our PSHA in favor of the AG model.

Table 2. GMMs and Relative Weights for Crustal Sources

Ground Motion Model (GMM)	GMM Abbreviation	GMM Weights
Abrahamson et al. NGA-West2 (2014)	ASK	0.25
Boore et al. NGA-West2 (2014)	BSSA	0.25
Campbell and Bozorgnia NGA-West2 (2014)	CB	0.25
Chiou and Youngs NGA-West2 (2014)	CY	0.25

Table 3.GMMs and Relative Weights for Subduction Intraslab Sources

Ground Motion Model (GMM)	GMM Abbreviation	GMM Weights
Parker et al. (2022) [a]	PSHAB	0.3333
Kuehn et al. (2020)[b]	KBCG	0.3333
Abrahamson and Gulerce (2020) [c]	AG	0.3334

Notes:

a. *Cascadia, outside Basin with $Z_{2.5}$.*

b. *Cascadia, Non-Seattle Basin.*

c. *Cascadia with adjustments.*

Table 4. GMMs and Relative Weights for Subduction Interface Sources		
Ground Motion Model (GMM)	**GMM Abbreviation**	**GMM Weights**
Parker et al. (2022) [a]	PSHAB	0.3333
Kuehn et al. (2020)[b]	KBCG	0.3333
Abrahamson and Gulerce (2020) [c]	AG	0.3334

Notes:

a. *Cascadia, outside Basin with $Z_{2.5}$.*
b. *Cascadia, Non-Seattle Basin.*
c. *Cascadia with adjustments.*

5.3.2.3 Site Properties

Basin depth terms ($Z_{1.0}$ and $Z_{2.5}$) are required to compute ground motion intensity for all of the above-selected shallow crustal and subduction GMMs. $Z_{1.0}$ is defined as the depth a V_S horizon of 1,000 meters per second while $Z_{2.5}$ represents the depth to a V_S horizon of 2,500 meters per second.

CB, AG, KBCG, and PSHAB rely upon the $Z_{2.5}$ depth parameter for their basin response term. We used a site-specific $Z_{2.5}$ value of 1.85 kilometers within our PSHA. This site-specific value was calculated from the $Z_{2.5}$ iso-surface extracted from the Stephenson et. al., (2017) velocity model using an inverse-distance weighted average of the $Z_{2.5}$ values taken from the four closest grid points surrounding the site.

ASK, BSSA, and CY rely upon the $Z_{1.0}$ term instead of $Z_{2.5}$. For these three NGA-West2 models, we used a $Z_{1.0,eff}$ value of 0.405 kilometers, consistent with the site-specific $Z_{2.5}$ value. This $Z_{1.0,eff}$ value was determined using an equal weight average of the empirical correlation models described in Petersen et. al. (2020), as shown in the following equations ($Z_{1.0}$ and $Z_{2.5}$ are depths in kilometers).

$$Z_{1.0,eff} = 0.1146\ Z_{2.5} + 0.2826$$

$$Z_{1.0,eff} = 0.0933\ Z_{2.5} + 0.1444$$

This approach is consistent with the USGS approach for basin adjustments in the Seattle region used in the 2018 National Seismic Hazard Maps and can be reasonably adopted for the Portland region as well, in our opinion. As the Portland basin is relatively shallow, the effects of these basin adjustments are generally minor.

5.3.2.4 Haley & Aldrich Site-Specific PSHA Results

Using the framework described in this section, the site-specific PSHA results included probabilistic MCE uniform hazard spectrum (UHS) at half-space conditions, total mean hazard curves, source-specific hazard curves, and disaggregation hazard contribution results. Table 5 (attached) summarizes the Haley & Aldrich site-specific MCE UHS at half-space condition. More detailed results produced from PSHA results are presented in Appendix D of this report.

5.3.3 Site-Specific Deterministic Seismic Hazard Analysis (DSHA)

The 84th percentile deterministic (MCE_R) seismic hazard was computed per ASCE 7-16 Section 21.2.2. RotD50, deterministic response spectra were computed for the Portland Hills Fault, CSZ intraslab, and the CSZ interface sources using the same suite of GMMs and epistemic weights documented in Tables 2 through 4, utilizing the best-estimate design V_{S30}.

Table 6 summarizes the primary input parameters selected for each of the deterministic scenarios. Distance metrics were selected to be consistent with the modeled source geometry and location of the site. Characteristic magnitudes were selected considering existing literature related to each source type and disaggregation results for the site.

Table 6. Deterministic Scenario Input Parameters			
Parameter	**Portland Hills**	**CSZ Intraslab**	**CSZ Interface**
M_W	7.1	7.2	9.0
R_{Rup} (km)	10.4	75	94
R_{JB} (km)	10.4	N/A	N/A
Z_{TOR} (km)	0	50	5
Hypocentral Depth (km)	N/A	65	N/A
Note: *V_{S30} = 388 m/s, $Z_{1.0}$ = 0.405 km, $Z_{2.5}$ = 1.85 km*			

The calculated deterministic response spectrum is summarized in Table 5 (attached). The calculated 84th percentile deterministic response spectrum is taken as the envelope of the three source-specific deterministic spectra and is presented in Figure 7. More detailed results including the development of the deterministic response spectra for the three source types summarized in Table 6 are presented in Appendix D. As presented in Appendix D, the intraslab subduction spectrum is highest at very short periods with the Portland Hills Fault and interface subduction spectra controlling at longer periods.

5.3.4 Probabilistic Response Spectrum Modification for Targeted Risk

The probabilistic MCE hazard is risk-adjusted to achieve a 1 percent probability of collapse in 50 years. We calculated the risk coefficients using Method 2 in ASCE 7-16, Section 21.2.1.2, by using an iterative integration procedure that combines the probability of exceedance of a given spectral acceleration with a lognormal probability density function representing the probability of collapse for that spectral acceleration (also known as a fragility curve).

The risk coefficients were calculated using a MATLAB script obtained from USGS and were determined using a lognormal standard deviation of 0.6. The input to the MATLAB script consisted of seismic hazard curves at each period (i.e., annual exceedance frequency versus spectral acceleration), which were obtained from the PSHA. The primary outputs of the code are the MCE_R and 2 percent in 50-year UHS spectra. The risk coefficients, which the MATLAB script also computes, are simply the ratio of these two response spectra. The computed risk coefficients are listed in Table 5 (attached).

5.3.5 MCE_R Response Spectrum Modification for Maximum Component

The results of the PSHA and DSHA are RotD50 response spectra. However, the maximum spectral acceleration over all orientations (known as the maximum component or RotD100 accelerations) is a potentially more significant parameter for structural design (BSSC, 2009). To develop the maximum component spectrum, the RotD50 response spectrum obtained from the PSHA and DSHA was adjusted by period-dependent factors that relate maximum component to RotD50 spectral accelerations. We used the scale factors from Shahi and Baker (2014) to develop the MCE_R. These factors are shown in Table 5 (attached).

5.3.6 Target Half-Space MCE_R Response Spectrum

Per ASCE 7-16 Section 21.2.3, the site-specific MCE_R response spectrum is taken as the lesser of the probabilistic and deterministic MCE_R response spectra. Figure 7 presents a comparison of the probabilistic and deterministic MCE_R response spectra, and it is observed that the deterministic spectrum is higher at all periods. As such, the probabilistic MCE_R spectrum is adopted as the recommended MCE_R spectrum.

The recommended site-specific MCE_R response spectra, shown in Figure 7, is also tabulated in the last column of Table 5. Table 5 compares the calculated MCE_R response spectrum with the Site Class C code-based spectrum. As shown in Figure 7, the target half-space MCE_R response spectrum meets the requirement to be greater than or equal to the minimum allowable spectrum (80 percent code-based Site Class C) for all spectral periods.

5.4 INPUT GROUND MOTION SELECTION

This section describes the framework used to select and scale input ground motion time histories for use in as inputs to our seismic analyses (2D NDA and 1D SRA).

5.4.1 Spectral Periods of Interest

Based on email discussions with B&M in late May to early June of 2023, we understand that the impulsive period of the proposed fuel tank is 0.202 seconds and the natural period of the first mode of sloshing (convective period) is 7.5 seconds. To deal with these different fundamental periods in a reasonable manner, two suites of five input ground motions (10 total) are developed: One suite developed relative to the impulsive period (T = 0.2 seconds) and a second suite developed relative to the sloshing period (T = 7.5 seconds). As an additional consideration, the estimated fundamental site period (as discussed in Section 5.3.1) is approximately 1.2 seconds. The identified period ranges of interest for each suite of ground motions are summarized as follows:

- For the impulsive period (T = 0.2 seconds) scenario, the spectral period range interest for selection and scaling of the selected ground motions will be taken from 0.04 seconds (0.2 times the structure impulsive period) to 1.6 seconds (1.3 times the fundamental site period, representative of a degraded site period).
- For the convective period (T = 7.5 seconds) scenario, spectral period range interest for selection and scaling of the selected ground motions will be taken from 3.75 seconds (0.5 times the structure convective period) to 10 seconds.

5.4.2 Disaggregated Hazard Contributions

The recommended ground motion source distributions for each suite of five ground motions were derived based on the disaggregation results at spectral periods of 0.2 seconds and 7.5 seconds, respectively. Table 7 summarizes the results of disaggregation results for each period and earthquake source, as well as the identified number or ground motions to be selected for each source type.

Table 7. Seismic Hazard Contributions at 2,475-year Return Period										
Source	T = 0.2 seconds (Impulsive)					T = 7.5 seconds (Convective)				
	Percent Contribution	ε	M_w	R_{rup} (km)	# of Motion	Percent Contribution	ε	M_w	R_{rup} (km)	# of Motion
Interface Subduction	20	1.52	9.0	93	1	76	0.88	8.9	112	4
Intraslab Subduction	30	1.22	6.9	81	2	< 0.5	2.91	7.2	75	0
Crustal	50	1.12	6.3	13.6	2	24	0.99	7.1	31	1
Note: The tabulated ε, M_w, and R_{rup} are the mean disaggregated values calculated from disaggregation analysis.										

5.4.3 Ground Motion Selection

Table 7 served as the basis for performing ground motion suite selection for each scenario. We selected 5, 1-component ground motion time histories for both impulsive and convective period suites, resulting in 10 selected input motions total. Five motions for each suite were selected to be consistent with the site response analysis requirements in Section 21.1.1 of ASCE 7-16. We chose the processed ground motion records published by the Pacific Earthquake Engineering Research (PEER) center for both crustal earthquakes (NGA West2) and subduction earthquakes (NGA Sub). An amplitude scaling approach was selected for use rather than a spectral matching approach to minimize modification of potentially important characteristics of the earthquake recordings. The ground motion suites were selected based primarily on the following criteria:

1. Multiply original ground motion records by scaling factors ranging from 0.5 to 3.0 (amplitude scaling method)
2. Spectral shape fit, with respect to the target spectrum within the spectral period of interest for either the Impulsive or Convective period;
3. Appropriate source mechanism (i.e., shallow crustal, subduction interface, subduction intraslab);
4. Moment magnitude and source-to-site distance.
5. Earthquake duration using significant duration metric ($D_{5\text{-}95}$) estimated using Bahrampouri et. al. (2021).
6. Cumulative absolute velocity (CAV) estimated using and M_w and R_{rup} from disaggregation result in Table 7 using Macedo et. al. (2020) and Liu & Macedo (2022) for crustal and subduction source conditional ground motion models, respectively.

Tables 8 and 9 (attached) summarize the metadata and information for selected ground motion for impulsive and convective period suite, respectively. Figure 8 presents the selected input motion spectra for each suite and the target MCE_R half-space spectrum. Figure 8 shows that the average amplitude-scaled ground motion response spectra matches the level of the MCE_R target spectrum well across all periods, meeting the intent of ASCE 7-16 Chapter 21.1.1 ground motion selection criteria. Detailed plots of acceleration, displacement, velocity time histories, and ground motion parameters for each selected ground motion are presented in Appendix D.

5.5 2D EFFECTIVE-STRESS NONLINEAR DEFORMATION ANALYSES

5.5.1 Limit-Equilibrium Flow Failure Evaluation

Limit-equilibrium flow failure analysis was performed to evaluate the potential for a flow failure that affects our site, assuming liquefaction of the full ESU-3 layer occurs. Figure E-1 in Appendix E summarizes the results of limit-equilibrium stability analysis using the software program SLIDE. We assigned post-liquefied residual shear strength ratio (S_r/σ'_{vo}) to ESU-3a, ESU-3b, and ESU-3c of 0.08, 0.1, and 0.12, respectively. We compared the value recommended by Idriss & Boulanger (2008) and Robertson (2021) where all values are interpreted from CPT data. We found that the assigned values are relatively conservative assuming the q_{c1Ncs} values of 90, 110, and 120 for ESU-3a, ESU-3b, and ESU-3c, respectively (see Figure B-2).

As shown in Figure E-1, flow failure appears unlikely to occur and the failure planes with the lowest factors of safety (> 1.0) do not extend to the existing fuel tank facilities.

5.5.2 2D Numerical Model

A free field 2D model was used to predict the behavior of the site under seismic loading. The resulting deformations represent the conditions accordingly, and do not account for additional deformation, which would be imposed by shallow foundations and the associated structural loading as we understand that the new tanks will be founded on deep foundation elements or ground improvement.

5.5.2.1 2D FLAC Element Mesh

The cross-section B-B' shown in Figure 4 was used to derive a 2D model for nonlinear deformation analyses (NDA) using the finite difference program FLAC 8.1. The user defined PM4Sand (V3.1) and PM4Silt (V1.0) constitutive models were used to model ESUs reasonably likely to be susceptible to liquefaction or cyclic softening at the project site. The left boundary of the model was located 200 feet away from the left edge (southern perimeter) of the existing fuel tanks (near boring B-2 in Figure 2), and the model extends 2,850 feet northwards from the existing facilities toward the Columbia River. The full plane strain model is shown in Figure E2 in Appendix E.

As shown on the available topography and bathymetry data, the model captures a ground surface sloping slightly up approximately 0.5 to 1.0 percent from the existing facilities toward the levee, and then sloping down from the levee toward the river. In the vertical axis, the mesh was modeled from the ground surface (NAVD88 El. +22 feet at the existing facilities and approximately El. +45 feet at the crest of the levee) to the bottom of the model at El. –160 feet. To simplify the calculation, the geometry of the Columbia Riverbed was simplified as shown in Figure 4. The deepest elevation of the riverbed modeled in our analysis was at NAVD88 El. –34 feet.

The full model mesh is approximately 2,850 feet wide and 180 feet tall, comprising about 20,864 elements. The elements are typically 8 to 10 feet long and 3 feet tall, with an aspect ratio ranging from 2.7 to 3.3. This grid mesh resolutions were considered sufficiently fine to capture important aspects of wave propagation in a nonlinear time-domain dynamic simulation. By assuming 10 elements is sufficient to propagate a single wavelength, the average element height of 3 feet with shear wave velocity profile shown in Figure 6 are capable for propagating input motion with a maximum frequency of at least 25 hertz (Hz). Even if stiffness degradation during shaking is considered, this mesh resolution can still propagate motion with a frequency of at least 10 Hz.

5.5.2.2 Boundary Condition

The dynamic simulation used a compliant (quiet) model base, with the outcrop input motion (presented in Figure 8 and Appendix D) applied as a horizontal stress-time history at the bottom of the model (j = 1). The half-space layer from El. –130 to El. –160 feet was modeled as an elastic material. The dashpot coefficient factor was calibrated to ensure that the nodal velocity time history at the base of the 2D model (j = 1) matched the outcrop input motion velocity time history (FLAC 8.1 Technical Manual, Itasca 2019). This was done to avoid over- or underestimation of the input motion, as the dashpot coefficient factor is influenced by the model geometry and impedance contrast of the elastic half-space velocity and the nonlinear soil continuum above it. The 30-foot elastic half-space layer at the base of the model was modeled as an elastic material with a shear wave velocity of 1,271 feet per second (ft/s) and a Poisson's ratio of 0.33.

The left and right boundaries were modeled using radiating absorbent boundaries, also known as "free-field" side boundaries, and all columns within 10 feet of the boundaries were considered elastic to adequately confine all interior zones. The elastic column was set to have a 30-percent reduction in small-strain shear moduli to accommodate cyclic degradation during the simulation. We also performed a sensitivity analysis by extending the left boundary to evaluate the results and found that it produced only small differences, which will be discussed in the following section.

For all simulations, the nodal pore pressure boundary conditions were set to be impermeable at the left, right, and bottom of the model. For the top of the model (surface to riverbed), the nodal pore pressure was set to allow flow outside the model (i.e., permeable).

5.5.2.3 Initial State & Analysis Settings

The simulations were performed in several analysis stages. In the first stage, the model was solved for static equilibrium by assigning Mohr-Coulomb elastoplastic material to all elements, assuming dry conditions, using the drained friction angle, and small-strain shear modulus (derived from the shear wave velocity profile shown in Figure 6). The coefficient of earth pressure at rest (Ko) for all soil elements was calculated to be between 0.45 and 0.5. The water table was initialized by setting a static phreatic surface, as shown in cross-section B-B' in Figure 4. The initial state of stress of the model is presented in Figure E-2.

In the second stage, the pore-pressure conditions were solved for, and then the PM4Sand and PM4Silts materials were assigned to ESU3 and ESU2, respectively. The model was solved once again for static equilibrium using the updated parameters.

The last stage is the dynamic simulation stage, where the analysis is divided into several parts to run different time duration partitions. Rayleigh damping of 0.5 percent centered at a frequency of 1 Hz was applied during shaking, as it has been found to be sufficient by other researchers (Boulanger & Ziotopoulou, 2017). During the shaking simulation, the groundwater flow equation was also solved over the duration of the ground shaking. The simulation solved both for mechanical and flow (fully-coupled) at each time step.

5.5.2.4 *Monitored Engineering Demand Parameter (EDP)*

For this Seismic Vulnerability Assessment (SVA) study, we determined several Engineering Demand Parameters (EDPs) to evaluate the extent of liquefaction triggering and the deformation pattern of the 2D model. These EDPs include induced shear strain, nodal lateral deformation, and excess pore pressure ratios. These outputs were extracted for all elements at the end of the input motion for all motions. The contour maps presenting these outputs are shown in Appendix E (Figure E3 – E8).

Additionally, we also monitored several element responses, such as nodal displacement, velocity, and acceleration time history at the surface within the fuel tank facilities. We also monitored the profile of depth versus lateral displacement (Figure 9), shear strain increment (Figure E9, Appendix E), and excess pore pressure ratio (Figure E10, Appendix E) at the left edge (southern), middle, and right edge (northern) perimeter of the fuel tank facilities.

5.5.2.5 *Input Motion*

Selected, scaled, and processed ground motions for each impulsive and convective period were used as input motions. With a total of 10 input motions, we produced 10 simulation results as the baseline case. To eliminate numerical noise caused by the high-frequency components of each input motion, a 6th order Butterworth filter was applied to all motions with a cutoff frequency of approximately 20 to 25 Hz. The filtering process was monitored to ensure that the Arias Intensity of the filtered input motions were not less than 95 percent of the original Arias Intensity.

5.5.3 Calibration of Constitutive Soil Model

5.5.3.1 *ESU-1*

This section discusses the soil constitutive models assigned to each ESU, as presented in Figure E2 in Appendix E. During the dynamic simulation, ESU1 was changed from a Mohr-Coulomb material to an elastic material with hysteretic damping (Sigmoidal3) in FLAC. ESU1 was calibrated to match the Darendeli (2001) modulus reduction curve of clay with a plasticity index (PI) of 20. Table 10 provides a summary of the baseline soil parameters used for our 2D NDA.

5.5.3.2 *ESU-2 (Overbank Deposit)*

As shown in Figure 4, the lack of subsurface information in the northern part of the existing fuel tank facilities led us to project CPT-18 data from the Geotechnical Resources, Inc (GRI) report. This data indicates that ESU2 was observed only up to NAVD88 El. 0.0 feet. However, this assumption should be confirmed through more detailed subsurface investigation. The presence of a thicker and softer ESU2 layer toward the Columbia River may potentially impact the overall results presented in this report.

Based on laboratory testing (index testing, CRS, DSS, and CDSS results) and interpretation of CPTs (see Figure B1 in Appendix B), we believe ESU2 is not susceptible (Figure C-6) to experiencing zero effective stress (i.e., $R_{u\text{-}max} < 0.8 – 0.9$ from CDSS test), but it can still experience strength degradation and accumulate shear strain during cyclic loading (see Figure C2 – C5). The DSS test (Figure C1) indicates that ESU2 is composed of non-sensitive (S = 1.2) fine-grained material. Softening behavior (approximately 15 to 20 percent degradation) was observed at shear strain levels exceeding 30 percent. We expect the strength of ESU2 to experience 5 to 10 percent strength degradation during an earthquake event.

To capture the cyclic behavior, strength degradation, and shear strain accumulation of ESU2, we used the PM4Silt V1.0 constitutive model. We employed a conservative assumption of a baseline value of S_u/σ'_{vo} of 0.3. The shear modulus coefficient (G_o) was calibrated using the measured V_s values, which are presented in Figure B1. We set all secondary parameters to the recommended default values as discussed in Boulanger & Ziotopoulou (2018). Additionally, we checked the damping behavior to match the Darendeli (2001) modulus reduction curve for a material with an overconsolidation ratio (OCR) of 2 and a plasticity index (PI) of 16. Using the CDSS results presented in Appendix C, we calibrated the contraction rate parameter (h_{po}) to match the CRR vs $N_{c\text{-}liq}$ line under single-element undrained CDSS simulations up to 3 percent single amplitude shear strain. We found that h_{po} = 25 produced a reasonable agreement. The hydraulic conductivity of this ESU was estimated using the correlations by Robertson & Cabal (2015), and we set the horizontal to vertical hydraulic conductivity ratio to be 5.0.

Table 10. Summary of Soil Constitutive Model Parameters Used in 2D FLAC Simulation

Model Parameter	ESU-1 (Above GWL)	ESU-2 (Overbank Deposit)	ESU-3 (Columbia River Sand)	Elastic Half-Space
Top Elevation (feet)	23	3	–38	–160
Bot. Elevation (feet)	3	–38	–160	–180
Constitutive Model	***Elastic Hysteretic (Sig3)***	***PM4Silt***[a]	***PM4Sand***[a]	***Elastic***
Plasticity Index	15 - 20	16	Non-Plastic	N/A
MRD Curves	Darendeli (2001)	Darendeli (2001)	n.a	n.a
Unit Weight (pcf)	115	115	120	130
Mass Density (slugs/feet^3)	3.573	3.573	3.728	4.039
Shear Wave Velocity (ft/s)[b]	375	472	613 - 816	1271
Mohr-Coulomb Cohesion (psf)	500	n.a.	n.a.	n.a.
Mohr-Coulomb Friction Angle (°)	30	n.a.	n.a.	n.a.
Undrained Shear Strength Ratio[c] (S_u/σ'_{vo})	n.a.	**0.3** (0.17 - 0.86)	n.a.	n.a.
Relative Density, D_R (%)[c]	n.a.	n.a.	ESU-3a: **40%** ESU-3b: **50%** ESU-3c: **58%**	n.a.
Clean-sand equivalent CPT tip resistance [d], q_{c1Ncs}	n.a.	n.a.	ESU-3a: **90** ESU-3b: **110** ESU-3c: **120**	n.a.
Vertical Hydraulic Conductivity, k_v (ft/s)	6.5E-8	6.5E-8	ESU-3a: **2.0E-6** ESU-3b: **1.0E-5** ESU-3c: **1.0E-5**	1.0E-5
Horizontal Hydraulic Conductivity, k_h (ft/s)	5.0 k_v	5.0 k_v	2.0 k_v	2.0 k_v
h_{po}[e]	n.a.	25	ESU-3a: **1.8** ESU-3b: **1.9** ESU-3c: **2.0**	n.a.

Table 10. Summary of Soil Constitutive Model Parameters Used in 2D FLAC Simulation				
Model Parameter	**ESU-1 (Above GWL)**	**ESU-2 (Overbank Deposit)**	**ESU-3 (Columbia River Sand)**	**Elastic Half-Space**
G_o	n.a.	425 - 546	ESU-3a: **628 - 687** ESU-3b: **587 - 782** ESU-3c: **681 - 743**	n.a.

Notes:
a. All secondary parameters are set to default unless specified.
b. Baseline value from field geophysical measurement
c. Mean value from estimated values, see Appendix-A.
d. Based on Boulanger & Idriss (2016)
e. Calibration parameters to match cyclic resistance curves.

5.5.3.3 ESU-3 (Columbia River Sand)

We relied on the interpretation of CPTs shown in Figure B-2 to determine the engineering properties of ESU-3. Based on the tabulated data in Table 10 and Figure B-2, we discretized this ESU into three sub-layers with different relative densities ranging from 40 to 58 percent. The shear modulus coefficient (G_o) was calibrated using the measured V_s values, which are presented in Figure B2.

To estimate the cyclic resistance ratio (CRR), we utilized the liquefaction triggering line [CRR = f(q_{c1Ncs})] from Boulanger & Idriss (2016), along with their Magnitude Scale Factor (MSF) relationship, to estimate the relationship between CRR and Nc-liq. Subsequently, we performed single-element undrained CDSS simulations until 3 percent single amplitude shear strain to match the target CRR vs Nc-liq relationship. We calibrated the contraction rate parameter (h_{po}) to match the CRR vs Nc-liq, assuming a probability of liquefaction of 15 percent.

The hydraulic conductivity of this ESU was estimated using the correlations by Robertson & Cabal (2015). We set the horizontal to vertical hydraulic conductivity ratio to be 2.0.

5.5.4 Analysis Results

5.5.4.1 Lateral Deformation

The purpose of our simulation is to evaluate the extent of liquefaction triggering by evaluating the maximum induced shear strain during shaking, the generation of excess pore water pressure ratio ($R_{u\ max}$), and the lateral displacement pattern. We ran the selected 10 input ground motions described in Section 5.4.3 and 5.5.1.5 and produced contour maps of the monitored parameters, as presented in Appendix E. Our evaluation focuses on two parts of the model: the levee area and the existing fuel tank perimeter.

In general, based on the analysis of the 2D plane-strain model, the levee toe region experienced significant lateral deformation (more than 10 feet) due to high shear strain accumulation within the toe region, as shown in Figures E2 to E5. A wide extent of soil liquefaction (i.e., $R_{u\text{-}max} \approx 1.0$ and maximum shear strain, γ_{max} >10 percent) occurred within the levee area, reaching a depth of 80 feet bgs. Figure E6 to E7 display the $R_{u\text{-}max}$ contour map, illustrating the extent of liquefaction. Out of the 10 motions we analyzed, one long-duration input motion (NGASubRSN6001811_MET-EW) from a subduction interface source caused progressive failure that propagated toward the existing fuel tank facilities. The estimated lateral deformation within the levee area shaken by this motion exceeded 13 feet. This long-duration motion is observed to have the largest CAV of all the input motions, as well as a response spectrum that generally matches or exceeds the target MCE_R spectrum at most periods.

Within the existing fuel tank facilities area, the presence of a 0.5 to 1.0 percent upsloping ground helps to mitigate deformation toward the Columbia River direction. However, our simulations, based on the 10 motions we ran, showed that the existing fuel tank facilities area experienced lateral displacement toward the south direction, reaching a maximum displacement of 6 feet due to the modeled surficial topography for 9 of the motions, except the previously discussed NGASubRSN6001811_MET-EW motion. Figure 9 provides a summary of the lateral displacement profiles calculated from the 10 motions. Tables 8 and 9 (attached) showed that the NGASubRSN6001811_MET-EW motion represents the most intense earthquake event in terms of highest CAV and longest duration. This motion resulted in progressive failure propagating from the levee area to the middle of the fuel tank facility area. The maximum lateral deformation calculated due to the NGASubRSN6001811_MET-EW input motion was also 6 feet toward the north direction.

As shown in Figure 9, significant shear strain was observed within the depth range of 40 to 50 feet bgs. Based on our estimation, this depth range corresponds to the location of the failure sliding plane. Considering a 2,475-year hazard level, we estimated that the existing fuel tank facilities area will experience lateral displacement, either toward the north or south direction, of up to 6 feet. The cyclic shear strain accumulation within the depth range of 40 to 50 feet contributes the most to the resulting permanent deformation.

5.5.4.2 Post-Liquefaction Reconsolidation Settlement Calculation

The estimation of post-liquefaction reconsolidation settlement was performed by combining the maximum shear strain profile results calculated from the 2D FLAC NDA and laboratory-based volumetric strain–max shear strain models (ε_{vol}–γ_{max}). Figure E8 illustrates the maximum cyclic shear strain profiles induced by all 10 motions. By employing the laboratory-based ε_{vol}–γ_{max} models for Columbia River silty soil (Stuedlein et. al., 2022) and typical clean sand soil (Bray & Olaya, 2023), we were able to estimate the post-shaking settlement, as summarized in Figure 10.

The average calculated settlement from all 10 motions was approximately 11 inches at the left edge (southern), 9 inches at the middle, and 7 inches at the right edge (northern) perimeter of the fuel tank facilities.

We estimated that the soil within the depth range of 0 to 60 feet bgs contributes to more than 75 percent of the resulting post-shaking settlement. Notably, we observed higher settlement along the left edge perimeter, which may lead to significant differential settlement for the fuel tank facilities.

5.5.4.3 Summary of Primary 2D Modeling Results

As described earlier in this report, we selected two suites of 5 ground motions to capture the convective and impulsive periods of the tank, resulting in 10 total motions. For consistency with the intent of ASCE 7-16 Section 16.2.2 we have counted the ground motion with the largest deformation twice to take the average of eleven total ground motions. The resulting averages are provided in Tables 11 and 12.

Table 11. Summary of Total Settlement and Lateral Displacement		
Analysis Profile	**Average Vertical Settlement (inches)**	**Average Lateral Surface Displacement (inches)**
North (right)	8.1	18
Middle	10.2	20
South (left)	12.2	32
Notes: Distance between north edge to south edge is 440 feet		

Table 12. Summary of Differential Settlement and Lateral Displacement		
Analysis Profile	**Average Differential Settlement (inches/50 feet)**	**Average Differential Lateral Surface Displacement (inches/50 feet)**
Between North and South Profiles	0.5	1.6
Notes: Distance between north edge to south edge is 440 feet		

Note that for the tabulated average lateral surface displacements in Tables 11 and 12, we utilized the absolute value of all surface displacements. To calculate the average differential settlements/lateral displacements, we took the difference of the values at the north and south ends of the tank site, divided that value by the distance between them, and then normalized this difference to reflect a distance of 50 feet.

5.5.4.4 Other Modeling Considerations

We conducted additional analyses to assess the impact of two factors: the distance of the existing fuel tank facilities to the left boundary and the ground motion polarity. Our findings indicate that extending the left boundary to a distance of 700 feet away from the existing facilities still resulted in a similar magnitude of southward deformation, showing that the tendency to deform in that direction is primarily a function of the topography rather than edge effects of the model.

Furthermore, we evaluated the influence of ground motion polarity by multiplying –1.0 to the input time history. For this particular 2D model and ground motion, we observed that the ground motion polarity has a negligible effect, as it produced a very similar deformation pattern and magnitude compared to the baseline results.

5.6 SITE-SPECIFIC SITE RESPONSE ANALYSIS

The site-specific 1D site response analysis (SRA) conducted in this report serves two main purposes: first, to determine a recommended response spectrum at the ground surface, and second, to provide additional support and analysis to complement the results obtained from the 2D NDA (Numerical Dynamic Analysis).

Comparing the induced shear strain and displacement profiles calculated by the 2D NDA and 1D SRA is valuable for assessing the consistency and reliability of the results. To carry out the 1D SRA, the DEEPSOIL V7.0 computer program was employed. By conducting both the 2D NDA and 1D SRA analyses, a more comprehensive understanding of the site response is obtained.

5.6.1 One-Dimensional Model

A representative 1D soil profile was developed for the purpose of conducting ground response analysis, utilizing available subsurface information such as boring logs, CPT data, and geophysical measurements. The depth of the groundwater table was specified at 15 feet depth, as discussed earlier in this report. The soil profile and stratification for the ground response analysis is depicted in Figure 6 and Figure B1. This profile was developed to represent a generalized depiction of the subsurface conditions at the site suitable for development of a site-specific response spectrum for the site.

To explore the effects of variability in shear wave velocity, multiple V_S profiles were used for the ground response analyses. These profiles involved increasing and decreasing the baseline Vs profiles by 20 percent to assess the sensitivity of the results to changes in the Vs distribution.

To capture the response of each soil layer accurately, the thickness of each layer was set to 3 feet. This configuration ensures that each layer is capable of propagating harmonic motion with maximum frequencies of at least 25 Hz, allowing for a detailed analysis of the ground response. The specifics of the 1D ground response analysis can be found in Appendix E, where the results and interpretations are presented in detail.

5.6.2 Nonlinear Soil Properties

Nonlinear soil behavior, as described by nonlinear shear modulus reduction (G/G_{max}) and damping curves, was assigned to the analysis profile based on soil type and *in situ* effective stress. Empirical correlations for curves of soil G/G_{max} and damping with shear strain were used to generate the total stress nonlinear soil behavior for model layers, which were then fit to a hyperbolic soil model.

5.6.2.1 Soil Models and Empirical Modulus Reduction and Damping (MRD) Curves

The General Quadratic/Hyperbolic (GQ/H) soil model, developed by Groholski et. al. (2016), was selected for use in our analysis. This model incorporates the Modulus Reduction Factor (MRDF) concept proposed by Phillips and Hashash (2009). The GQ/H model is a strength-controlled soil model that ensures the shear strength of the soil never exceeds an asymptotic limit.

The GQ/H model's parameters are calibrated to fit the small-strain region of the G/G_{max} curve, capturing the initial onset of nonlinearity with shear strain in the soil. The large-strain behavior is controlled by a specified soil strength. The MRDF component of the model modifies the size of unload-reload hysteretic loops, deviating from the Masing behavior. The MRDF parameters are adjusted to match the hysteretic damping across all strain ranges.

Table 13 provides a summary of the selected MRD (Modulus Reduction-Damping) curves used in the analysis. The small-strain damping, D_{min}, is estimated empirically using the proposed MRD models. To obtain a more realistic surface spectrum, we multiply D_{min} by a factor of 3.0, following the recommendation by Tao & Rathje (2019). The profiles plot in Appendix E illustrates the selected D_{min} values, implied shear strength, and implied friction angle for each sublayer.

The GQ/H model is fit to the modulus reduction (G/G_{max}) and damping curves. By using shear strength as an input parameter, the GQ/H model corrects the empirical G/G_{max} curve to match the site's implied shear strength at higher shear strain values. This strength-corrected procedure ensures a more realistic stress-strain behavior at higher strains, which is crucial for producing accurate nonlinear ground response analyses.

Table 13. Nonlinear Curve Soil Index Properties

Depth Range in feet	Empirical MRD Curves	Unit Weight in pcf[a]	Friction Angle in degrees	Undrained Shear Strength Ratio	Additional Model Parameters
0 to 15	Darendeli (2001) Clay PI = 20	115	n.a.	0.5	K_0= 0.45 $(OCR)^{0.5}$
15 to 40	Darendeli (2001) Clay PI = 16	115	n.a.	0.3	K_0= 0.45 $(OCR)^{0.5}$
40 to 180	Darendeli (2001) Sand	120	29 to 32	0	$K_0 = 1 - \sin\phi$
> 180	Elastic Half-space	130	n.a.	n.a.	n.a.

Notes:

a. pcf = pounds per cubic foot

5.7 SURFACE RESPONSE SPECTRUM

The interpretation of 1D SRA results and development of the recommended spectrum are detailed in the following sections.

5.7.1 Results of 1D Site Response Analysis

In our analysis, we conducted 1D, nonlinear, time domain site-specific site response analyses on the representative soil profile described in Table 13 and Figure 6. We applied the five selected input ground motions from the impulsive period scenario to the base of the soil column and propagated them upward. For the 1D GRA, we excluded the convective period scenario input ground motion as the convective period (7.5 seconds) is much greater than the natural period of the 1D modeled profile (1.2 seconds). Stewart, Afshari, and Hashash (2014) note that at periods beyond the site period, SRA results have been found deficient in their ability to predict site response and a recommendation to use semi-empirical models at these periods is suggested instead.

The results of the analysis, including the propagation of peak acceleration through the soil profile, the maximum resulting strain in the soil profile, peak cyclic shear stress ratio, and peak displacement, are presented in Appendix E.

To measure the response of the soil column, we consider the spectral acceleration at the ground surface, which accounts for any amplification or deamplification of the input outcropping motions by the soil column, as shown in Figure 11.

The site effect, which represents the amplification or deamplification by the soil column, is typically characterized by amplification factors (see Figure 11). These factors are defined as the ratio between the surface and base response spectra. In our analysis, we computed linearly averaged amplification factors for each defined soil profile using all five ground motions. These amplification factors were then used to generate a surface spectrum by multiplying the amplification factor at each period by the base response spectrum at that period. The results of the amplified spectrum for all profile analyzed in this study is presented on Figure 11. This resulting surface spectrum is referred to as the amplified outcrop response spectrum and is consistent with the requirements for site response analyses outlined in ASCE 7-16.

5.7.2 Recommended Design MCE_R Spectrum

The recommended surface response spectrum has been developed based primarily on the results of the site response analysis. The spectrum is presented in Figure 11 and is observed to be generally equal to or larger than the full ASCE 7-16 Chapter 21 code-based spectrum in the impulsive period range of interest. At periods significantly beyond the estimated site period, a choice was made to set the recommended site-specific MCE_R response spectrum equal to the ASCE 7-22 Site Class DE response spectrum. This choice was made to avoid potential underestimation of the surface response spectrum at periods beyond where we trust the results of our SRA.

This recommended surface response spectrum satisfies the minimum bound requirement of ASCE 7-16, which states that the surface spectrum should not be lower than 80 percent of the Class E code-based spectrum. The site class E spectrum depicted on Figure 11 includes modifications performed in accordance with OSSC (2019) Section 1613.4.13.

To facilitate design, the design earthquake (DE) spectrum is determined as 2/3 of the MCE_R spectrum. Tabular values for both the MCE_R and DE spectra are provided in Table 14. Additionally, the design acceleration parameters, S_{D1} and S_{DS}, are computed from the recommended design spectrum in accordance with Section 21.4 of ASCE 7-16. These design acceleration parameters are included in the notes section of Table 14 and Figure 11 for reference.

By utilizing the recommended design spectrum, along with the calculated design acceleration parameters, designers can appropriately incorporate the seismic loading considerations into the structural design process in accordance with ASCE 7-16 guidelines.

Table 14. Recommended Surface Response Spectra		
Period (seconds)	**Recommended MCE_R Surface Response Spectrum (g)**	**Recommended Design Surface Response Spectrum (2/3 MCE_R) (g)**
0.01	0.34	0.23
0.03	0.40	0.27
0.05	0.45	0.30
0.10	0.58	0.39
0.20	0.89	0.59
1.20	0.89	0.59
1.50	0.74	0.49
1.70	0.65	0.43
2.00	0.52	0.35
3.00	0.36	0.24
4.00	0.27	0.18
5.00	0.21	0.14
7.50	0.13	0.09
10.00	0.10	0.07

Note:

S_{DS} = 0.59g, S_{D1} = 0.74g

6. Limitations

The recommendations presented in this report should be subject to review and modification as necessary during the final design stages of the project. As further details and information become available, it is essential to reassess and refine the recommendations to ensure their alignment with the specific project requirements and conditions.

6.1 ANALYSIS LIMITATIONS

While this SVA study involved advanced and high-level numerical analysis, it is important to acknowledge that there are limitations due to the limited subsurface information available for the project site. These limitations include:

1. **Limited subsurface explorations within the levee area:** The lack of detailed subsurface explorations in the levee area has resulted in a simplified 2D model derived from cross-section B-B'. The model geometry and interpreted soil layering are important factors that impact the calculated results. The extension of ESU-2 toward the levee area or the presence of thicker ESU-3a in that region may have an impact on the outcomes presented in this report.
2. **Assumptions on soil properties for the Levee structure:** Reasonable assumptions have been made regarding the soil properties of the Levee structure. It is worth noting, however, that, while not a major factor, the properties of the levee soil can influence the calculated lateral deformation at the existing facilities.
3. **Free-Field Analysis:** The numerical model evaluated free-field conditions for the site to estimate the ground deformations at the planned tank location. The values presented do not account for additional deformations induced by structures on shallow foundations on unmitigated soil conditions, or the effects of liquefaction mitigation measures. Additionally, it does not account for structure-soil-structure interaction that has been documented showing that structures founded on mitigated soils may significantly increase the rotation and seismic demand on adjacent structures over unmitigated soils (Hwang et. al., 2021, 2023).

Acknowledging these limitations is important to ensure a comprehensive understanding of the analysis results. It is recommended to address these limitations through additional investigations, explorations, and characterization of the subsurface conditions to improve the accuracy and reliability of the assessments and recommendations.

7. Closure

The recommendations provided in this report are formulated based on our current understanding of the project. It is important to note that these recommendations should be revisited and reassessed if there are any changes to the design that significantly impact the fundamental period of the structure.

This seismic design report presents data obtained from field explorations, advanced laboratory testing, and geophysical surveys conducted at the fuel tank facilities using the procedures outlined in this report. All analyses and calculations presented herein are based on the information provided in this report and the associated geotechnical data report. It is important to acknowledge that the subsurface conditions interpreted from the data presented in this report should not be considered as a guarantee of those interpreted conditions.

We assume the subsurface conditions encountered during the explorations are representative of the overall subsurface conditions throughout the project site. However, it is crucial to recognize that unanticipated soil conditions are commonly encountered during construction projects and cannot be fully determined solely by evaluating soil samples from a single boring. Therefore, continuous monitoring and assessment of the subsurface conditions during construction are necessary to address any unexpected variations or challenges that may arise.

8. References

1. Abrahamson, N. A., and Gulerce, Z. 2020. Regionalized ground-motion models for subduction earthquakes based on the NGA-SUB database. Report No. 2020/25, Berkeley, CA: Pacific Earthquake Engineering Research Center, University of California, Berkeley.

2. Abrahamson, N. A., et al. 2018. Update of the BC Hydro Subduction Ground-Motion Model using the NGA-Subduction Dataset. PEER Report No. 2018/02.

3. Abrahamson, N.A., W.J Silva, and R. Kamai 2014. Summary of the ASK14 ground-motion relation for active crustal regions; Earthquake Spectra, Vol. 30, No. 3, August 2014.

4. American Society of Civil Engineers 2017. Minimum Design Loads and Associated Criteria for Buildings and Other Structures, ASCE/SEI 7-16.

5. American Society of Civil Engineers 2022. Minimum Design Loads and Associated Criteria for Buildings and Other Structures, ASCE/SEI 7-22.

6. Atik, L. A., & Youngs, R. R. 2014. Epistemic Uncertainty for NGA-West2 Models. Earthquake Spectra, 30(3), 1301–1318. https://doi.org/10.1193/062813EQS173M.

7. Atkinson G. M., Macias M., 2009. Predicted ground motions for great interface earthquakes in the Cascadia Subduction Zone. Bulletin of the Seismological Society of America, Vol. 99, No. 3, 1552–1578

8. Atwater, B.F., S. Musumi-Rokkaku, K. Satake, T. Yoshinobu, K. Ueda, D. Yamaguchi, 2005. “The orphan tsunami of 1700,” U.S. Geological Survey Professional Paper 1707.

9. Bahrampouri, M., Rodriguez-Marek, A. and Green, R.A., 2021. Ground motion prediction equations for significant duration using the KiK-net database. *Earthquake Spectra*, *37*(2), pp.903-920.

10. Boore, D.M, J.P. Stewart, Emel Seyhan, and G.A. Atkinson 2014. NGA-West2 equations for predicting PGA, PGV, and 5% damped PSA for shallow crustal earthquakes. Earthquake Spectra Vol. 30, No. 3, August 2014.

11. Boulanger, Ross W., and I. M. Idriss. "CPT-based liquefaction triggering procedure." Journal of Geotechnical and Geoenvironmental Engineering 142.2 (2016): 04015065.

12. Boulanger, R.W., and Ziotopoulou, K. (2017). “PM4Sand (version 3.1): A sand plasticity model for earthquake engineering applications.” Report No. UCD/CGM-17/01, Center for Geotechnical Modeling, Department of Civil and Environmental Engineering, University of California, Davis, CA, March, 112 pp.

13. Boulanger, R. W., and Ziotopoulou, K. (2018). “PM4Silt (Version 1): A silt plasticity model for earthquake engineering applications.” Report No. UCD/CGM-18/01, Center for Geotechnical Modeling, Department of Civil and Environmental Engineering, University of California, Davis, CA.

14. Bray, J.B., Olaya, F. (2023). 2022 H. Bolton Seed Memorial Lecture: Evaluating Liquefaction Effects. ASCE Journal of Geotechnical & Geoenviornmental Engineering. https://ascelibrary.org/doi/10.1061/JGGEFK.GTENG-11242.

15. Bray, J.B., Sancio, R.B. (2006). Assessment of the Liquefaction Susceptibility of Fine-Grained Soils. ASCE JGGE. https://doi.org/10.1061/(ASCE)1090-0241(2006)132:9(116

16. Building Seismic Safety Council (BSSC), 2009. NEHRP Recommended Provisions for Seismic Regulations for New Buildings and Other Structures, FEMA P-749, Federal Emergency Management Agency, Washington, D.C.

17. Campbell, K.W. and Y. Bozorgnia 2014. NGA-West2 Ground motion model for the average horizontal components of PGA, PGV, and 5% damped linear acceleration response spectra; Earthquake Spectra, Vol. 30, No. 3, August 2014.

18. Chiou, B.S.J. and R.R. Youngs, 2014. Update of the Chiou and Youngs NGA model for the average horizontal component of peak ground motion and response spectra; Earthquake Spectra, Vol. 30, No. 3, August 2014.

19. Darendeli, M. B. 2001. Development of a New Family of Normalized Modulus Reduction and Material Damping Curves, Department of Civil, Architectural and Environmental Engineering, The University of Texas, Austin, Texas.

20. Groholski, D., Hashash, Y., Kim, B., Musgrove, M., Harmon, J., and Stewart, J., 2016. “Simplified Model for Small-Strain Nonlinearity and Strength in 1D Seismic Site Response Analysis.” J. Geotech. Geoenviron. Eng., 10.1061/(ASCE)GT.1943-5606.0001496, 04016042.

21. Hashash, Y.M.A., Musgrove, M.I., Harmon, J.A., Ilhan, O., Xing, G., Numanoglu, O., Groholski, D.R., Phillips, C.A., and Park, D. (2020) “DEEPSOIL 7.0, User Manual”. Urbana, IL, Board of Trustees of University of Illinois at Urbana-Champaign.

22. Haley & Aldrich 2023. Geotechnical Data Report. PDX Fuel Tank Project, Portland International Airport. 17 July 2023.

23. Hutabarat, D., and Bray, J.D. 2022. Estimating the Severity of Liquefaction Ejecta Using the Cone Penetration Test. ASCE Journal of Geotechnical & Geoenvironmental Engineering, Vol. 148-3-2022.

24. Hwang, Y.W., Ramirez, J., Dashti, S., Kirkwood, P., Liel, A.B., Camata, G., Petracca, M. (2021). “Seismic Interaction of Adjacent Structures on Liquefiable Soils: Insight from Centrifuge and Numerical Modeling,” ASCE JGGE.

25. Hwang, Y.W., Dashti, S. (2023). “Seismic Interactions Among Multiple Structures Founded on Liquefiable Soils in a City Block,” ASCE JGGE.

26. Idriss, I.M. and Boulanger, R.W. (2008) Soil Liquefaction during Earthquake. EERI Publication, Monograph MNO-12, Earthquake Engineering Research Institute, Oakland.

27. Idriss I. M., 2014. An NGA-West2 empirical model for estimating the horizontal spectral values generated by shallow crustal earthquakes, Earthquake Spectra, Vol. 30, No. 3, August 2014.

28. International Code Council 2022. Oregon Structural Specialty Code (OSSC) 2022.

29. Itasca Consulting Group, Inc. (2019) FLAC — Fast Lagrangian Analysis of Continua, Ver. 8.1. Minneapolis: Itasca.

30. Kuehn N., Bozorgnia Y., Campbell K. W., and Gregor N. (2020). Partially nonergodic ground-motion model for subduction regions using NGA-Subduction database, PEER Report No. 2020/04, Pacific Earthquake Engineering Research Center, University of California, Berkeley, CA.

31. Liu C, Macedo J. New conditional, scenario-based, and non-conditional cumulative absolute velocity models for subduction tectonic settings. Earthquake Spectra. 2022;38(1):615-647. doi:10.1177/87552930211043897

32. Macedo J, Abrahamson N, Liu C (2021) New scenario-based cumulative absolute velocity models for shallow crustal tectonic settings. Bulletin of the Seismological Society of America 111(1): 157–172.

33. Parker GA, Stewart JP, Boore DM, Atkinson GM, Hassani B. NGA-subduction global ground motion models with regional adjustment factors. Earthquake Spectra. 2022; 38(1):456-493. doi:10.1177/87552930211034889.

34. Petersen, M.D., et al. (2014). Documentation for the 2014 Update of the United States National Seismic Hazard Maps: U.S. Geological Survey Open-File Report 2014-1091.

35. Petersen, M.D., Shumway, A.M., Powers, P.M., et al. (2020) The 2018 update of the US National Seismic Hazard Model: Overview of model and implications. Earthquake Spectra.;36(1):5-41. doi:10.1177/8755293019878199.

36. Phillips, C. and Y. M. A. Hashash, 2009. Damping formulation for non-linear 1D site response analyses. Soil Dynamics and Earthquake Engineering, 29(7): Pages 1143-1158.

37. Robertson, P.K., Cabal, K. (2015). Guide to Cone Penetration Testing 7th Edition. Gregg Drilling LLC.

38. Robertson, P.K.(2021). Evaluation of flow liquefaction and liquefied strength using the cone penetration test: an update. Canadian Geotechnical Journal. https://cdnsciencepub.com/doi/10.1139/cgj-2020-0657.

39. Rocscience Slide2, Version 9.028. Accessed 13 July 2023.

40. Shahi, Shrey K. and Jack W. Baker 2014. NGA-West2 Models for Ground-Motion Directionality, Earthquake Spectra: August 2014. Vol. 30, No. 3, pp. 1285-1300.

41. Stephenson, W. J., Reitman, N. G., and Angster, S. J. (2017). P- and S-wave velocity models incorporating the Cascadia subduction zone for 3D earthquake ground motion simulations—Update for Open-File Report 2007-1348, Version 1.6: U.S. Geological Survey Open-File Report 2017-1152.

42. Stuedlein, A.W., Dadashiderej, A., Jana, A., Evans. M.T. (2022). Liquefaction Susceptibility and Cyclic Response of Intact Nonplastic and Plastic Silts. ASCE Journal of Geotechnical & Geoenvironmental Engineering. https://ascelibrary.org/doi/10.1061/%28ASCE%29GT.1943-5606.0002935.

43. Stewart, J.P., Afshari, K., Hashash, Y.M.A. Guidelines for performing hazard-consistent one-dimensional ground response analysis for ground motion prediction. PEER Report 2014/16, October 2014.

44. Tao, Y. and Rathje, E.M. (2019). Insights into Modeling Small-Strain Site Response Derived from Downhole Array Data. ASCE JGGE. https://ascelibrary.org/doi/10.1061/%28ASCE%29GT.1943-5606.0002048.

\\haleyaldrich.com\share\pdx_data\Notebooks\0204679-001_PDX_Fuel_Project_Tank_Design\Deliverables\Reports\Final Enhanced Seismic Design Report\2023_0929_HAI_PDX_Tank_EnhancedSeismicDesignReport_F.docx

FIGURES

FOR REFERENCE ONLY

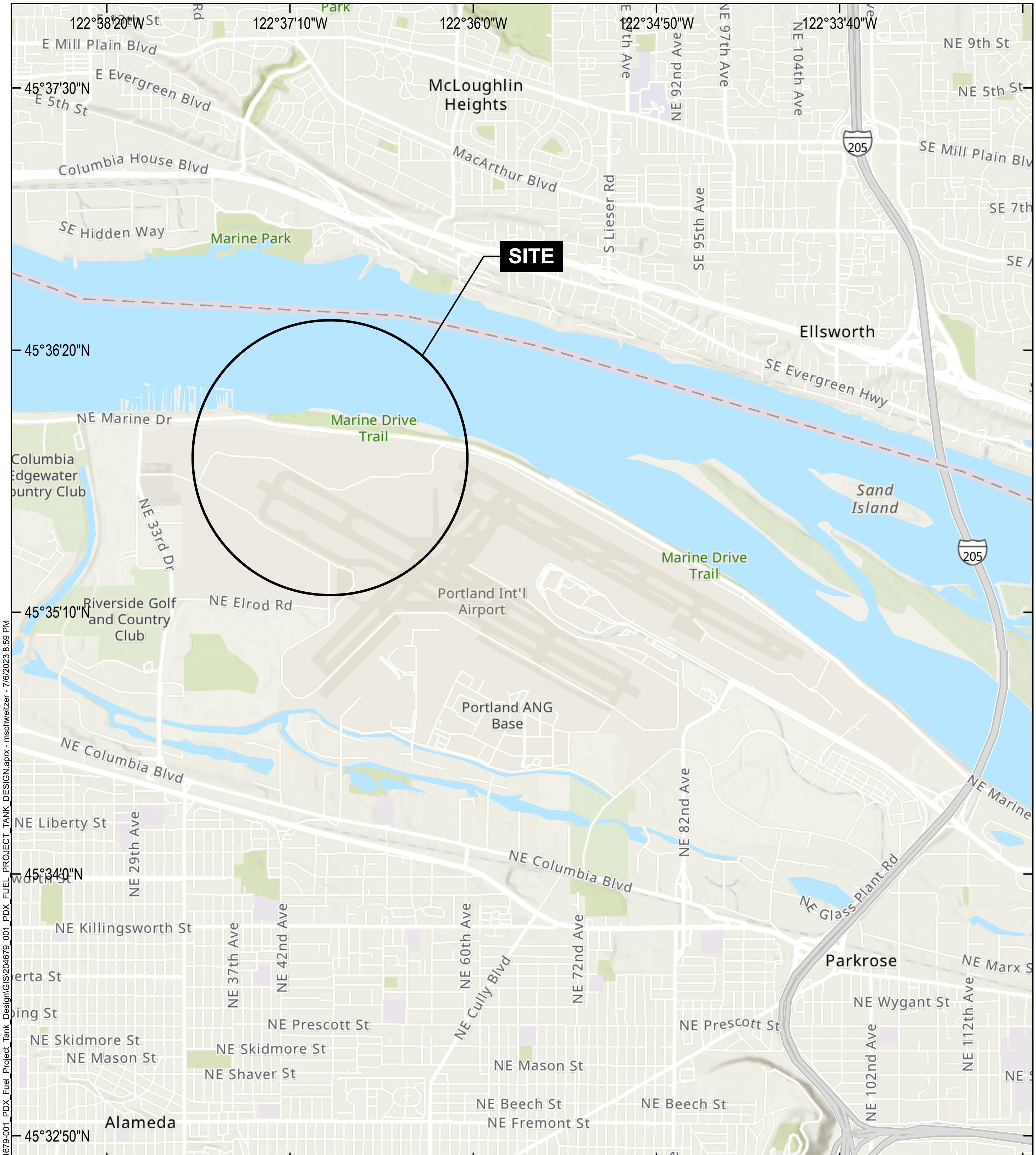

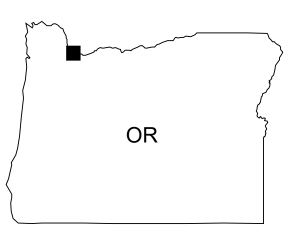

MAP SOURCE: ESRI
SITE COORDINATES: 45°35'06"N, 122°35'39"W

HALEY ALDRICH

PDX FUEL TANKS – SEISMIC VULNERABILITY ASSESSMENT
PORTLAND, OREGON 97218

VICINITY MAP

APPROXIMATE SCALE: 1 IN = 1 MILE
JULY 2023

FIGURE 1

GIS: \\haleyaldrich.com\share\pdx_data\Notebooks\0204679-001_PDX_Fuel_Project_Tank_Design\GIS\204679_001_PDX_FUEL_PROJECT_TANK_DESIGN.aprx - mschweitzer - 7/6/2023 8:59 PM

LEGEND

- CURRENT EXPLORATION (H&A, 2023)
- PREVIOUS EXPLORATION (GRI, 2017)
- PREVIOUS EXPLORATION (H&A, 2019)
- TEST PITS CURRENT EXPLORATION (H&A, 2023)
- CROSS SECTION
- BATHYMETRIC ELEVATION CONTOUR, 5-FT INTERVAL (NAVD 88)
- TOPOGRAPHIC ELEVATION CONTOUR, 5-FT INTERVAL (NAVD 88)
- NORTHERN, MIDDLE, AND SOUTHERN PERIMETER OF FUEL TANK FACILITY

NOTES

1. ALL LOCATIONS AND DIMENSIONS ARE APPROXIMATE.
2. TOPOGRAPHY/BATHYMETRY SOURCE: US ARMY CORPS OF ENGINEERS, 2010.
3. AERIAL IMAGERY SOURCE: NEARMAP, 14 AUGUST 2022.
4. NORTH AMERICAN VCERTICAL DATUM OF 1988 (NAVD88)

N

0 800 1,600
SCALE IN FEET

HALEY ALDRICH

PDX FUEL TANKS – SEISMIC VULNERABILITY ASSESSMENT
PORTLAND, OREGON 97218

SITE PLAN

JULY 2023

FIGURE 2

GIS FILE PATH: \\haleyaldrich.com\share\pdx_data\Notebooks\0204679-001_PDX_Fuel_Project_Tank_Design\GIS\204679_001_PDX_FUEL_PROJECT_TANK_DESIGN.aprx - USER: elindquist - LAST SAVED: 7/6/2023 10:38 PM

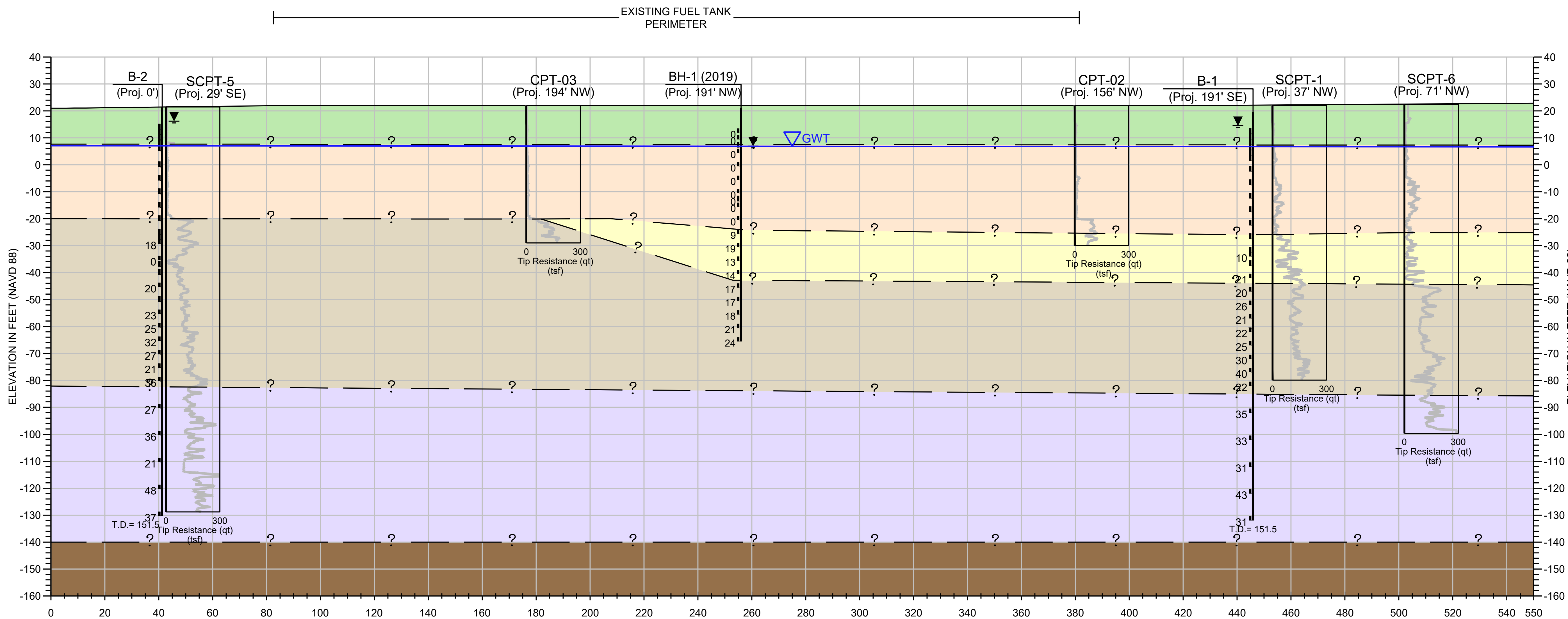

LEGEND

EXPLORATION

B-1
(Proj. 221' E)

STANDARD PENETRATION RESISTANCE IN BLOWS PER FOOT — 10, 21, 20

WATER LEVEL

USCS CLASSIFICATION — SP

T.D.= 151.5 — EXPLORATION DEPTH IN FEET

CPT EXPLORATION

CPT-18
(Proj. 1905' E)

0 300
Tip Resistance (qt)
(tsf)

ESU-1 - FILL & OVERBANK DEPOSIT (ABOVE G.W.T)

ESU-2 - OVERBANK DEPOSIT

ESU-3A - COLUMBIA RIVER SAND (DR =40%)

ESU-3B - COLUMBIA RIVER SAND (SP)(DR = 50%)

ESU-3C - COLUMBIA RIVER SAND (SP)(DR = 58%)

VERY DENSE SANDY GRAVEL (ELASTIC HALFSPACE VS = 1271 FT/SEC)

NOTES

1. CONTACTS BETWEEN SOIL UNITS ARE BASED UPON INTERPOLATION BETWEEN BORINGS AND REPRESENT OUR INTERPRETATION OF SUBSURFACE CONDITIONS BASED ON CURRENTLY AVAILABLE DATA.
2. PROFILE SURFACE CREATED FROM A DIGITAL ELEVATION MODEL (DEM) CREATED BY THE LOWER COLUMBIA ESTUARY PARTNERSHIP.

0 40 80
SCALE IN FEET

HALEY ALDRICH

PDX FUEL TANK - SEISMIC VULNERABILITY ASSESSMENT
PORTLAND INTERNATIONAL AIRPORT
5000 NE MARINE DRIVE
PORTLAND, OREGON 97218

SUBSURFACE CROSS SECTION A-A'

JULY 2023

FIGURE 3

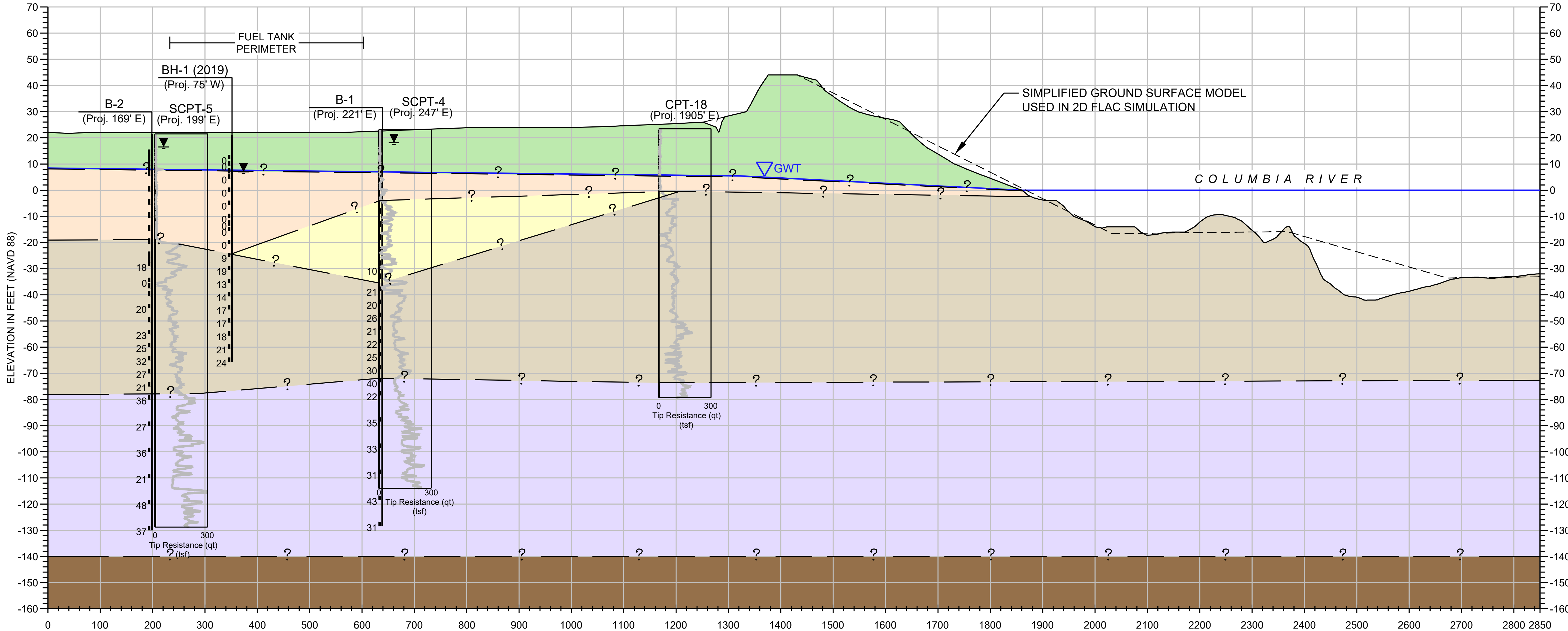

LEGEND

EXPLORATION

B-1
(Proj. 221' E)

STANDARD PENETRATION RESISTANCE IN BLOWS PER FOOT — 10, 21, 20

WATER LEVEL

SP — USCS CLASSIFICATION

T.D.= 151.5 — EXPLORATION DEPTH IN FEET

CPT EXPLORATION

CPT-18
(Proj. 1905' E)

0 300
Tip Resistance (qt)
(tsf)

ESU-1 - FILL & OVERBANK DEPOSIT (ABOVE G.W.T)

ESU-2 - OVERBANK DEPOSIT

ESU-3A - COLUMBIA RIVER SAND (DR =40%)

ESU-3B - COLUMBIA RIVER SAND (SP)(DR = 50%)

ESU-3C - COLUMBIA RIVER SAND (SP)(DR = 58%)

VERY DENSE SANDY GRAVEL (ELASTIC HALFSPACE VS = 1271 FT/SEC)

NOTES

1. CONTACTS BETWEEN SOIL UNITS ARE BASED UPON INTERPOLATION BETWEEN BORINGS AND REPRESENT OUR INTERPRETATION OF SUBSURFACE CONDITIONS BASED ON CURRENTLY AVAILABLE DATA.
2. PROFILE SURFACE CREATED FROM A DIGITAL ELEVATION MODEL (DEM) CREATED BY THE LOWER COLUMBIA ESTUARY PARTNERSHIP.

HORIZ. 0 200 400
VERT. 0 40 80
SCALE IN FEET

HALEY ALDRICH

PDX FUEL TANK - SEISMIC VULNERABILITY ASSESSMENT
PORTLAND INTERNATIONAL AIRPORT
5000 NE MARINE DRIVE
PORTLAND, OREGON 97218

SUBSURFACE CROSS SECTION B-B'

JULY 2023

FIGURE 4

Saved by: ELINDQUIST Printed: 7/7/2023 12:53 PM Sheet: HA-SEC-B
\\HALEYALDRICH.COM\SHARE\PDX_DATA\NOTEBOOKS\0204679-001_PDX_FUEL_PROJECT_TANK_DESIGN\CAD\C3D\204679_001_CROSS_SECTION.DWG

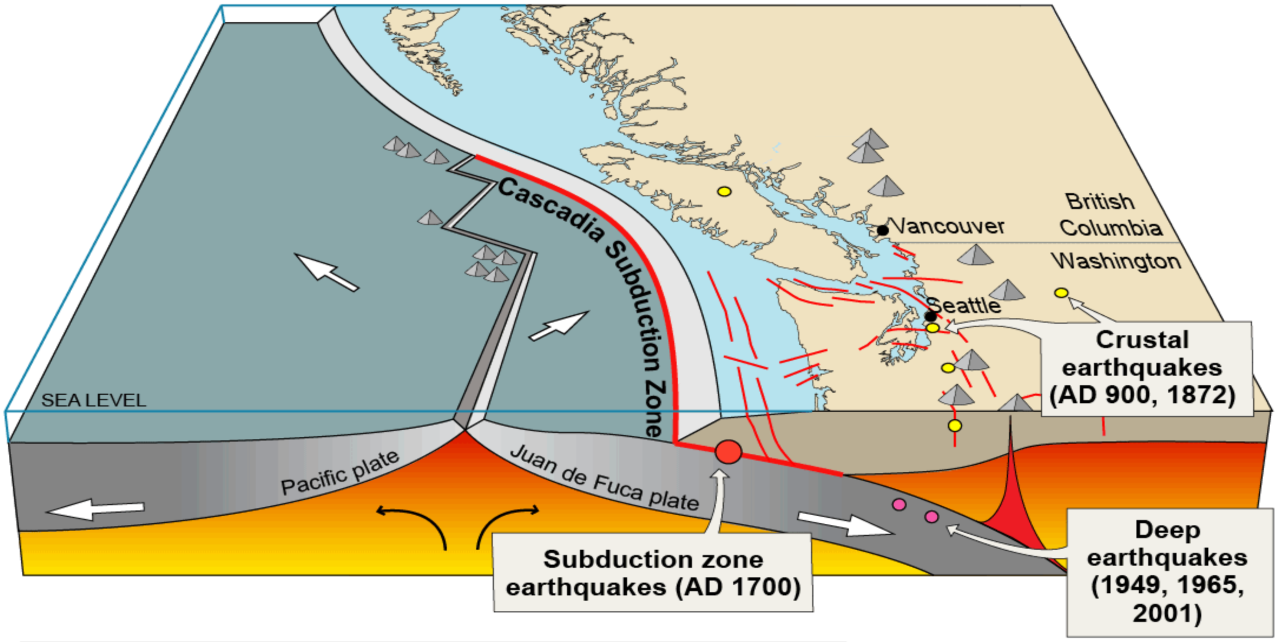

Source	Max. Size	Recurrence
Subduction zone	M 9+	200–600 years
Deep Juan de Fuca plate	M 7+	30–50 years
Crustal faults	M 7+	Hundreds of years?

Volcano

Active crustal fault

Active plate boundary fault

Source: https://www.dnr.wa.gov/pictures/ger/ger_hazards_eq_wa_faults_1140.png

PDX Fuel Tank
Seismic Vulnerability Assessment
Portland, Oregon

Seismotectonic Characteristic of The Pacific Northwest

0204679-001 July 2023

HALEY ALDRICH

Fig. 5

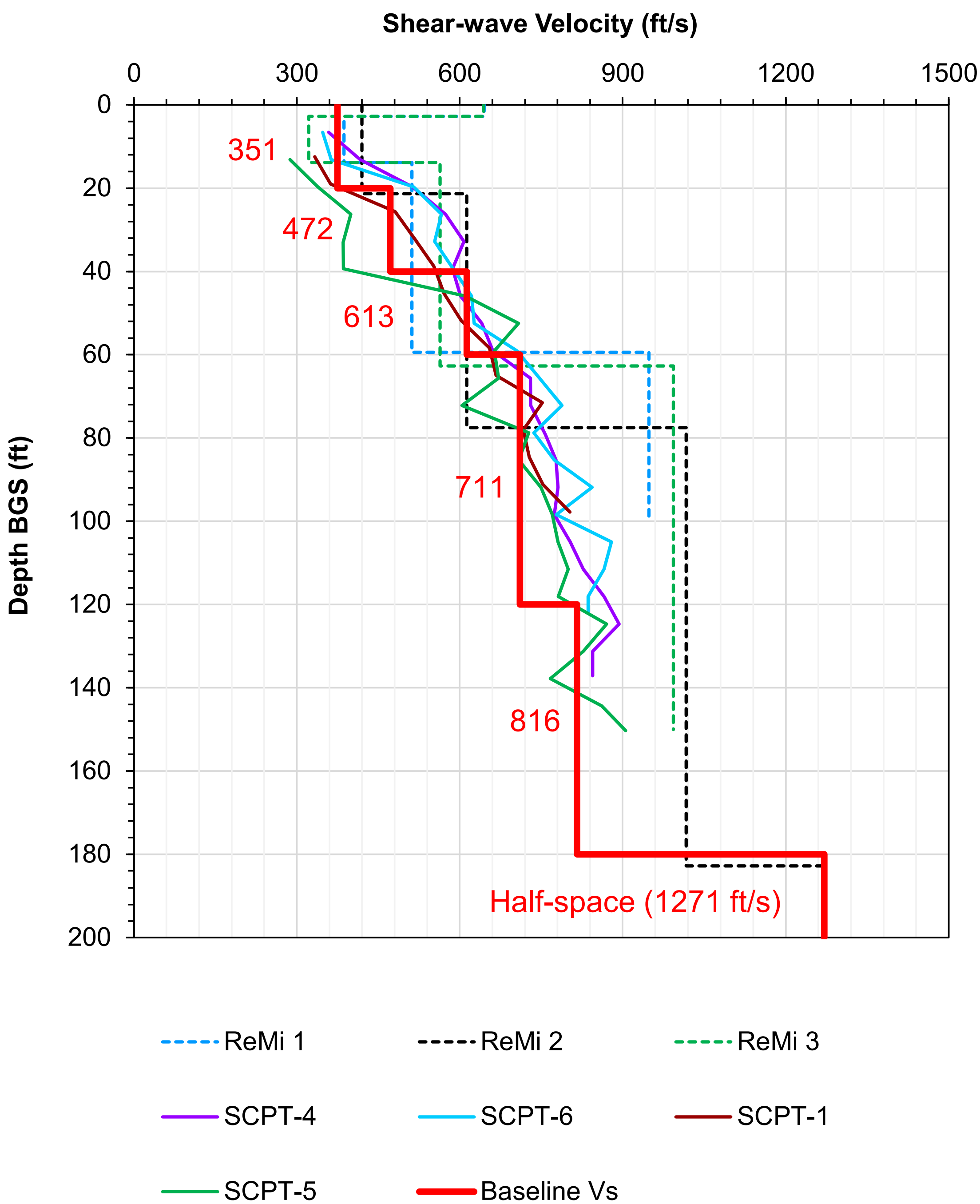

Notes:
1. Half-space Vs = 1271 ft/s

PDX Fuel Tank
Seismic Vulnerability Assessment
Portland, Oregon

Measured Shear Wave Velocity Profile at Fuel Tank Facilities Area

0204679-001 July 2023

HALEY ALDRICH

Fig. 6

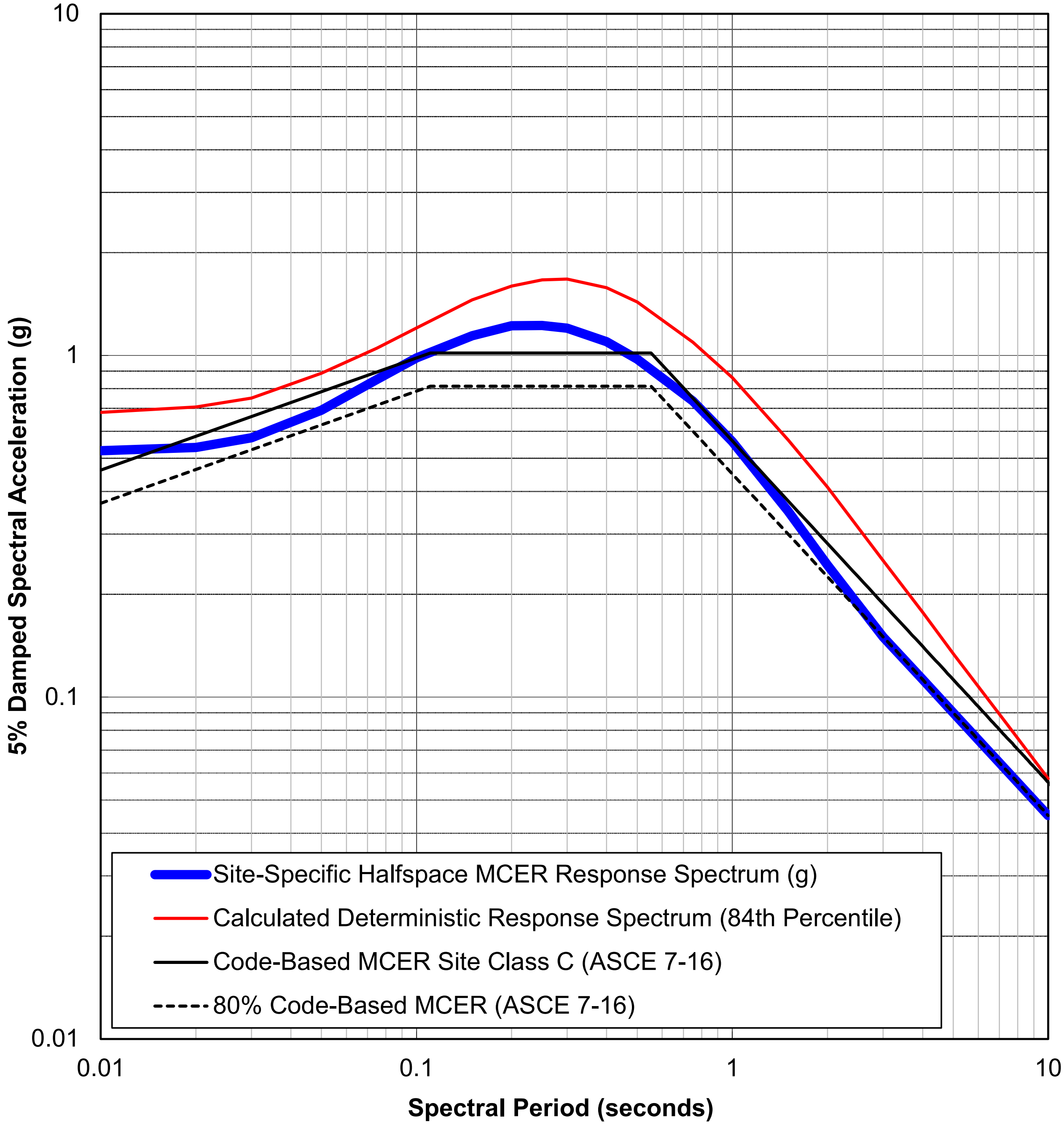

Notes:
1. Half-space Vs = 1271 ft/s
2. This response spectrum was used as the target spectrum for selection of ground motion time histories. It is not intended for use in design

PDX Fuel Tank Seismic Vulnerability Assessment Portland, Oregon
Site-Specific **(Half-space) MCE_R Target** **Response Spectrum**
0204679-001 July 2023
HALEY ALDRICH **Fig. 7**

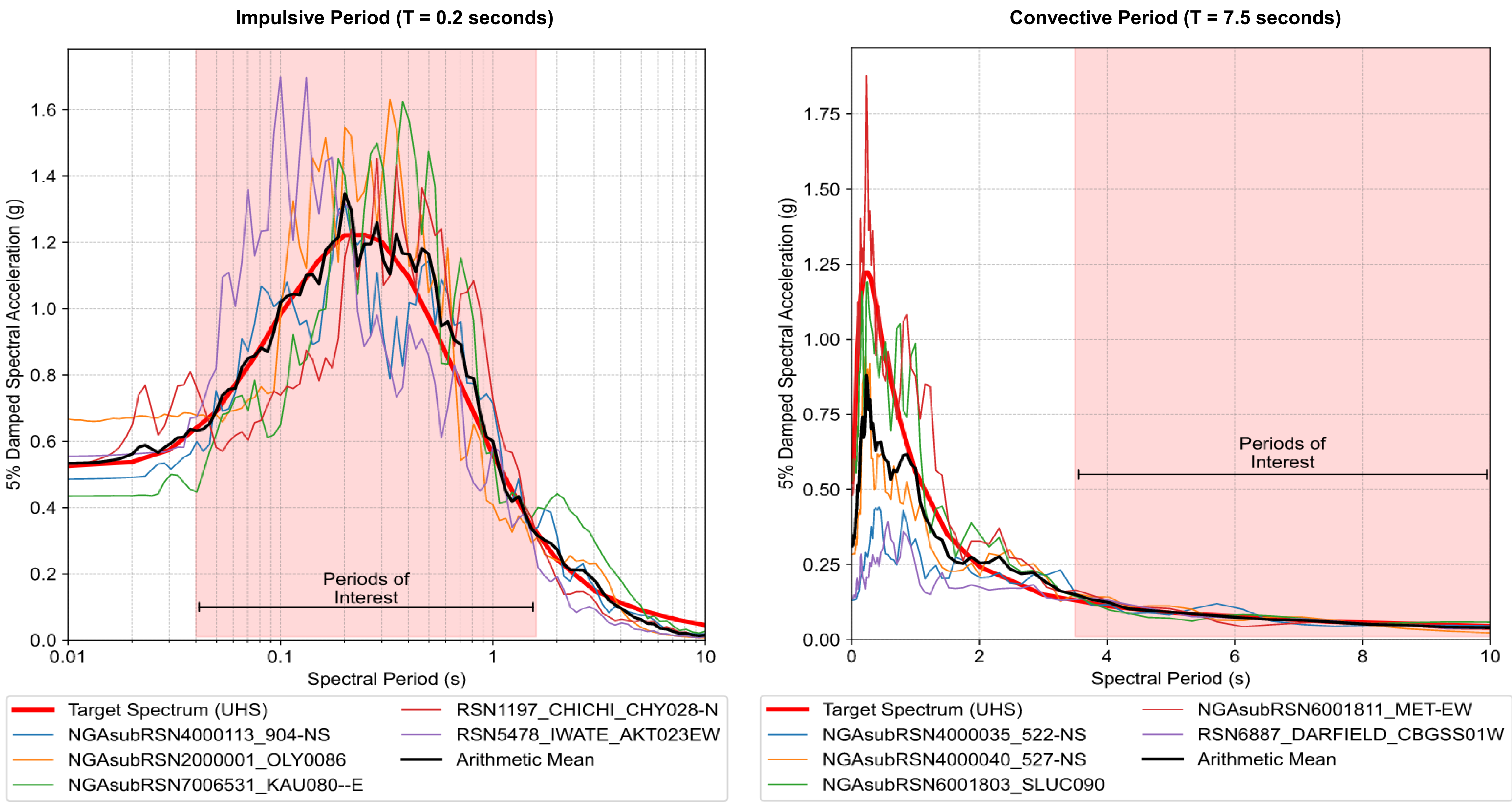

Notes:
1. Half-space condition with Vs = 1271 ft/sec
2. Amplitude-scaled one component ground motion

PDX Fuel Tanks SVA
Portland, Oregon

Selected Amplitude-Scaled Ground Motion for Impulsive and Convective Period

0204679-001 July 2023

HALEY ALDRICH

Figure 8

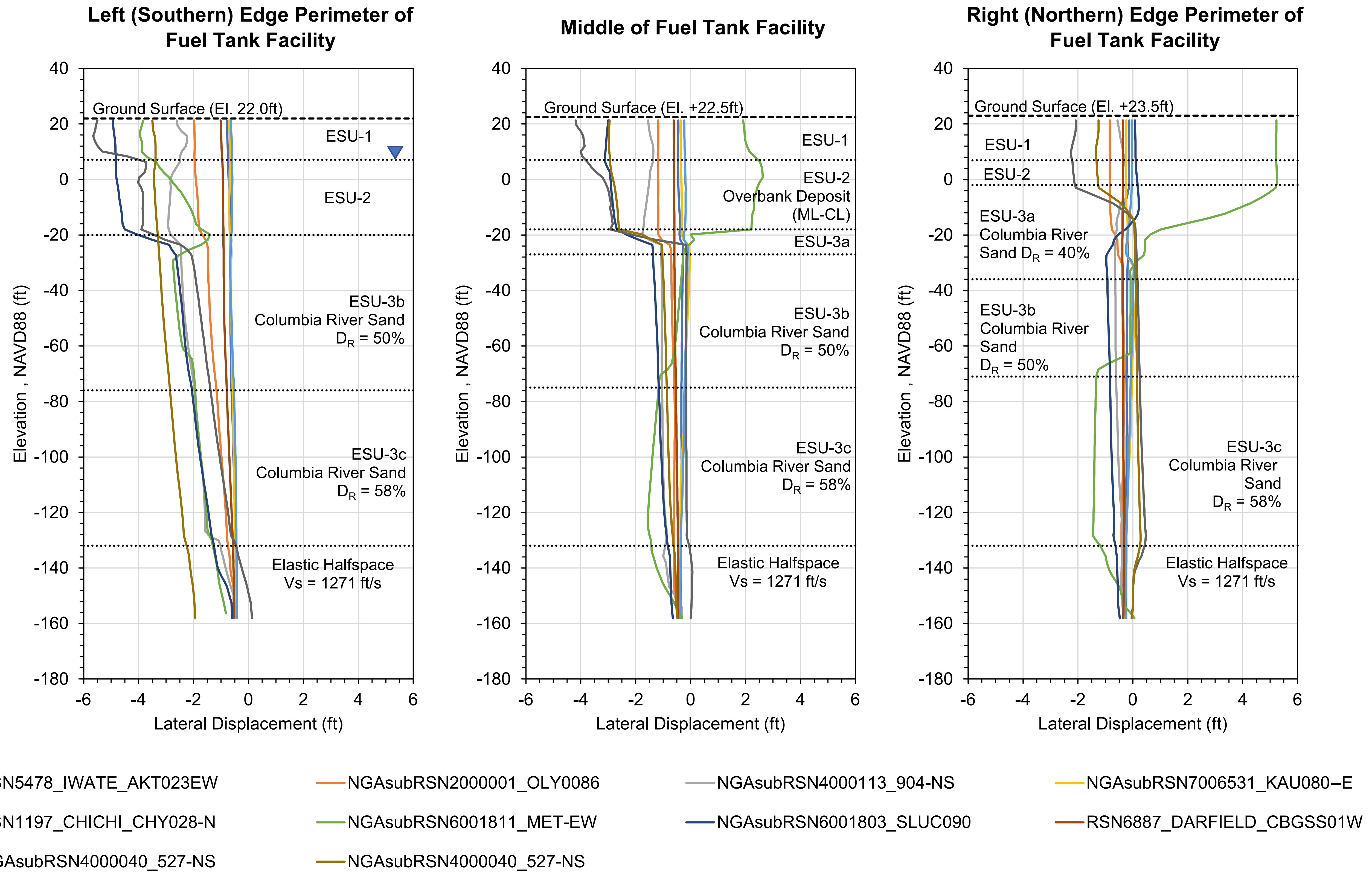

Notes:
1. The displacement profile show results at the end of the FLAC 2D Nonlinear Deformation Analysis (NDA) for each motions
2. The depth of contact for every ESU are consistent with the FLAC 2D NDA model

PDX Fuel Tanks SVA
Portland, Oregon

Calculated Lateral Displacement Profile: FLAC 2D NDA

0204679-001 July 2023

HALEY ALDRICH

Figure 9

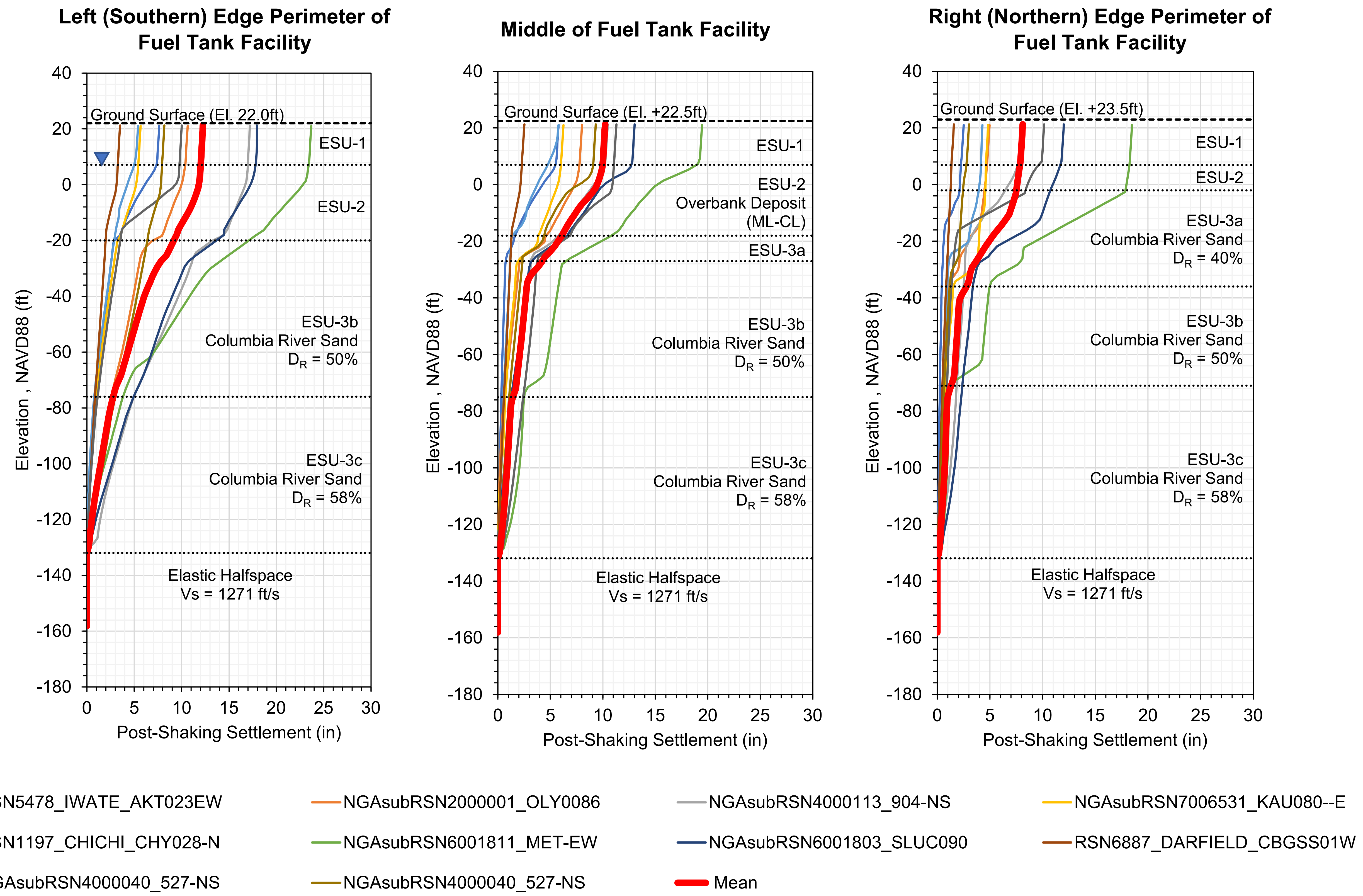

Notes:

1. Post-Liquefaction Volumetric Strain for ESU-2 (Overbank Deposit) is estimated using Stuedlein et al. (2022) ε_{vol} (%) = 0.139 EXP(0.04$r_{u\text{-}max}$)
2. Post-Liquefaction Volumetric Strain for ESU-3a,3b,3c (Columbia River Sand) is estimated using Bray & Olaya (2023) ε_{vol} (%) = 1.14 EXP(-2.0 D_R) (MIN(γ_{max},8%))
3. $$S_e(inch) = \sum_{i=1}^{n} \varepsilon_{vol_i} \Delta H_i$$,where ΔH = thickness of sub layer *i*, and n = number of layers
4. $r_{u\text{-}max}$ and γ_{max} were the maximum pore pressure ratio and shear strain value calculated from FLAC 2D NDA simulation
5. The calculated settlement does not include the primary and secondary consolidation settlement of ESU-2 layer

PDX Fuel Tanks SVA
Portland, Oregon

Estimated Post Liquefaction Reconsolidation Settlement Profile

0204679-001 July 2023

Figure
10

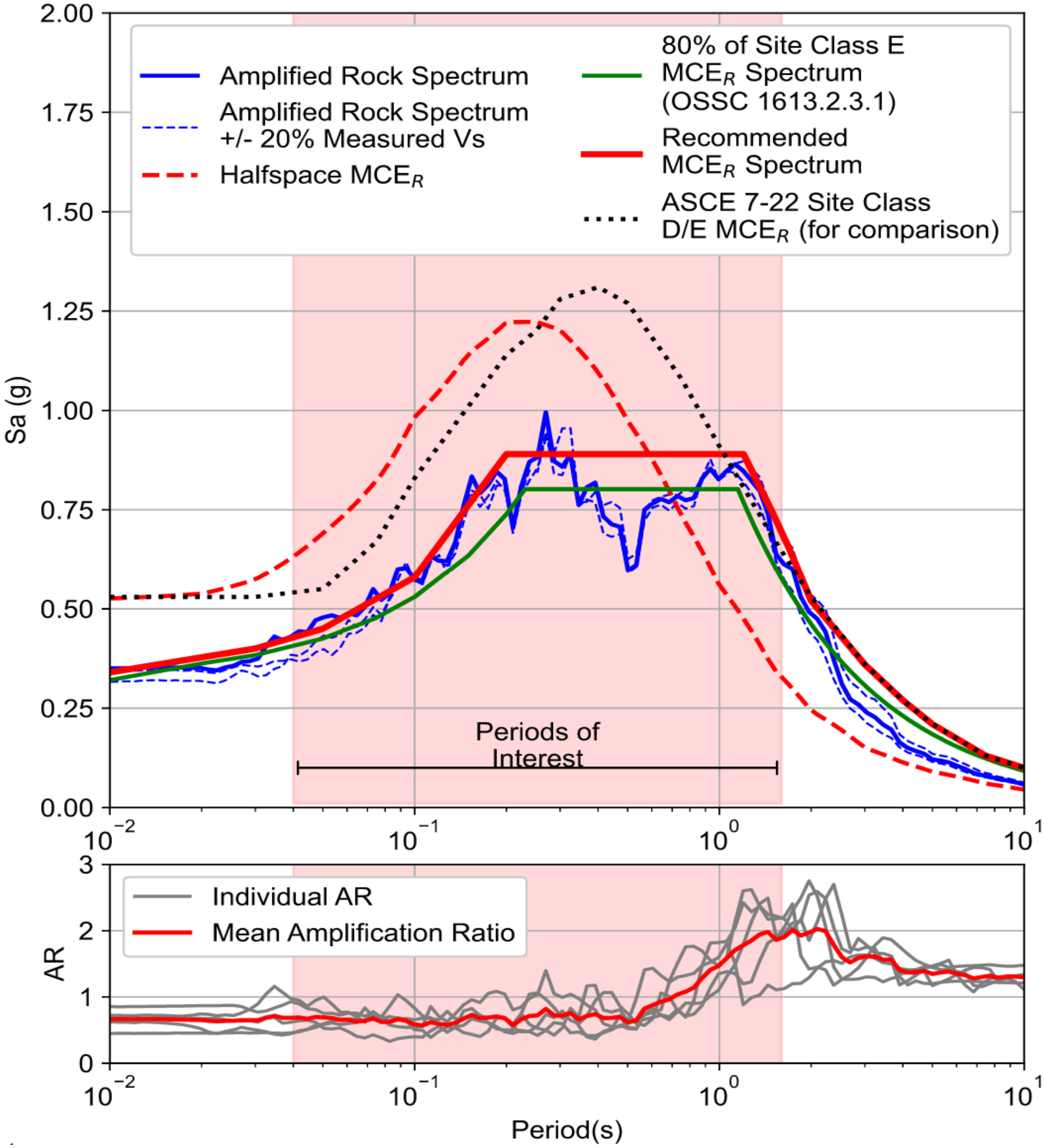

Notes:

1. Amplified Rock Spectrum = Halfspace MCER x Mean Amplification Ratio
2. Site-specfic Design Parameters are S_{DS} = 0.59g, S_{D1} = 0.74 g

PDX Fuel Tank
Seismic Vulnerability Assessment
Portland, Oregon

Recommended Surface MCE$_R$ Spectrum From 1D Site Response Analysis

0204679-001 July 2023

HALEY ALDRICH

Fig. 11

\\haleyaldrich.com\share\pdx_data\Notebooks\0204679-001_PDX_Fuel_Project_Tank_Design\Analysis and Calcs\4 Seismic Hazard & Ground Motions\MCER Development\[Development of MCER - PDXFuelTan

TABLES

Table 5 - Development of Site-Specific Halfspace MCE_R Response Spectrum

Period (s)	Haley & Aldrich PSHA Site-Specific (V_{S30} = 1271 ft/s) 2,475-year Response Spectrum (g)[1] (RotD50)	Risk Coefficients (ASCE 7-16 Method 2)[2]	Maximum Component Factor (Shahi and Baker, 2014)	Calculated MCE_R Response Spectrum (g)	ASCE 7-16 Code-Based MCE_R Response Spectrum for Site Class C (g)	Ratio of Calculated MCE_R Response Spectrum to Code-Based MCE_R Spectrum	Calculated Deterministic Response Spectrum (84th Percentile)	**Site-Specific Halfspace MCE_R Response Spectrum (g)**
0.01	0.50	0.89	1.19	0.53	0.46	1.14	0.68	**0.53**
0.02	0.51	0.89	1.19	0.54	0.52	1.04	0.71	**0.54**
0.03	0.54	0.90	1.19	0.57	0.57	1.00	0.75	**0.57**
0.05	0.65	0.89	1.19	0.69	0.68	1.01	0.89	**0.69**
0.075	0.79	0.90	1.19	0.85	0.82	1.04	1.05	**0.85**
0.1	0.92	0.90	1.19	0.98	0.96	1.03	1.20	**0.98**
0.15	1.08	0.89	1.19	1.14	1.02	1.12	1.46	**1.14**
0.2	1.13	0.89	1.21	1.22	1.02	1.20	1.60	**1.22**
0.25	1.14	0.89	1.21	1.22	1.02	1.20	1.66	**1.22**
0.3	1.11	0.89	1.22	1.20	1.02	1.18	1.67	**1.20**
0.4	1.00	0.89	1.23	1.10	1.02	1.08	1.58	**1.10**
0.5	0.89	0.89	1.23	0.97	1.02	0.96	1.43	**0.97**
0.75	0.67	0.88	1.24	0.73	0.75	0.98	1.09	**0.73**
1	0.51	0.89	1.24	0.56	0.56	0.99	0.86	**0.56**
1.5	0.32	0.88	1.24	0.35	0.38	0.93	0.57	**0.35**
2	0.22	0.88	1.24	0.24	0.28	0.86	0.41	**0.24**
3	0.13	0.88	1.25	0.14	0.19	0.75	0.25	**0.15**
4	0.087	0.88	1.26	0.097	0.141	0.69	0.18	**0.113**
5	0.064	0.88	1.26	0.071	0.113	0.63	0.13	**0.090**
7.5	0.038	0.87	1.28	0.042	0.075	0.56	0.08	**0.060**
10	0.026	0.87	1.29	0.030	0.056	0.53	0.06	**0.045**

Notes:

1. Values were obtained from Haley & Aldrich's PSHA using site-specific basin depth terms ($Z_{1.0}$ = 0.405 km and $Z_{2.5}$ = 1.85 km), as described in the report.
2. Risk coefficients based were obtained at each period using a Matlab routine provided to us by USGS.

Table 8 - Metadata of Selected Input Ground Motion for Impulsive Period (T = 0.2 sec)

Record ID	Earthquake	Recording Station	Magnitude	Distances (km)		V_{S30} (m/s)	Max. Useable Period[a,b] (s)	Fault Mechanism	Pulse-Like? (Period of Pulse in Seconds)	Component ID	Data Source & PEER ID Number	Scale Factor	Hanging Wall Indicators	$D_{5\text{-}95}$ (seconds)[c]		CAV (ft/s)[d]		Sources
				R_{rup}	R_{JB}									Estimated	Selected	Estimated	Selected	
1–1	Tohoku_Japan 2011	42308	9.1	91.8	78.8	411	66.0	Subduction - Interface	n.a.	NGAsubRSN4000113_904-NS.AT2	PEER NGA-Sub	2.22	n.a.	34 / 51 / 76	61	133 / 175 / 231	175	Cascadia Interface
1–2	Olympia_WA 1949	OLY0	6.7	47.6	0.8	399	2.7	Subduction - Intraslab	n.a.	NGAsubRSN2000001_OLY0086.AT2	PEER NGA-Sub	2.20	n.a.	12 / 19 / 30	17.2	50 / 68 / 93	85	Juan De-Fuca Intraslab
1–3	Pingtung.Doublet2 Taiwan 2006	KAU080	6.9	34.7	23.4	400	10.5	Subduction - Intraslab	n.a.	NGAsubRSN7006531_KAU080--E.AT2	PEER NGA-Sub	2.21	n.a.	12 / 19 / 30	10.2	50 / 68 / 93	58	Juan De-Fuca Intraslab
1–4	Chi-Chi_ Taiwan 1999	1197	7.6	3.1	3.1	543	6.7	Reverse Oblique (Dip 33°)	No	RSN1197_CHICHI_CHY028-N.AT2	PEER NGA-West2	0.68	FW	6 / 9 / 14	8.7	21 / 28 / 38	40	Portland Hills
1–5	Iwate_ Japan 2008	5478	6.9	17.0	11.7	556	8.0	Reverse (40° Dip)	No	RSN5478_IWATE_AKT023EW.AT2	PEER NGA-West2	1.51	HW	6 / 9 / 14	10.1	21 / 28 / 38	54	Gridded Seismicity Background

Notes:

a. Interface records were downloaded as corrected accelerograms from a preliminary subset of the NGA-Sub database. The maximum usable periods are documented by PEER.

b. Crustal records were downloaded as corrected accelerograms from the NGA-West2 database. The maximum usable periods are documented by PEER.

c. $D_{5\text{-}95}$ in column Model is the estimated (-1 Std.Dev / Mean / +1 Std. Dev) value using Bahrampouri et al. (2020) ground motion model and disaggreagtion resuls, $D_{5\text{-}95}$ in column Selected is the actual $D_{5\text{-}95}$ of the motion

d. CAV in column Estimated is the estimated (-1 Std.Dev / Mean / +1 Std. Dev) value using disaggregation results and Liu et al (2022) and Macedo et al. (2020) conditional ground motion for subduction and crustal sources, respectively. CAV in column Selected is the actual CAV of the motion

Table 9 - Metadata of Selected Input Ground Motion for Convective Period (T = 7.5 sec)

Record ID	Earthquake	Recording Station	Magnitude	Distances (km)		V_{S30} (m/s)	Max. Useable Period[a,b] (s)	Fault Mechanism	Pulse-Like? (Period of Pulse in Seconds)	Component ID	Data Source & PEER ID Number	Scale Factor	Hanging Wall Indicators	$D_{5\text{-}95}$ (seconds)[c]		CAV (ft/s)[d]		Sources
				R_{rup}	R_{JB}									Estimated	Selected	Estimated	Selected	
1–1	Tohoku_Japan 2011	41314	9.1	107.8	96.9	257	127.5	Subduction - Interface	n.a.	NGAsubRSN4000035_522-NS.AT2	PEER NGA-Sub	2.03	n.a.	33 / 50 / 74	141	127 / 168 / 222	114	Cascadia Interface
1–2	Tohoku_Japan 2011	41319	9.1	124.5	115.2	270	52.1	Subduction - Interface	n.a.	NGAsubRSN4000040_527-NS.AT2	PEER NGA-Sub	2.44	n.a.	33 / 50 / 74	95.1	127 / 168 / 222	159	Cascadia Interface
1–3	2010 Chile	STL	8.8	123.7	113.1	1411	23.3	Subduction - Interface	n.a.	NGAsubRSN6001803_SLUC090.AT2	PEER NGA-Sub	1.56	n.a.	33 / 50 / 74	37.7	127 / 168 / 222	136	Cascadia Interface
1–4	2010 Chile	MET	8.8	121.9	111.1	598	40.4	Subduction - Interface	n.a.	NGAsubRSN6001811_MET-EW.AT2	PEER NGA-Sub	2.89	n.a.	33 / 50 / 74	41.7	127 / 168 / 222	207	Cascadia Interface
1–5	Darfield_NZ 2010	CBGS	7.0	18.0	18.0	187	20.0	Strike-Slip	Yes (12.621)	RSN6887_DARFIELD_CBGSS01W.AT2	PEER NGA-West2	0.71	n.a.	6 / 9.7 / 16	28.5	30 / 41 / 56	26	Gridded Seismicity Background

Notes:

a. Interface records were downloaded as corrected accelerograms from a preliminary subset of the NGA-Sub database. The maximum usable periods are documented by PEER.

b. Crustal records were downloaded as corrected accelerograms from the NGA-West2 database. The maximum usable periods are documented by PEER.

c. $D_{5\text{-}95}$ in column Estimated is the estimated (-1 Std.Dev / Mean / +1 Std. Dev) value using Bahrampouri et al. (2020) ground motion model and disaggreagtion resuls, $D_{5\text{-}95}$ in column Selected is the actual $D_{5\text{-}95}$ of the motion

d. CAV in column Estimated is the estimated (-1 Std.Dev / Mean / +1 Std. Dev) value using Liu et al (2022) and Macedo et al. (2020) conditional ground motion for subduction and crustal sources, respectively. CAV in column Selected is the actual CAV of the motion

APPENDIX A
Boring Logs

Sample Description

Identification of soils in this report is based on visual field and laboratory observations which include density/consistency, moisture condition, grain size, and plasticity estimates and should not be construed to imply field nor laboratory testing unless presented herein. ASTM D 2488 visual-manual identification methods were used as a guide. Where laboratory testing confirmed visual-manual identifications, then ASTM D 2487 was used to classify the soils.

Relative Density/Consistency

Soil density/consistency in borings is related primarily to the standard penetration resistance (N). Soil density/consistency in test pits and probes is estimated based on visual observation and is presented parenthetically on the logs.

SAND or GRAVEL Relative Density	N (Blows/Foot)	SILT or CLAY Consistency	N (Blows/Foot)
Very loose	0 to 4	Very soft	0 to 1
Loose	5 to 10	Soft	2 to 4
Medium dense	11 to 30	Medium stiff	5 to 8
Dense	31 to 50	Stiff	9 to 15
Very dense	>50	Very stiff	16 to 30
		Hard	>30

Moisture

Dry	Absence of moisture, dusty, dry to the touch
Moist	Damp but no visible water
Wet	Visible free water, usually soil is below water table

USCS Soil Classification Chart (ASTM D 2487)

Major Divisions			Symbols: Graph	Symbols: USCS	Typical Descriptions
Coarse Grained Soils More than 50% of Material Retained on No. 200 Sieve	Gravel and Gravelly Soils More than 50% of Coarse Fraction Retained on No. 4 Sieve	Clean Gravels *(<5% fines)*		GW	Well-Graded Gravel; Well-Graded Gravel with Sand
				GP	Poorly Graded Gravel; Poorly Graded Gravel with Sand
		Gravels *(5-12% fines)*		GW-GM	Well-Graded Gravel with Silt; Well-Graded Gravel with Silt and Sand
				GW-GC	Well-Graded Gravel with Clay; Well-Graded Gravel with Clay and Sand
				GP-GM	Poorly Graded Gravel with Silt; Poorly Graded Gravel with Silt and Sand
				GP-GC	Poorly Graded Gravel with Clay; Poorly Graded Gravel with Clay and Sand
		Gravels with Fines *(>12% fines)*		GM	Silty Gravel; Silty Gravel with Sand
				GC	Clayey Gravel; Clayey Gravel with Sand
	Sand and Sandy Soils More than 50% of Coarse Fraction Passing No. 4 Sieve	Sands with few Fines *(<5% fines)*		SW	Well-Graded Sand; Well-Graded Sand with Gravel
				SP	Poorly Graded Sand; Poorly Graded Sand with Gravel
		Sands *(5-12% fines)*		SW-SM	Well-Graded Sand with Silt Well-Graded Sand with Silt and Gravel
				SW-SC	Well-Graded Sand with Clay; Well-Graded Sand with Clay and Gravel
				SP-SM	Poorly Graded Sand with Silt; Poorly Graded Sand with Silt and Gravel
				SP-SC	Poorly Graded Sand with Clay; Poorly Graded Sand with Clay and Gravel
		Sands with Fines *(>12% fines)*		SM	Silty Sand; Silty Sand with Gravel
				SC	Clayey Sand; Clayey Sand with Gravel
Fine Grained Soils More than 50% of Material Passing No. 200 Sieve	Silts			ML	Silt; Silt with Sand or Gravel; Sandy or Gravelly Silt
				MH	Elastic Silt; Elastic Silt with Sand or Gravel; Sandy or Gravelly Elastic Silt
	Silty Clay *(based on Atterberg Limits)*			CL-ML	Silty Clay; Silty Clay with Sand or Gravel; Gravelly or Sandy Silty Clay
	Clays			CL	Lean Clay; Lean Clay with Sand or Gravel; Sandy or Gravelly Lean Clay
				CH	Fat Clay; Fat Clay with Sand or Gravel; Sandy or Gravelly Fat Clay
	Organics			OL/OH	Organic Soil; Organic Soil with Sand or Gravel; Sandy or Gravelly Organic Soil
Highly Organic *(>50% organic material)*				PT	Peat - Decomposing Vegetation - Fibrous to Amorphous Texture

Minor Constituents

	Estimated Percentage
Sand, Gravel	
Trace	<5
Few	5 - 15
Cobbles, Boulders	
Trace	<5
Few	5 - 10
Little	15 - 25
Some	30 - 45

Soil Test Symbols

%F	Percent Passing No. 200 Sieve
AL	Atterberg Limits (%)
	Liquid Limit (LL)
	Water Content (WC)
	Plastic Limit (PL)
CA	Chemical Analysis
CAUC	Consolidated Anisotropic Undrained Compression
CAUE	Consolidated Anisotropic Undrained Extension
CBR	California Bearing Ratio
CIDC	Consolidated Drained Isotropic Triaxial Compression
CIUC	Consolidated Isotropic Undrained Compression
CK0DC	Consolidated Drained k0 Triaxial Compression
CK0DSS	Consolidated k0 Undrained Direct Simple Shear
CK0UC	Consolidated k0 Undrained Compression
CK0UE	Consolidated k0 Undrained Extension
CRSCN	Constant Rate of Strain Consolidation
DSS	Direct Simple Shear
DT	In Situ Density
GS	Grain Size Classification
HYD	Hydrometer
ILCN	Incremental Load Consolidation
K0CN	k0 Consolidation
kc	Constant Head Permeability
kf	Falling Head Permeability
MD	Moisture Density Relationship
OC	Organic Content
OT	Tests by Others
P	Pressuremeter
PID	Photoionization Detector Reading
PP	Pocket Penetrometer
SG	Specific Gravity
TRS	Torsional Ring Shear
TV	Torvane
UC	Unconfined Compression
UUC	Unconsolidated Undrained Triaxial Compression
VS	Vane Shear
WC	Water Content (%)

Groundwater Indicators

- Groundwater Level on Date or At Time of Drilling (ATD)
- Groundwater Level on Date Measured in Piezometer
- Groundwater Seepage (Test Pits)

Sample Symbols

1.5" I.D. Split Spoon	Rock Core Run	Grab
3.25" O.D. Split Spoon	Sonic Core	Cuttings
Modified California Sampler	Shelby Tube/Push Probe/GeoProbe®	

Well Symbols

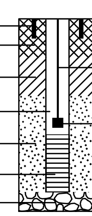

HARTCROWSER

Project: PDX Fueling Facility Improvements
Location: Portland, Oregon
Project No.: 154-118-001

Key to Exploration Logs

Figure **A-1**
Sheet **1 of 1**

Date Started: 6/27/19	Date Completed: 6/27/19
Logged by: D. Knapp	Checked by: T. Anderson
Location: Lat: 45.596739 Long: -122.612754	
Ground Surface Elevation: 6.5 feet	
Horizontal Datum: WGS 84	
Vertical Datum: NAVD 88	
Comments: Location and ground surface elevations are approximate.	

Drilling Contractor/Crew: Western States Soil Conservation, Inc. / Lucas	
Drilling Method: Mud Rotary/Hollow Stem Auger	
Rig Model/Type: GeoProbe® 7822DT / Track-mounted push-probe rig	
Hammer Type: Auto-hammer	
Hammer Weight (pounds): 140	Hammer Drop Height (inches): 30
Measured Hammer Efficiency (%): 91	
Hole Diameter:	Casing Diameter: NA
Total Depth: 86.5 feet	Depth to Groundwater: 14 feet

Material Description

Depth (feet)	Elevation (feet)	Material Description
0	6.5	Topsoil (2-inches grass, 10-inches roots/topsoil)
1	5.5	SILTY SAND (SM), medium dense, brown, moist, fine to medium sand, homogenous, no layering. [FILL]
4	2.5	POORLY GRADED SAND WITH SILT (SP-SM), loose, brown, wet, fine to medium sand. caving observed 4-7 feet bgs
7.5	-1	ELASTIC SILT (MH), trace fine sand, very soft, gray-brown/brown mottled, moist, mild organic odor, numerous organic and woody debris. [OVERBANK DEPOSITS]
10		grades to moist to wet
15		grades to wet, fine to medium sand, laminated to stratified silt and sand seams and layers, micaceous, trace organic debris
20		grades to gray/gray-green mottled
30	-23.5	SILT (ML), trace fine sand, very soft, gray-brown/green mottled, moist to wet, low to medium plasticity, micaceous, trace to numerous organic and woody debris.

Water Level: ATD at 14 feet

Sample Data

Depth (feet)	Blow Count	Recovery	Length (inches)	Number / Tests	SPT N Value	WC (%)
8	0 0 0	12in.	18	S-1 AL, WC	0	82.5
10.5	0 0 0	18in.	18	S-2 WC	0	71.7
13		7in.	24	S-3 DT, CN, MD, WC		
15.5	0 0 0	18in.	18	S-4 AL, WC	0	59.1
20.5	0 0 0	16in.	18	S-5 WC	0	
25.5	0 0 0	18in.	18	S-6 WC	0	
30.5	0 0 0	18in.	18	S-7 AL, WC	0	55.3
33	0 0 0	2in.	24	S-8	0	
35.5	0 0 0	18in.	18	S-9 WC	0	58.3

Legend: PL — WC (%) — LL; ✖ Fines Content (%); ▲ SPT N Value

General Notes:
1. Refer to Figure A-1 for explanation of descriptions and symbols.
2. Material descriptions and stratum lines are interpretive and actual changes may be gradual. Solid stratum lines indicate distinct contact between material strata or geologic units. Dashed stratum lines indicate gradual or approximate change between material strata or geologic units.
3. USCS designations are based on visual-manual identification (ASTM D 2488) unless otherwise supported by laboratory testing (ASTM D 2487).
4. Groundwater level, if indicated, is at time of drilling/excavation (ATD) or for date specified. Level may vary with time.

Date Started: 6/27/19	Date Completed: 6/27/19
Logged by: D. Knapp	Checked by: T. Anderson
Location: Lat: 45.596739 Long: -122.612754	
Ground Surface Elevation: 6.5 feet	
Horizontal Datum: WGS 84	
Vertical Datum: NAVD 88	
Comments: Location and ground surface elevations are approximate.	
Drilling Contractor/Crew: Western States Soil Conservation, Inc. / Lucas	
Drilling Method: Mud Rotary/Hollow Stem Auger	
Rig Model/Type: GeoProbe® 7822DT / Track-mounted push-probe rig	
Hammer Type: Auto-hammer	
Hammer Weight (pounds): 140	Hammer Drop Height (inches): 30
Measured Hammer Efficiency (%): 91	
Hole Diameter:	Casing Diameter: NA
Total Depth: 86.5 feet	Depth to Groundwater: 14 feet

Depth (feet)	Blow Count	Recovery	Length (inches)	Number / Tests	Material Description	SPT N Value	Fines Content (%)
40	0 0 0	18in.	18	S-10 / WC	SILT (ML), trace fine sand, very soft, gray-brown/green mottled, moist to wet, low to medium plasticity, micaceous, trace to numerous organic and woody debris. *(continued)* numerous fine to coarse sand lenses and layers, blocky, trace clay	0	
45	5 5 4	12in.	18	S-11 / WC	POORLY GRADED SAND WITH SILT (SP-SM), loose, gray, wet, fine to medium sand, rapid dilatancy, micaceous, quartz-rich. [COLUMBIA RIVER SAND AQUIFER]	9	
50	8 9 10	11in.	18	S-12 / GS, WC	grades to medium dense	19	6
55	4 6 7	10in.	18	S-13 / WC		13	
60	5 6 8	12in.	18	S-14 / WC		14	
65	6 8 9	9in.	18	S-15 / WC		17	
70	5 8 9	10in.	18	S-16 / WC		17	
75	8 7 11	12in.	18	S-17 / WC	increase in silt content	18	

Elevation (feet): -35, -40, -45, -50, -55, -60, -65, -70

Legend: PL — WC (%) — LL; ✖ Fines Content (%); ▲ SPT N Value; scale 10, 20, 30, 40

General Notes:
1. Refer to Figure A-1 for explanation of descriptions and symbols.
2. Material descriptions and stratum lines are interpretive and actual changes may be gradual. Solid stratum lines indicate distinct contact between material strata or geologic units. Dashed stratum lines indicate gradual or approximate change between material strata or geologic units.
3. USCS designations are based on visual-manual identification (ASTM D 2488) unless otherwise supported by laboratory testing (ASTM D 2487).
4. Groundwater level, if indicated, is at time of drilling/excavation (ATD) or for date specified. Level may vary with time.

Date Started: 6/27/19	Date Completed: 6/27/19	Drilling Contractor/Crew: Western States Soil Conservation, Inc. / Lucas	
Logged by: D. Knapp	Checked by: T. Anderson	Drilling Method: Mud Rotary/Hollow Stem Auger	
Location: Lat: 45.596739 Long: -122.612754		Rig Model/Type: GeoProbe® 7822DT / Track-mounted push-probe rig	
Ground Surface Elevation: 6.5 feet		Hammer Type: Auto-hammer	
Horizontal Datum: WGS 84		Hammer Weight (pounds): 140	Hammer Drop Height (inches): 30
Vertical Datum: NAVD 88		Measured Hammer Efficiency (%): 91	
Comments: Location and ground surface elevations are approximate.		Hole Diameter:	Casing Diameter: NA
		Total Depth: 86.5 feet	Depth to Groundwater: 14 feet

Elevation (feet)	Depth (feet)	Blow Count	Type	Recovery	Length (inches)	Number / Tests	Graphic Log	Material Description	Water Level	PL — WC (%) — LL; ✖ Fines Content (%); ▲ SPT N Value (10, 20, 30, 40)	Depth (feet)
	80	4 8 13		13in.	18	S-18		POORLY GRADED SAND WITH SILT (SP-SM), medium dense, gray, wet, fine to medium sand, rapid dilatancy, micaceous, quartz-rich. [COLUMBIA RIVER SAND AQUIFER]		▲ 21	80
-75											
	85	8 11 13		12in.	18	S-19 / WC				▲ 24, ●	85
-80								Bottom of Borehole at 86.5 feet.			
	90										90
-85											
	95										95
-90											
	100										100
-95											
	105										105
-100											
	110										110
-105											
	115										115
-110											

General Notes:
1. Refer to Figure A-1 for explanation of descriptions and symbols.
2. Material descriptions and stratum lines are interpretive and actual changes may be gradual. Solid stratum lines indicate distinct contact between material strata or geologic units. Dashed stratum lines indicate gradual or approximate change between material strata or geologic units.
3. USCS designations are based on visual-manual identification (ASTM D 2488) unless otherwise supported by laboratory testing (ASTM D 2487).
4. Groundwater level, if indicated, is at time of drilling/excavation (ATD) or for date specified. Level may vary with time.

Date Started: 03/02/2023	Date Completed: 03/03/2023	Drilling Contractor/Crew: Western States Soil Conservation, Inc. / Shane, Alfredo, Chaz	
Logged by: DCH	Checked by:	Drilling Method: Mud Rotary/ Push Probe	
Location: Lat: 45.597583 Long: -122.613906 (WGS 84)		Rig Model/Type: CME-55 / Track-mounted drill rig	
Ground Surface Elevation: 19.53 feet (NAVD 88)		Hammer Type: Auto-hammer	
Comments:		Hammer Weight (pounds): 140	Hammer Drop Height (inches): 30
		Measured Hammer Efficiency (%): Not Available	
		Hole Diameter: 4.875 inches	Well Casing Diameter: NA
		Total Depth: 151.5 feet	Depth to Groundwater: 5 feet

Elevation (feet)	Depth (feet)	Blow Count	Recovery	Length (inches)	Number / Tests	Material Description	Water Level	PL / WC (%) / LL; Fines Content (%); SPT N Value
	0					topsoil (3-inch thick)		
						vacuum excavated to 6 ft. bgs.		
15	5						⊲ 2/28/2023	
						SILT (ML), very soft, wet, gray, micaceous.		
			19.5in.	24	U-1 / PP, TV	(PP = 0.0 tsf, TV = 0.175 tsf)		
			20in.	24	U-2 / PP, TV	grades to mottled with gray-brown and iron-oxide staining (PP = 0.0 tsf, TV = 0.2 tsf)		
10	10		21.5in.	24	U-3 / PP, TV	grades to soft (PP = 0.5 tsf, TV = 0.325 tsf)		
			22.5in.	24	U-4 / PP, TV	grades to no iron-oxide staining (PP = 0.5 tsf, TV = 0.25 tsf)		
5	15		24in.	24	U-5 / PP, TV	grades to medium stiff (PP = 0.75 tsf, TV = 0.25 tsf)		
			23in.	24	U-6 / PP, TV	(PP = 0.5 tsf, TV = 0.225 tsf)		
0	20							
			15in.	24	U-7			
-5	25							
			19.5in.	24	U-8 / PP	(PP = 0.5 tsf)		
-10	30					POORLY GRADED SAND (SP), loose to medium dense, wet, gray, mostly fine sand, micaceous.		
			18in.	24	U-9			
-15	35							
			22.5in.	24	U-10 / GS, WC			47
-20								

General Notes:
1. Refer to Figure A-1 for explanation of descriptions and symbols.
2. Material stratum lines are interpretive and actual changes may be gradual. Solid lines indicate distinct contacts and dashed lines indicate gradual or approximate contacts.
3. USCS designations are based on visual-manual identification (ASTM D 2488), unless otherwise supported by laboratory testing (ASTM D 2487).
4. Groundwater level, if indicated, is at time of drilling/excavation (ATD) or for date specified. Level may vary with time.
5. Location and ground surface elevations are approximate.

Date Started: 03/02/2023	Date Completed: 03/03/2023
Logged by: DCH	Checked by:
Location: Lat: 45.597583 Long: -122.613906 (WGS 84)	
Ground Surface Elevation: 19.53 feet (NAVD 88)	
Comments:	

Drilling Contractor/Crew: Western States Soil Conservation, Inc. / Shane, Alfredo, Chaz	
Drilling Method: Mud Rotary/ Push Probe	
Rig Model/Type: CME-55 / Track-mounted drill rig	
Hammer Type: Auto-hammer	
Hammer Weight (pounds): 140	Hammer Drop Height (inches): 30
Measured Hammer Efficiency (%): Not Available	
Hole Diameter: 4.875 inches	Well Casing Diameter: NA
Total Depth: 151.5 feet	Depth to Groundwater: 5 feet

Elevation (feet)	Depth (feet)	Blow Count	Type	Recovery	Length (inches)	Number / Tests	Graphic Log	Material Description	Water Level	PL / WC (%) / LL; Fines Content (%); SPT N Value
	40							POORLY GRADED SAND (SP), loose to medium dense, wet, gray, mostly fine sand, micaceous. *(continued)*		
				14in.	24	U-11 / PP, TV		(PP = 0.75 tsf, TV = 0.15 tsf) layer of silt observed at 41.2 ft (0.079-inch thick), material is likely interbedded		
-25	45							flowing water observed in sand in hole		
				17in.	24	U-12 / AL, GS, WC				95; 53.7
-30	50			8in.	24	U-13 / PP		(PP = 1.5 tsf)		
		2 4 6		13in.	18	S-1 / GS, WC		frequent silt lamination througout sample, trace coarse sand		23; 10
-35	55							grades to medium dense		
				2.5in.	24	U-14				
-40	60	7 10 11		12in.	18	S-2		grades to no silt lamination, coarse sand		21
-45	65	6 9 11		10in.	18	S-3				20
-50	70	6 11 15		10in.	18	S-4 / WC				26
-55	75	6 9 12		11in.	18	S-5				21
-60										

General Notes:
1. Refer to Figure A-1 for explanation of descriptions and symbols.
2. Material stratum lines are interpretive and actual changes may be gradual. Solid lines indicate distinct contacts and dashed lines indicate gradual or approximate contacts.
3. USCS designations are based on visual-manual identification (ASTM D 2488), unless otherwise supported by laboratory testing (ASTM D 2487).
4. Groundwater level, if indicated, is at time of drilling/excavation (ATD) or for date specified. Level may vary with time.
5. Location and ground surface elevations are approximate.

Date Started: 03/02/2023	Date Completed: 03/03/2023
Logged by: DCH	Checked by:
Location: Lat: 45.597583 Long: -122.613906 (WGS 84)	
Ground Surface Elevation: 19.53 feet (NAVD 88)	
Comments:	

Drilling Contractor/Crew: Western States Soil Conservation, Inc. / Shane, Alfredo, Chaz	
Drilling Method: Mud Rotary/ Push Probe	
Rig Model/Type: CME-55 / Track-mounted drill rig	
Hammer Type: Auto-hammer	
Hammer Weight (pounds): 140	Hammer Drop Height (inches): 30
Measured Hammer Efficiency (%): Not Available	
Hole Diameter: 4.875 inches	Well Casing Diameter: NA
Total Depth: 151.5 feet	Depth to Groundwater: 5 feet

Elevation (feet)	Depth (feet)	Sample Data: Blow Count	Type	Recovery	Length (inches)	Number / Tests	Graphic Log	Material Description	Water Level	SPT N Value	Depth (feet)
	80	7 10 12	X	10in.	18	S-6a S-6b WC		POORLY GRADED SAND (SP), loose to medium dense, wet, gray, mostly fine sand, micaceous. *(continued)* layer of silty sand observed (approximately 3-inch thick)		22	80
-65	85	9 11 14	X	12in.	18	S-7				25	85
-70	90	9 14 16	X	12in.	18	S-8 WC				30	90
-75	95	14 20 20	X	13in.	18	S-9		grades to dense		40	95
-80	100	7 9 13	X	8in.	18	S-10		grades to medium dense		22	100
-85	105										105
-90	110	9 16 19	X	11in.	18	S-11 WC		grades to dense		35	110
-95	115										115
-100											

Chart legend: PL — WC (%) — LL; ✖ Fines Content (%); ▲ SPT N Value; scale 10 20 30 40

General Notes:
1. Refer to Figure A-1 for explanation of descriptions and symbols.
2. Material stratum lines are interpretive and actual changes may be gradual. Solid lines indicate distinct contacts and dashed lines indicate gradual or approximate contacts.
3. USCS designations are based on visual-manual identification (ASTM D 2488), unless otherwise supported by laboratory testing (ASTM D 2487).
4. Groundwater level, if indicated, is at time of drilling/excavation (ATD) or for date specified. Level may vary with time.
5. Location and ground surface elevations are approximate.

Date Started: 03/02/2023 | Date Completed: 03/03/2023
Logged by: DCH | Checked by:
Location: Lat: 45.597583 Long: -122.613906 (WGS 84)
Ground Surface Elevation: 19.53 feet (NAVD 88)
Comments:

Drilling Contractor/Crew: Western States Soil Conservation, Inc. / Shane, Alfredo, Chaz
Drilling Method: Mud Rotary/ Push Probe
Rig Model/Type: CME-55 / Track-mounted drill rig
Hammer Type: Auto-hammer
Hammer Weight (pounds): 140 | Hammer Drop Height (inches): 30
Measured Hammer Efficiency (%): Not Available
Hole Diameter: 4.875 inches | Well Casing Diameter: NA
Total Depth: 151.5 feet | Depth to Groundwater: 5 feet

Elevation (feet)	Depth (feet)	Blow Count	Type	Recovery	Length (inches)	Number / Tests	Graphic Log	Material Description	Water Level	PL / WC (%) / LL; Fines Content (%); SPT N Value
	120	10 15 18		9in.	18	S-12		POORLY GRADED SAND (SP), loose to medium dense, wet, gray, mostly fine sand, micaceous. *(continued)* occasional laminations of medium white sand		SPT N = 33
-105	125									
-110	130	10 14 17		10in.	18	S-13 / WC				SPT N = 31; WC
-115	135									
-120	140	13 20 23		15in.	18	S-14				SPT N = 43
-125	145									
-130	150	11 14 17		9in.	18	S-15				SPT N = 31
								Bottom of Borehole at 151.5 feet.		
-135	155									
-140										

Plot scale: 10, 20, 30, 40

General Notes:
1. Refer to Figure A-1 for explanation of descriptions and symbols.
2. Material stratum lines are interpretive and actual changes may be gradual. Solid lines indicate distinct contacts and dashed lines indicate gradual or approximate contacts.
3. USCS designations are based on visual-manual identification (ASTM D 2488), unless otherwise supported by laboratory testing (ASTM D 2487).
4. Groundwater level, if indicated, is at time of drilling/excavation (ATD) or for date specified. Level may vary with time.
5. Location and ground surface elevations are approximate.

Date Started: 02/28/2023	Date Completed: 03/02/2023
Logged by: DCH	Checked by:
Location: Lat: 45.596374 Long: -122.613728 (WGS 84)	
Ground Surface Elevation: 21.21 feet (NAVD 88)	
Comments:	

Drilling Contractor/Crew: Western States Soil Conservation, Inc. / Shane, Alfredo, Chaz	
Drilling Method: Mud Rotary/ Push Probe	
Rig Model/Type: CME-55 / Track-mounted drill rig	
Hammer Type: Auto-hammer	
Hammer Weight (pounds): 140	Hammer Drop Height (inches): 30
Measured Hammer Efficiency (%): Not Available	
Hole Diameter: 4.875 inches	Well Casing Diameter: NA
Total Depth: 151.5 feet	Depth to Groundwater: 5 feet

Sample Data

Elevation (feet)	Depth (feet)	Blow Count	Type	Recovery	Length (inches)	Number Tests	Material Description	Water Level
21.21	0						topsoil (3-inch thick)	
							vacuum excavated to 6 ft. bgs.	
	5							∇ 2/28/2023
15	6						SILT (ML), soft, moist to wet, gray.	
				0in.	24	U-1		
							(PP = 0.75 tsf, TV = 0.15 tsf)	
				24in.	24	U-2 PP, TV		
10	10						wood observed in cuttings from 10 to 12 ft.	
							(PP = 0.35 tsf, TV = 0.75 tsf)	
				24in.	24	U-3 PP, TV		
				0in.	24	U-4		
							(PP = 0.2 tsf, TV = 0.5 tsf)	
5	15			24in.	24	U-5 PP, TV		
0	20						(PP = 0.35 tsf, TV = 0.75 tsf)	
				22.5in.	24	U-6 PP, TV		
							layer of SAND WITH SILT (0.079-inch thick), material is likely interbedded	
-5	25						(PP = 1.0 tsf, TV = 0.15 tsf)	
				20in.	24	U-7 PP, TV		
-10	30						(PP = 1.5 tsf, TV = 0.3 tsf)	
				23.5in.	24	U-8 PP, TV		
							grades to mottled with gray and brown iron-oxide staining	
-15	35						grades to no iron-oxide staining	
							(PP = 0.75 tsf, TV = 0.15 tsf)	
				24in.	24	U-9 PP, TV		

WC (%) ●
✖ Fines Content (%)
▲ SPT N Value
10 20 30 40

Depth (feet): 0, 5, 10, 15, 20, 25, 30, 35

General Notes:
1. Refer to Figure A-1 for explanation of descriptions and symbols.
2. Material stratum lines are interpretive and actual changes may be gradual. Solid lines indicate distinct contacts and dashed lines indicate gradual or approximate contacts.
3. USCS designations are based on visual-manual identification (ASTM D 2488), unless otherwise supported by laboratory testing (ASTM D 2487).
4. Groundwater level, if indicated, is at time of drilling/excavation (ATD) or for date specified. Level may vary with time.
5. Location and ground surface elevations are approximate.

Date Started: 02/28/2023 | Date Completed: 03/02/2023 | Drilling Contractor/Crew: Western States Soil Conservation, Inc. / Shane, Alfredo, Chaz
Logged by: DCH | Checked by: | Drilling Method: Mud Rotary/ Push Probe
Location: Lat: 45.596374 Long: -122.613728 (WGS 84) | Rig Model/Type: CME-55 / Track-mounted drill rig
Ground Surface Elevation: 21.21 feet (NAVD 88) | Hammer Type: Auto-hammer
Comments: | Hammer Weight (pounds): 140 | Hammer Drop Height (inches): 30
Measured Hammer Efficiency (%): Not Available
Hole Diameter: 4.875 inches | Well Casing Diameter: NA
Total Depth: 151.5 feet | Depth to Groundwater: 5 feet

Elevation (feet)	Depth (feet)	Blow Count	Type	Recovery	Length (inches)	Number / Tests	Material Description
-18.8	40						SILT (ML), soft, moist to wet, gray. *(continued)*
-19.8	41		Shelby	24in.	24	U-10 / GS, WC	POORLY GRADED SAND WITH SILT (SP-SM), medium dense, wet, gray, fine sand, micaceous.
	45		Shelby	0in.	24	U-11	
	47		Shelby	5in.	24	U-12	
	49	1 6 12	SPT	15in.	18	S-1 / GS, WC	
-33.8	55	0 0 0	SPT	9in.	18	S-2	SILT (ML), soft, moist to wet, gray.
-35.8	57		Shelby	12in.	24	U-13	POORLY GRADED SAND WITH SILT (SP-SM), medium dense, wet, gray, fine sand, micaceous.
	60		Shelby	7in.	24	U-14	
	65	5 9 11	SPT	8in.	18	S-3 / WC	
	69						wood observed in cuttings from 69 to 70 ft.
	71		Shelby	8in.	24	U-15	
	75	7 11 12	SPT	8in.	18	S-4	

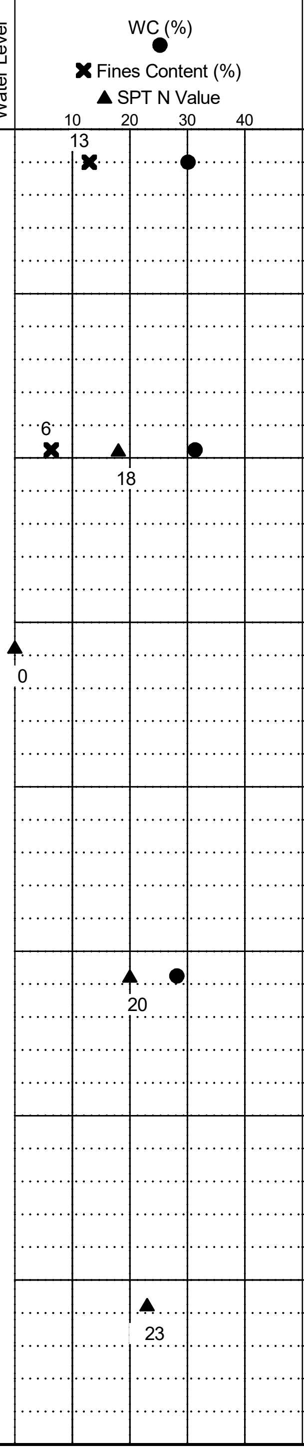

General Notes:
1. Refer to Figure A-1 for explanation of descriptions and symbols.
2. Material stratum lines are interpretive and actual changes may be gradual. Solid lines indicate distinct contacts and dashed lines indicate gradual or approximate contacts.
3. USCS designations are based on visual-manual identification (ASTM D 2488), unless otherwise supported by laboratory testing (ASTM D 2487).
4. Groundwater level, if indicated, is at time of drilling/excavation (ATD) or for date specified. Level may vary with time.
5. Location and ground surface elevations are approximate.

HALEY ALDRICH

Project: PDX Fuel Project Tank Design
Location: Portland, Oregon
Project No.: 0204679-001

Push Probe Log
B-2

Figure **A**

Date Started: 02/28/2023	Date Completed: 03/02/2023	Drilling Contractor/Crew: Western States Soil Conservation, Inc. / Shane, Alfredo, Chaz	
Logged by: DCH	Checked by:	Drilling Method: Mud Rotary/ Push Probe	
Location: Lat: 45.596374 Long: -122.613728 (WGS 84)		Rig Model/Type: CME-55 / Track-mounted drill rig	
Ground Surface Elevation: 21.21 feet (NAVD 88)		Hammer Type: Auto-hammer	
Comments:		Hammer Weight (pounds): 140	Hammer Drop Height (inches): 30
		Measured Hammer Efficiency (%): Not Available	
		Hole Diameter: 4.875 inches	Well Casing Diameter: NA
		Total Depth: 151.5 feet	Depth to Groundwater: 5 feet

Elevation (feet)	Depth (feet)	Blow Count	Type	Recovery	Length (inches)	Number / Tests	Material Description	WC (%) ● / Fines Content (%) ✖ / SPT N Value ▲
-60	80	8 12 13	⊠	9in.	18	S-5 / WC	POORLY GRADED SAND WITH SILT (SP-SM), medium dense, wet, gray, fine sand, micaceous. *(continued)*	25
-65	85	8 15 17	⊠	9in.	18	S-6	grades to dense	32
-70	90	7 11 16	⊠	9in.	18	S-7 / GS, WC	grades to medium dense	6 ✖; 27
-75	95	11 12 9	⊠	9in.	18	S-8		21
-80	100	9 17 19	⊠	9in.	18	S-9 / WC	grades to dense	36
-85	105							
-90	110	8 11 16	⊠	9in.	18	S-10	grades to medium dense	27
-95	115							

General Notes:
1. Refer to Figure A-1 for explanation of descriptions and symbols.
2. Material stratum lines are interpretive and actual changes may be gradual. Solid lines indicate distinct contacts and dashed lines indicate gradual or approximate contacts.
3. USCS designations are based on visual-manual identification (ASTM D 2488), unless otherwise supported by laboratory testing (ASTM D 2487).
4. Groundwater level, if indicated, is at time of drilling/excavation (ATD) or for date specified. Level may vary with time.
5. Location and ground surface elevations are approximate.

Date Started: 02/28/2023	Date Completed: 03/02/2023	Drilling Contractor/Crew: Western States Soil Conservation, Inc. / Shane, Alfredo, Chaz	
Logged by: DCH	Checked by:	Drilling Method: Mud Rotary/ Push Probe	
Location: Lat: 45.596374 Long: -122.613728 (WGS 84)		Rig Model/Type: CME-55 / Track-mounted drill rig	
Ground Surface Elevation: 21.21 feet (NAVD 88)		Hammer Type: Auto-hammer	
Comments:		Hammer Weight (pounds): 140	Hammer Drop Height (inches): 30
		Measured Hammer Efficiency (%): Not Available	
		Hole Diameter: 4.875 inches	Well Casing Diameter: NA
		Total Depth: 151.5 feet	Depth to Groundwater: 5 feet

Elevation (feet)	Depth (feet)	Sample Data: Blow Count	Type	Recovery	Length (inches)	Number / Tests	Graphic Log	Material Description	Water Level	WC (%) ● / Fines Content (%) ✖ / SPT N Value ▲
-100	120	13 15 21	⊠	9in.	18	S-11 / WC		POORLY GRADED SAND WITH SILT (SP-SM), medium dense, wet, gray, fine sand, micaceous. *(continued)* grades to dense		● ▲ 36
-105	125									
-110	130	8 9 12	⊠	9in.	18	S-12		grades to medium dense		▲ 21
-115	135									
-120	140	19 23 25	⊠	9in.	18	S-13 / WC		grades to dense		● ▲ 48
-125	145									
-130	150	16 19 18	⊠	10in.	18	S-14				▲ 37
								Bottom of Borehole at 151.5 feet.		
-135	155									

General Notes:
1. Refer to Figure A-1 for explanation of descriptions and symbols.
2. Material stratum lines are interpretive and actual changes may be gradual. Solid lines indicate distinct contacts and dashed lines indicate gradual or approximate contacts.
3. USCS designations are based on visual-manual identification (ASTM D 2488), unless otherwise supported by laboratory testing (ASTM D 2487).
4. Groundwater level, if indicated, is at time of drilling/excavation (ATD) or for date specified. Level may vary with time.
5. Location and ground surface elevations are approximate.

Date Started: 03/09/2023 Date Completed: 03/09/2023 Contractor/Crew:
Logged by: Checked by: Rig Model/Type: Backhoe
Location: Lat: 45.596585 Long: -122.612579 (WGS 84) Total Depth: 3.5 feet Depth to Seepage: Not Encountered
Ground Surface Elevation: 20.97 feet (NAVD 88)
Comments: Single ring falling head infiltration test conducted from 1050 to 1200.

Elevation (feet)	Depth (feet)	Sample Data: Type	Sample Data: Length (inches)	Sample Data: Number / Tests	Graphic Log	Material Description	Depth (feet)
	0					topsoil (2-inch thick)	0
20						SILTY SAND (SM), (medium dense), moist, gray-brown. [NATIVE]	
						POORLY GRADED SAND WITH SILT (SP), (medium dense), moist, gray, mostly fine to medium sand.	
		⊠		G-1			
						Bottom of Test Pit at 3.5 feet.	
	5						5
15							
	10						10
10							
	15						15
5							
	20						20
0							
	25						25
-5							
	30						30
-10							
	35						35
-15							

General Notes:
1. Refer to Figure A-1 for explanation of descriptions and symbols.
2. Material stratum lines are interpretive and actual changes may be gradual. Solid lines indicate distinct contacts and dashed lines indicate gradual or approximate contacts.
3. USCS designations are based on visual-manual identification (ASTM D 2488), unless otherwise supported by laboratory testing (ASTM D 2487).
4. Groundwater level, if indicated, is at time of drilling/excavation (ATD) or for date specified. Level may vary with time.
5. Location and ground surface elevations are approximate.

Date Started: 03/09/2023 Date Completed: 03/09/2023 Contractor/Crew:
Logged by: Checked by: Rig Model/Type: Backhoe
Location: Lat: 45.597209 Long: -122.612269 (WGS 84) Total Depth: 2.25 feet Depth to Seepage: Not Encountered
Ground Surface Elevation: 21.93 feet (NAVD 88)
Comments: Double ring falling head infiltration test conducted from 1050 to 1200.

Elevation (feet)	Depth (feet)	Sample Data: Type	Sample Data: Length (inches)	Sample Data: Number / Tests	Graphic Log	Material Description	Depth (feet)
	0					topsoil (3-inch thick)	0
						SILTY SAND (SM), (medium dense), moist, gray-brown. [NATIVE]	
20				G-1		POORLY GRADED SAND WITH SILT (SP), (medium dense), moist, gray, mostly fine to medium sand.	
						Bottom of Test Pit at 2.3 feet.	
	5						5
15							
	10						10
10							
	15						15
5							
	20						20
0							
	25						25
-5							
	30						30
-10							
	35						35
-15							

General Notes:
1. Refer to Figure A-1 for explanation of descriptions and symbols.
2. Material stratum lines are interpretive and actual changes may be gradual. Solid lines indicate distinct contacts and dashed lines indicate gradual or approximate contacts.
3. USCS designations are based on visual-manual identification (ASTM D 2488), unless otherwise supported by laboratory testing (ASTM D 2487).
4. Groundwater level, if indicated, is at time of drilling/excavation (ATD) or for date specified. Level may vary with time.
5. Location and ground surface elevations are approximate.

Date Started: 03/09/2023	Date Completed: 03/09/2023	Contractor/Crew:	
Logged by:	Checked by:	Rig Model/Type: Backhoe	
Location: Lat: 45.597973 Long: -122.612933 (WGS 84)		Total Depth: 3.5 feet	Depth to Seepage: Not Encountered
Ground Surface Elevation: 24.05 feet (NAVD 88)			

Comments: Single ring falling head infiltration test conducted from 1215 to 1430.

Elevation (feet)	Depth (feet)	Sample Type	Length (inches)	Number / Tests	Material Description	WC (%)	Fines Content (%)
24.05	0				SILTY SAND (SM), (loose to medium dense), moist, gray-brown.		
					SANDY SILT (ML), (medium stiff to stiff), moist, brown.		
	3.5	⊠		G-1 / GS, WC			45
					Bottom of Test Pit at 3.5 feet.		

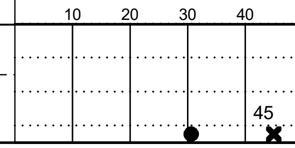

General Notes:
1. Refer to Figure A-1 for explanation of descriptions and symbols.
2. Material stratum lines are interpretive and actual changes may be gradual. Solid lines indicate distinct contacts and dashed lines indicate gradual or approximate contacts.
3. USCS designations are based on visual-manual identification (ASTM D 2488), unless otherwise supported by laboratory testing (ASTM D 2487).
4. Groundwater level, if indicated, is at time of drilling/excavation (ATD) or for date specified. Level may vary with time.
5. Location and ground surface elevations are approximate.

HALEY ALDRICH

Project: PDX Fuel Project Tank Design
Location: Portland, Oregon
Project No.: 0204679-001

Test Pit Log
IT-3

Figure **A**
Sheet **1 of 1**

Date Started: 03/09/2023 Date Completed: 03/09/2023 Contractor/Crew:
Logged by: Checked by: Rig Model/Type: Backhoe
Location: Lat: 45.598133 Long: -122.614312 (WGS 84) Total Depth: 10 feet Depth to Seepage: Not Encountered
Ground Surface Elevation: 24.28 feet (NAVD 88)
Comments:

Elevation (feet)	Depth (feet)	Sample Data: Type	Sample Data: Length (inches)	Sample Data: Number / Tests	Graphic Log	Material Description	Depth (feet)
	0					topsoil (3-inch thick)	0
		☒		G-1		SILTY SAND (SM), trace fine and coarse gravel, (loose to medium dense), moist, trace organics.	
						grades to no organics, increase in sand content	
20	5					SANDY SILT (ML), (soft to medium stiff), moist, dark gray-brown to brown.	5
						increase in moisture	
15						grades to dark gray-brown	
	10					water begins to seep into test pit at 10 ft.	10
						Bottom of Test Pit at 10.0 feet.	
10	15						15
5	20						20
0	25						25
-5	30						30
-10	35						35
-15							

General Notes:
1. Refer to Figure A-1 for explanation of descriptions and symbols.
2. Material stratum lines are interpretive and actual changes may be gradual. Solid lines indicate distinct contacts and dashed lines indicate gradual or approximate contacts.
3. USCS designations are based on visual-manual identification (ASTM D 2488), unless otherwise supported by laboratory testing (ASTM D 2487).
4. Groundwater level, if indicated, is at time of drilling/excavation (ATD) or for date specified. Level may vary with time.
5. Location and ground surface elevations are approximate.

HA TEST PIT - \\HALEYALDRICH.COM\SHARE\SEA_DATA\GINT\HC_LIBRARY.GLB - 16/5/23 12:58 - \\HALEYALDRICH.COM\SHARE\PDX_DATA\NOTEBOOKS\0204679-001_PDX_FUEL_PROJECT_TANK_DESIGN\FIELD DATA\PERM_GINT FILES\0204679-001_PDX FUEL PROJECT TANK DESIGN_GINT.GPJ - kbubel

Date Started: 03/09/2023 Date Completed: 03/09/2023 Contractor/Crew:

Logged by: Checked by: Rig Model/Type: Backhoe

Location: Lat: 45.597348 Long: -122.611951 (WGS 84) Total Depth: 5.5 feet Depth to Seepage: Not Encountered

Ground Surface Elevation: 23.00 feet (NAVD 88)

Comments:

Elevation (feet)	Depth (feet)	Sample Data: Type	Length (inches)	Number / Tests	Graphic Log	Material Description	Depth (feet)
	0					POORLY GRADED SAND WITH SILT AND GRAVEL (SP-SM), trace cobbles, (loose to medium dense), moist to wet, gray-brown. [FILL]	0
		⊠		G-1		SANDY SILT (ML), (medium dense), moist, brown mottled with gray-brown.	
20		⊠		G-2		SILTY SAND (SM), (medium dense), moist, brown. grades to gray	
						POORLY GRADED SAND (SP), few silt, (loose), moist.	
	5	⊠		G-3		water begins to seep into test pit	5
						Bottom of Test Pit at 5.5 feet.	
15	10						10
10	15						15
5	20						20
0	25						25
-5	30						30
-10	35						35
-15							

General Notes:
1. Refer to Figure A-1 for explanation of descriptions and symbols.
2. Material stratum lines are interpretive and actual changes may be gradual. Solid lines indicate distinct contacts and dashed lines indicate gradual or approximate contacts.
3. USCS designations are based on visual-manual identification (ASTM D 2488), unless otherwise supported by laboratory testing (ASTM D 2487).
4. Groundwater level, if indicated, is at time of drilling/excavation (ATD) or for date specified. Level may vary with time.
5. Location and ground surface elevations are approximate.

HALEY ALDRICH

Project: PDX Fuel Project Tank Design
Location: Portland, Oregon
Project No.: 0204679-001

Test Pit Log
TP-2

Figure **A**
Sheet **1 of 1**

HA TEST PIT - \\HALEYALDRICH.COM\SHARE\SEA_DATA\GINT\HC_LIBRARY.GLB - 16/5/23 12:58 - \\HALEYALDRICH.COM\SHARE\PDX_DATA\NOTEBOOKS\0204679-001_PDX_FUEL_PROJECT_TANK_DESIGN\FIELD DATA\PERM_GINT FILES\0204679-001_PDX FUEL PROJECT TANK DESIGN_GINT.GPJ - kbubel

APPENDIX B
Summary of Subsurface Engineering Properties Derived from CPT Interpretation

Soil Constitutive Model Parameters for ESU-2: PM4Silt Version 1 (Boulanger & Ziotopoulou 2018)

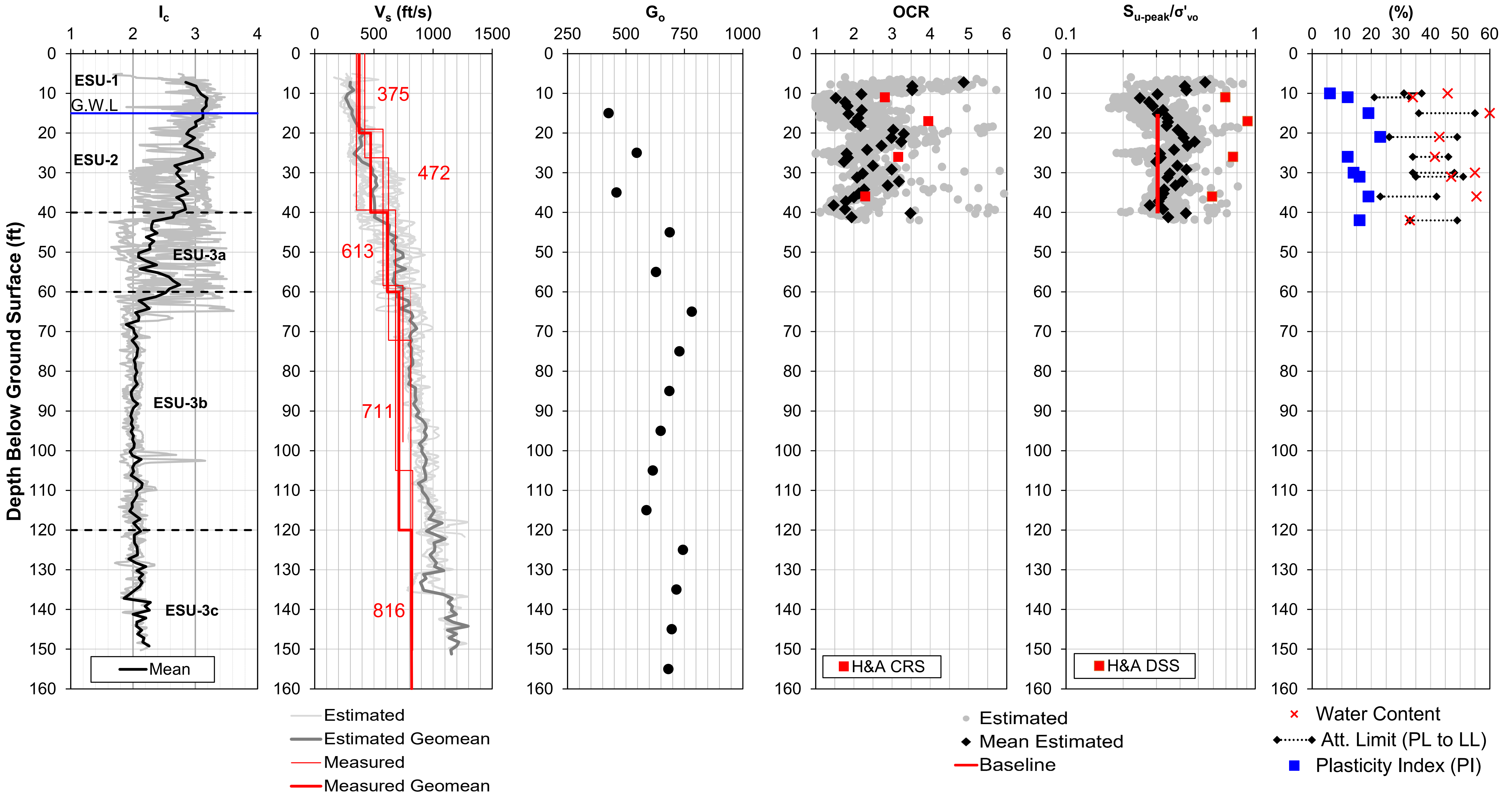

Notes:

1. Estimated Vs values are computed using Robertson 2009 CPT-Vs correlation
2. Measured Vs values are based on Seismic CPT data
3. G_o values for PM4Silt parameters are calibrated to "Measured Geomean" Vs value for every 10 ft elevation ($G_o = (G_{max}/p_{atm}) / (p'/p_{atm})^{0.75}$)
4. Estimated OCR values are computed using procedure proposed by Agaiby & Mayne (2019)
5. Peak undrained shear strength is $S_{u\text{-peak}}/\sigma'_{vo} = 0.5 \sin(\phi'_{NTH})\, OCR^{0.8}$, where ϕ'_{NTH} is estimated using Ouyang & Mayne (2019)
6. H&A CRS and DSS were the laboratory Constant Rate Strain consolidation and Direct Simple Shear test results performed by Haley & Aldrich, Inc

PDX Fuel Tank SVA
Portland, OR

Estimated Engineering Soil Properties for ESU-2: Overbank Deposit (ML / CL)

0204679-001 07 - 2023

HALEY ALDRICH

Fig. **B-1**

Soil Constitutive Model Parameters for ESU-3: PM4Sand Version 3.1 (Boulanger & Ziotopoulou 2017)

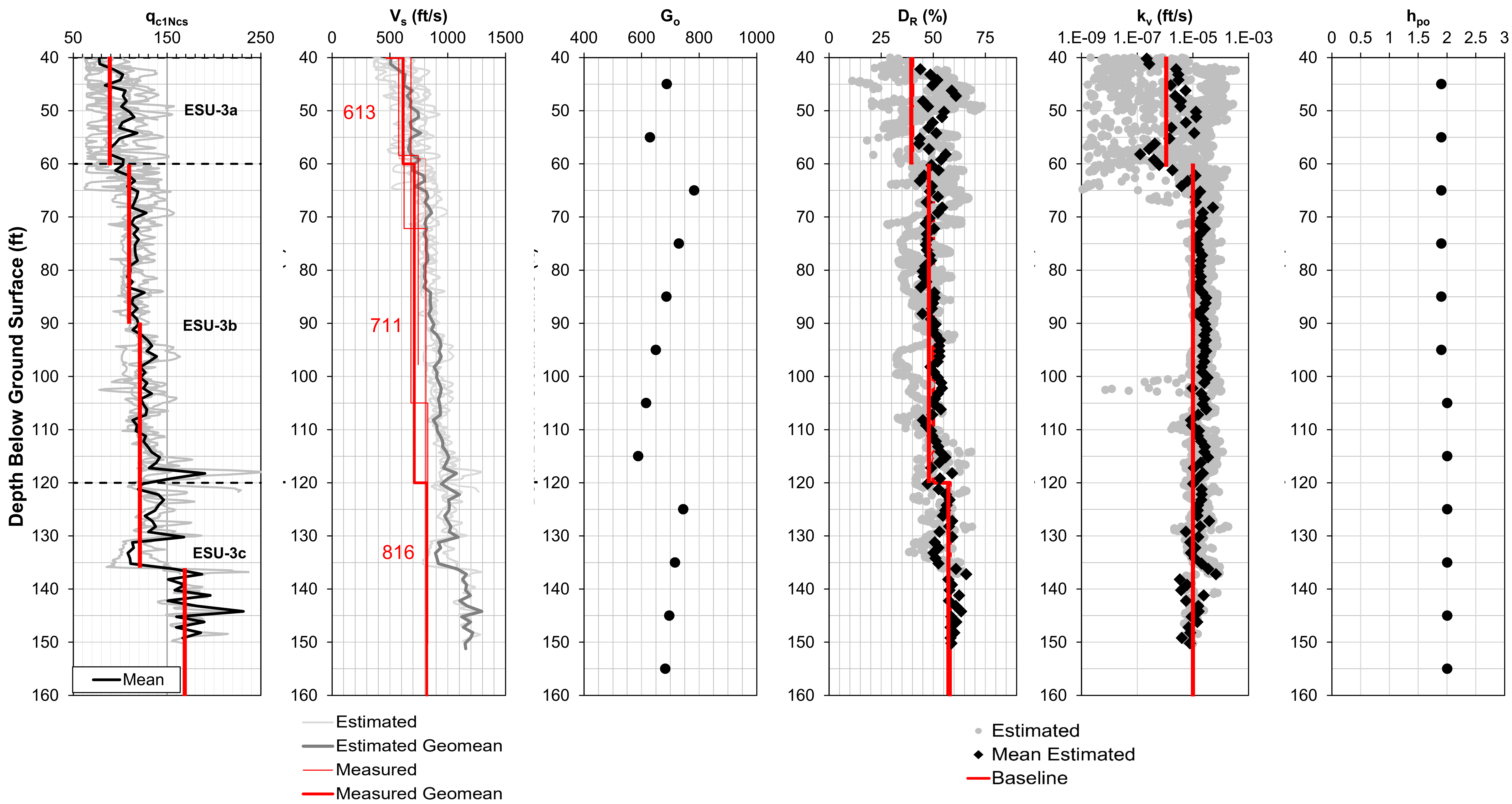

Notes:

1. q_{c1Ncs} values is computed following Idriss & Boulanger (2016)
2. Estimated Vs values are computed using Robertson (2009), Measured Vs values are based on Seismic CPT data
3. G_o values for PM4Sand parameters are calibrated to Measured Geomean value and every 10 ft elevation ($G_o = (G_{max}/p_{atm}) / (p'/p_{atm})^{0.5}$
4. Relative density (DR) values are estimated using Idriss & Boulanger (2008), Jamiolkowski et al. (2001), and Kulhawy & Mayne (1991) with weighting factor of 0.4, 0.3, 0.3, respectively
5. Hydraulic conductivity value are estimated using Robertson & Cabal (2015) CPT correlations
6. h_{po} value is calibrated to match Boulanger & Idriss (2016) CRR-N_c within P_{Liq} of 15 to 85%

PDX Fuel Tanks SVA
Portland, OR

Estimated Engineering Soil Properties for ESU-3: Columbia River Sand (SP)

0204679-001 07 - 2023

HALEY ALDRICH

Fig.
B-2

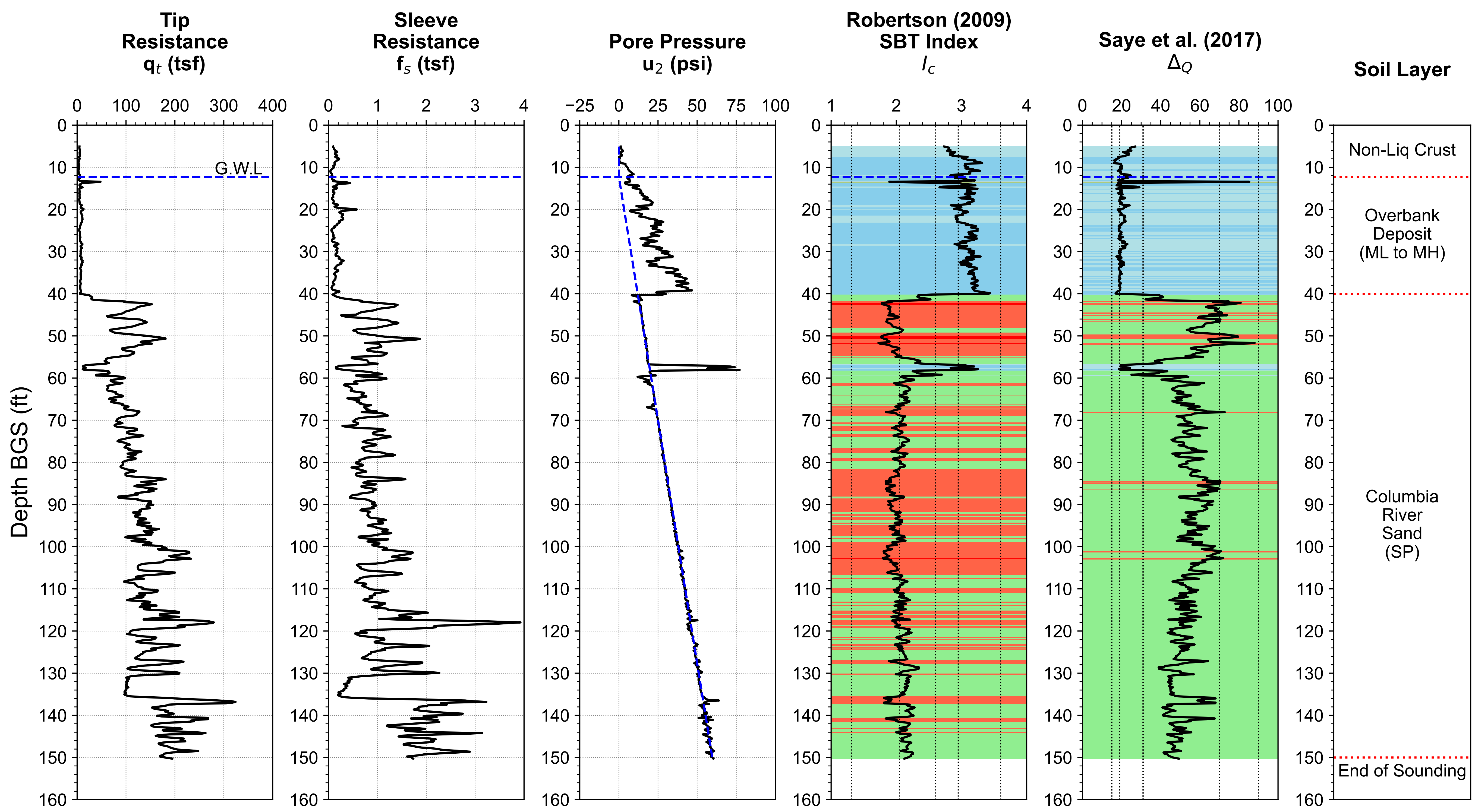

Robertson (2009) SBTn Zone:

- Gravelly Sands (I_c < 1.31)
- Clean sands (1.31 ≤ I_c < 1.8)
- Silty Sands (1.8 ≤ I_c < 2.05)
- Sand mixture: Sandy silt (2.05 ≤ I_c < 2.6)
- Silt mixture: Clayey silt to silty clay (2.6 ≤ I_c < 2.95)
- Clays (2.95 ≤ I_c ≤ 3.6)
- Organic Soils (I_c > 3.6)

Saye et al. (2017) Δ_Q Zone (Typical USCS):

- SP, SW (FC ≤ 5%, $\Delta_Q > 90$)
- SP-SM, SP-SC (FC ≈ 5-12%, $70 \le \Delta_Q < 90$)
- SM, SC, GM, GC (FC ≈ 12-50%, $31 \le \Delta_Q < 70$)
- ML, CL (FC > 50%, $D_{50} = 75\mu m$, $19 \le \Delta_Q < 31$)
- MH, CH (Liquid Limit, $w_L > 50$, $15 \le \Delta_Q < 19$)
- OL, OH, Pt (Highly Organic Soil, $\Delta_Q < 15$)

PDX Fuel Tank SVA
Portland, OR

CPT-Based Interpretation Summary
Basic Measurement
SCPT-5 : (45.597485 , -122.612872)

0204679-001 July 2023

HALEY ALDRICH

Figure
B-3

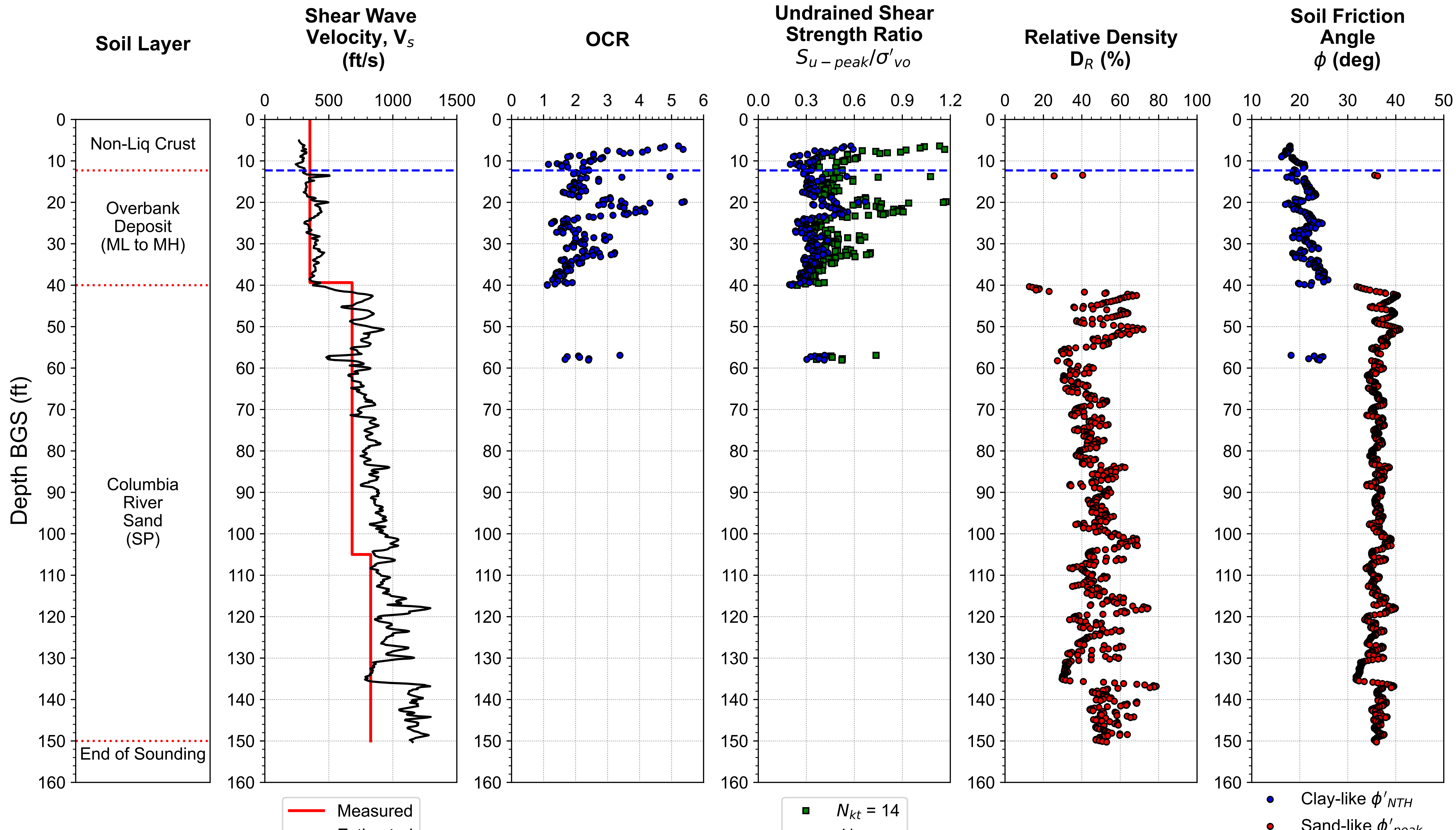

Notes:

1a. V_s is estimated using Robertson (2009) CPT-V_s Correlation
1b. Measured V_s is calculated using Slope method
2. OCR is determined using Agaiby & Mayne (2019) procedure
3a. S_{u-peak}/σ'_{vo} = ($q_t - \sigma_{vo}$) / ($N_{kt}\sigma'_{vo}$) and S_{u-peak}/σ'_{vo} = 0.5 sin(ϕ'_{NTH}) OCR $^{0.8}$
3b. N_{kt} = 14 ; ϕ_{NTH} = Effective friction angles calculated using modified NTH method (Ouyang & Mayne 2019)
4. Relative Density is estimated using Idriss & Boulanger 2008, Jamiolkowski et al. 2001, and Kulhawy & Mayne 1991 with weighting average factor 0.4, 0.3, 0.3, respectively
5. ϕ_{peak} = Peak friction angle calculated using Robertson (2010) equation for sandy soils, assuming ϕ'_{cv} = 33^o

PDX Fuel Tank SVA Portland, OR	
CPT-Based Interpretation Summary **Engineering Properties** **SCPT-5 : (45.597485 , -122.612872)** 0204679-001 July 2023	
HALEY ALDRICH	Figure **B-4**

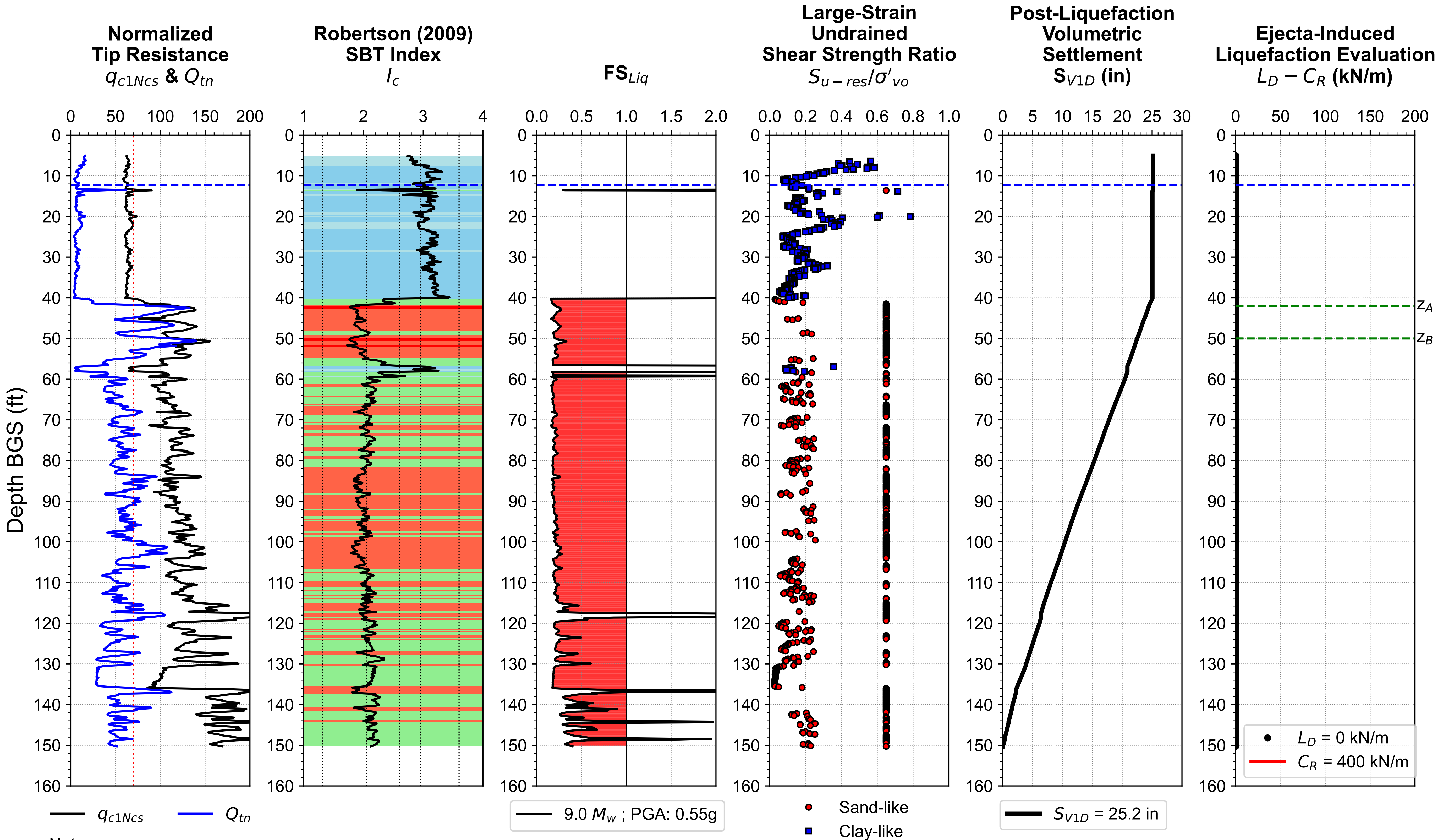

Notes:

1a. q_{c1Ncs}: Equivalent clean sand tip resistance following Boulanger & Idriss (2016) to estimate cyclic resistance ratio
1b. Q_{tn}: Normalized tip resistance following Robertson 2020 to estimate large-strain undrained shear strength ratio
2. FS_{Liq} is calculated using Boulanger & Idriss (2016) with P_{Liq} = 0.15 ; I_{c-cut} = 2.6 ; C_{FC} = 0.0
3. Large-strain undrained shear strength ratio is estimated using Robertson (2020) for clay-like and sand-like soil:
   Sand-like: Post-liquefied strength ratio (S_{u-liq}/σ'_{vo}) = tan (ϕ'_{cv}) for Q_{tn} > 70, where ϕ'_{cv} is assumed to be 33^o
   Clay-like: S_{u-res} is the same as remolded strength S_{u-rem}
4. Post-Liquefaction volumetric settlement is calculated using Zhang et al. (2002) procedure
5. Ejecta-induced settlement & severity are calculated based on Hutabarat & Bray (2022)

PDX Fuel Tank SVA
Portland, OR

CPT-based Liquefaction Evaluation
2475-yrs Hazard Level
SCPT-5 : (45.597485 , -122.612872)

0204679-001 July 2023

HALEY ALDRICH

Figure
B-5

Modified SBT$_n$
Robertson (2016)

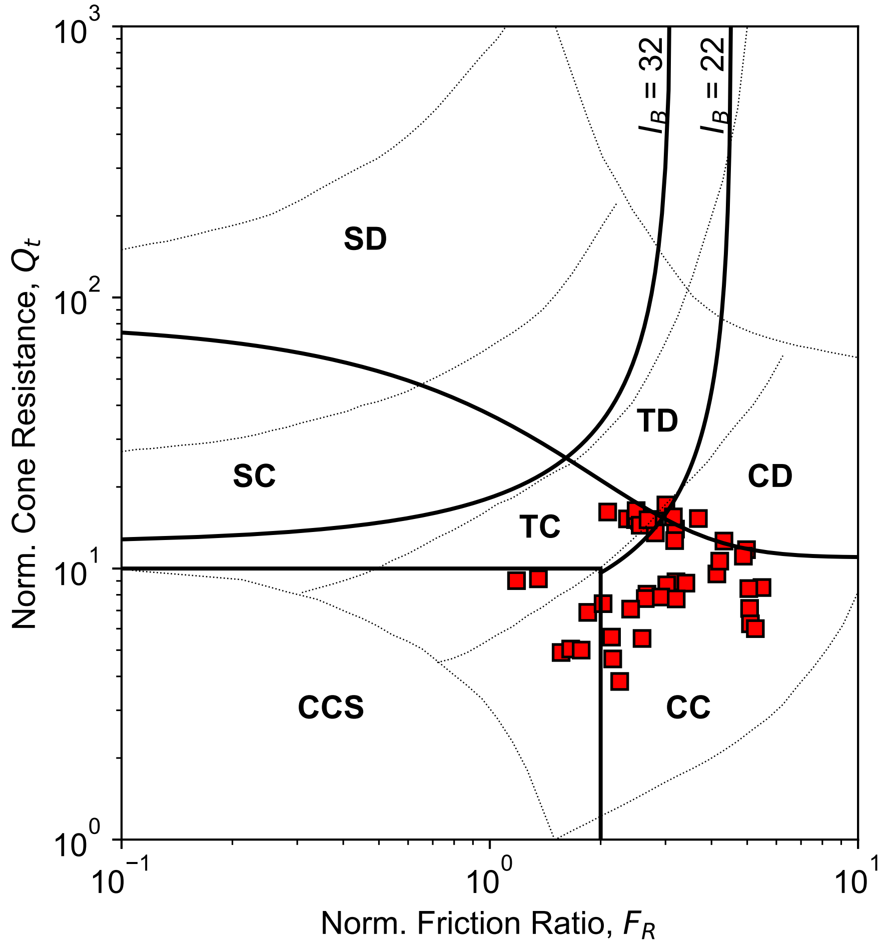

Δ_Q Index Soil Classification Chart
Saye et al. (2017)

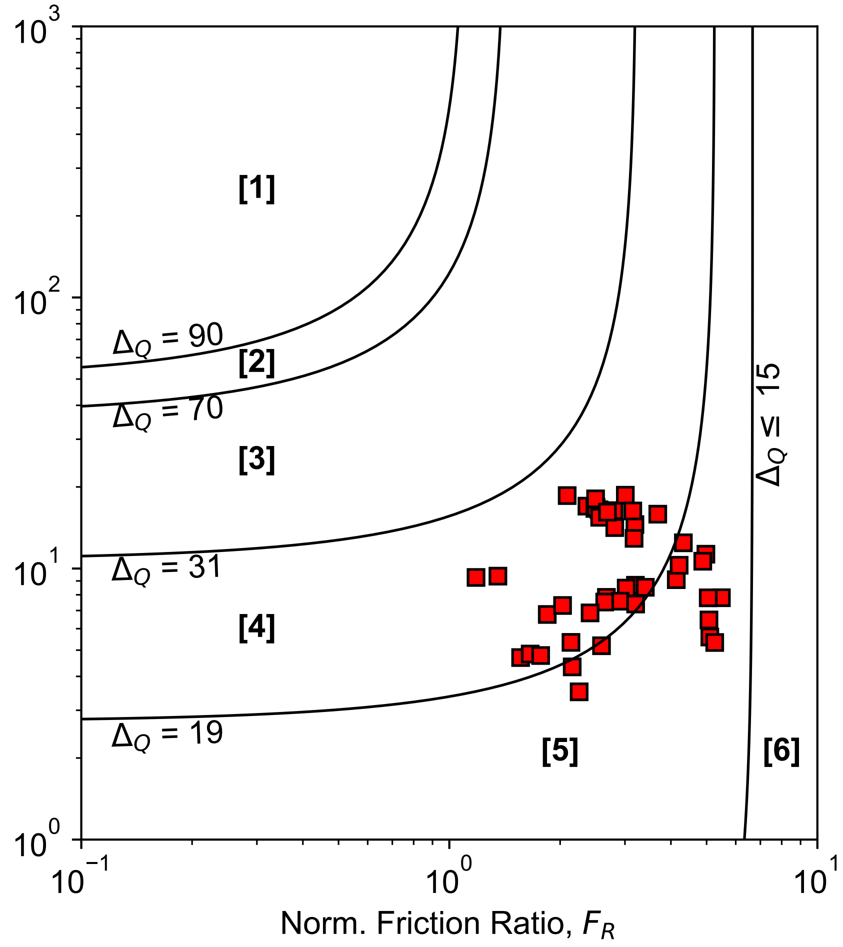

Soil Classification Chart
Schneider et al. (2012)

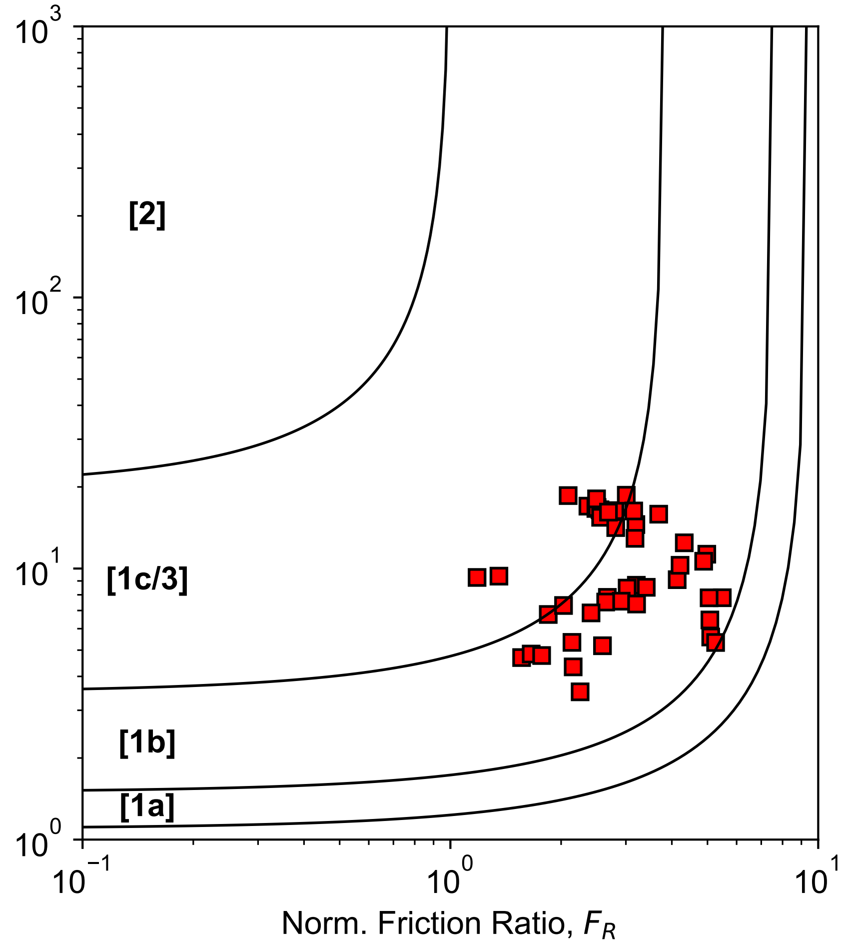

Robertson (2016) SBTn Zone:
SD = Sand-like - Dilative
SC = Sand-like - Contractive
TD = Transitional - Dilative
TC = Transitional - Contractive
CD = Clay-like - Dilative
CC = Clay-like - Contractive
CCS = Clay-like Contractive Sensitive

Typical USCS (Saye et al. 2017):
[1] $\Delta_Q > 90$ = SP, SW (FC ≤ 5%)
[2] $70 \le \Delta_Q < 90$ = SP-SM, SP-SC (FC ≈ 5-12%)
[3] $31 \le \Delta_Q < 70$ = SM, SC, GM, GC (FC ≈ 12-50%)
[4] $19 \le \Delta_Q < 31$ = ML, CL (FC > 50%, $D_{50} = 75\mu$m)
[5] $15 \le \Delta_Q < 19$ = MH, CH (Liquid Limit, $w_L > 50$)
[6] $\Delta_Q < 15$ = OL, OH, Pt (Highly Organic Soil)

Classification Zone Schneider et al. 2012:
Zone-[1a] = Low-I_R clays ($I_R = G/S_u$)
Zone-[1b] = Clays
Zone-[1c] = Sensitive clays
Zone-[3] = Silts and transitional soils
Zone-[2] = Essentially drained sands

PDX Fuel Tank SVA
Portland, OR

Soil Classification Chart
Layer-1: 5 ft to 12 ft
SCPT-5 : (45.597485 , -122.612872)

0204679-001 July 2023

HALEY ALDRICH

Figure
B-6

\\haleyaldrich.com\share\pdx_data\Notebooks\0204679-001_PDX_Fuel_Project_Tank_Design\Analysis and Calcs\5 2D FLAC NDA\CPTBased Assessment\SCPT-5.pdf

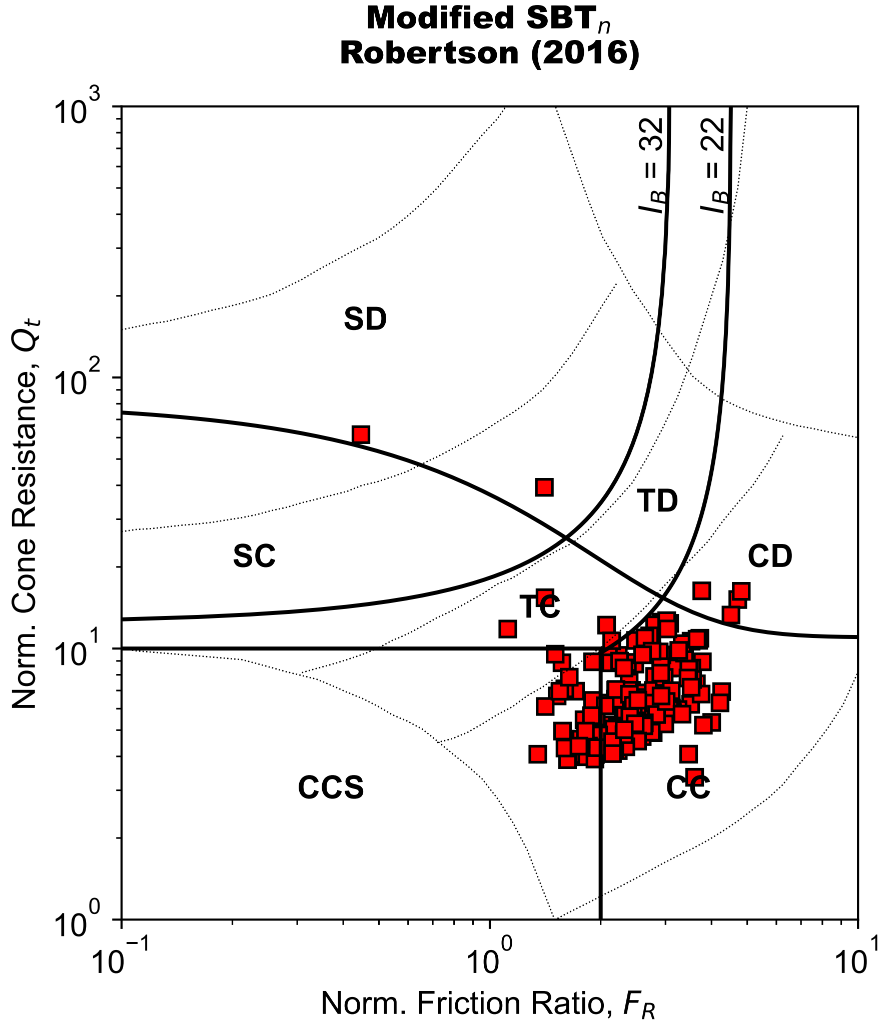

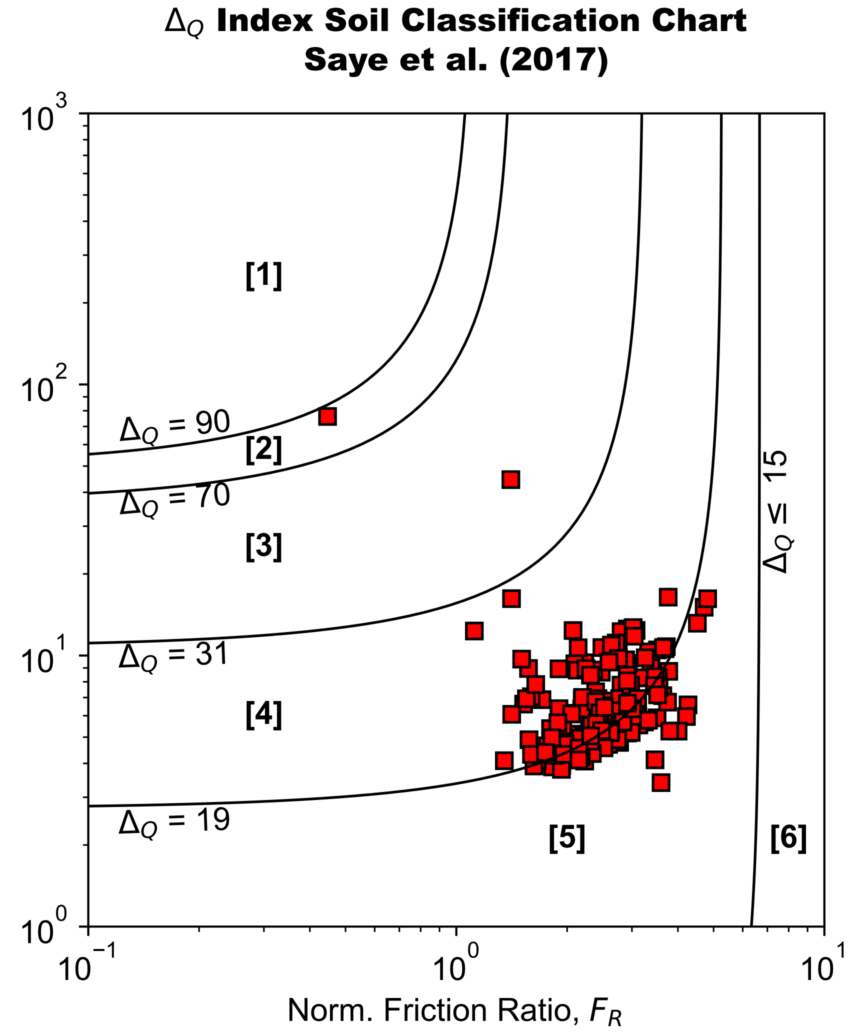

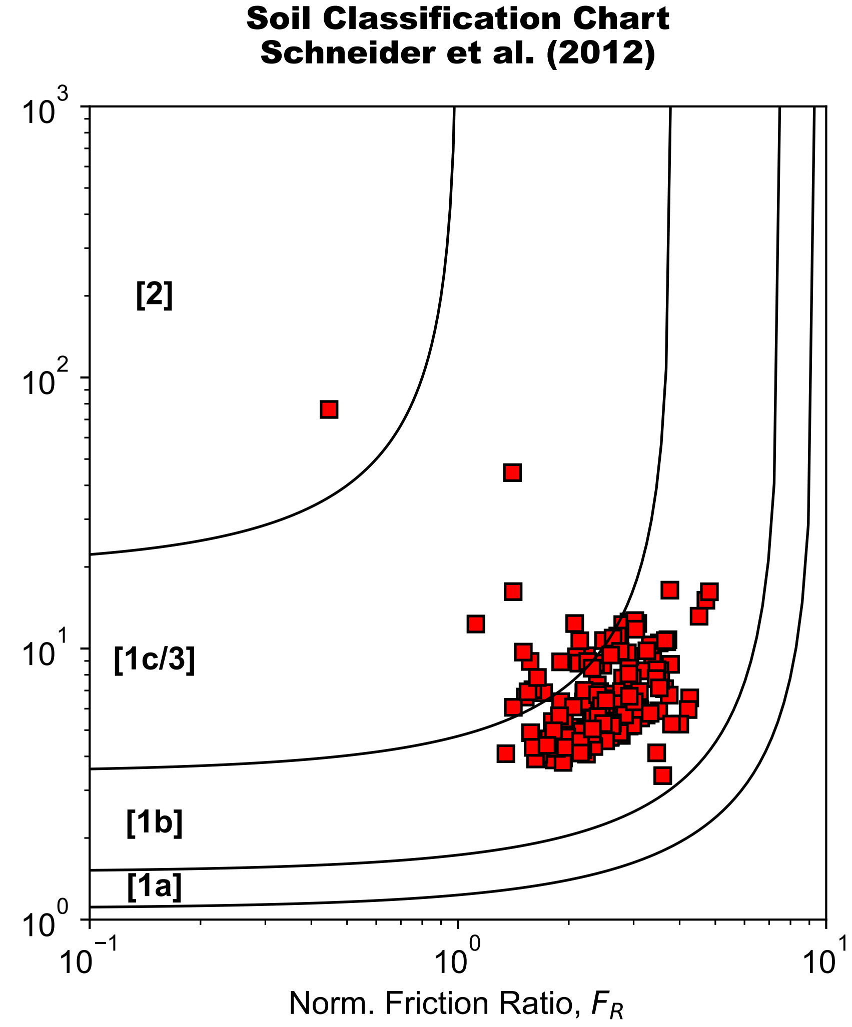

Robertson (2016) SBTn Zone:
SD = Sand-like - Dilative
SC = Sand-like - Contractive
TD = Transitional - Dilative
TC = Transitional - Contractive
CD = Clay-like - Dilative
CC = Clay-like - Contractive
CCS = Clay-like Contractive Sensitive

Typical USCS (Saye et al. 2017):
[1] $\Delta_Q > 90$ = SP, SW (FC ≤ 5%)
[2] $70 \leq \Delta_Q < 90$ = SP-SM, SP-SC (FC ≈ 5-12%)
[3] $31 \leq \Delta_Q < 70$ = SM, SC, GM, GC (FC ≈ 12-50%)
[4] $19 \leq \Delta_Q < 31$ = ML, CL (FC > 50%, $D_{50} = 75\mu$m)
[5] $15 \leq \Delta_Q < 19$ = MH, CH (Liquid Limit, $w_L > 50$)
[6] $\Delta_Q < 15$ = OL, OH, Pt (Highly Organic Soil)

Classification Zone Schneider et al. 2012:
Zone-[1a] = Low-I_R clays ($I_R = G/S_u$)
Zone-[1b] = Clays
Zone-[1c] = Sensitive clays
Zone-[3] = Silts and transitional soils
Zone-[2] = Essentially drained sands

PDX Fuel Tank SVA
Portland, OR

Soil Classification Chart
Layer-2: 12 ft to 40 ft
SCPT-5 : (45.597485 , -122.612872)

0204679-001 July 2023

HALEY ALDRICH

Figure
B-7

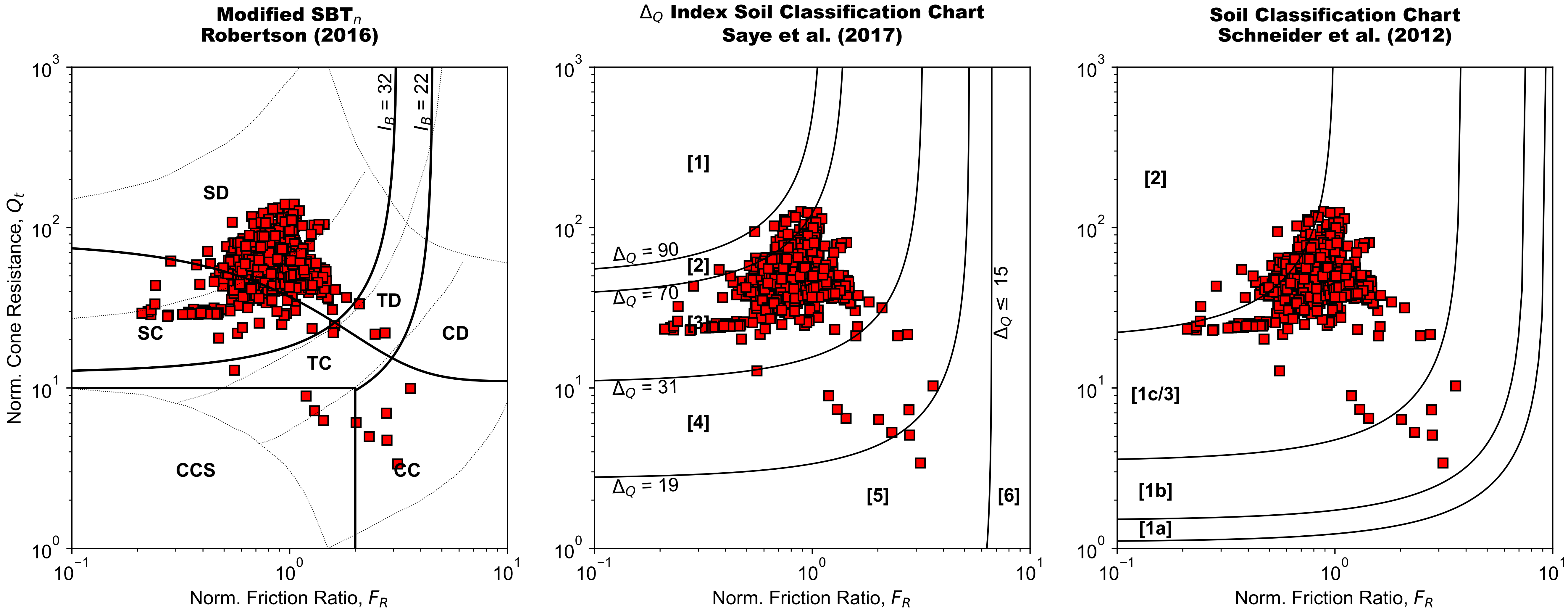

Robertson (2016) SBTn Zone:
SD = Sand-like - Dilative
SC = Sand-like - Contractive
TD = Transitional - Dilative
TC = Transitional - Contractive
CD = Clay-like - Dilative
CC = Clay-like - Contractive
CCS = Clay-like Contractive Sensitive

Typical USCS (Saye et al. 2017):
[1] $\Delta_Q > 90$ = SP, SW (FC $\leq$ 5%)
[2] $70 \leq \Delta_Q < 90$ = SP-SM, SP-SC (FC $\approx$ 5-12%)
[3] $31 \leq \Delta_Q < 70$ = SM, SC, GM, GC (FC $\approx$ 12-50%)
[4] $19 \leq \Delta_Q < 31$ = ML, CL (FC > 50%, $D_{50} = 75\mu$m)
[5] $15 \leq \Delta_Q < 19$ = MH, CH (Liquid Limit, $w_L > 50$)
[6] $\Delta_Q < 15$ = OL, OH, Pt (Highly Organic Soil)

Classification Zone Schneider et al. 2012:
Zone-[1a] = Low-I_R clays ($I_R = G/S_u$)
Zone-[1b] = Clays
Zone-[1c] = Sensitive clays
Zone-[3] = Silts and transitional soils
Zone-[2] = Essentially drained sands

PDX Fuel Tank SVA
Portland, OR

Soil Classification Chart
Layer-3: 40 ft to 150 ft
SCPT-5 : (45.597485 , -122.612872)

0204679-001 July 2023

HALEY ALDRICH

Figure
B-8

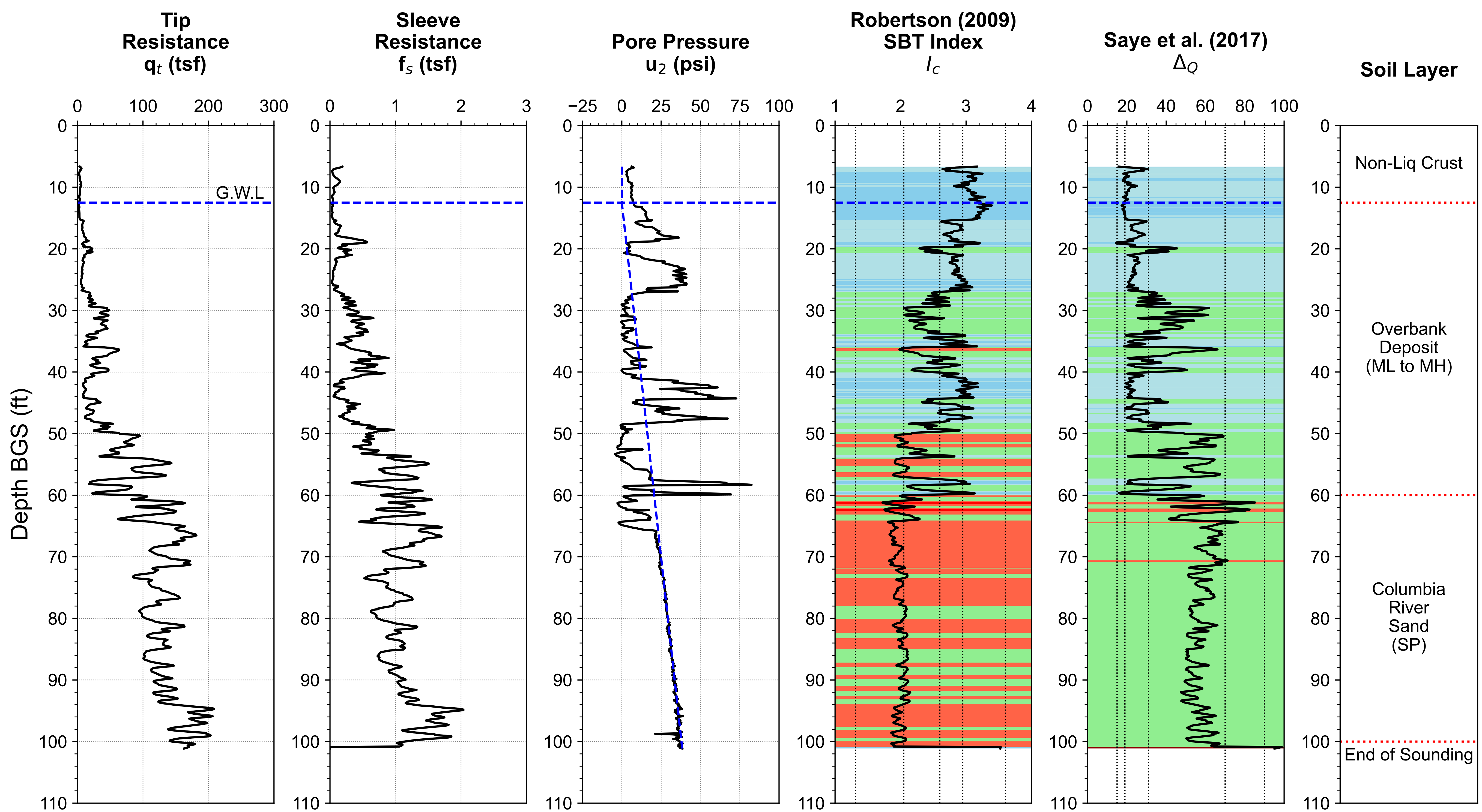

Robertson (2009) SBTn Zone:

- Gravelly Sands (I_c < 1.31)
- Clean sands (1.31 ≤ I_c < 1.8)
- Silty Sands (1.8 ≤ I_c < 2.05)
- Sand mixture: Sandy silt (2.05 ≤ I_c < 2.6)
- Silt mixture: Clayey silt to silty clay (2.6 ≤ I_c < 2.95)
- Clays (2.95 ≤ I_c ≤ 3.6)
- Organic Soils (I_c > 3.6)

Saye et al. (2017) Δ_Q Zone (Typical USCS):

- SP, SW (FC ≤ 5%, $\Delta_Q > 90$)
- SP-SM, SP-SC (FC ≈ 5-12%, $70 \leq \Delta_Q < 90$)
- SM, SC, GM, GC (FC ≈ 12-50%, $31 \leq \Delta_Q < 70$)
- ML, CL (FC > 50%, $D_{50} = 75\mu m$, $19 \leq \Delta_Q < 31$)
- MH, CH (Liquid Limit, $w_L > 50$, $15 \leq \Delta_Q < 19$)
- OL, OH, Pt (Highly Organic Soil, $\Delta_Q < 15$)

PDX Fuel Tank SVA
Portland, OR

CPT-Based Interpretation Summary
Basic Measurement
SCPT-1 : (45.59739 , -122.61306)

0204679-001 July 2023

HALEY ALDRICH

Figure
B-9

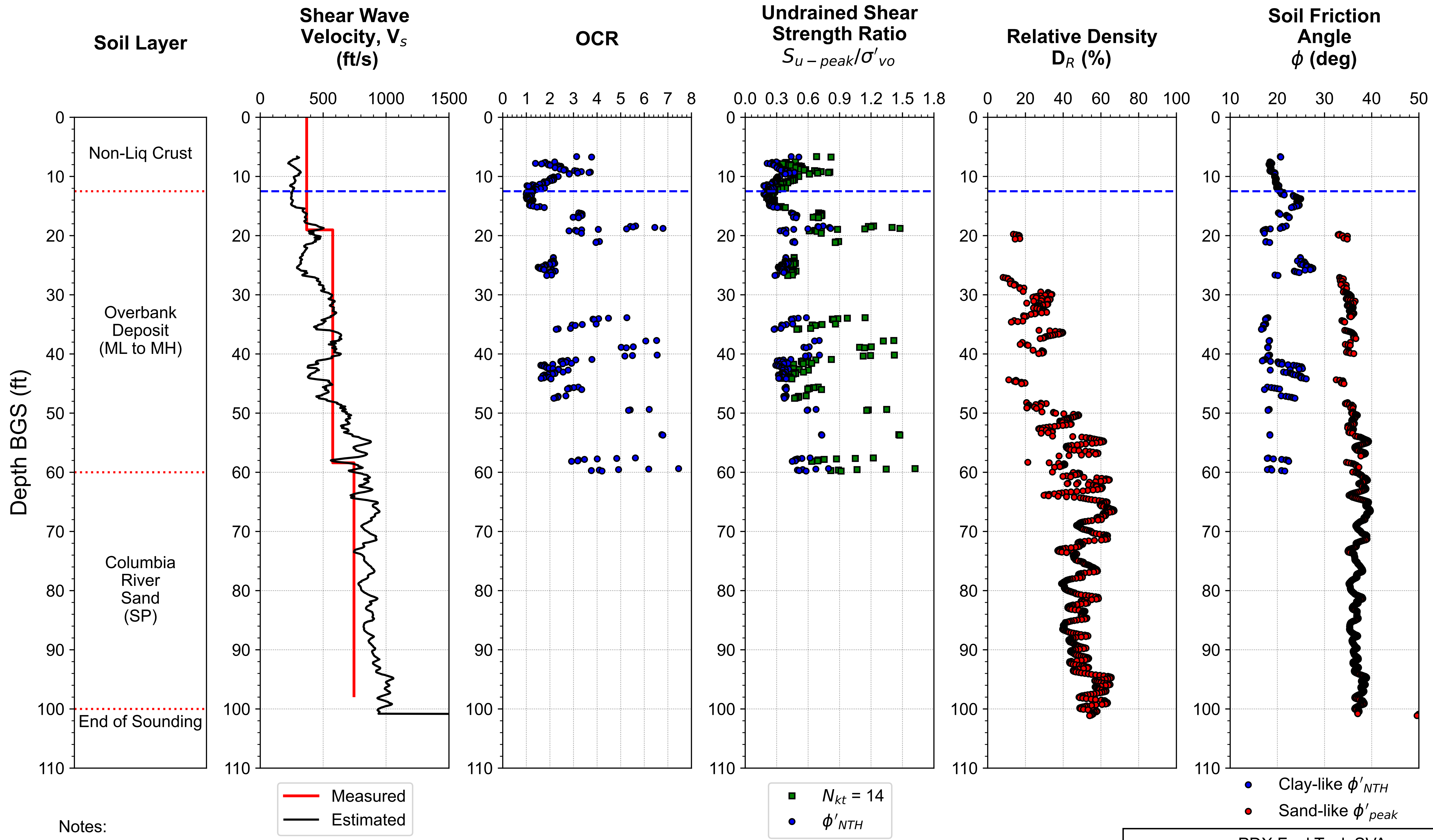

Notes:

1a. V_s is estimated using Robertson (2009) CPT-V_s Correlation
1b. Measured V_s is calculated using Slope method
2. OCR is determined using Agaiby & Mayne (2019) procedure
3a. S_{u-peak}/σ'_{vo} = ($q_t - \sigma_{vo}$) / ($N_{kt}\sigma'_{vo}$) and S_{u-peak}/σ'_{vo} = 0.5 sin(ϕ'_{NTH}) OCR $^{0.8}$
3b. N_{kt} = 14 ; ϕ_{NTH} = Effective friction angles calculated using modified NTH method (Ouyang & Mayne 2019)
4. Relative Density is estimated using Idriss & Boulanger 2008, Jamiolkowski et al. 2001, and Kulhawy & Mayne 1991 with weighting average factor 0.4, 0.3, 0.3, respectively
5. ϕ_{peak} = Peak friction angle calculated using Robertson (2010) equation for sandy soils, assuming ϕ'_{cv} = 33^o

PDX Fuel Tank SVA
Portland, OR

CPT-Based Interpretation Summary
Engineering Properties
SCPT-1 : (45.59739 , -122.61306)

0204679-001 July 2023

HALEY ALDRICH

Figure
B-10

\\haleyaldrich.com\share\pdx_data\Notebooks\0204679-001_PDX_Fuel_Project_Tank_Design\Analysis and Calcs\5 2D FLAC NDA\CPTBased Assessment\SCPT-1.pdf

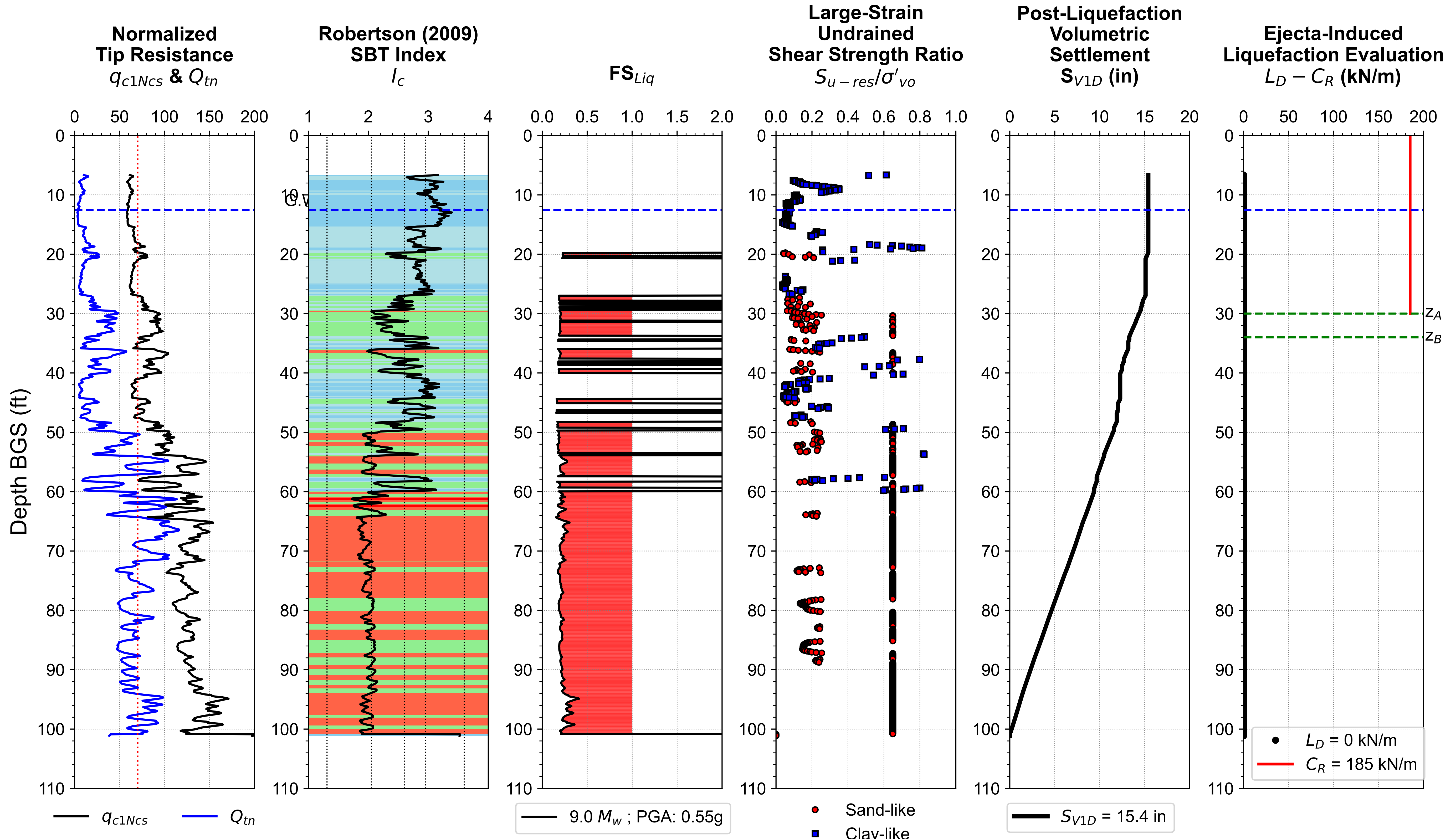

Notes:

1a. q_{c1Ncs}: Equivalent clean sand tip resistance following Boulanger & Idriss (2016) to estimate cyclic resistance ratio
1b. Q_{tn}: Normalized tip resistance following Robertson 2020 to estimate large-strain undrained shear strength ratio
2. FS_{Liq} is calculated using Boulanger & Idriss (2016) with P_{Liq} = 0.15 ; I_{c-cut} = 2.6 ; C_{FC} = 0.0
3. Large-strain undrained shear strength ratio is estimated using Robertson (2020) for clay-like and sand-like soil:
   Sand-like: Post-liquefied strength ratio (S_{u-liq}/σ'_{vo}) = tan (ϕ'_{cv}) for Q_{tn} > 70, where ϕ'_{cv} is assumed to be 33^o
   Clay-like: S_{u-res} is the same as remolded strength S_{u-rem}
4. Post-Liquefaction volumetric settlement is calculated using Zhang et al. (2002) procedure
5. Ejecta-induced settlement & severity are calculated based on Hutabarat & Bray (2022)

PDX Fuel Tank SVA
Portland, OR

CPT-based Liquefaction Evaluation
2475-yrs Hazard Level
SCPT-1 : (45.59739 , -122.61306)

0204679-001 July 2023

HALEY ALDRICH

Figure
B-11

Modified SBT$_n$
Robertson (2016)

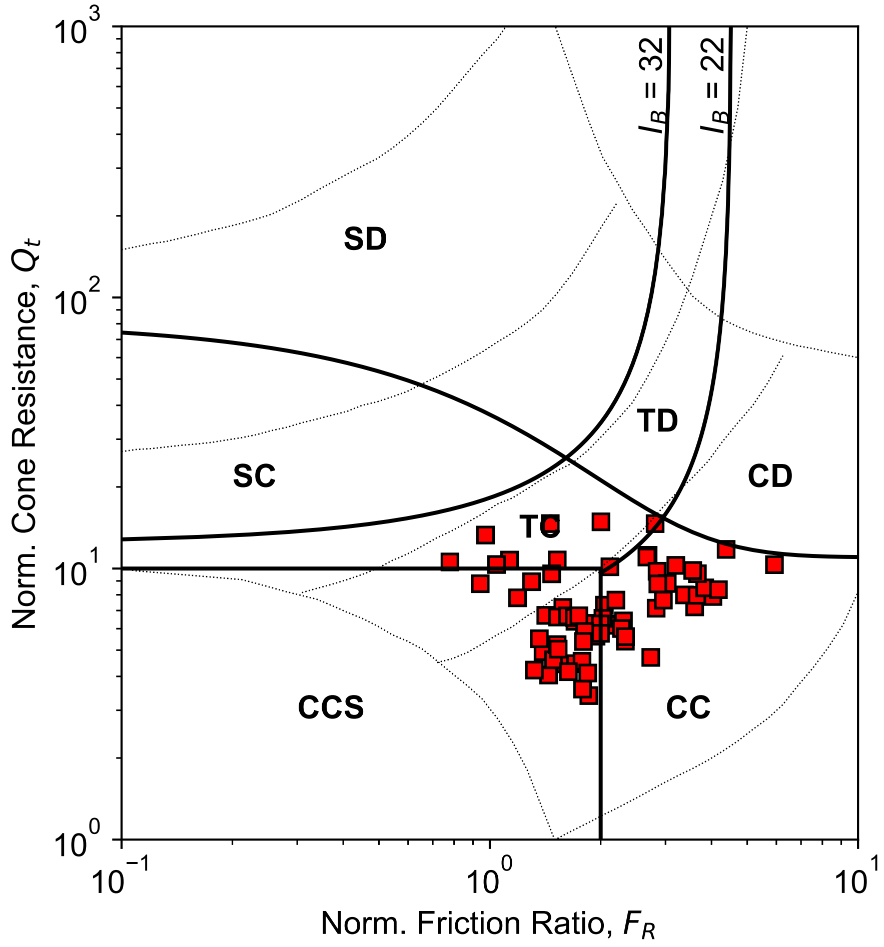

Δ_Q Index Soil Classification Chart
Saye et al. (2017)

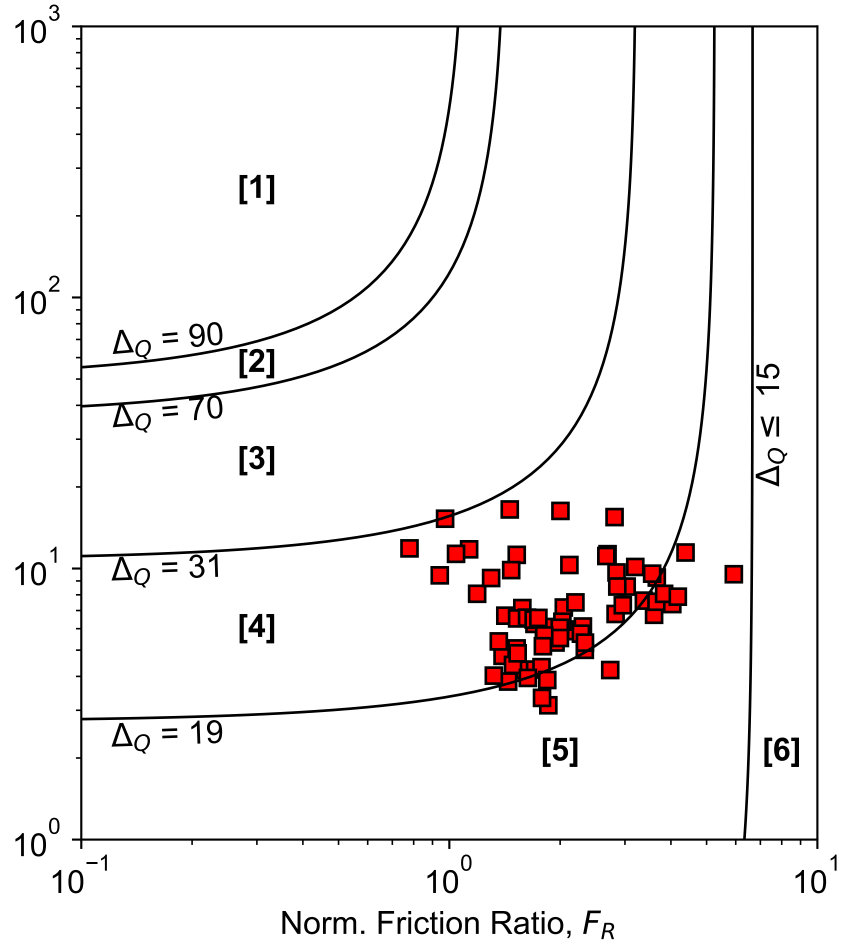

Soil Classification Chart
Schneider et al. (2012)

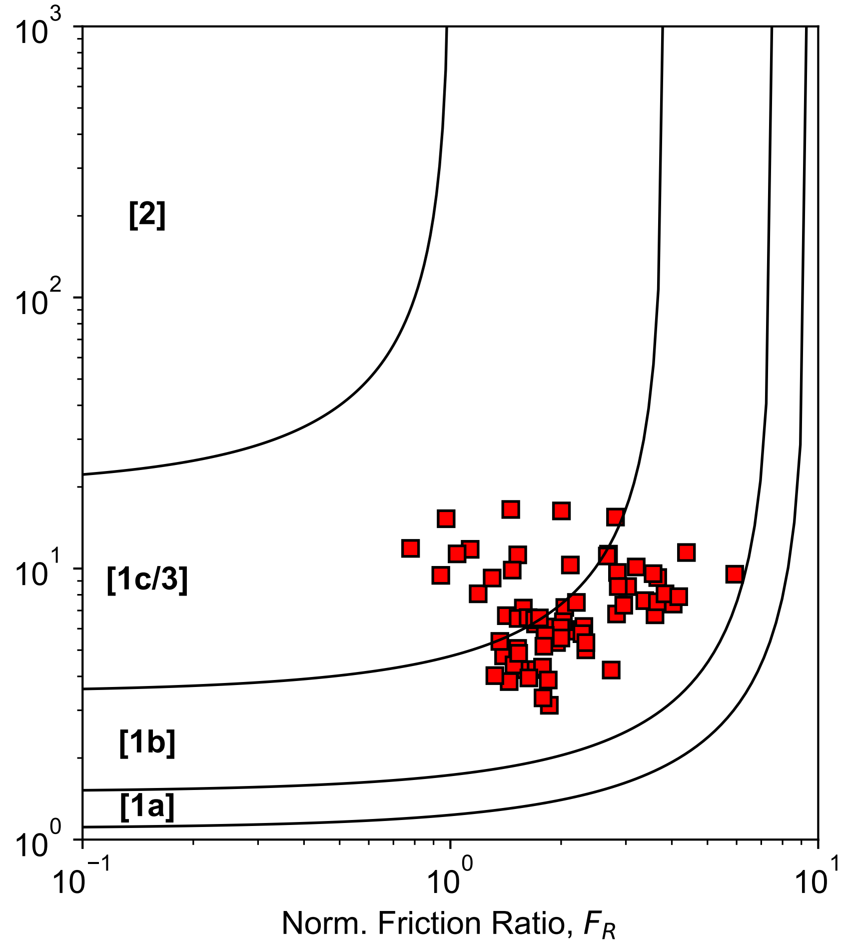

Robertson (2016) SBTn Zone:
SD = Sand-like - Dilative
SC = Sand-like - Contractive
TD = Transitional - Dilative
TC = Transitional - Contractive
CD = Clay-like - Dilative
CC = Clay-like - Contractive
CCS = Clay-like Contractive Sensitive

Typical USCS (Saye et al. 2017):
[1] $\Delta_Q > 90$ = SP, SW (FC ≤ 5%)
[2] $70 \leq \Delta_Q < 90$ = SP-SM, SP-SC (FC ≈ 5-12%)
[3] $31 \leq \Delta_Q < 70$ = SM, SC, GM, GC (FC ≈ 12-50%)
[4] $19 \leq \Delta_Q < 31$ = ML, CL (FC > 50%, $D_{50} = 75\mu m$)
[5] $15 \leq \Delta_Q < 19$ = MH, CH (Liquid Limit, $w_L > 50$)
[6] $\Delta_Q < 15$ = OL, OH, Pt (Highly Organic Soil)

Classification Zone Schneider et al. 2012:
Zone-[1a] = Low-I_R clays ($I_R = G/S_u$)
Zone-[1b] = Clays
Zone-[1c] = Sensitive clays
Zone-[3] = Silts and transitional soils
Zone-[2] = Essentially drained sands

PDX Fuel Tank SVA
Portland, OR

Soil Classification Chart
Layer-1: 7 ft to 12 ft
SCPT-1 : (45.59739 , -122.61306)

0204679-001 July 2023

HALEY ALDRICH

Figure
B-12

\\haleyaldrich.com\share\pdx_data\Notebooks\0204679-001_PDX_Fuel_Project_Tank_Design\Analysis and Calcs\5 2D FLAC NDA\CPTBased Assessment\SCPT-1.pdf

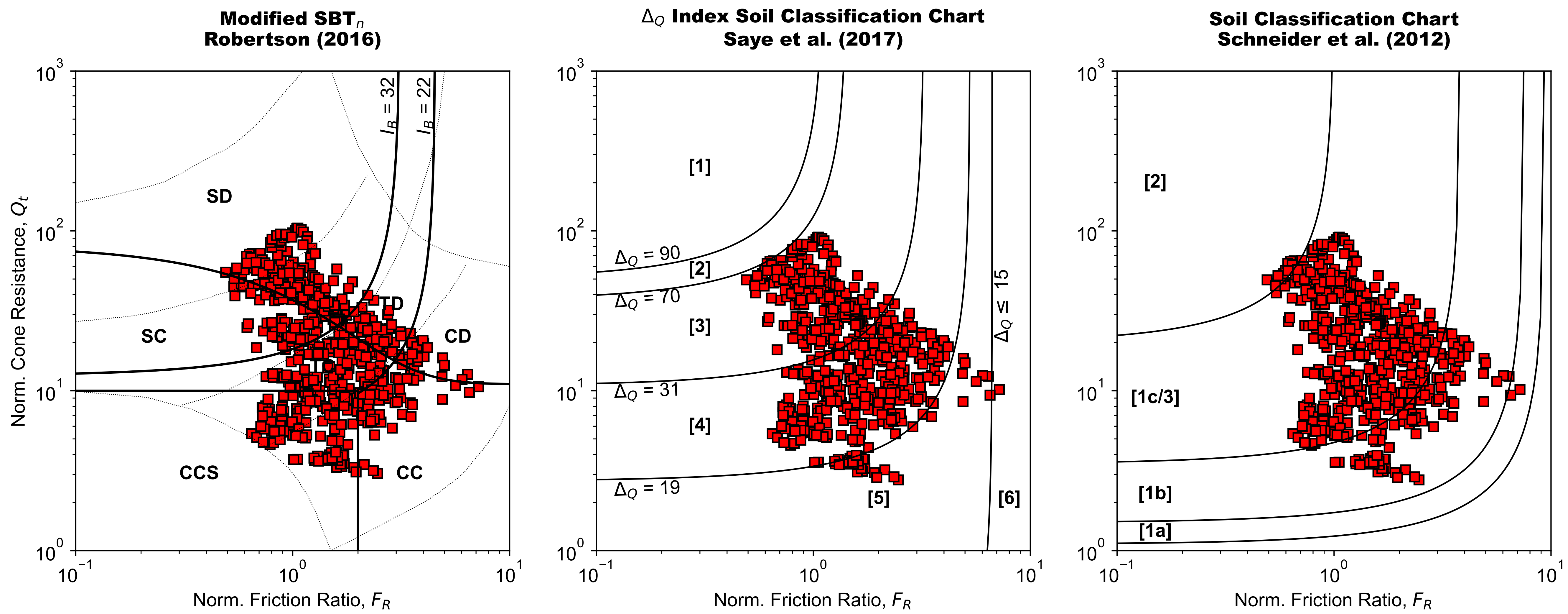

Robertson (2016) SBTn Zone:
SD = Sand-like - Dilative
SC = Sand-like - Contractive
TD = Transitional - Dilative
TC = Transitional - Contractive
CD = Clay-like - Dilative
CC = Clay-like - Contractive
CCS = Clay-like Contractive Sensitive

Typical USCS (Saye et al. 2017):
[1] $\Delta_Q > 90$ = SP, SW (FC $\leq$ 5%)
[2] $70 \leq \Delta_Q < 90$ = SP-SM, SP-SC (FC $\approx$ 5-12%)
[3] $31 \leq \Delta_Q < 70$ = SM, SC, GM, GC (FC $\approx$ 12-50%)
[4] $19 \leq \Delta_Q < 31$ = ML, CL (FC > 50%, $D_{50} = 75\mu$m)
[5] $15 \leq \Delta_Q < 19$ = MH, CH (Liquid Limit, $w_L > 50$)
[6] $\Delta_Q < 15$ = OL, OH, Pt (Highly Organic Soil)

Classification Zone Schneider et al. 2012:
Zone-[1a] = Low-I_R clays ($I_R = G/S_u$)
Zone-[1b] = Clays
Zone-[1c] = Sensitive clays
Zone-[3] = Silts and transitional soils
Zone-[2] = Essentially drained sands

PDX Fuel Tank SVA
Portland, OR

Soil Classification Chart
Layer-2: 12 ft to 60 ft
SCPT-1 : (45.59739 , -122.61306)

0204679-001 July 2023

HALEY ALDRICH

Figure
B-13

Modified SBT$_n$
Robertson (2016)

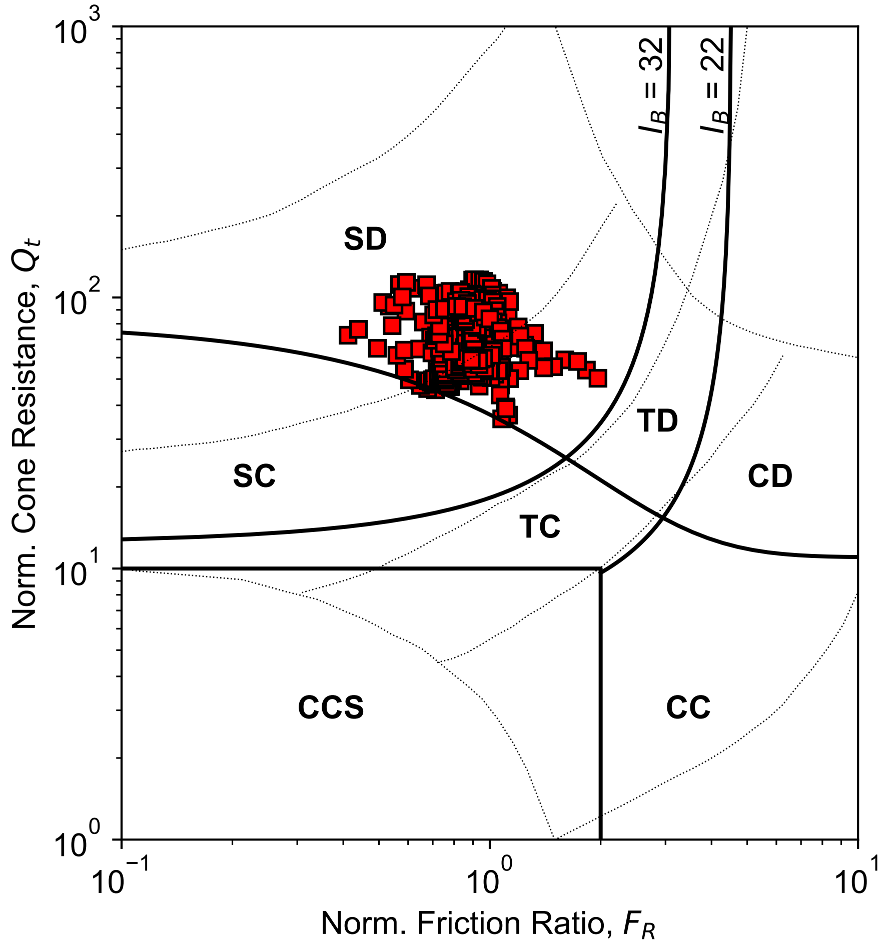

Δ_Q Index Soil Classification Chart
Saye et al. (2017)

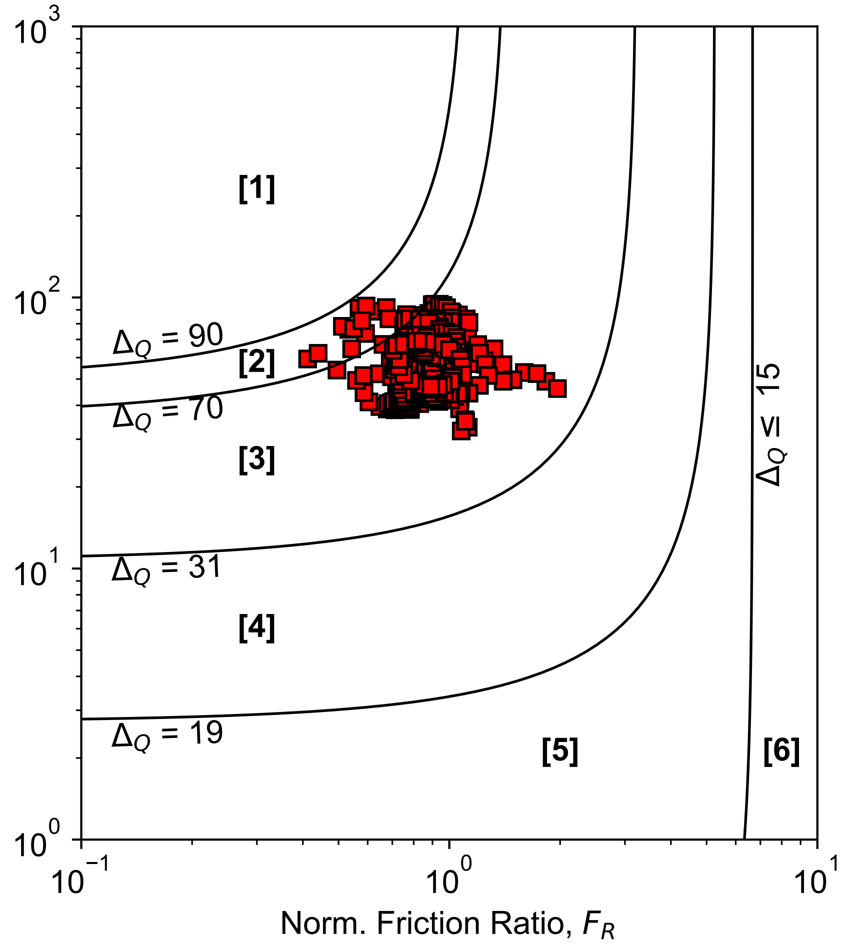

Soil Classification Chart
Schneider et al. (2012)

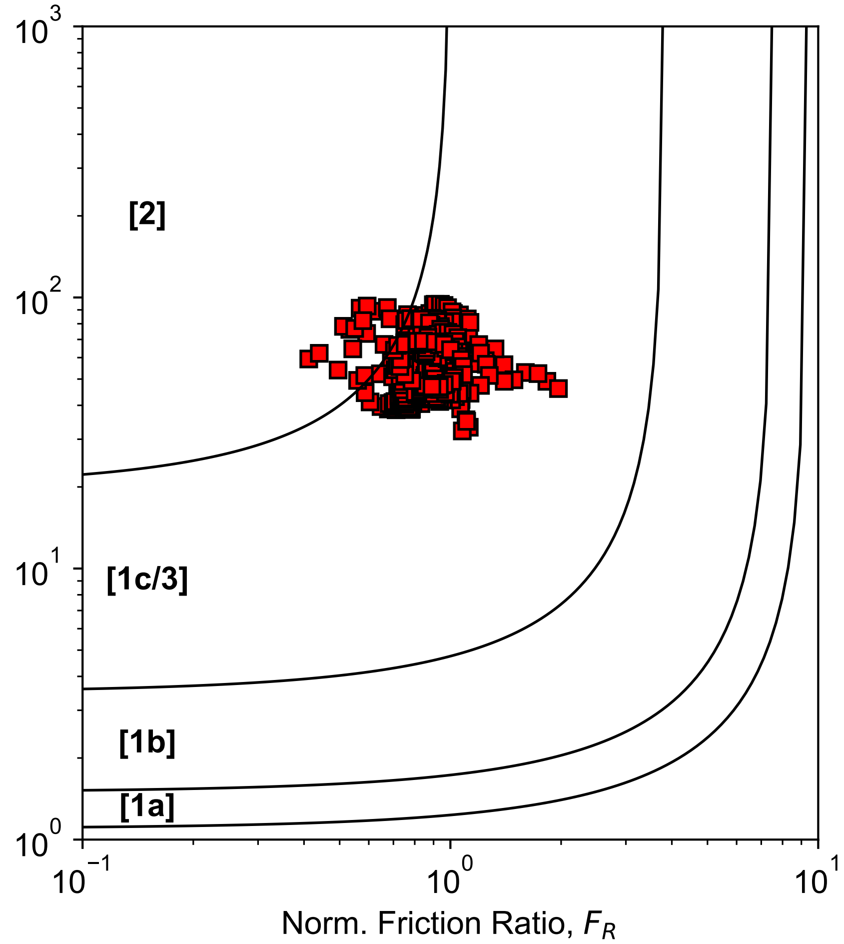

Robertson (2016) SBTn Zone:
SD = Sand-like - Dilative
SC = Sand-like - Contractive
TD = Transitional - Dilative
TC = Transitional - Contractive
CD = Clay-like - Dilative
CC = Clay-like - Contractive
CCS = Clay-like Contractive Sensitive

Typical USCS (Saye et al. 2017):
[1] $\Delta_Q > 90$ = SP, SW (FC ≤ 5%)
[2] $70 \leq \Delta_Q < 90$ = SP-SM, SP-SC (FC ≈ 5-12%)
[3] $31 \leq \Delta_Q < 70$ = SM, SC, GM, GC (FC ≈ 12-50%)
[4] $19 \leq \Delta_Q < 31$ = ML, CL (FC > 50%, $D_{50} = 75\mu m$)
[5] $15 \leq \Delta_Q < 19$ = MH, CH (Liquid Limit, $w_L > 50$)
[6] $\Delta_Q < 15$ = OL, OH, Pt (Highly Organic Soil)

Classification Zone Schneider et al. 2012:
Zone-[1a] = Low-I_R clays ($I_R = G/S_u$)
Zone-[1b] = Clays
Zone-[1c] = Sensitive clays
Zone-[3] = Silts and transitional soils
Zone-[2] = Essentially drained sands

PDX Fuel Tank SVA
Portland, OR

Soil Classification Chart
Layer-3: 60 ft to 100 ft
SCPT-1 : (45.59739 , -122.61306)

0204679-001 July 2023

HALEY ALDRICH

Figure
B-14

\\haleyaldrich.com\share\pdx_data\Notebooks\0204679-001_PDX_Fuel_Project_Tank_Design\Analysis and Calcs\5 2D FLAC NDA\CPTBased Assessment\SCPT-1.pdf

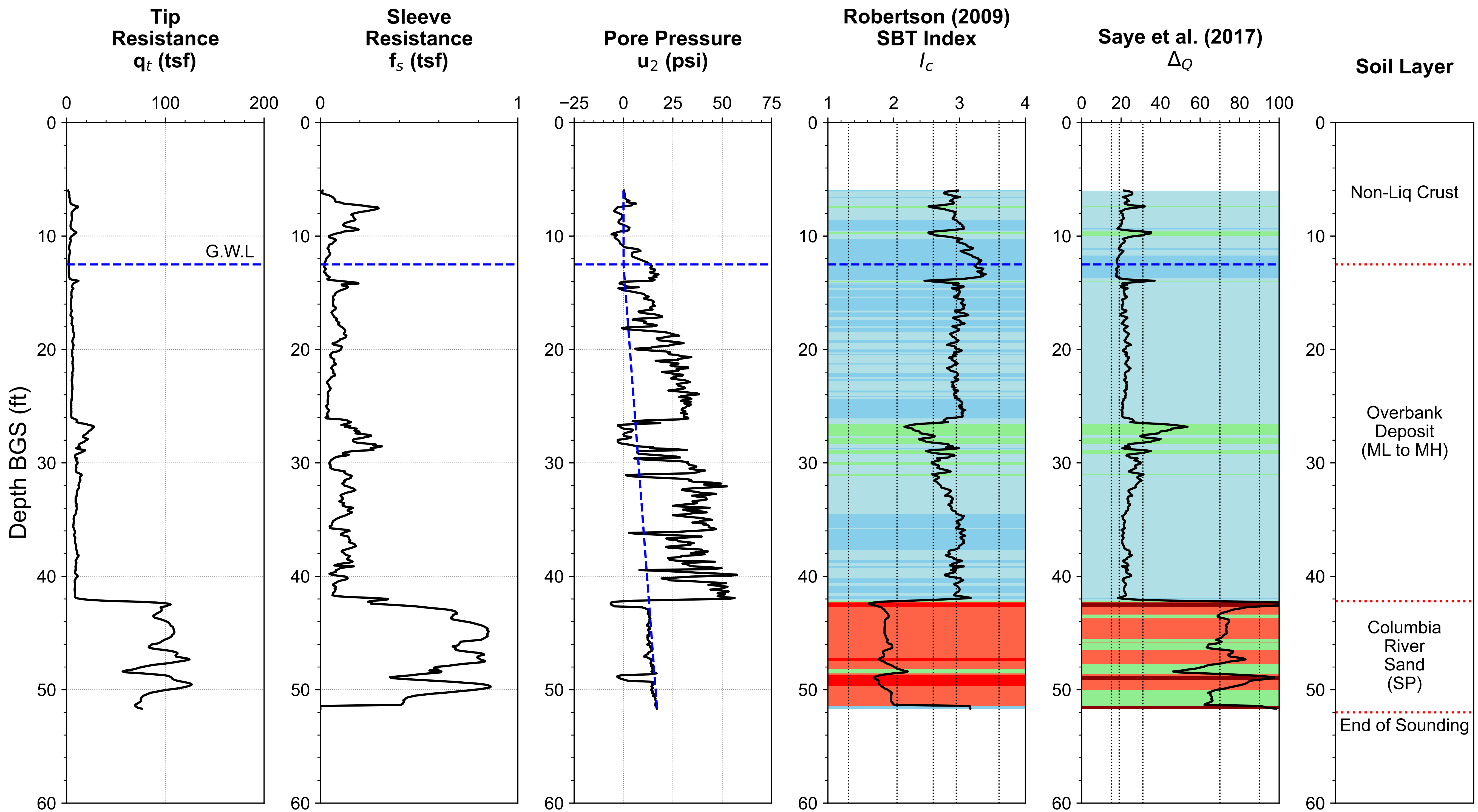

Robertson (2009) SBTn Zone:

- Gravelly Sands (I_c < 1.31)
- Clean sands (1.31 ≤ I_c < 1.8)
- Silty Sands (1.8 ≤ I_c < 2.05)
- Sand mixture: Sandy silt (2.05 ≤ I_c < 2.6)
- Silt mixture: Clayey silt to silty clay (2.6 ≤ I_c < 2.95)
- Clays (2.95 ≤ I_c ≤ 3.6)
- Organic Soils (I_c > 3.6)

Saye et al. (2017) Δ_Q Zone (Typical USCS):

- SP, SW (FC ≤ 5%, $\Delta_Q > 90$)
- SP-SM, SP-SC (FC ≈ 5-12%, $70 \leq \Delta_Q < 90$)
- SM, SC, GM, GC (FC ≈ 12-50%, $31 \leq \Delta_Q < 70$)
- ML, CL (FC > 50%, $D_{50} = 75\mu m$, $19 \leq \Delta_Q < 31$)
- MH, CH (Liquid Limit, $w_L > 50$, $15 \leq \Delta_Q < 19$)
- OL, OH, Pt (Highly Organic Soil, $\Delta_Q < 15$)

PDX Fuel Tank SVA
Portland, OR

CPT-Based Interpretation Summary
Basic Measurement
CPT-2 : (45.59709 , -122.61272)

0204679-001 July 2023

HALEY ALDRICH

Figure **B-15**

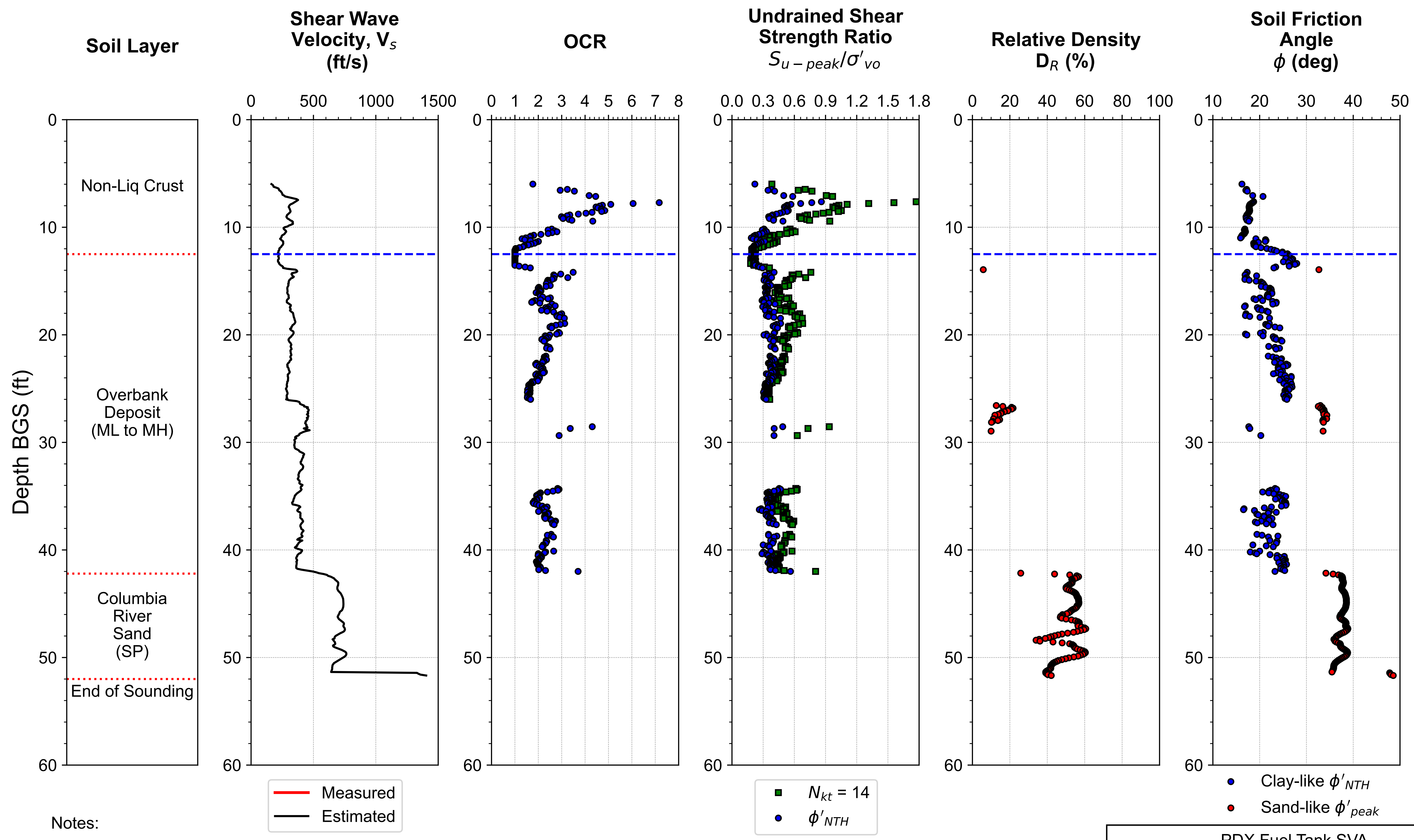

Notes:

1a. V_s is estimated using Robertson (2009) CPT-V_s Correlation
1b. Measured V_s is calculated using Slope method
2. OCR is determined using Agaiby & Mayne (2019) procedure
3a. S_{u-peak}/σ'_{vo} = ($q_t - \sigma_{vo}$) / ($N_{kt}\sigma'_{vo}$) and S_{u-peak}/σ'_{vo} = 0.5 sin(ϕ'_{NTH}) OCR $^{0.8}$
3b. N_{kt} = 14 ; ϕ_{NTH} = Effective friction angles calculated using modified NTH method (Ouyang & Mayne 2019)
4. Relative Density is estimated using Idriss & Boulanger 2008, Jamiolkowski et al. 2001, and Kulhawy & Mayne 1991 with weighting average factor 0.4, 0.3, 0.3, respectively
5. ϕ_{peak} = Peak friction angle calculated using Robertson (2010) equation for sandy soils, assuming ϕ'_{cv} = 33^o

PDX Fuel Tank SVA
Portland, OR

CPT-Based Interpretation Summary
Engineering Properties
CPT-2 : (45.59709 , -122.61272)

0204679-001 July 2023

HALEY ALDRICH

Figure **B-16**

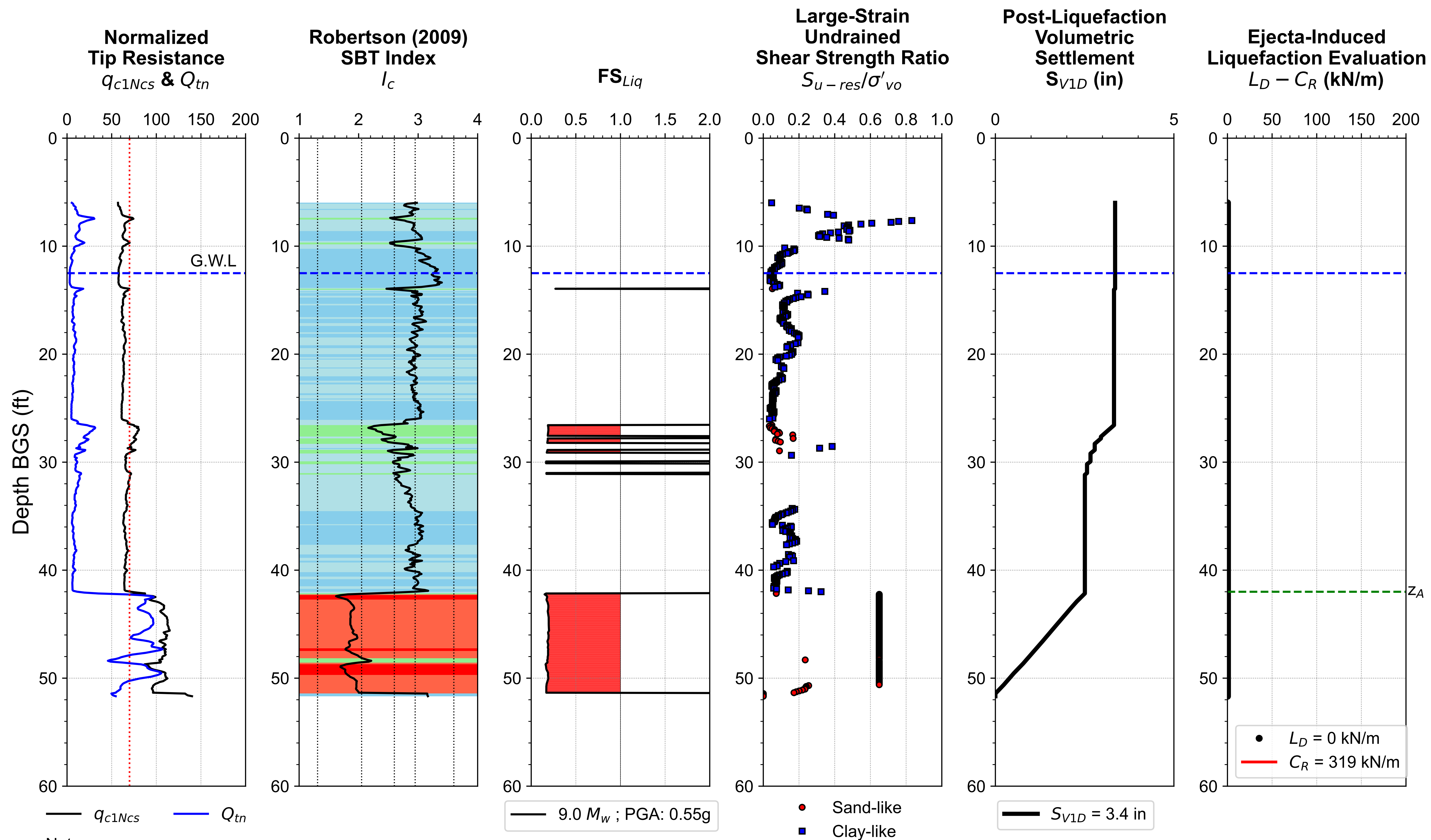

Notes:

1a. q_{c1Ncs}: Equivalent clean sand tip resistance following Boulanger & Idriss (2016) to estimate cyclic resistance ratio
1b. Q_{tn}: Normalized tip resistance following Robertson 2020 to estimate large-strain undrained shear strength ratio
2. FS_{Liq} is calculated using Boulanger & Idriss (2016) with P_{Liq} = 0.15 ; I_{c-cut} = 2.6 ; C_{FC} = 0.0
3. Large-strain undrained shear strength ratio is estimated using Robertson (2020) for clay-like and sand-like soil:
   Sand-like: Post-liquefied strength ratio (S_{u-liq}/σ'_{vo}) = tan (ϕ'_{cv}) for Q_{tn} > 70, where ϕ'_{cv} is assumed to be 33^o
   Clay-like: S_{u-res} is the same as remolded strength S_{u-rem}
4. Post-Liquefaction volumetric settlement is calculated using Zhang et al. (2002) procedure
5. Ejecta-induced settlement & severity are calculated based on Hutabarat & Bray (2022)

PDX Fuel Tank SVA
Portland, OR

CPT-based Liquefaction Evaluation
2475-yrs Hazard Level
CPT-2 : (45.59709 , -122.61272)

0204679-001 July 2023

HALEY ALDRICH

Figure
B-17

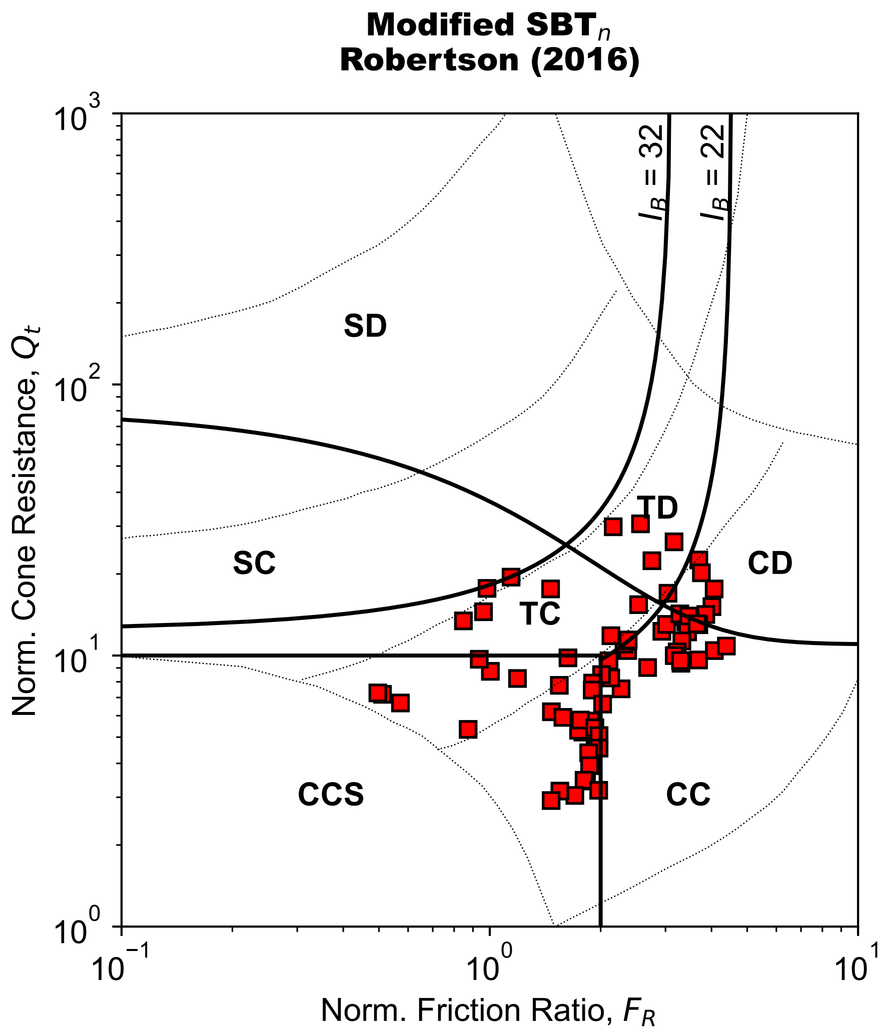

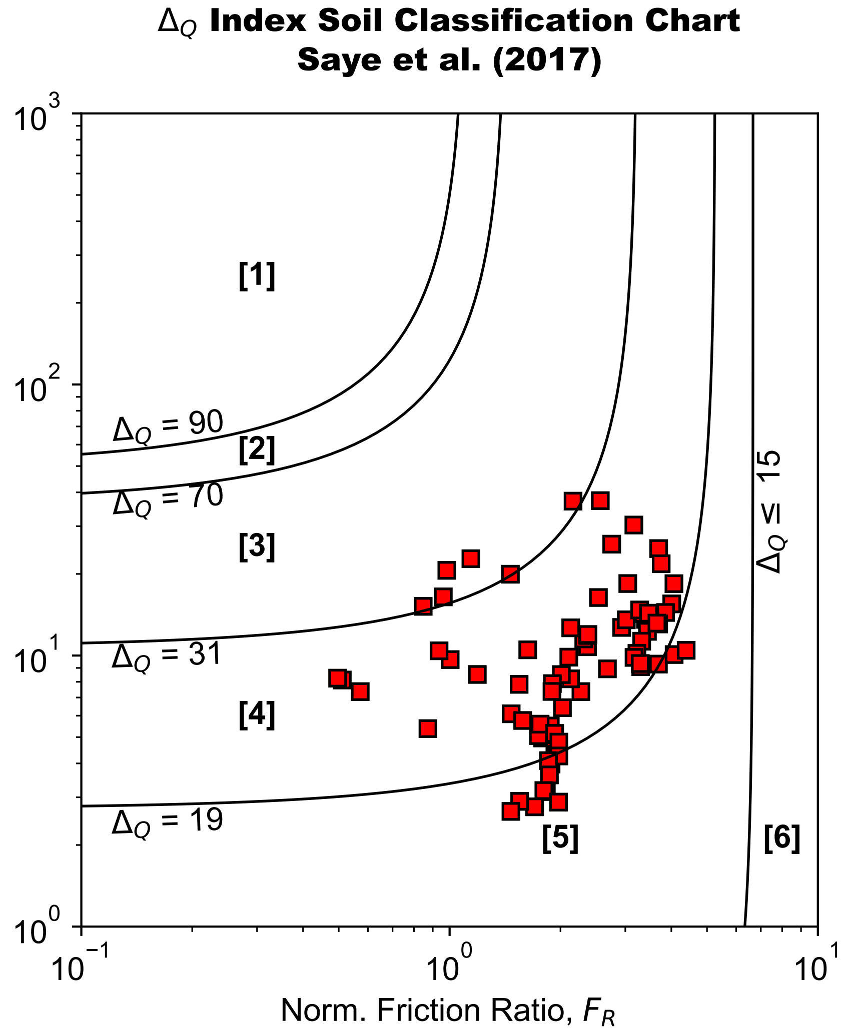

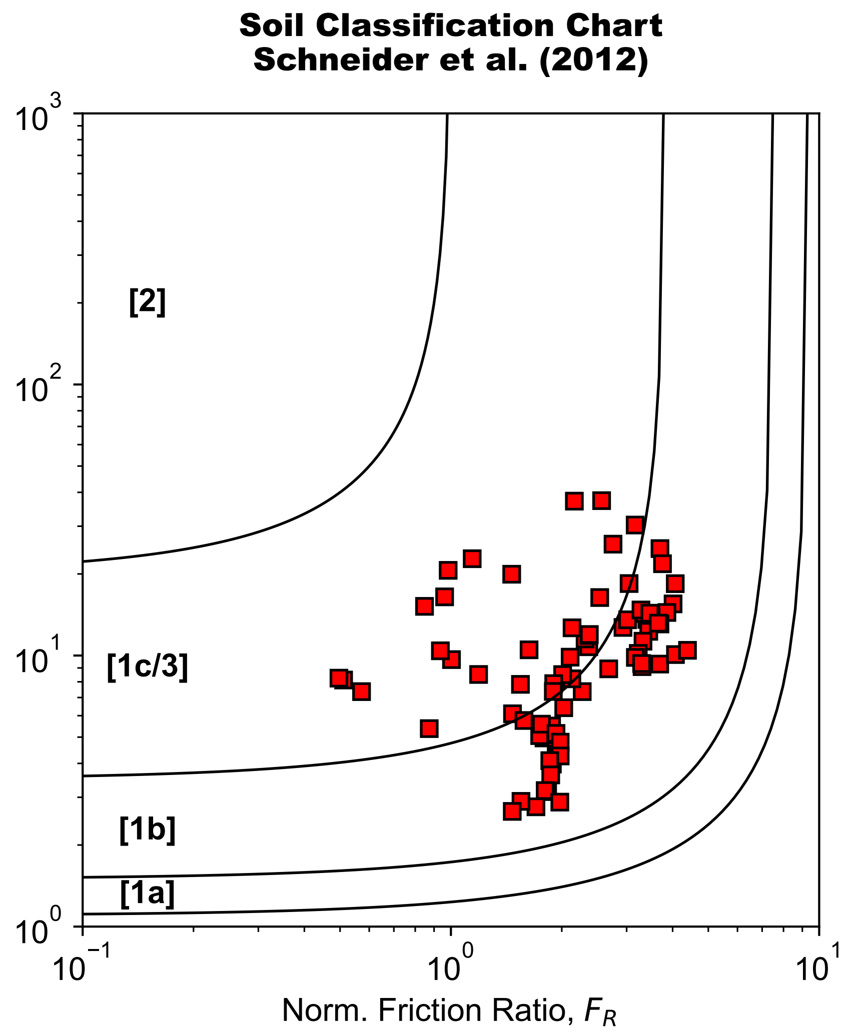

Robertson (2016) SBTn Zone:
SD = Sand-like - Dilative
SC = Sand-like - Contractive
TD = Transitional - Dilative
TC = Transitional - Contractive
CD = Clay-like - Dilative
CC = Clay-like - Contractive
CCS = Clay-like Contractive Sensitive

Typical USCS (Saye et al. 2017):
[1] $\Delta_Q > 90$ = SP, SW (FC $\leq$ 5%)
[2] $70 \leq \Delta_Q < 90$ = SP-SM, SP-SC (FC $\approx$ 5-12%)
[3] $31 \leq \Delta_Q < 70$ = SM, SC, GM, GC (FC $\approx$ 12-50%)
[4] $19 \leq \Delta_Q < 31$ = ML, CL (FC > 50%, $D_{50} = 75\mu$m)
[5] $15 \leq \Delta_Q < 19$ = MH, CH (Liquid Limit, $w_L > 50$)
[6] $\Delta_Q < 15$ = OL, OH, Pt (Highly Organic Soil)

Classification Zone Schneider et al. 2012:
Zone-[1a] = Low-I_R clays ($I_R = G/S_u$)
Zone-[1b] = Clays
Zone-[1c] = Sensitive clays
Zone-[3] = Silts and transitional soils
Zone-[2] = Essentially drained sands

PDX Fuel Tank SVA
Portland, OR

Soil Classification Chart
Layer-1: 6 ft to 12 ft
CPT-2 : (45.59709 , -122.61272)

0204679-001 July 2023

HALEY ALDRICH

Figure
B-18

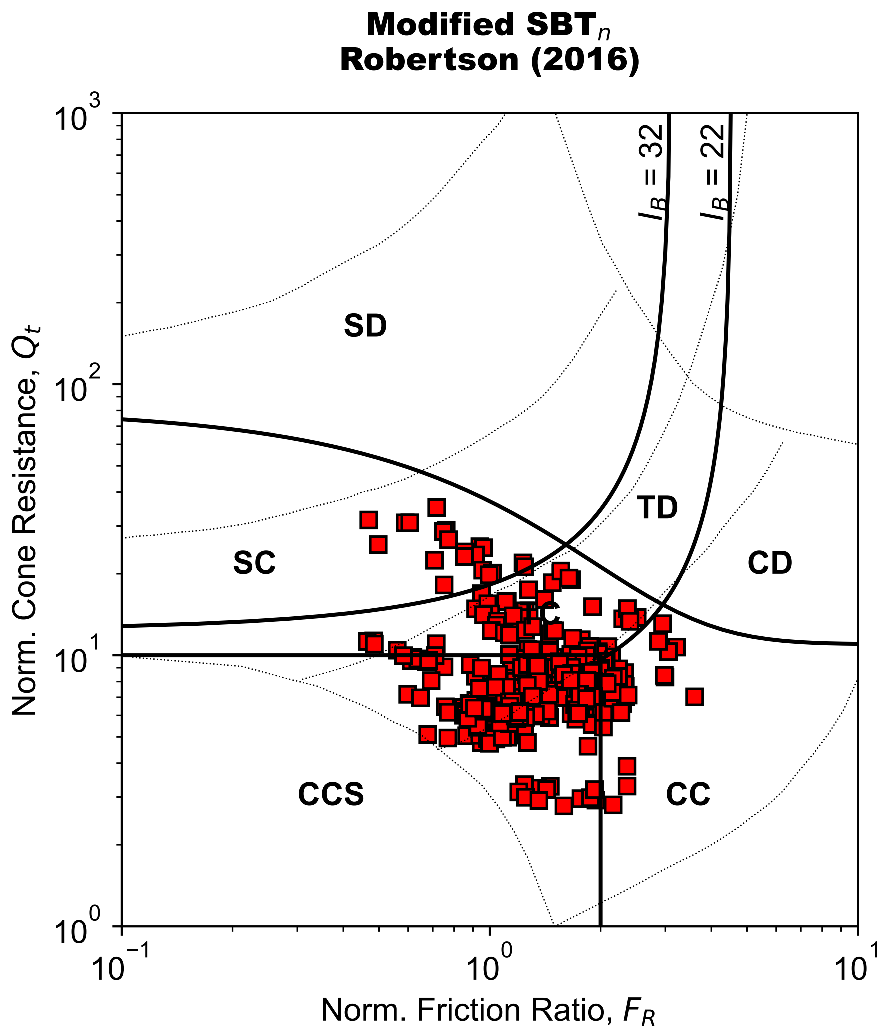

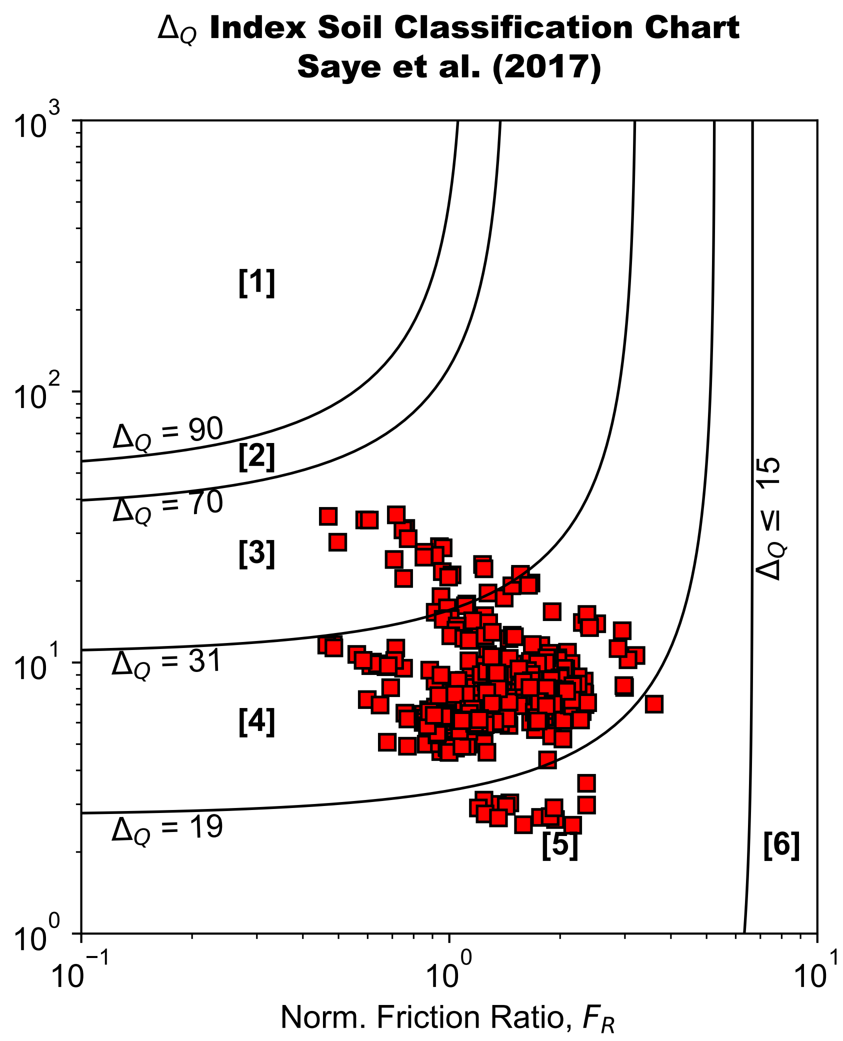

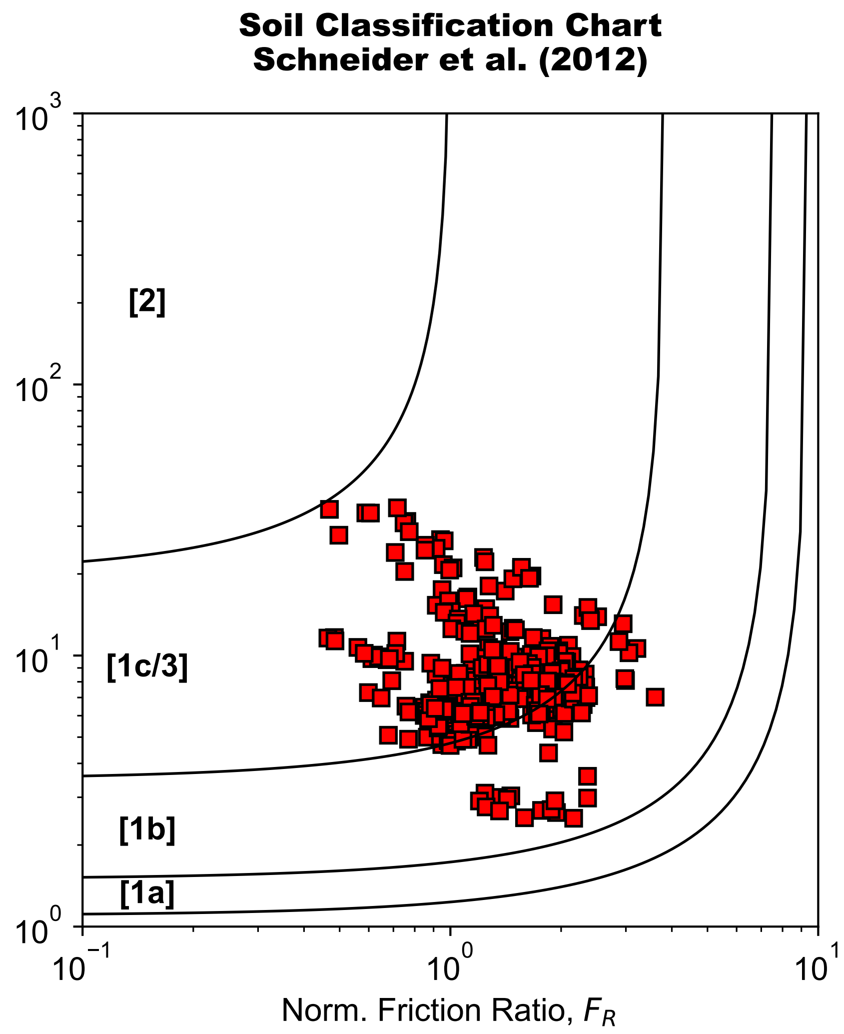

Robertson (2016) SBTn Zone:
SD = Sand-like - Dilative
SC = Sand-like - Contractive
TD = Transitional - Dilative
TC = Transitional - Contractive
CD = Clay-like - Dilative
CC = Clay-like - Contractive
CCS = Clay-like Contractive Sensitive

Typical USCS (Saye et al. 2017):
[1] $\Delta_Q > 90$ = SP, SW (FC ≤ 5%)
[2] $70 \leq \Delta_Q < 90$ = SP-SM, SP-SC (FC ≈ 5-12%)
[3] $31 \leq \Delta_Q < 70$ = SM, SC, GM, GC (FC ≈ 12-50%)
[4] $19 \leq \Delta_Q < 31$ = ML, CL (FC > 50%, $D_{50} = 75\mu$m)
[5] $15 \leq \Delta_Q < 19$ = MH, CH (Liquid Limit, $w_L > 50$)
[6] $\Delta_Q < 15$ = OL, OH, Pt (Highly Organic Soil)

Classification Zone Schneider et al. 2012:
Zone-[1a] = Low-I_R clays ($I_R = G/S_u$)
Zone-[1b] = Clays
Zone-[1c] = Sensitive clays
Zone-[3] = Silts and transitional soils
Zone-[2] = Essentially drained sands

PDX Fuel Tank SVA
Portland, OR

Soil Classification Chart
Layer-2: 12 ft to 42 ft
CPT-2 : (45.59709 , -122.61272)

0204679-001 July 2023

HALEY ALDRICH

Figure
B-19

Modified SBT$_n$
Robertson (2016)

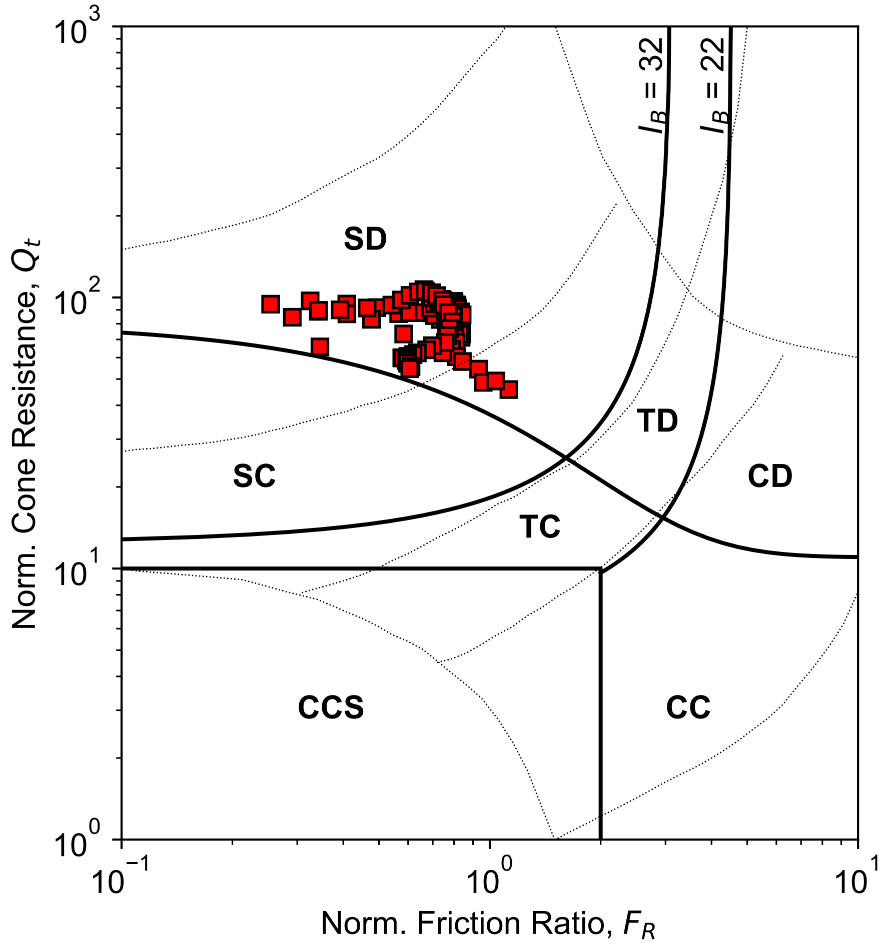

Δ_Q Index Soil Classification Chart
Saye et al. (2017)

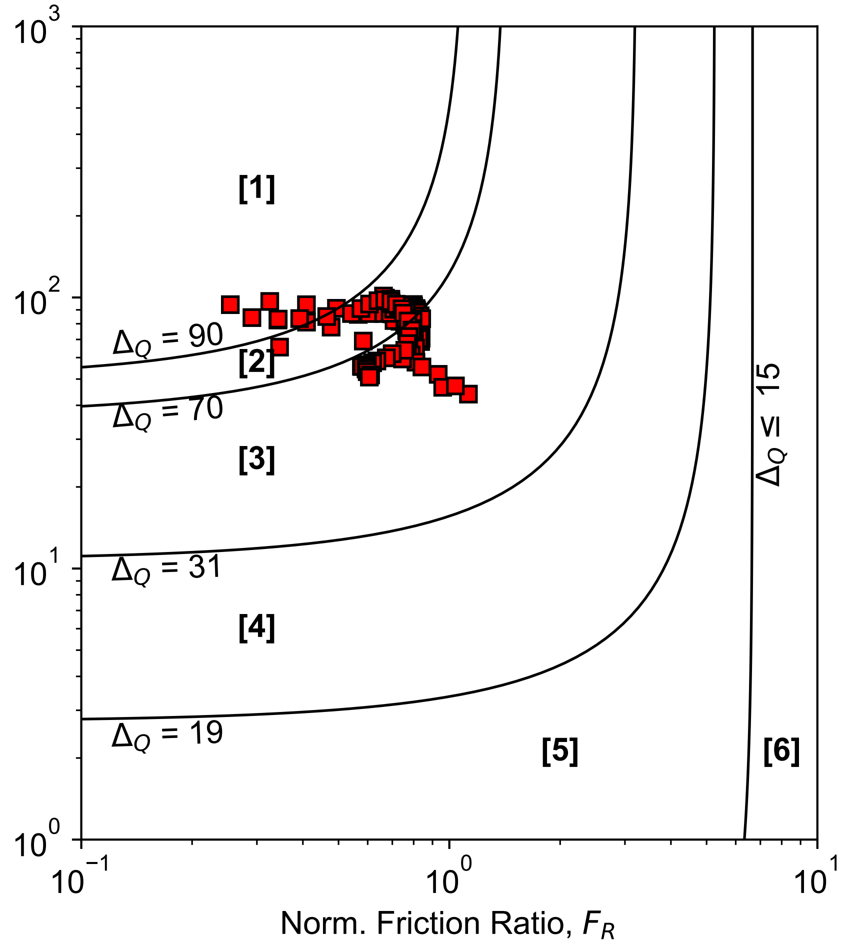

Soil Classification Chart
Schneider et al. (2012)

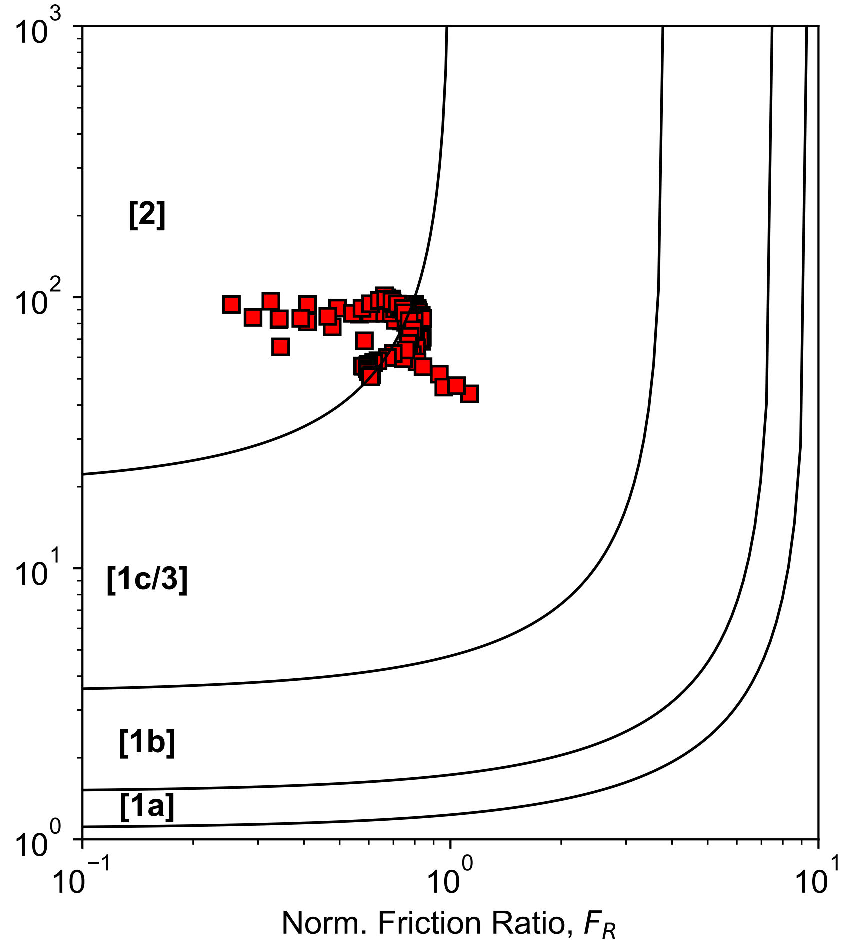

Robertson (2016) SBTn Zone:
SD = Sand-like - Dilative
SC = Sand-like - Contractive
TD = Transitional - Dilative
TC = Transitional - Contractive
CD = Clay-like - Dilative
CC = Clay-like - Contractive
CCS = Clay-like Contractive Sensitive

Typical USCS (Saye et al. 2017):
[1] $\Delta_Q > 90$ = SP, SW (FC ≤ 5%)
[2] $70 \leq \Delta_Q < 90$ = SP-SM, SP-SC (FC ≈ 5-12%)
[3] $31 \leq \Delta_Q < 70$ = SM, SC, GM, GC (FC ≈ 12-50%)
[4] $19 \leq \Delta_Q < 31$ = ML, CL (FC > 50%, $D_{50} = 75\mu$m)
[5] $15 \leq \Delta_Q < 19$ = MH, CH (Liquid Limit, $w_L > 50$)
[6] $\Delta_Q < 15$ = OL, OH, Pt (Highly Organic Soil)

Classification Zone Schneider et al. 2012:
Zone-[1a] = Low-I_R clays ($I_R = G/S_u$)
Zone-[1b] = Clays
Zone-[1c] = Sensitive clays
Zone-[3] = Silts and transitional soils
Zone-[2] = Essentially drained sands

PDX Fuel Tank SVA
Portland, OR

Soil Classification Chart
Layer-3: 42 ft to 52 ft
CPT-2 : (45.59709 , -122.61272)

0204679-001 July 2023

HALEY ALDRICH

Figure
B-20

\\haleyaldrich.com\share\pdx_data\Notebooks\0204679-001_PDX_Fuel_Project_Tank_Design\Analysis and Calcs\5 2D FLAC NDA\CPTBased Assessment\CPT-2.pdf

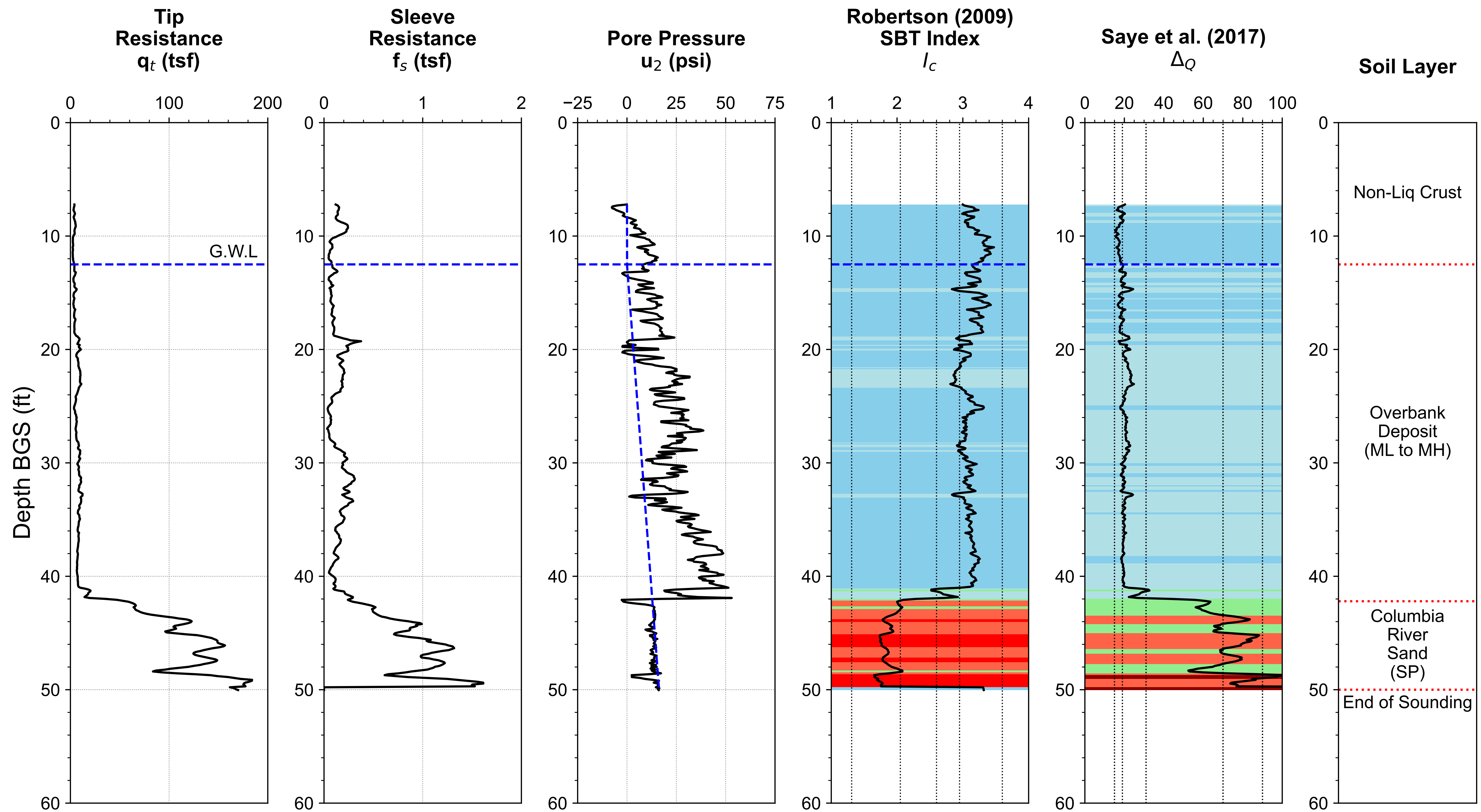

Robertson (2009) SBTn Zone:

- Gravelly Sands ($I_c < 1.31$)
- Clean sands ($1.31 \leq I_c < 1.8$)
- Silty Sands ($1.8 \leq I_c < 2.05$)
- Sand mixture: Sandy silt ($2.05 \leq I_c < 2.6$)
- Silt mixture: Clayey silt to silty clay ($2.6 \leq I_c < 2.95$)
- Clays ($2.95 \leq I_c \leq 3.6$)
- Organic Soils ($I_c > 3.6$)

Saye et al. (2017) Δ_Q Zone (Typical USCS):

- SP, SW (FC ≤ 5%, $\Delta_Q > 90$)
- SP-SM, SP-SC (FC ≈ 5-12%, $70 \leq \Delta_Q < 90$)
- SM, SC, GM, GC (FC ≈ 12-50%, $31 \leq \Delta_Q < 70$)
- ML, CL (FC > 50%, $D_{50} = 75\mu m$, $19 \leq \Delta_Q < 31$)
- MH, CH (Liquid Limit, $w_L > 50$, $15 \leq \Delta_Q < 19$)
- OL, OH, Pt (Highly Organic Soil, $\Delta_Q < 15$)

PDX Fuel Tank SVA
Portland, OR

CPT-Based Interpretation Summary
Basic Measurement
CPT-3 : (45.59653 , -122.61285)

0204679-001 July 2023

HALEY ALDRICH

Figure
B-21

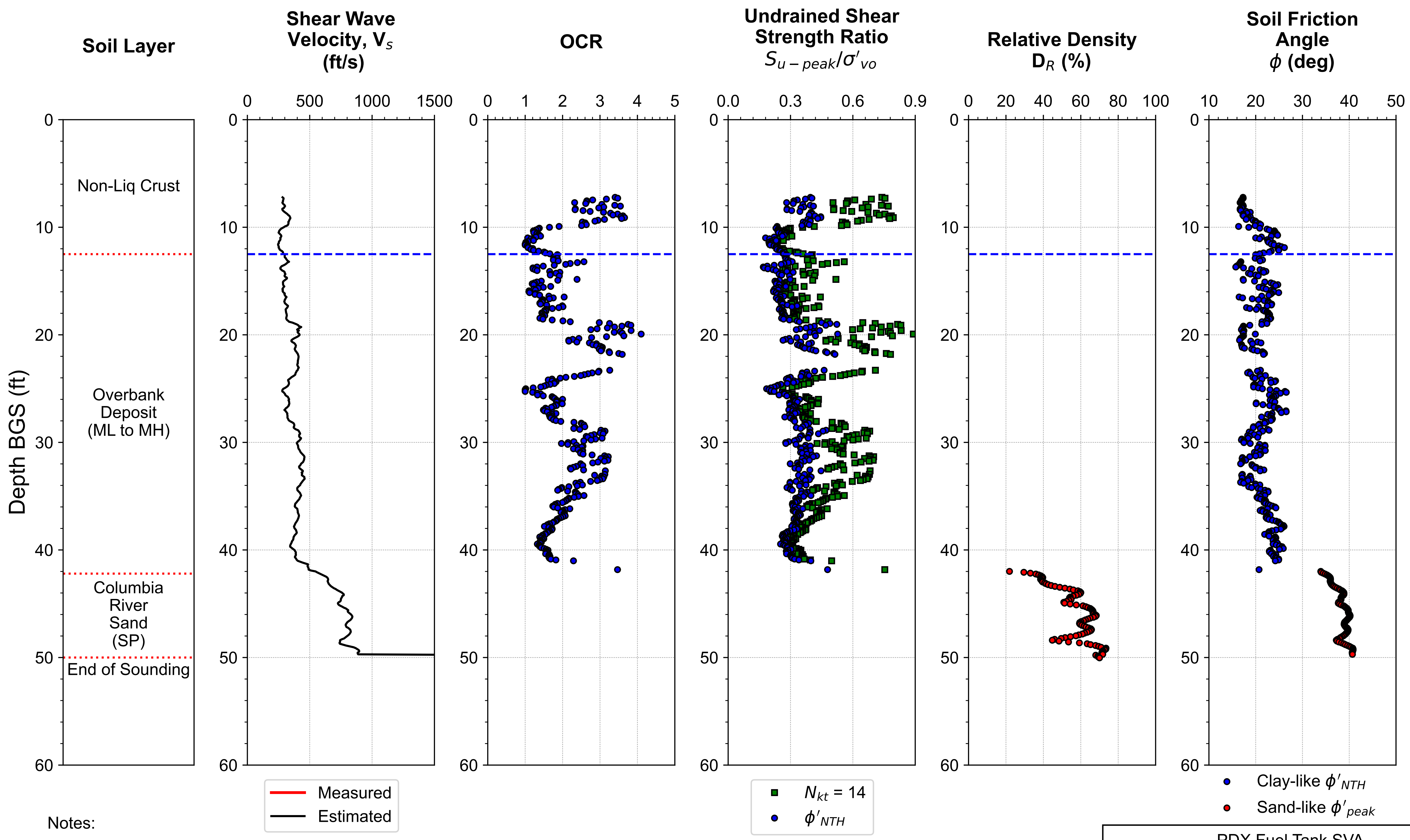

Notes:

1a. V_s is estimated using Robertson (2009) CPT-V_s Correlation
1b. Measured V_s is calculated using Slope method
2. OCR is determined using Agaiby & Mayne (2019) procedure
3a. S_{u-peak}/σ'_{vo} = ($q_t - \sigma_{vo}$) / ($N_{kt}\sigma'_{vo}$) and S_{u-peak}/σ'_{vo} = 0.5 sin(ϕ'_{NTH}) OCR $^{0.8}$
3b. N_{kt} = 14 ; ϕ_{NTH} = Effective friction angles calculated using modified NTH method (Ouyang & Mayne 2019)
4. Relative Density is estimated using Idriss & Boulanger 2008, Jamiolkowski et al. 2001, and Kulhawy & Mayne 1991 with weighting average factor 0.4, 0.3, 0.3, respectively
5. ϕ_{peak} = Peak friction angle calculated using Robertson (2010) equation for sandy soils, assuming ϕ'_{cv} = 33^o

PDX Fuel Tank SVA
Portland, OR

CPT-Based Interpretation Summary
Engineering Properties
CPT-3 : (45.59653 , -122.61285)

0204679-001 July 2023

HALEY ALDRICH

Figure **B-22**

FOR REFERENCE ONLY

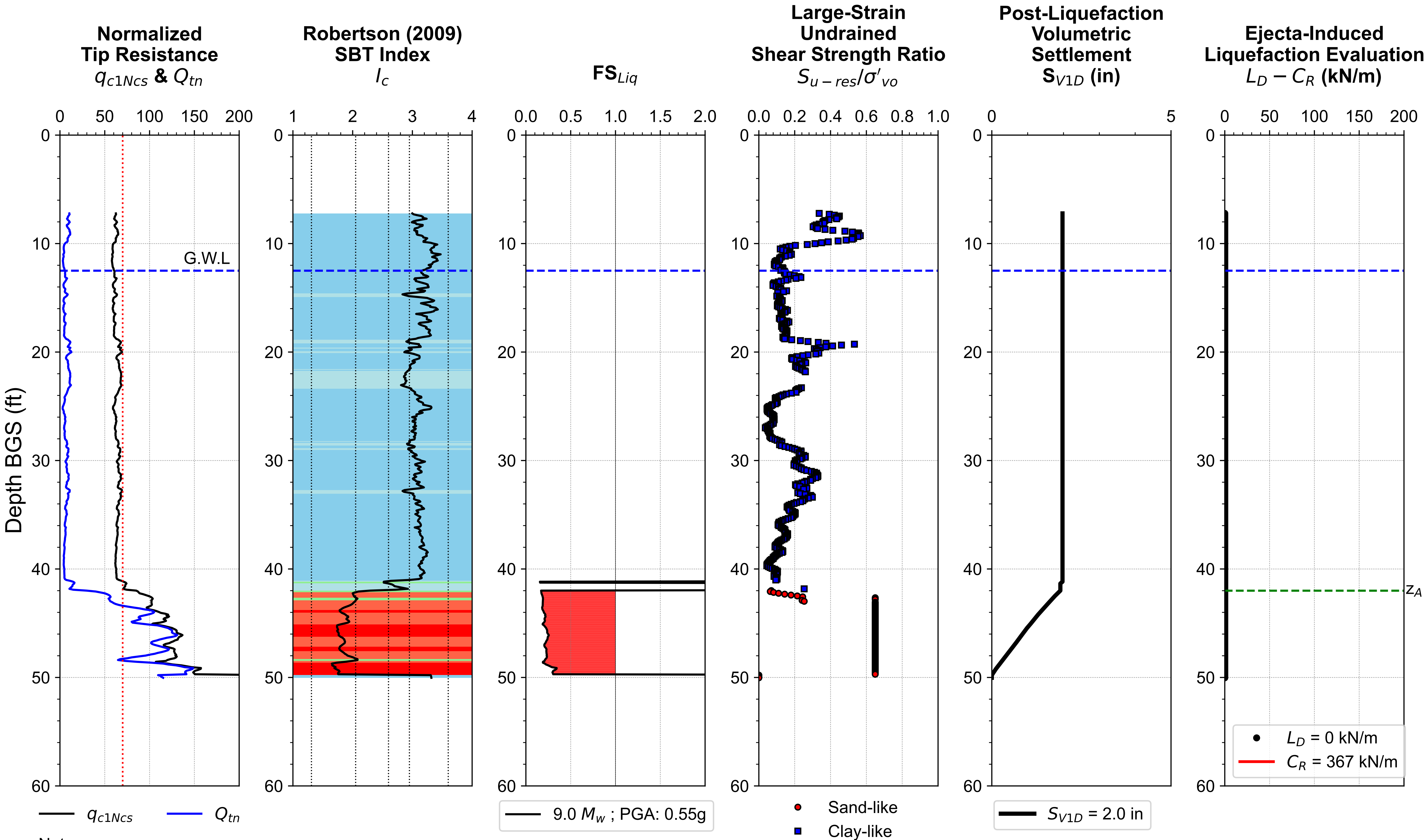

Notes:

1a. q_{c1Ncs}: Equivalent clean sand tip resistance following Boulanger & Idriss (2016) to estimate cyclic resistance ratio
1b. Q_{tn}: Normalized tip resistance following Robertson 2020 to estimate large-strain undrained shear strength ratio
2. FS_{Liq} is calculated using Boulanger & Idriss (2016) with P_{Liq} = 0.15 ; I_{c-cut} = 2.6 ; C_{FC} = 0.0
3. Large-strain undrained shear strength ratio is estimated using Robertson (2020) for clay-like and sand-like soil:
   Sand-like: Post-liquefied strength ratio (S_{u-liq}/σ'_{vo}) = tan (ϕ'_{cv}) for Q_{tn} > 70, where ϕ'_{cv} is assumed to be 33^o
   Clay-like: S_{u-res} is the same as remolded strength S_{u-rem}
4. Post-Liquefaction volumetric settlement is calculated using Zhang et al. (2002) procedure
5. Ejecta-induced settlement & severity are calculated based on Hutabarat & Bray (2022)

PDX Fuel Tank SVA
Portland, OR

CPT-based Liquefaction Evaluation
2475-yrs Hazard Level
CPT-3 : (45.59653 , -122.61285)

0204679-001 July 2023

HALEY ALDRICH

Figure **B-23**

\\haleyaldrich.com\share\pdx_data\Notebooks\0204679-001_PDX_Fuel_Project_Tank_Design\Analysis and Calcs\5 2D FLAC NDA\CPTBased Assessment\CPT-3.pdf

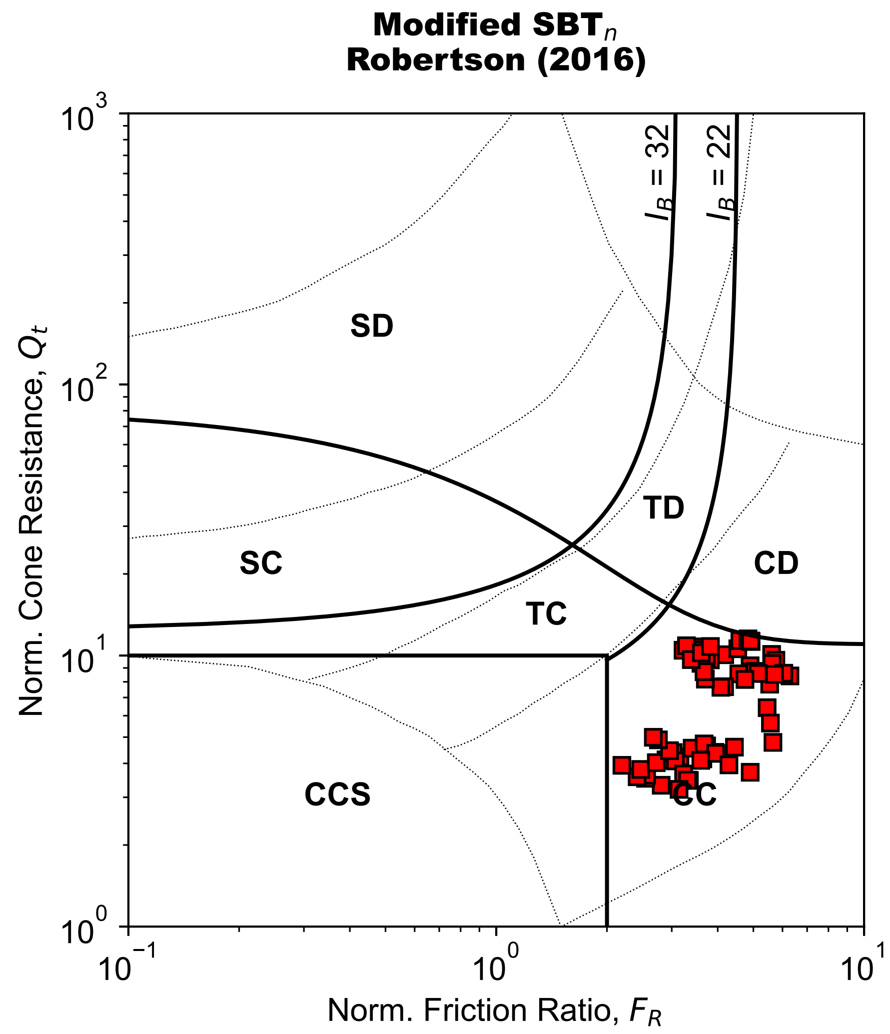

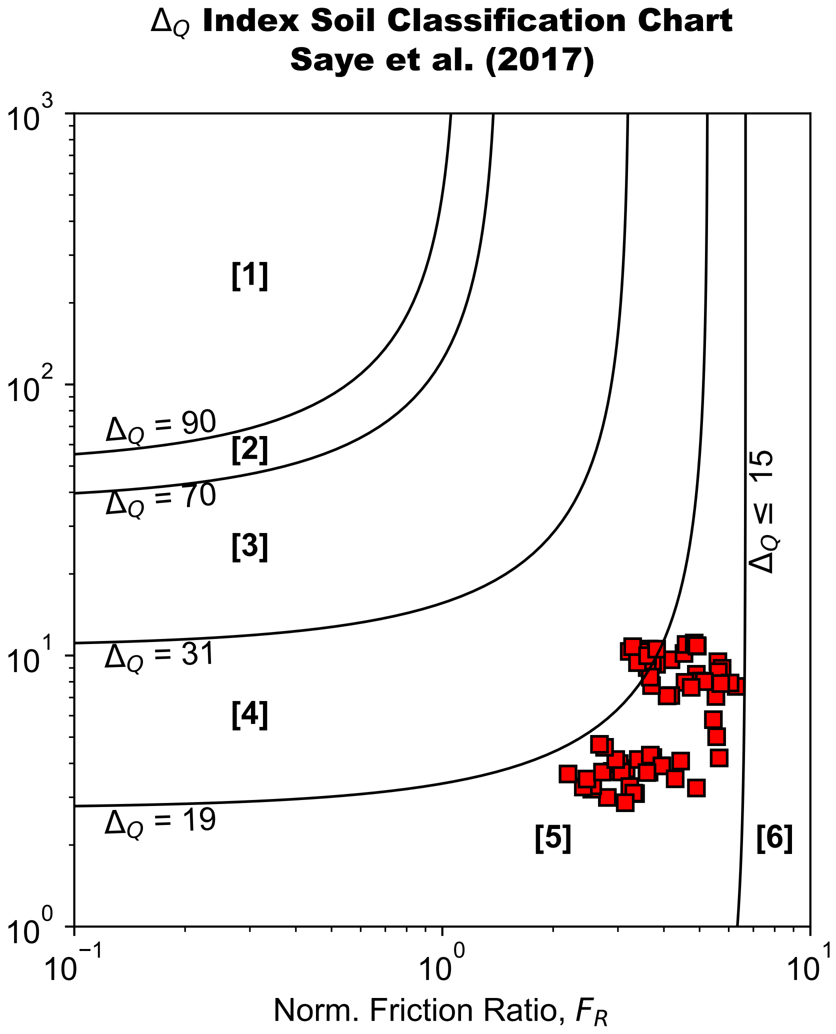

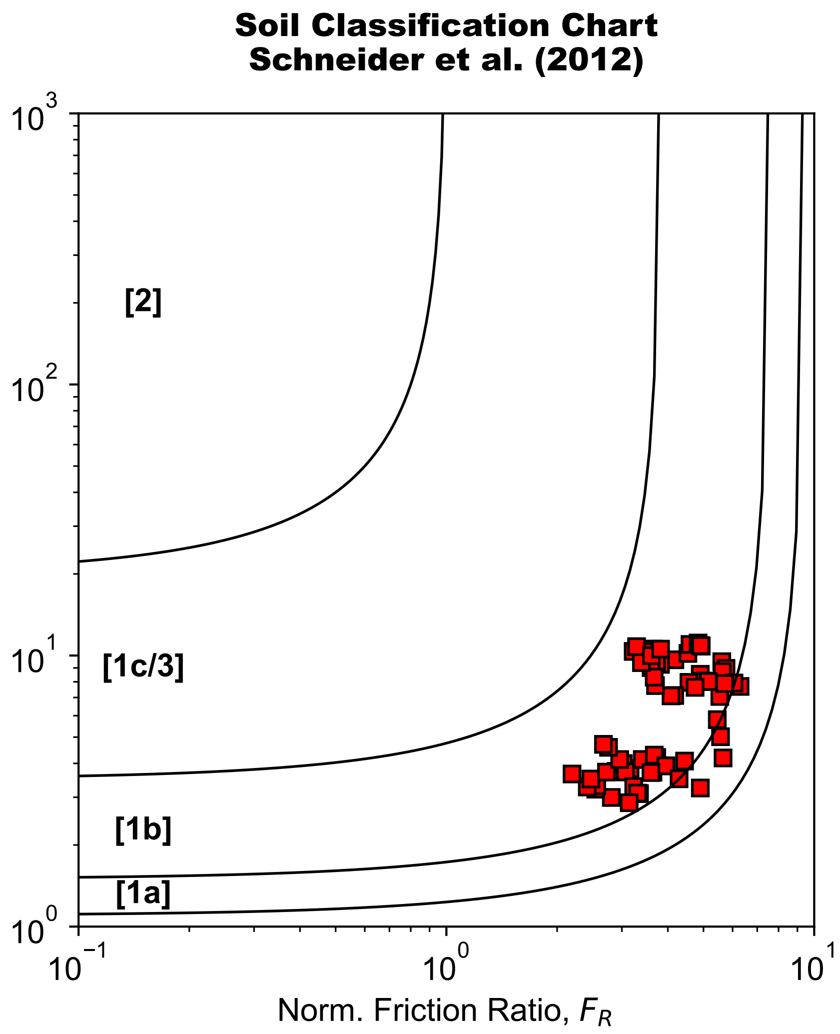

Robertson (2016) SBTn Zone:
SD = Sand-like - Dilative
SC = Sand-like - Contractive
TD = Transitional - Dilative
TC = Transitional - Contractive
CD = Clay-like - Dilative
CC = Clay-like - Contractive
CCS = Clay-like Contractive Sensitive

Typical USCS (Saye et al. 2017):
[1] $\Delta_Q > 90$ = SP, SW (FC $\leq$ 5%)
[2] $70 \leq \Delta_Q < 90$ = SP-SM, SP-SC (FC $\approx$ 5-12%)
[3] $31 \leq \Delta_Q < 70$ = SM, SC, GM, GC (FC $\approx$ 12-50%)
[4] $19 \leq \Delta_Q < 31$ = ML, CL (FC > 50%, $D_{50} = 75\mu$m)
[5] $15 \leq \Delta_Q < 19$ = MH, CH (Liquid Limit, $w_L > 50$)
[6] $\Delta_Q < 15$ = OL, OH, Pt (Highly Organic Soil)

Classification Zone Schneider et al. 2012:
Zone-[1a] = Low-I_R clays ($I_R = G/S_u$)
Zone-[1b] = Clays
Zone-[1c] = Sensitive clays
Zone-[3] = Silts and transitional soils
Zone-[2] = Essentially drained sands

PDX Fuel Tank SVA
Portland, OR

Soil Classification Chart
Layer-1: 7 ft to 12 ft
CPT-3 : (45.59653 , -122.61285)

0204679-001 July 2023

HALEY ALDRICH

Figure
B-24

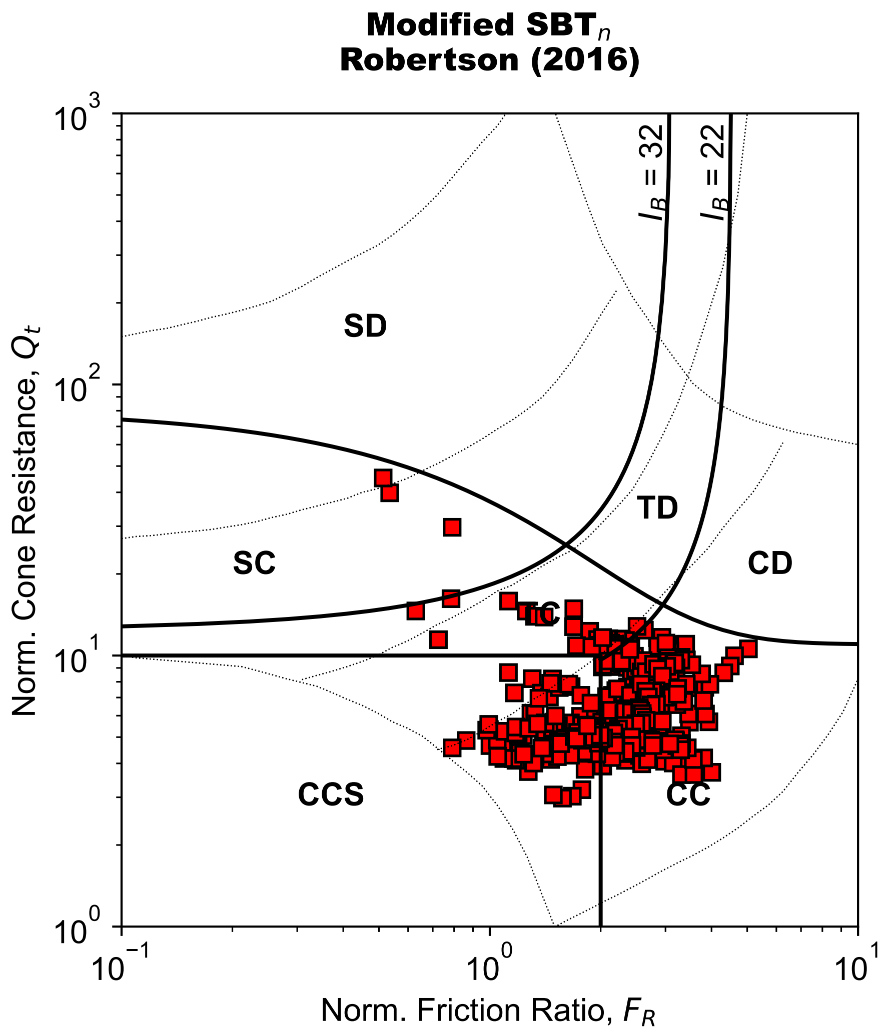

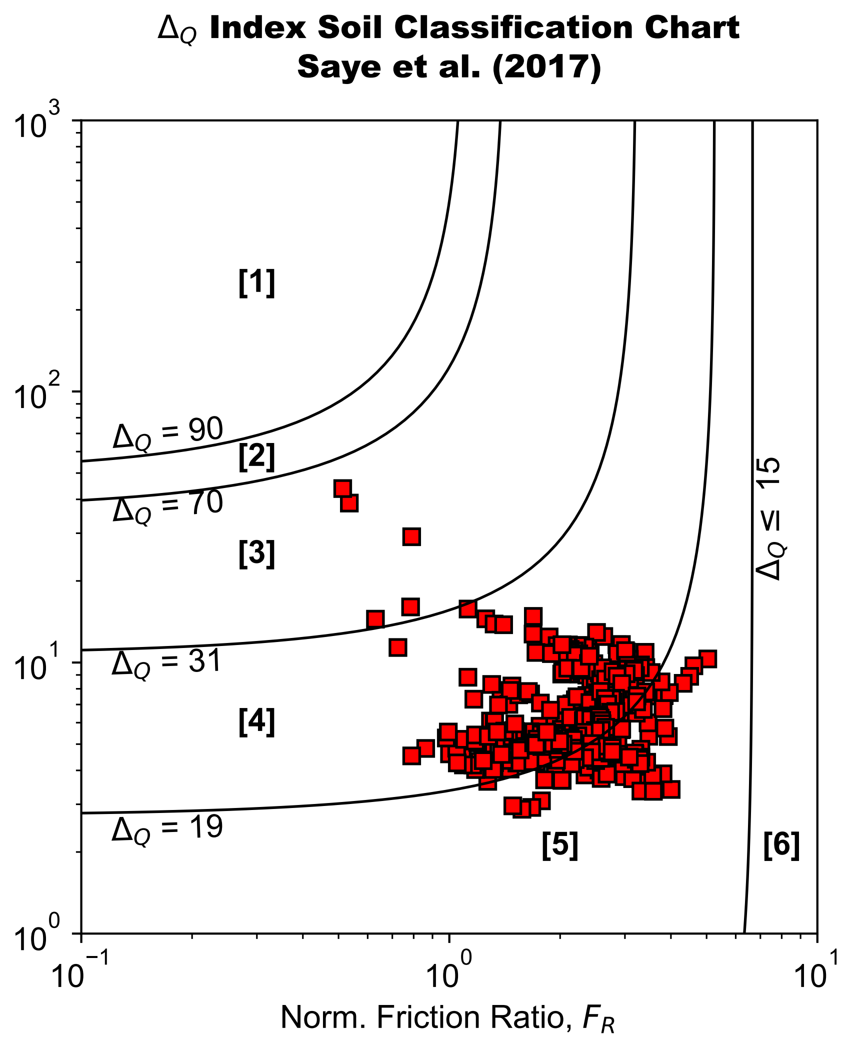

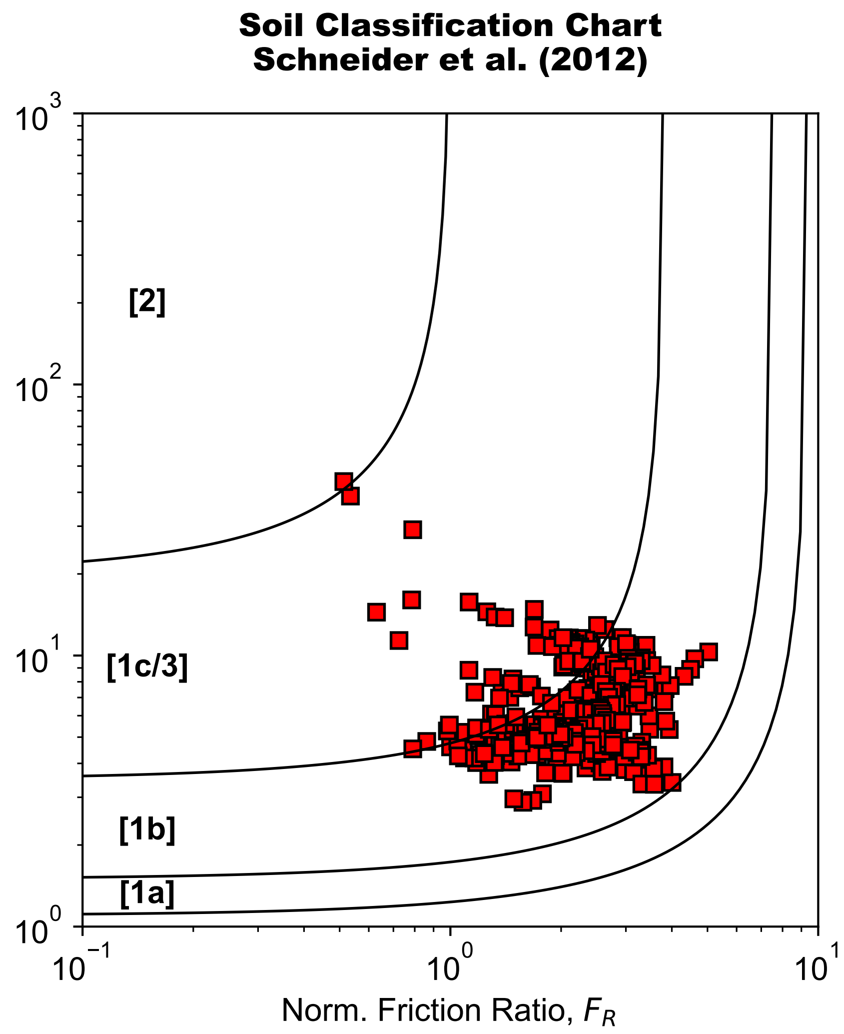

Robertson (2016) SBTn Zone:
SD = Sand-like - Dilative
SC = Sand-like - Contractive
TD = Transitional - Dilative
TC = Transitional - Contractive
CD = Clay-like - Dilative
CC = Clay-like - Contractive
CCS = Clay-like Contractive Sensitive

Typical USCS (Saye et al. 2017):
[1] $\Delta_Q > 90$ = SP, SW (FC ≤ 5%)
[2] $70 \leq \Delta_Q < 90$ = SP-SM, SP-SC (FC ≈ 5-12%)
[3] $31 \leq \Delta_Q < 70$ = SM, SC, GM, GC (FC ≈ 12-50%)
[4] $19 \leq \Delta_Q < 31$ = ML, CL (FC > 50%, $D_{50} = 75\mu$m)
[5] $15 \leq \Delta_Q < 19$ = MH, CH (Liquid Limit, $w_L > 50$)
[6] $\Delta_Q < 15$ = OL, OH, Pt (Highly Organic Soil)

Classification Zone Schneider et al. 2012:
Zone-[1a] = Low-I_R clays ($I_R = G/S_u$)
Zone-[1b] = Clays
Zone-[1c] = Sensitive clays
Zone-[3] = Silts and transitional soils
Zone-[2] = Essentially drained sands

PDX Fuel Tank SVA
Portland, OR

Soil Classification Chart
Layer-2: 12 ft to 42 ft
CPT-3 : (45.59653 , -122.61285)

0204679-001 July 2023

HALEY ALDRICH

Figure
B-25

\\haleyaldrich.com\share\pdx_data\Notebooks\0204679-001_PDX_Fuel_Project_Tank_Design\Analysis and Calcs\5 2D FLAC NDA\CPTBased Assessment\CPT-3.pdf

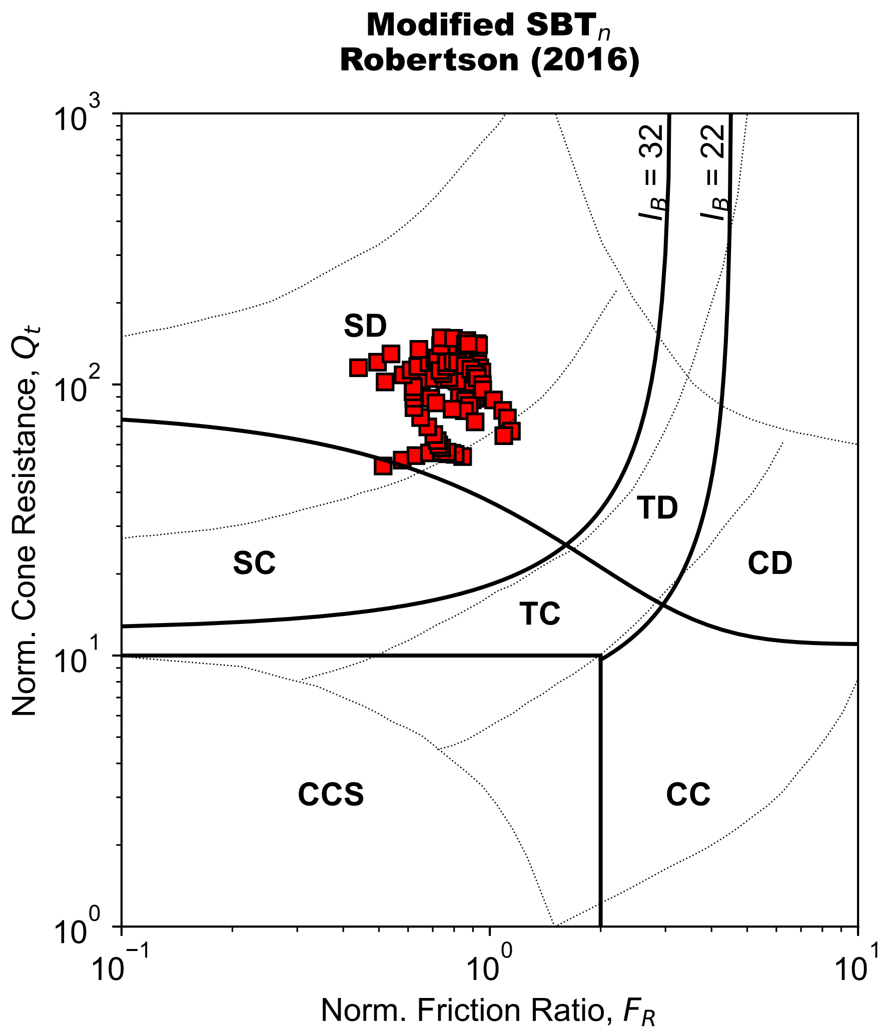

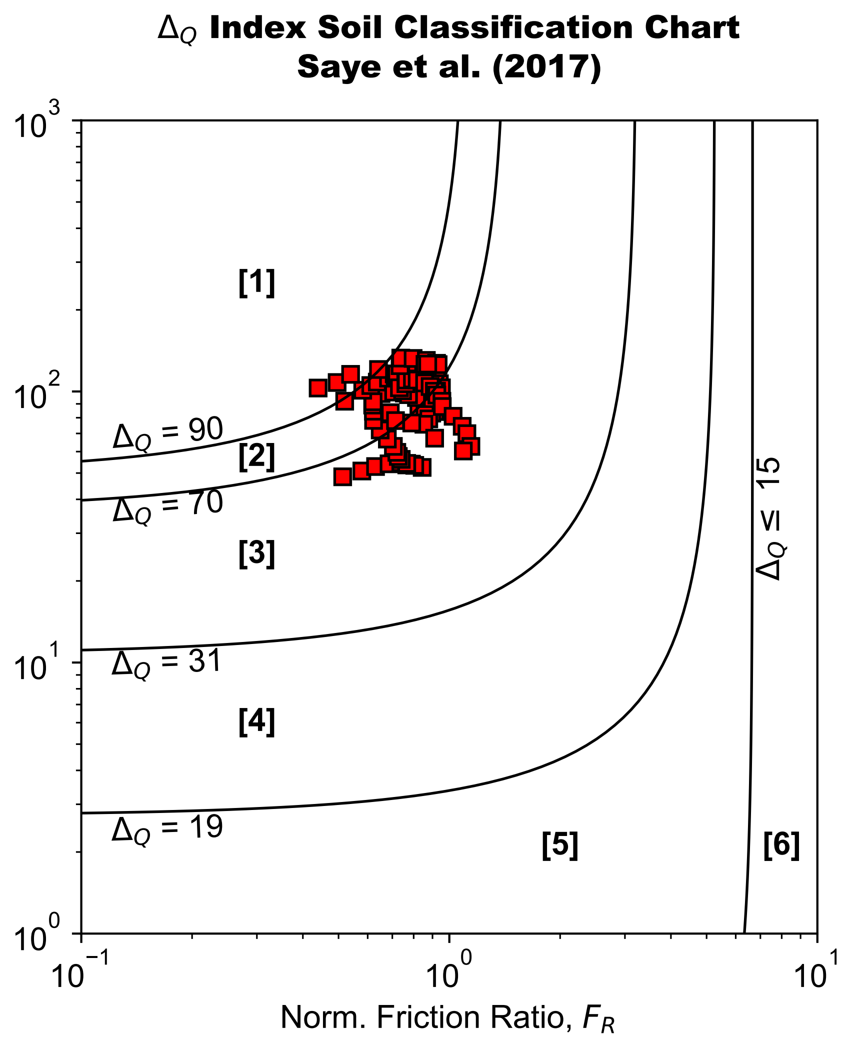

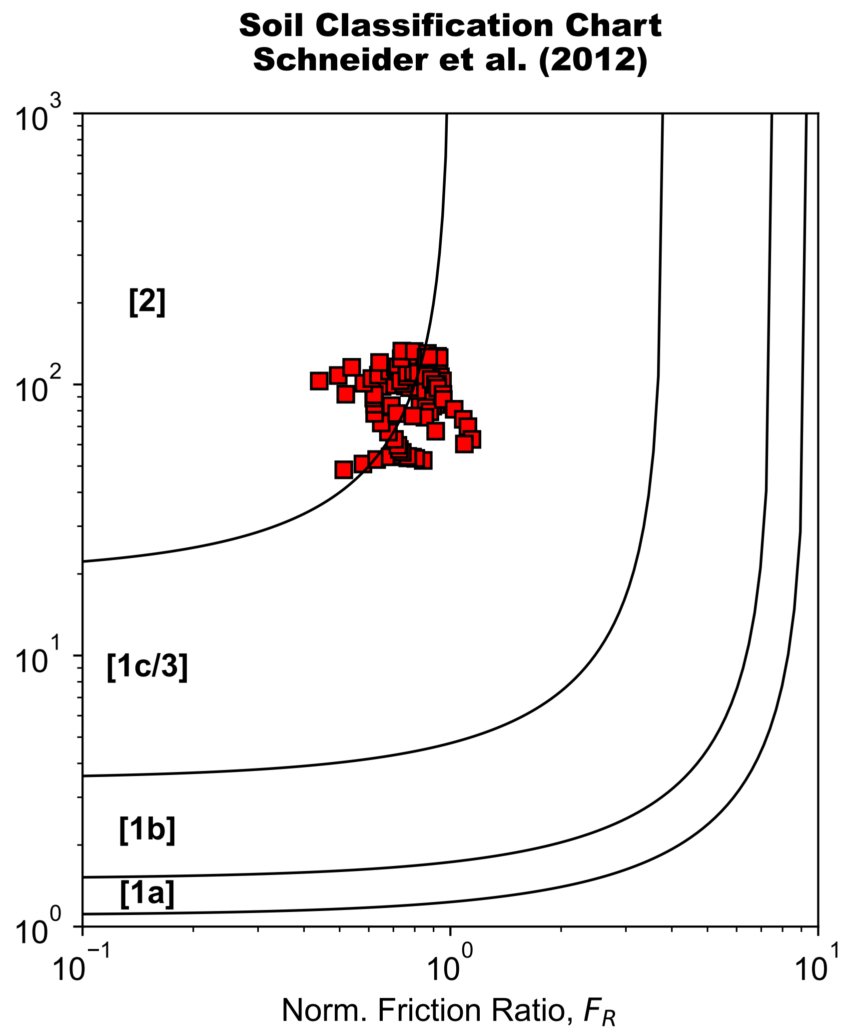

Robertson (2016) SBTn Zone:
SD = Sand-like - Dilative
SC = Sand-like - Contractive
TD = Transitional - Dilative
TC = Transitional - Contractive
CD = Clay-like - Dilative
CC = Clay-like - Contractive
CCS = Clay-like Contractive Sensitive

Typical USCS (Saye et al. 2017):
[1] $\Delta_Q > 90$ = SP, SW (FC ≤ 5%)
[2] $70 \leq \Delta_Q < 90$ = SP-SM, SP-SC (FC ≈ 5-12%)
[3] $31 \leq \Delta_Q < 70$ = SM, SC, GM, GC (FC ≈ 12-50%)
[4] $19 \leq \Delta_Q < 31$ = ML, CL (FC > 50%, $D_{50} = 75\mu$m)
[5] $15 \leq \Delta_Q < 19$ = MH, CH (Liquid Limit, $w_L > 50$)
[6] $\Delta_Q < 15$ = OL, OH, Pt (Highly Organic Soil)

Classification Zone Schneider et al. 2012:
Zone-[1a] = Low-I_R clays (I_R = G/S_u)
Zone-[1b] = Clays
Zone-[1c] = Sensitive clays
Zone-[3] = Silts and transitional soils
Zone-[2] = Essentially drained sands

PDX Fuel Tank SVA
Portland, OR

Soil Classification Chart
Layer-3: 42 ft to 50 ft
CPT-3 : (45.59653 , -122.61285)

0204679-001 July 2023

HALEY ALDRICH

Figure
B-26

\\haleyaldrich.com\share\pdx_data\Notebooks\0204679-001_PDX_Fuel_Project_Tank_Design\Analysis and Calcs\5 2D FLAC NDA\CPTBased Assessment\CPT-3.pdf

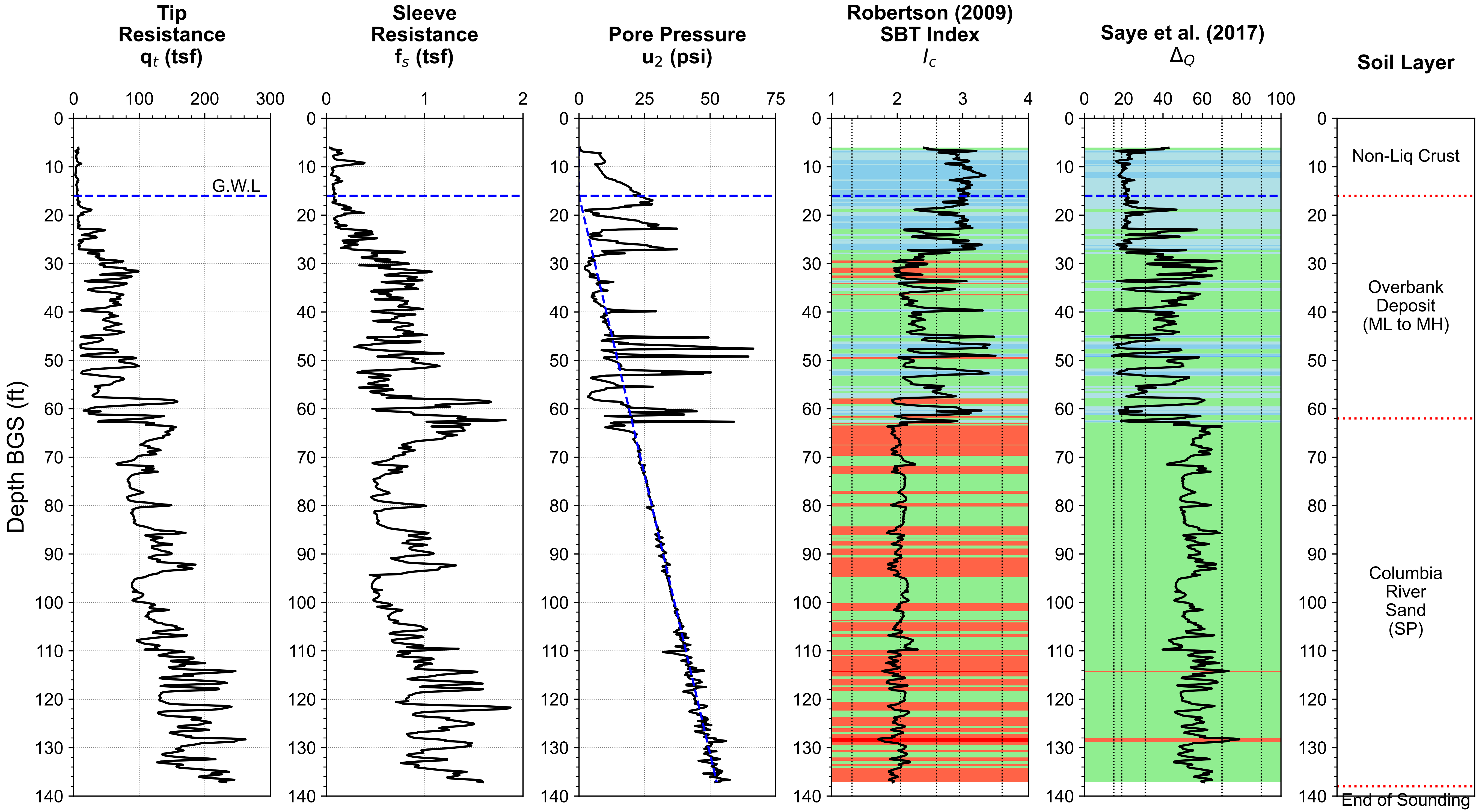

Robertson (2009) SBTn Zone:

- Gravelly Sands ($I_c < 1.31$)
- Clean sands ($1.31 \leq I_c < 1.8$)
- Silty Sands ($1.8 \leq I_c < 2.05$)
- Sand mixture: Sandy silt ($2.05 \leq I_c < 2.6$)
- Silt mixture: Clayey silt to silty clay ($2.6 \leq I_c < 2.95$)
- Clays ($2.95 \leq I_c \leq 3.6$)
- Organic Soils ($I_c > 3.6$)

Saye et al. (2017) Δ_Q Zone (Typical USCS):

- SP, SW (FC $\leq$ 5%, $\Delta_Q > 90$)
- SP-SM, SP-SC (FC $\approx$ 5-12%, $70 \leq \Delta_Q < 90$)
- SM, SC, GM, GC (FC $\approx$ 12-50%, $31 \leq \Delta_Q < 70$)
- ML, CL (FC > 50%, $D_{50} = 75\mu m$, $19 \leq \Delta_Q < 31$)
- MH, CH (Liquid Limit, $w_L > 50$, $15 \leq \Delta_Q < 19$)
- OL, OH, Pt (Highly Organic Soil, $\Delta_Q < 15$)

PDX Fuel Tank SVA
Portland, OR

CPT-Based Interpretation Summary
Basic Measurement
SCPT-4 : (45.597566 , -122.614008)

0204679-001 July 2023

HALEY ALDRICH

Figure
B-27

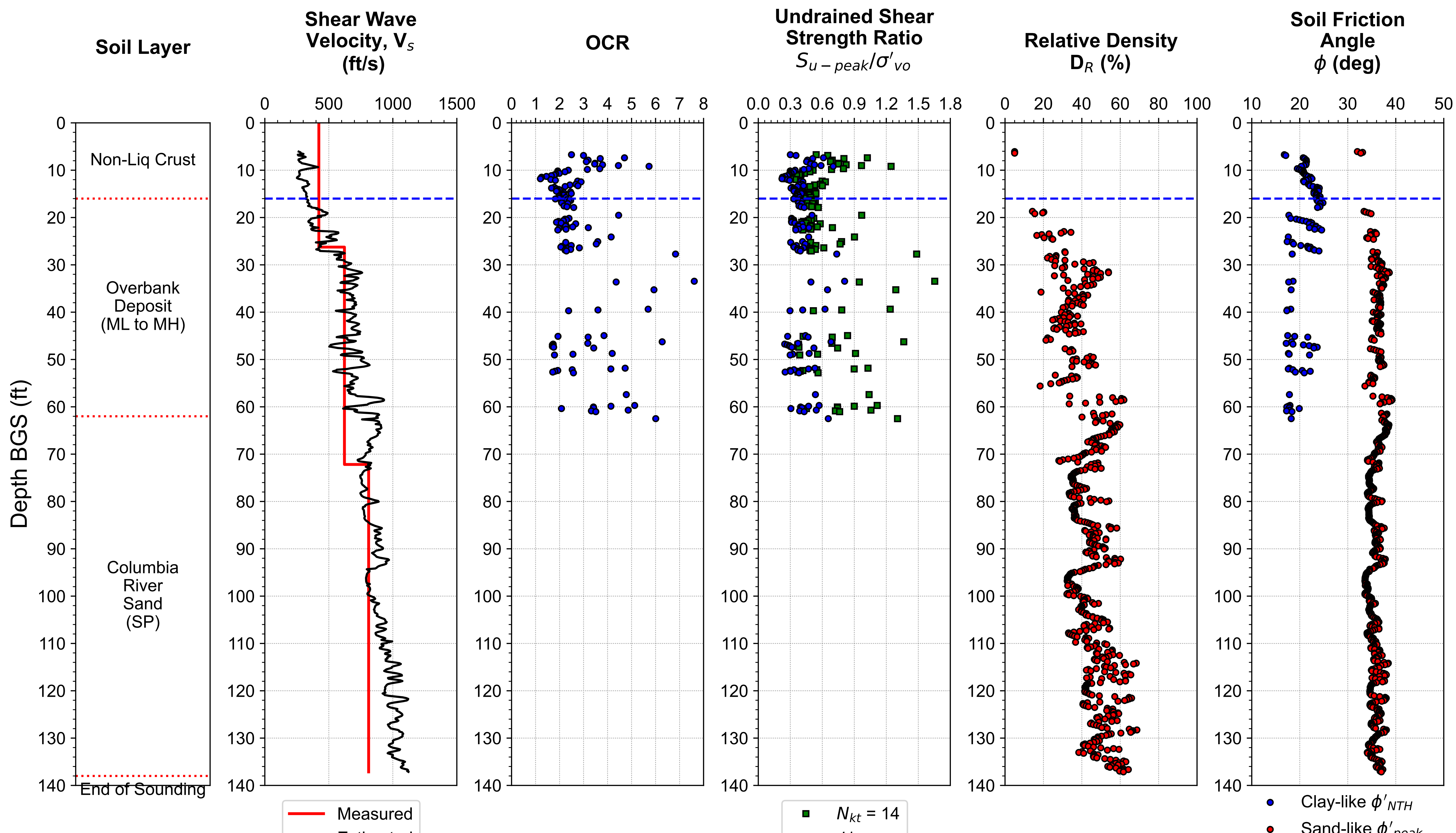

Notes:

1a. V_s is estimated using Robertson (2009) CPT-V_s Correlation

1b. Measured V_s is calculated using Slope method

2. OCR is determined using Agaiby & Mayne (2019) procedure

3a. S_{u-peak}/σ'_{vo} = ($q_t - \sigma_{vo}$) / ($N_{kt}\sigma'_{vo}$) and S_{u-peak}/σ'_{vo} = 0.5 sin(ϕ'_{NTH}) OCR $^{0.8}$

3b. N_{kt} = 14 ; ϕ_{NTH} = Effective friction angles calculated using modified NTH method (Ouyang & Mayne 2019)

4. Relative Density is estimated using Idriss & Boulanger 2008, Jamiolkowski et al. 2001, and Kulhawy & Mayne 1991 with weighting average factor 0.4, 0.3, 0.3, respectively

5. ϕ_{peak} = Peak friction angle calculated using Robertson (2010) equation for sandy soils, assuming ϕ'_{cv} = 33^o

PDX Fuel Tank SVA
Portland, OR

CPT-Based Interpretation Summary
Engineering Properties
SCPT-4 : (45.597566 , -122.614008)

0204679-001 July 2023

HALEY ALDRICH

Figure **B-28**

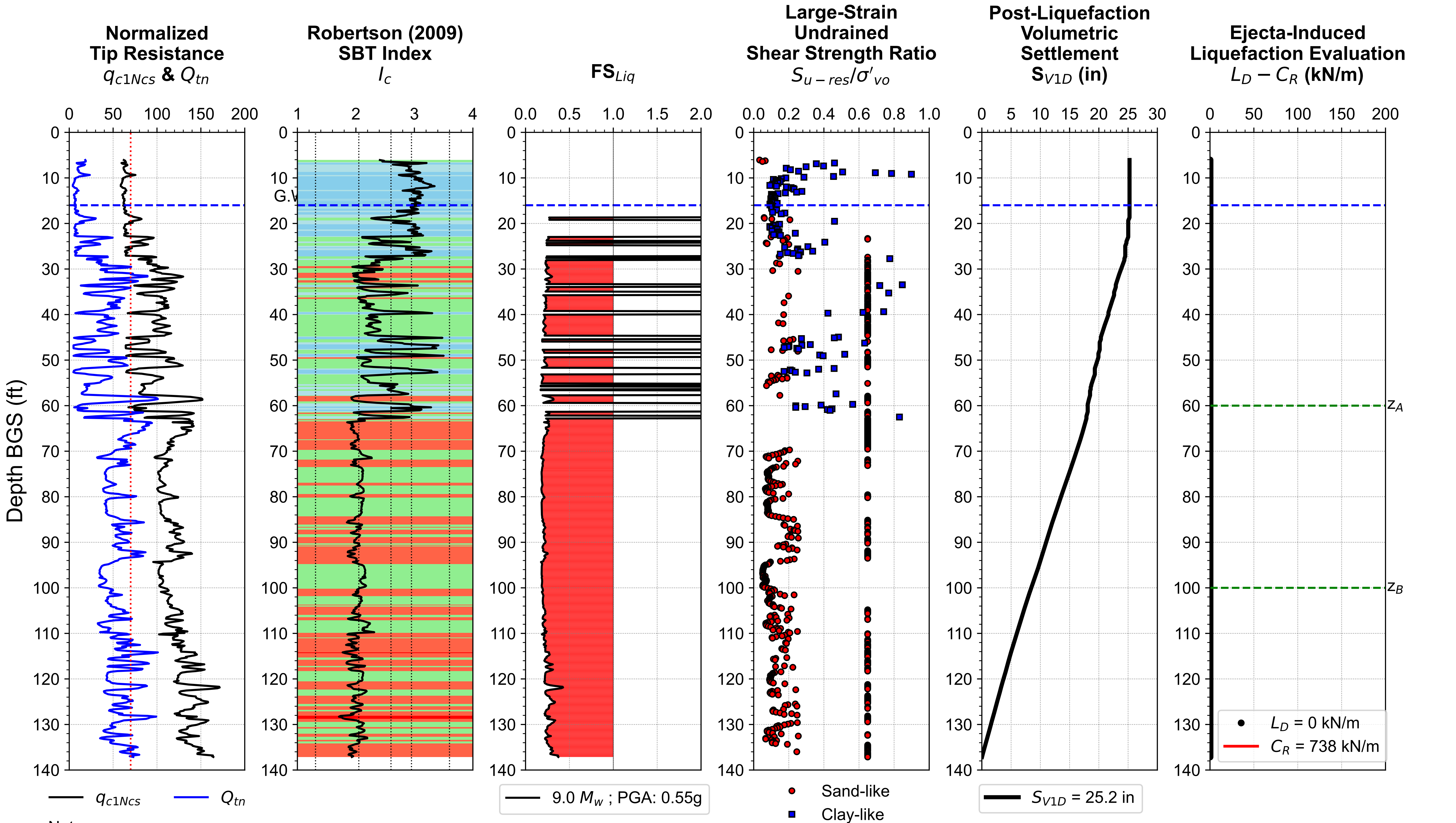

Notes:

1a. q_{c1Ncs}: Equivalent clean sand tip resistance following Boulanger & Idriss (2016) to estimate cyclic resistance ratio
1b. Q_{tn}: Normalized tip resistance following Robertson 2020 to estimate large-strain undrained shear strength ratio
2. FS_{Liq} is calculated using Boulanger & Idriss (2016) with P_{Liq} = 0.15 ; I_{c-cut} = 2.6 ; C_{FC} = 0.0
3. Large-strain undrained shear strength ratio is estimated using Robertson (2020) for clay-like and sand-like soil:
   Sand-like: Post-liquefied strength ratio (S_{u-liq}/σ'_{vo}) = tan (ϕ'_{cv}) for Q_{tn} > 70, where ϕ'_{cv} is assumed to be 33^o
   Clay-like: S_{u-res} is the same as remolded strength S_{u-rem}
4. Post-Liquefaction volumetric settlement is calculated using Zhang et al. (2002) procedure
5. Ejecta-induced settlement & severity are calculated based on Hutabarat & Bray (2022)

PDX Fuel Tank SVA
Portland, OR

CPT-based Liquefaction Evaluation
2475-yrs Hazard Level
SCPT-4 : (45.597566 , -122.614008)

0204679-001 July 2023

HALEY ALDRICH

Figure
B-29

Modified SBT$_n$
Robertson (2016)

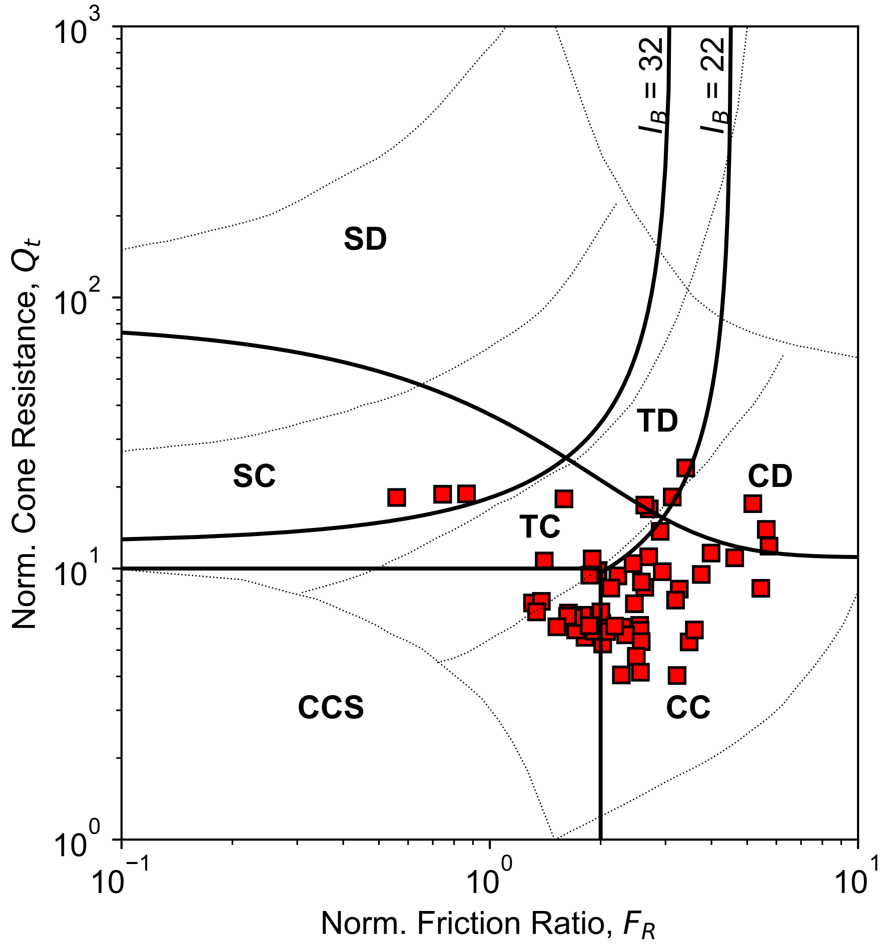

Δ_Q Index Soil Classification Chart
Saye et al. (2017)

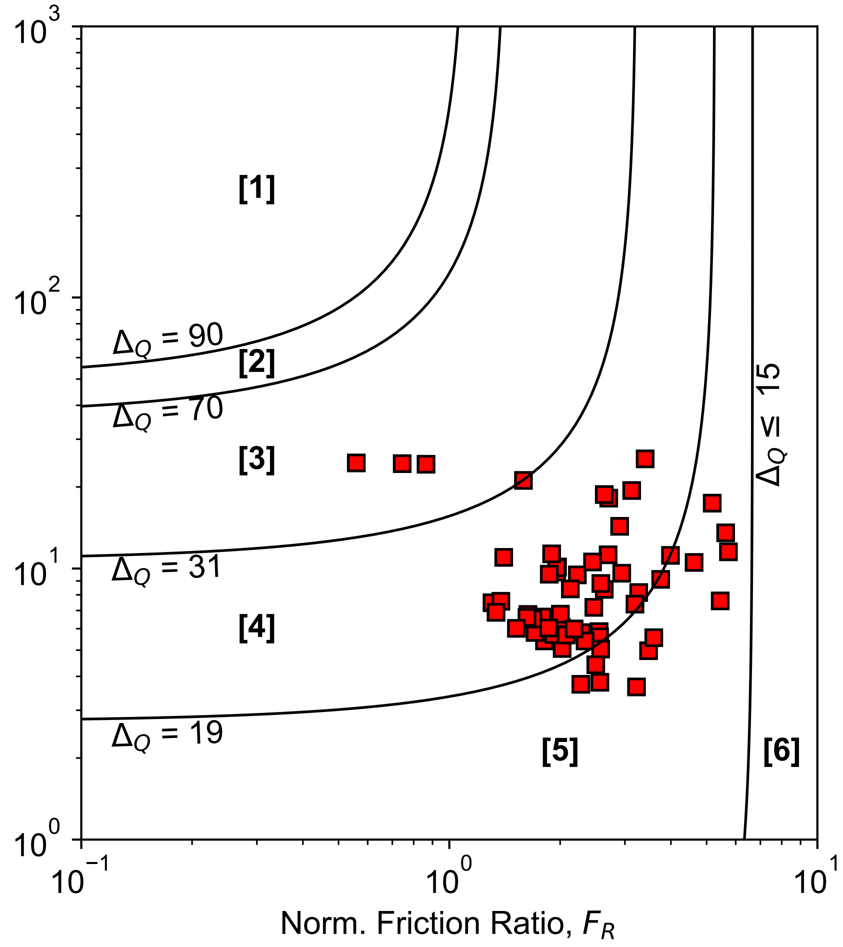

Soil Classification Chart
Schneider et al. (2012)

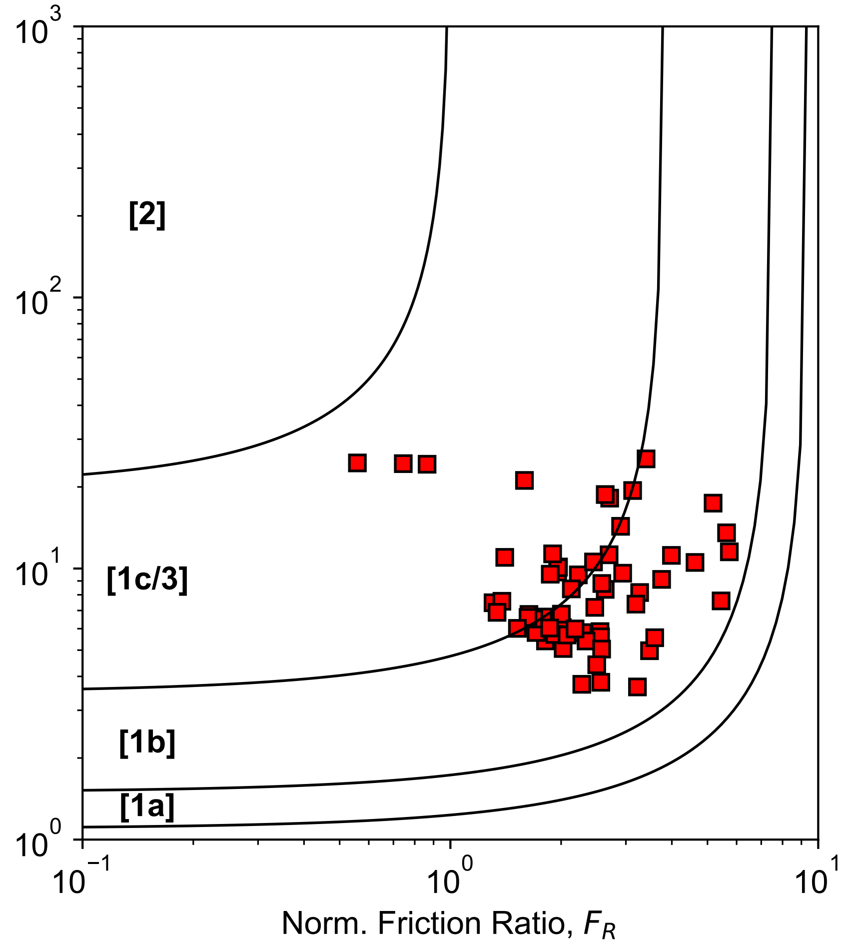

Robertson (2016) SBTn Zone:
SD = Sand-like - Dilative
SC = Sand-like - Contractive
TD = Transitional - Dilative
TC = Transitional - Contractive
CD = Clay-like - Dilative
CC = Clay-like - Contractive
CCS = Clay-like Contractive Sensitive

Typical USCS (Saye et al. 2017):
[1] $\Delta_Q > 90$ = SP, SW (FC $\leq$ 5%)
[2] $70 \leq \Delta_Q < 90$ = SP-SM, SP-SC (FC $\approx$ 5-12%)
[3] $31 \leq \Delta_Q < 70$ = SM, SC, GM, GC (FC $\approx$ 12-50%)
[4] $19 \leq \Delta_Q < 31$ = ML, CL (FC > 50%, $D_{50} = 75\mu$m)
[5] $15 \leq \Delta_Q < 19$ = MH, CH (Liquid Limit, $w_L > 50$)
[6] $\Delta_Q < 15$ = OL, OH, Pt (Highly Organic Soil)

Classification Zone Schneider et al. 2012:
Zone-[1a] = Low-I_R clays ($I_R = G/S_u$)
Zone-[1b] = Clays
Zone-[1c] = Sensitive clays
Zone-[3] = Silts and transitional soils
Zone-[2] = Essentially drained sands

PDX Fuel Tank SVA
Portland, OR

Soil Classification Chart
Layer-1: 6 ft to 16 ft
SCPT-4 : (45.597566 , -122.614008)

0204679-001 July 2023

HALEY ALDRICH

Figure
B-30

Modified SBT$_n$
Robertson (2016)

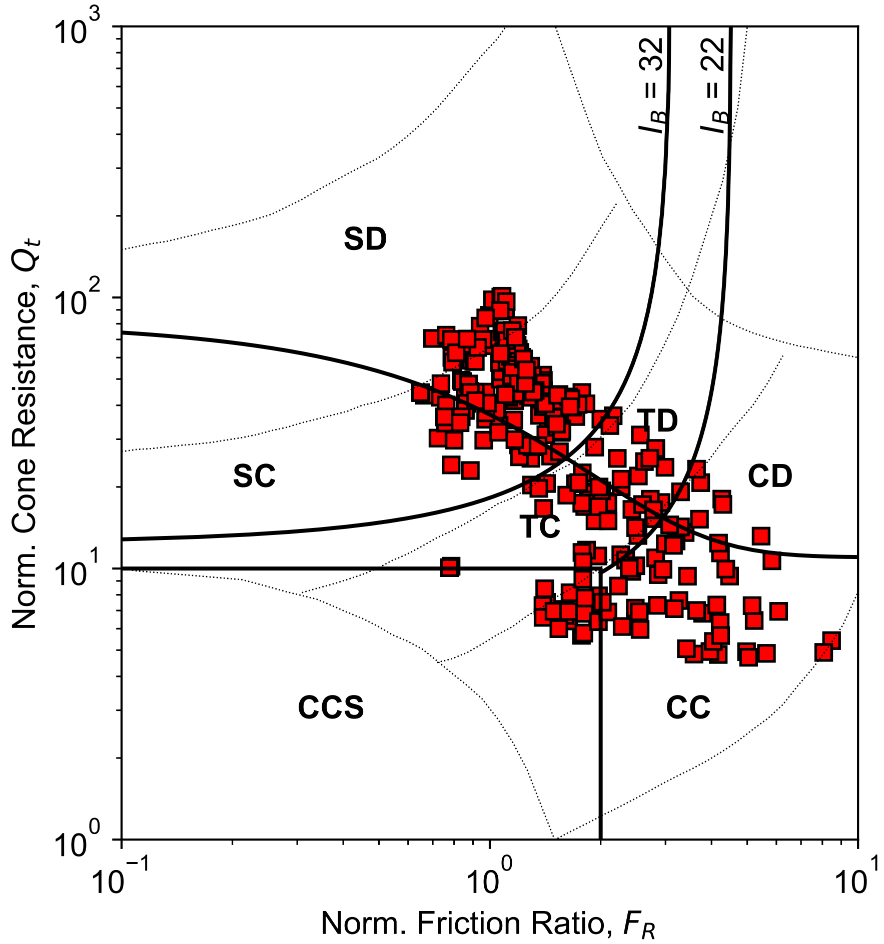

Δ_Q Index Soil Classification Chart
Saye et al. (2017)

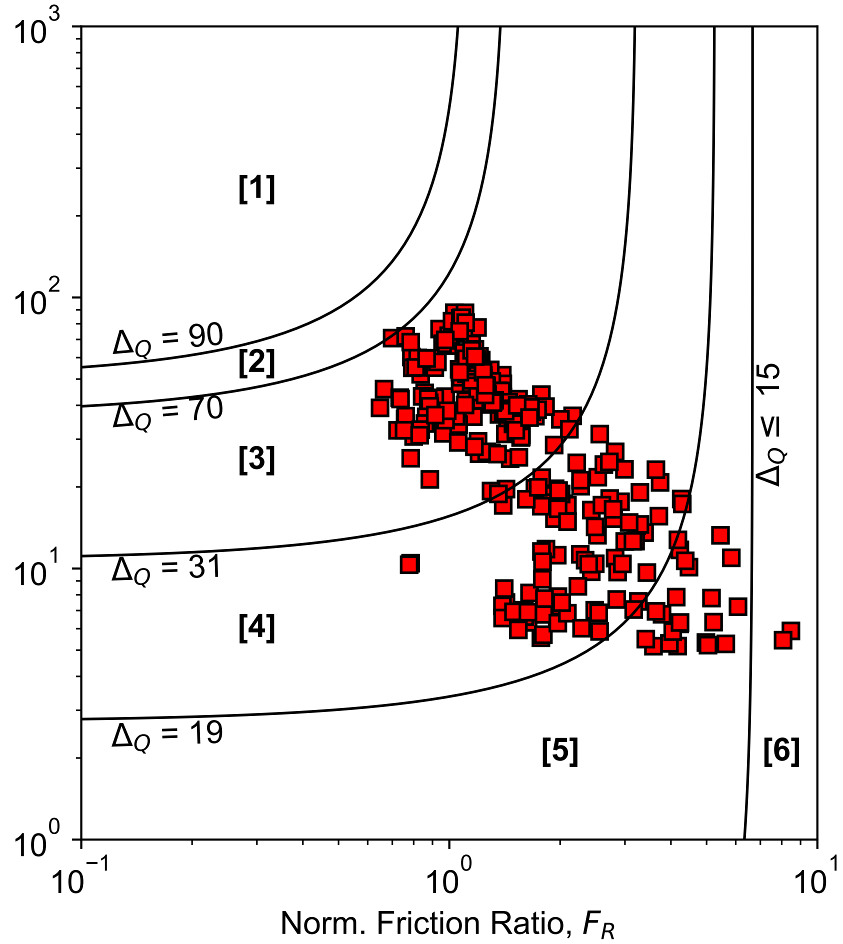

Soil Classification Chart
Schneider et al. (2012)

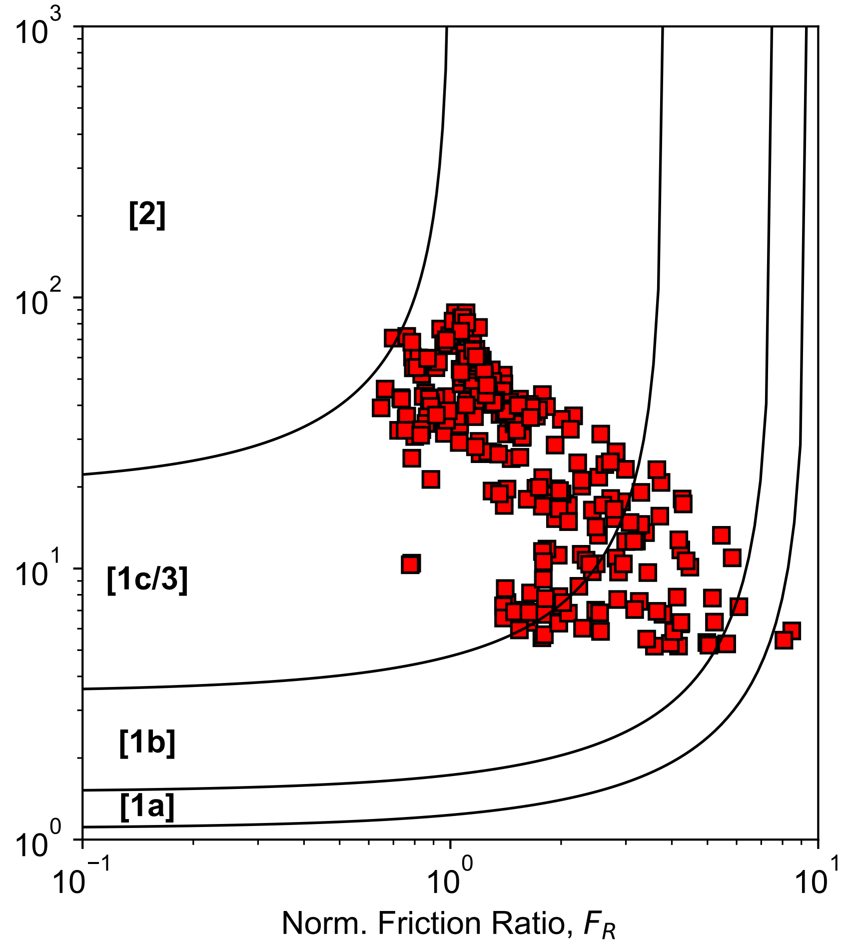

Robertson (2016) SBTn Zone:
SD = Sand-like - Dilative
SC = Sand-like - Contractive
TD = Transitional - Dilative
TC = Transitional - Contractive
CD = Clay-like - Dilative
CC = Clay-like - Contractive
CCS = Clay-like Contractive Sensitive

Typical USCS (Saye et al. 2017):
[1] $\Delta_Q > 90$ = SP, SW (FC $\leq$ 5%)
[2] $70 \leq \Delta_Q < 90$ = SP-SM, SP-SC (FC $\approx$ 5-12%)
[3] $31 \leq \Delta_Q < 70$ = SM, SC, GM, GC (FC $\approx$ 12-50%)
[4] $19 \leq \Delta_Q < 31$ = ML, CL (FC > 50%, $D_{50} = 75\mu$m)
[5] $15 \leq \Delta_Q < 19$ = MH, CH (Liquid Limit, $w_L > 50$)
[6] $\Delta_Q < 15$ = OL, OH, Pt (Highly Organic Soil)

Classification Zone Schneider et al. 2012:
Zone-[1a] = Low-I_R clays ($I_R = G/S_u$)
Zone-[1b] = Clays
Zone-[1c] = Sensitive clays
Zone-[3] = Silts and transitional soils
Zone-[2] = Essentially drained sands

PDX Fuel Tank SVA
Portland, OR

Soil Classification Chart
Layer-2: 16 ft to 62 ft
SCPT-4 : (45.597566 , -122.614008)

0204679-001 July 2023

HALEY ALDRICH

Figure
B-31

\\haleyaldrich.com\share\pdx_data\Notebooks\0204679-001_PDX_Fuel_Project_Tank_Design\Analysis and Calcs\5 2D FLAC NDA\CPTBased Assessment\SCPT-4.pdf

Modified SBT$_n$
Robertson (2016)

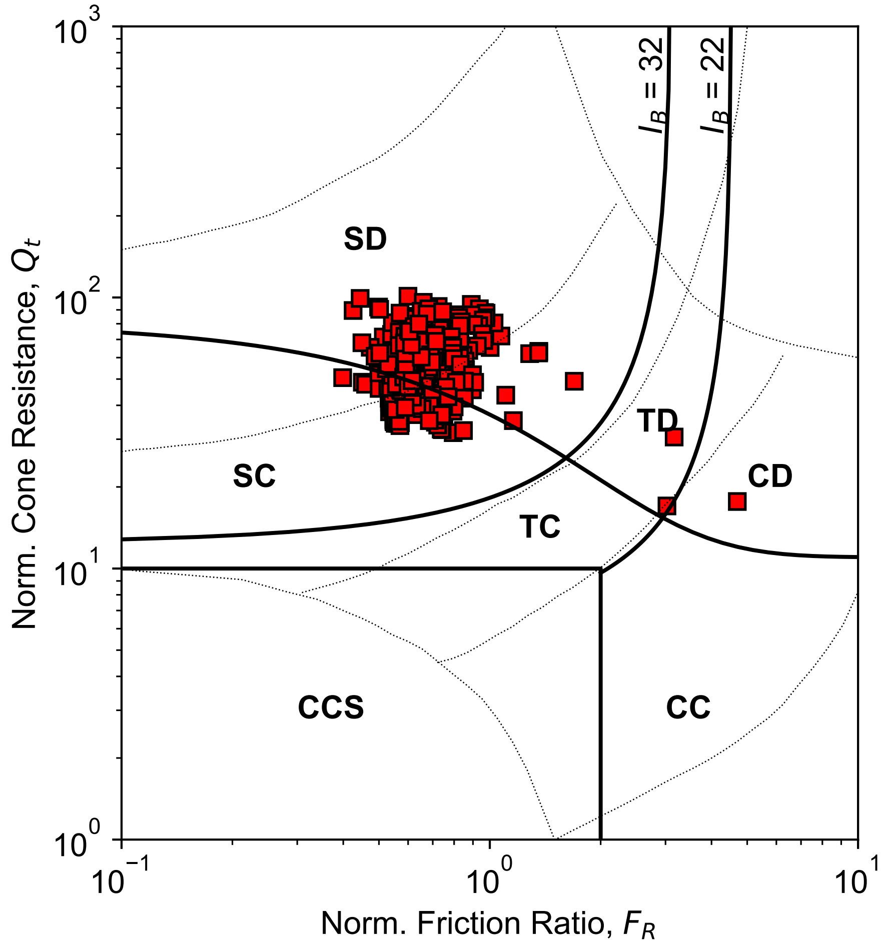

Robertson (2016) SBTn Zone:
SD = Sand-like - Dilative
SC = Sand-like - Contractive
TD = Transitional - Dilative
TC = Transitional - Contractive
CD = Clay-like - Dilative
CC = Clay-like - Contractive
CCS = Clay-like Contractive Sensitive

Δ_Q Index Soil Classification Chart
Saye et al. (2017)

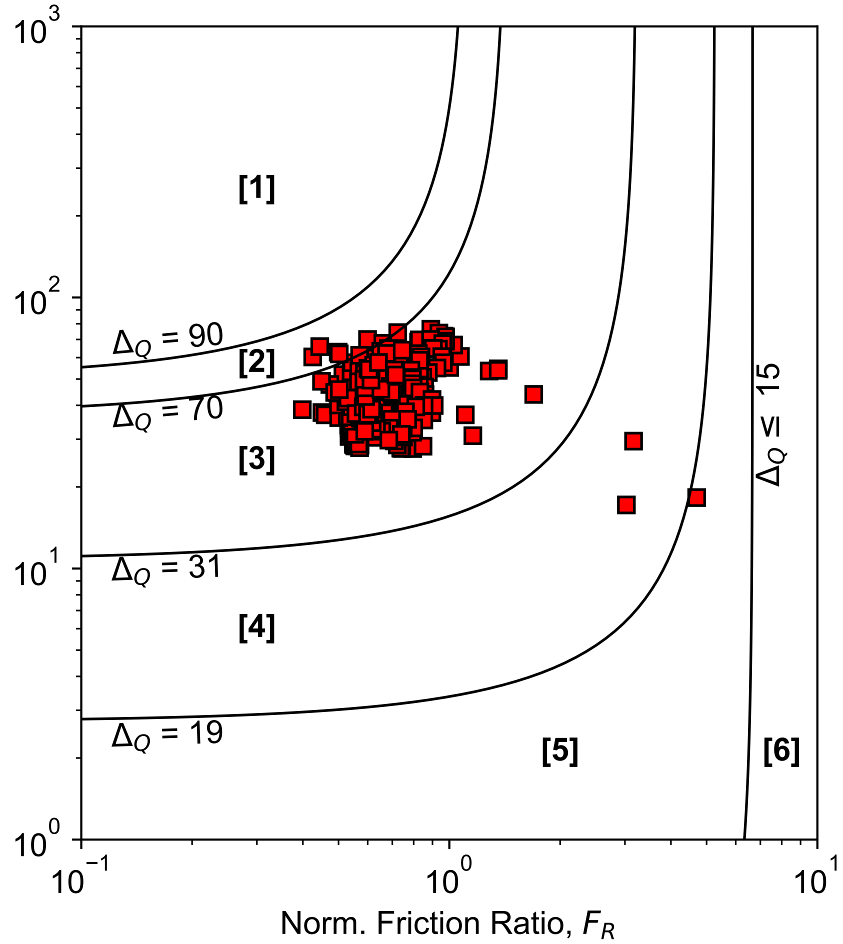

Typical USCS (Saye et al. 2017):
[1] $\Delta_Q > 90$ = SP, SW (FC ≤ 5%)
[2] $70 \leq \Delta_Q < 90$ = SP-SM, SP-SC (FC ≈ 5-12%)
[3] $31 \leq \Delta_Q < 70$ = SM, SC, GM, GC (FC ≈ 12-50%)
[4] $19 \leq \Delta_Q < 31$ = ML, CL (FC > 50%, $D_{50} = 75\mu$m)
[5] $15 \leq \Delta_Q < 19$ = MH, CH (Liquid Limit, $w_L > 50$)
[6] $\Delta_Q < 15$ = OL, OH, Pt (Highly Organic Soil)

Soil Classification Chart
Schneider et al. (2012)

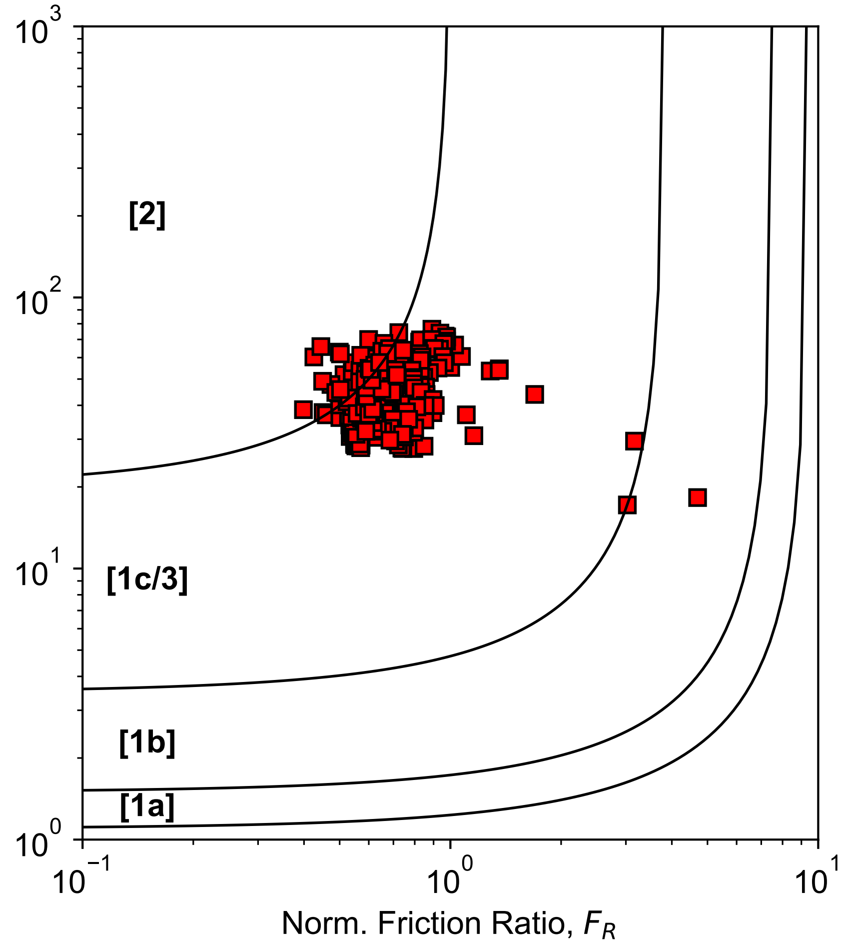

Classification Zone Schneider et al. 2012:
Zone-[1a] = Low-I_R clays ($I_R = G/S_u$)
Zone-[1b] = Clays
Zone-[1c] = Sensitive clays
Zone-[3] = Silts and transitional soils
Zone-[2] = Essentially drained sands

PDX Fuel Tank SVA
Portland, OR

Soil Classification Chart
Layer-3: 62 ft to 137 ft
SCPT-4 : (45.597566 , -122.614008)

0204679-001 July 2023

HALEY ALDRICH

Figure
B-32

\\haleyaldrich.com\share\pdx_data\Notebooks\0204679-001_PDX_Fuel_Project_Tank_Design\Analysis and Calcs\5 2D FLAC NDA\CPTBased Assessment\SCPT-4.pdf

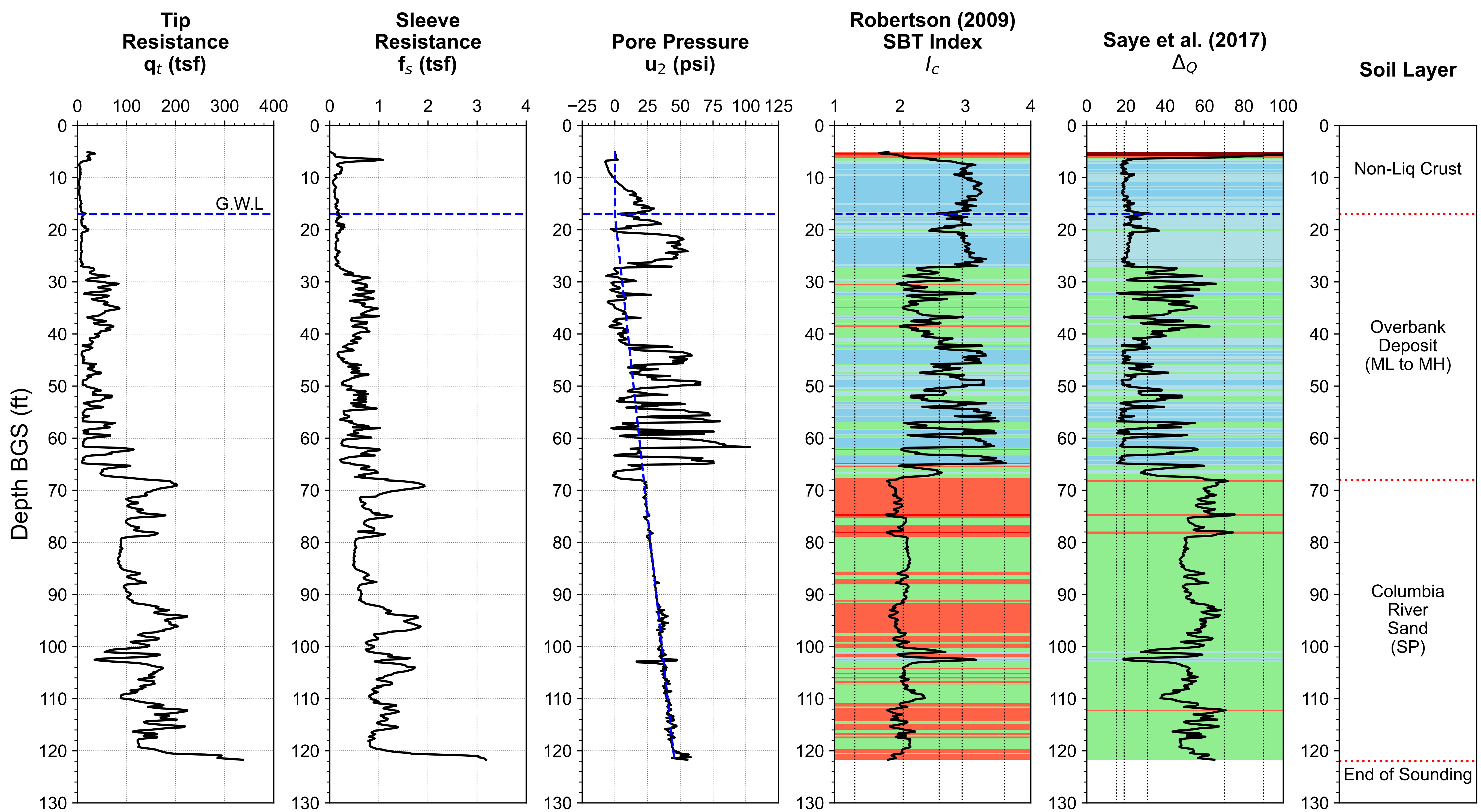

Robertson (2009) SBTn Zone:

- Gravelly Sands (I_c < 1.31)
- Clean sands (1.31 ≤ I_c < 1.8)
- Silty Sands (1.8 ≤ I_c < 2.05)
- Sand mixture: Sandy silt (2.05 ≤ I_c < 2.6)
- Silt mixture: Clayey silt to silty clay (2.6 ≤ I_c < 2.95)
- Clays (2.95 ≤ I_c ≤ 3.6)
- Organic Soils (I_c > 3.6)

Saye et al. (2017) Δ_Q Zone (Typical USCS):

- SP, SW (FC ≤ 5%, $\Delta_Q > 90$)
- SP-SM, SP-SC (FC ≈ 5-12%, $70 \le \Delta_Q < 90$)
- SM, SC, GM, GC (FC ≈ 12-50%, $31 \le \Delta_Q < 70$)
- ML, CL (FC > 50%, $D_{50} = 75\mu m$, $19 \le \Delta_Q < 31$)
- MH, CH (Liquid Limit, $w_L > 50$, $15 \le \Delta_Q < 19$)
- OL, OH, Pt (Highly Organic Soil, $\Delta_Q < 15$)

PDX Fuel Tank SVA
Portland, OR

CPT-Based Interpretation Summary
Basic Measurement
SCPT-6 : (45.597485 , -122.612872)

0204679-001 July 2023

HALEY ALDRICH

Figure **B-33**

\\haleyaldrich.com\share\pdx_data\Notebooks\0204679-001_PDX_Fuel_Project_Tank_Design\Analysis and Calcs\5 2D FLAC NDA\CPTBased Assessment\SCPT-6.pdf

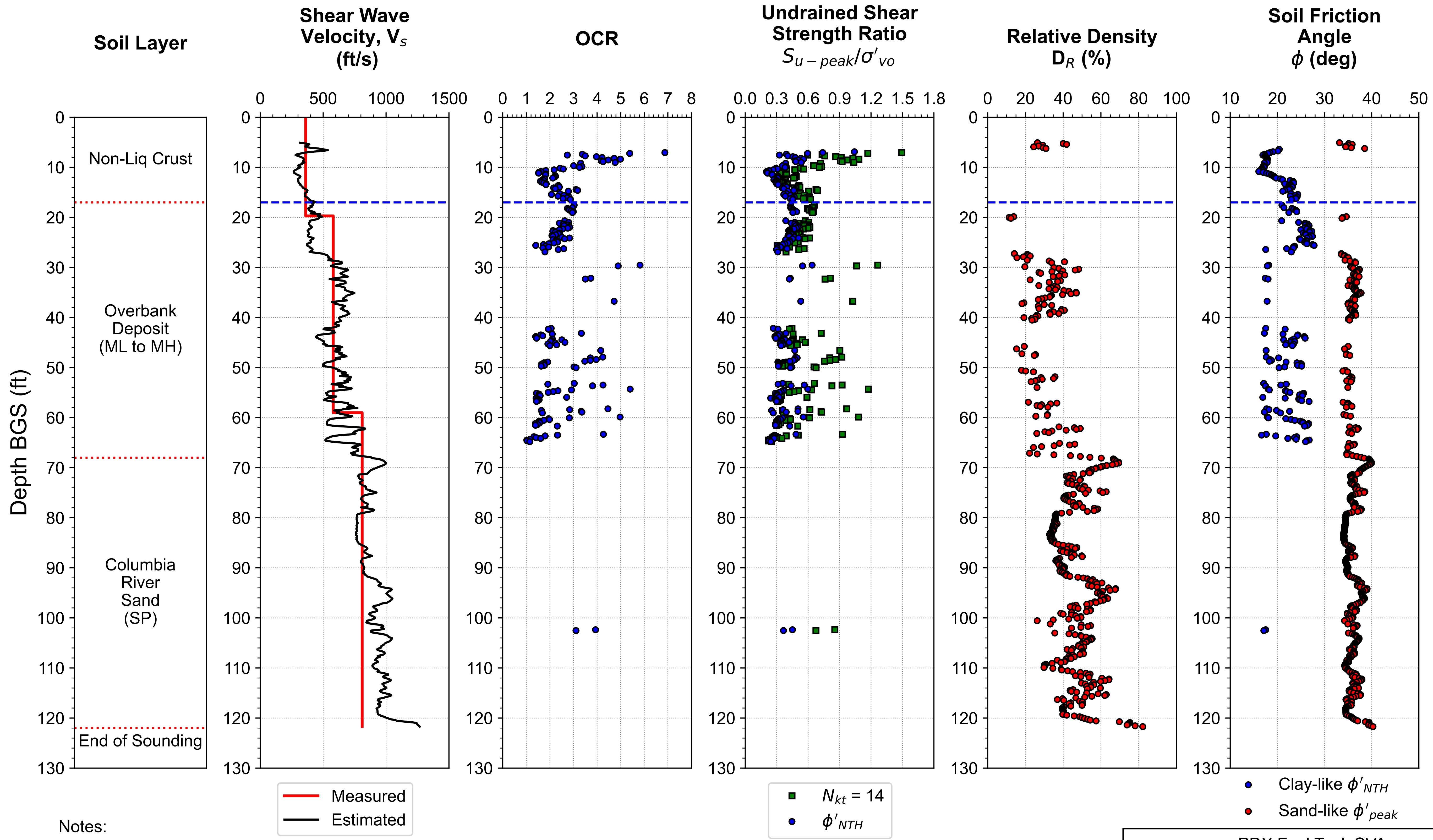

Notes:

1a. V_s is estimated using Robertson (2009) CPT-V_s Correlation
1b. Measured V_s is calculated using Slope method
2. OCR is determined using Agaiby & Mayne (2019) procedure
3a. S_{u-peak}/σ'_{vo} = ($q_t - \sigma_{vo}$) / ($N_{kt}\sigma'_{vo}$) and S_{u-peak}/σ'_{vo} = 0.5 sin(ϕ'_{NTH}) OCR $^{0.8}$
3b. N_{kt} = 14 ; ϕ_{NTH} = Effective friction angles calculated using modified NTH method (Ouyang & Mayne 2019)
4. Relative Density is estimated using Idriss & Boulanger 2008, Jamiolkowski et al. 2001, and Kulhawy & Mayne 1991 with weighting average factor 0.4, 0.3, 0.3, respectively
5. ϕ_{peak} = Peak friction angle calculated using Robertson (2010) equation for sandy soils, assuming ϕ'_{cv} = 33^o

PDX Fuel Tank SVA
Portland, OR

CPT-Based Interpretation Summary
Engineering Properties
SCPT-6 : (45.597485 , -122.612872)

0204679-001 July 2023

HALEY ALDRICH

Figure
B-34

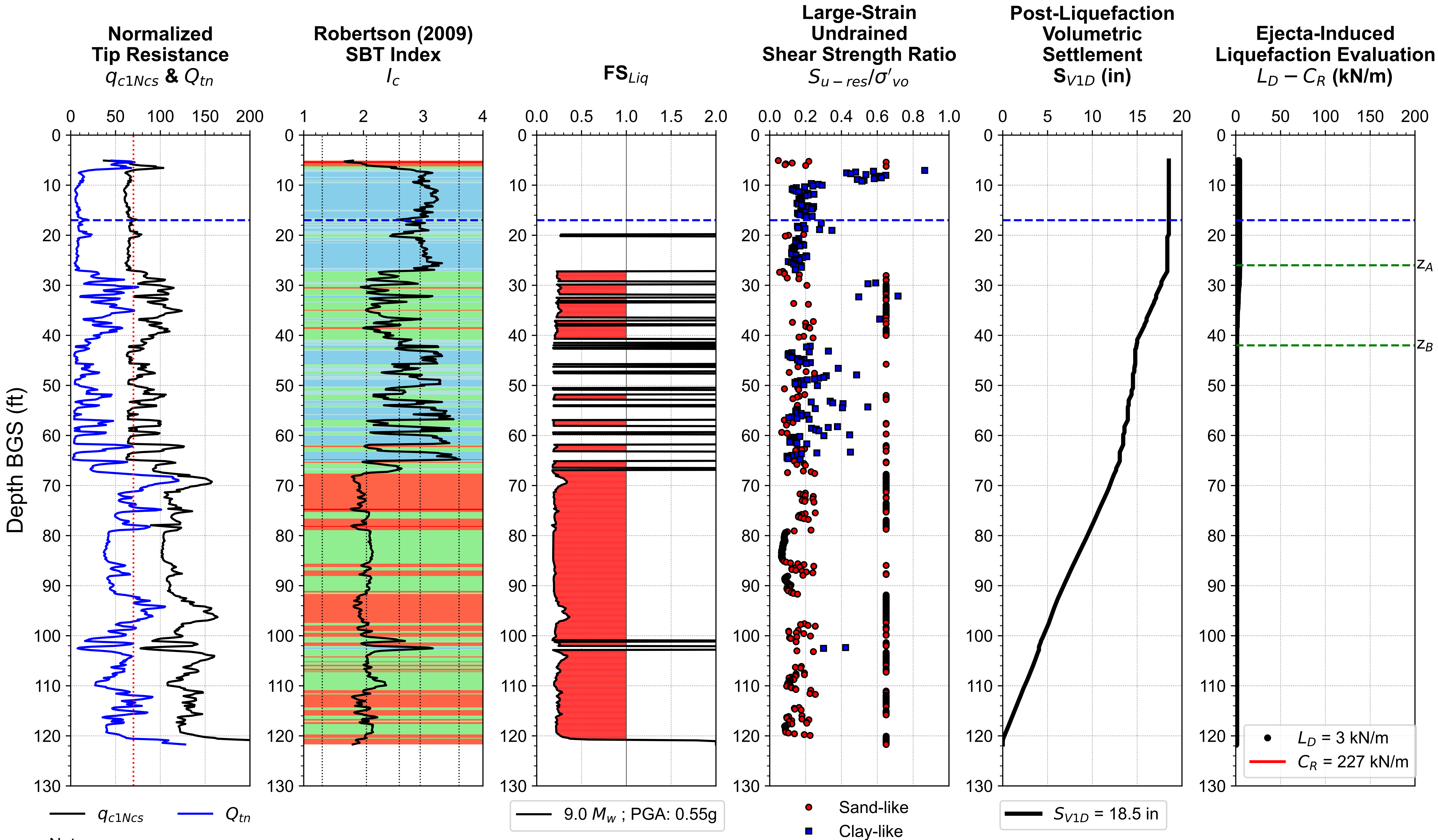

Notes:

1a. q_{c1Ncs}: Equivalent clean sand tip resistance following Boulanger & Idriss (2016) to estimate cyclic resistance ratio
1b. Q_{tn}: Normalized tip resistance following Robertson 2020 to estimate large-strain undrained shear strength ratio
2. FS_{Liq} is calculated using Boulanger & Idriss (2016) with P_{Liq} = 0.15 ; I_{c-cut} = 2.6 ; C_{FC} = 0.0
3. Large-strain undrained shear strength ratio is estimated using Robertson (2020) for clay-like and sand-like soil:
   Sand-like: Post-liquefied strength ratio (S_{u-liq}/σ'_{vo}) = tan (ϕ'_{cv}) for Q_{tn} > 70, where ϕ'_{cv} is assumed to be 33^o
   Clay-like: S_{u-res} is the same as remolded strength S_{u-rem}
4. Post-Liquefaction volumetric settlement is calculated using Zhang et al. (2002) procedure
5. Ejecta-induced settlement & severity are calculated based on Hutabarat & Bray (2022)

PDX Fuel Tank SVA
Portland, OR

CPT-based Liquefaction Evaluation
2475-yrs Hazard Level
SCPT-6 : (45.597485 , -122.612872)

0204679-001 July 2023

HALEY ALDRICH

Figure
B-35

Modified SBT$_n$
Robertson (2016)

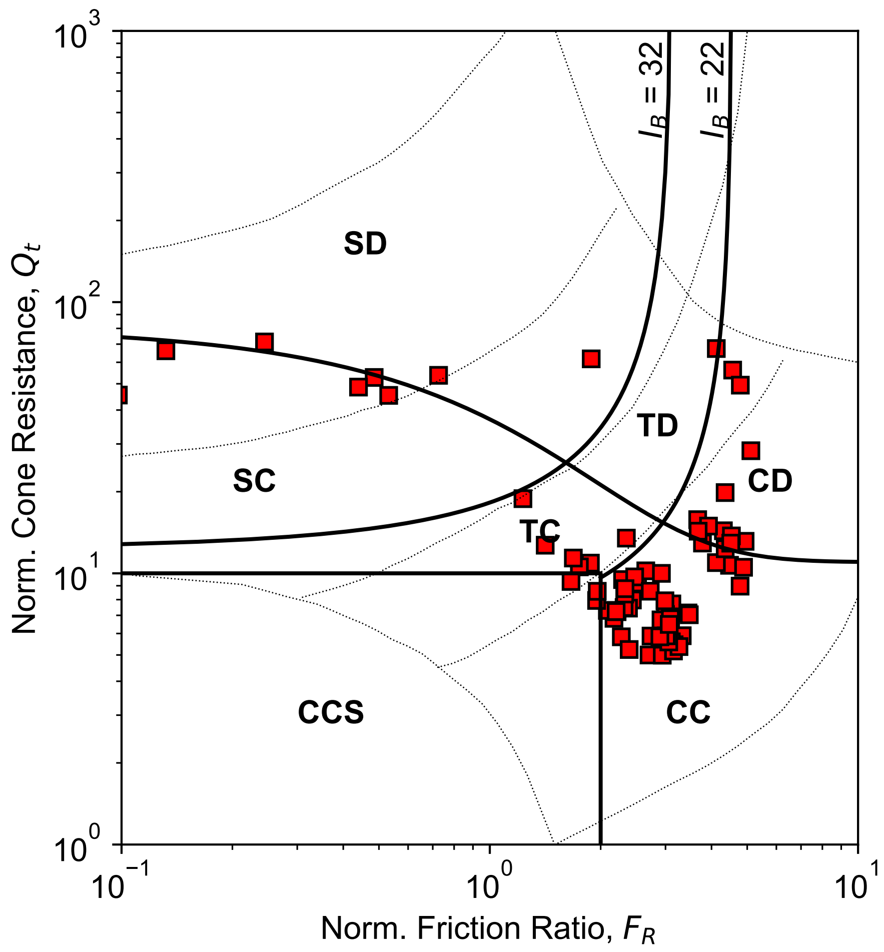

Δ_Q Index Soil Classification Chart
Saye et al. (2017)

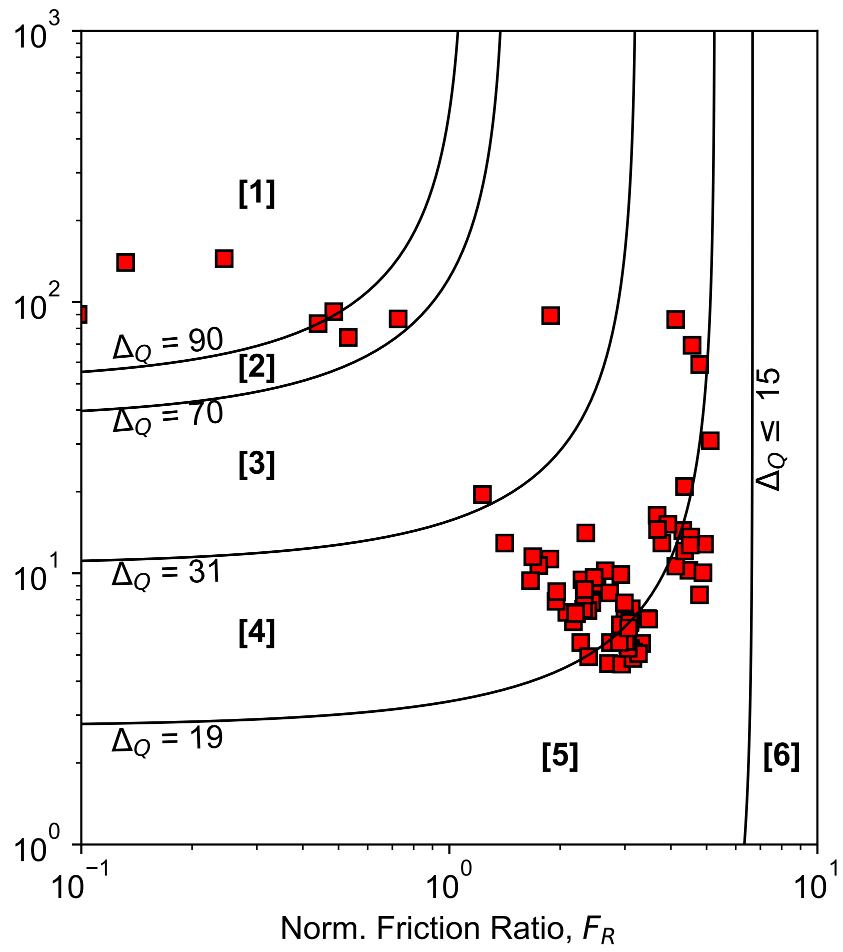

Soil Classification Chart
Schneider et al. (2012)

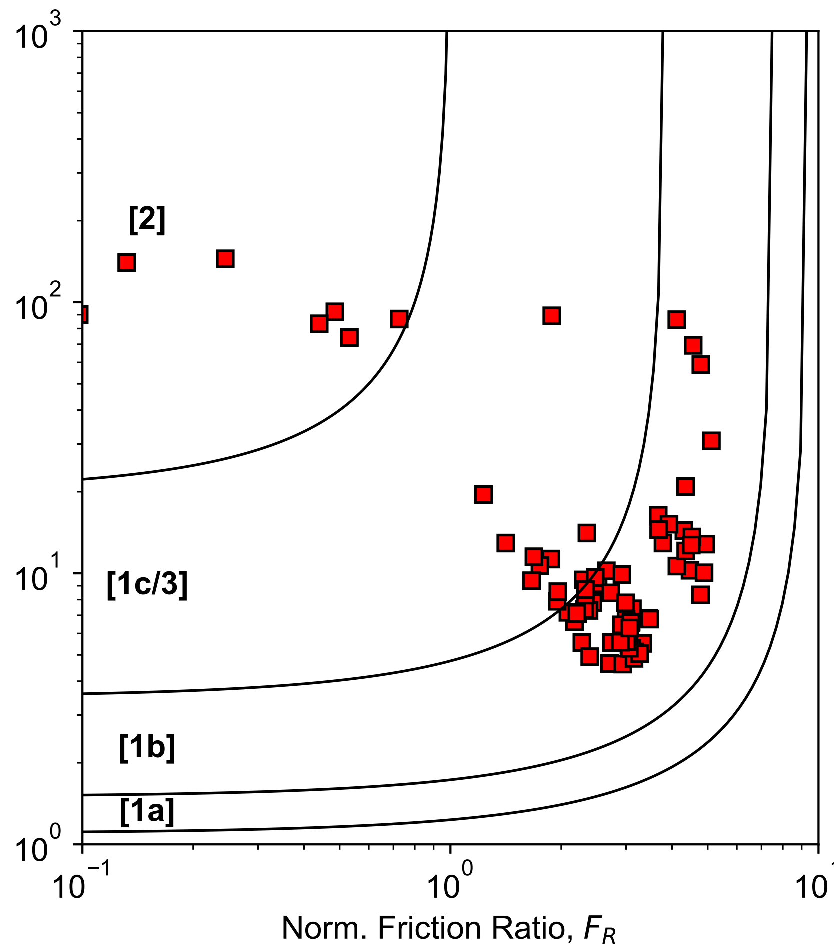

Robertson (2016) SBTn Zone:
SD = Sand-like - Dilative
SC = Sand-like - Contractive
TD = Transitional - Dilative
TC = Transitional - Contractive
CD = Clay-like - Dilative
CC = Clay-like - Contractive
CCS = Clay-like Contractive Sensitive

Typical USCS (Saye et al. 2017):
[1] $\Delta_Q > 90$ = SP, SW (FC ≤ 5%)
[2] $70 \le \Delta_Q < 90$ = SP-SM, SP-SC (FC ≈ 5-12%)
[3] $31 \le \Delta_Q < 70$ = SM, SC, GM, GC (FC ≈ 12-50%)
[4] $19 \le \Delta_Q < 31$ = ML, CL (FC > 50%, $D_{50} = 75\mu m$)
[5] $15 \le \Delta_Q < 19$ = MH, CH (Liquid Limit, $w_L > 50$)
[6] $\Delta_Q < 15$ = OL, OH, Pt (Highly Organic Soil)

Classification Zone Schneider et al. 2012:
Zone-[1a] = Low-I_R clays ($I_R = G/S_u$)
Zone-[1b] = Clays
Zone-[1c] = Sensitive clays
Zone-[3] = Silts and transitional soils
Zone-[2] = Essentially drained sands

PDX Fuel Tank SVA
Portland, OR

Soil Classification Chart
Layer-1: 5 ft to 17 ft
SCPT-6 : (45.597485 , -122.612872)

0204679-001 July 2023

HALEY ALDRICH

Figure
B-36

\\haleyaldrich.com\share\pdx_data\Notebooks\0204679-001_PDX_Fuel_Project_Tank_Design\Analysis and Calcs\5 2D FLAC NDA\CPTBased Assessment\SCPT-6.pdf

Modified SBT$_n$
Robertson (2016)

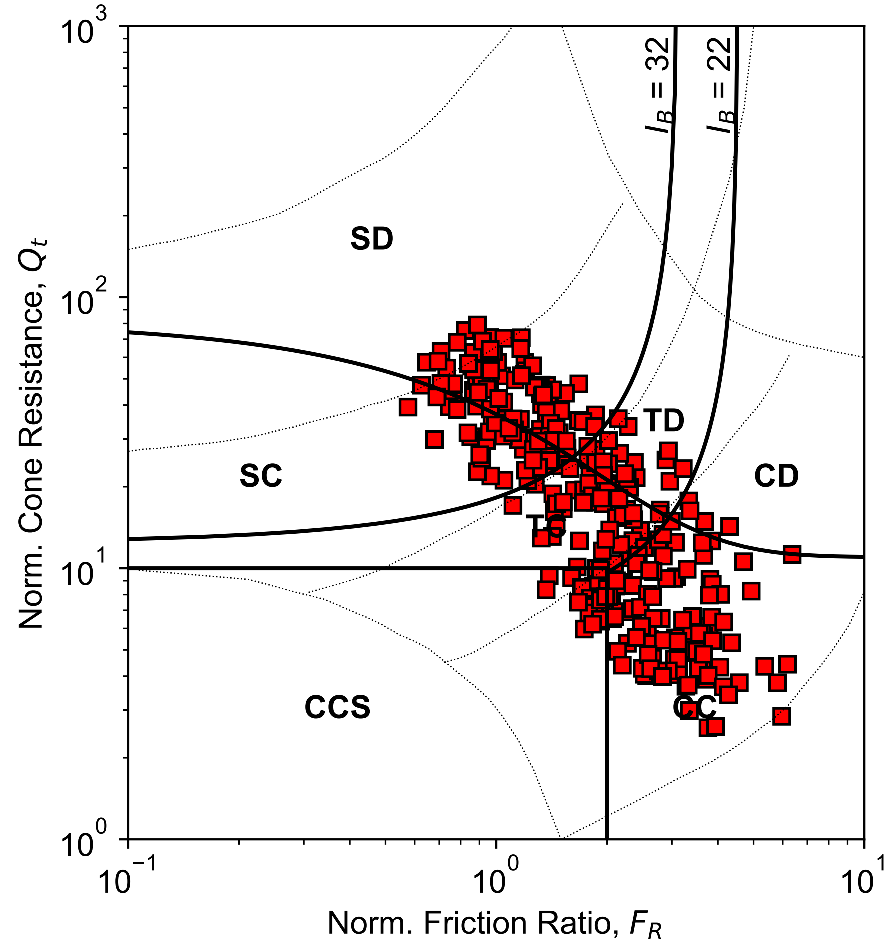

Δ_Q Index Soil Classification Chart
Saye et al. (2017)

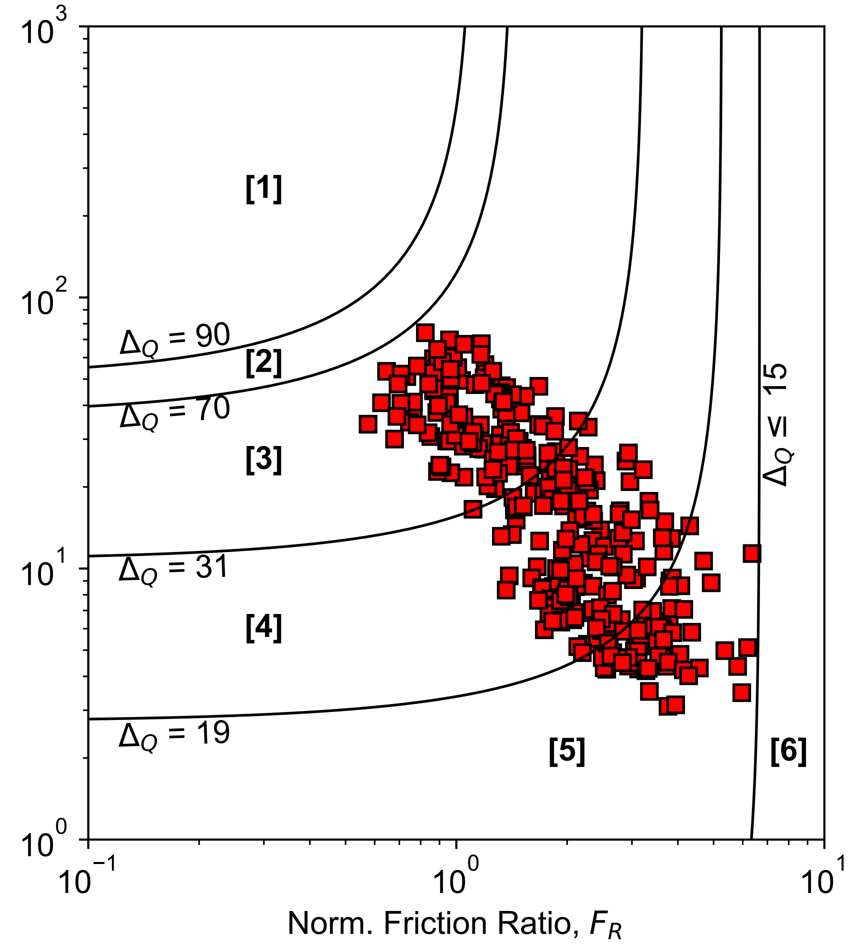

Soil Classification Chart
Schneider et al. (2012)

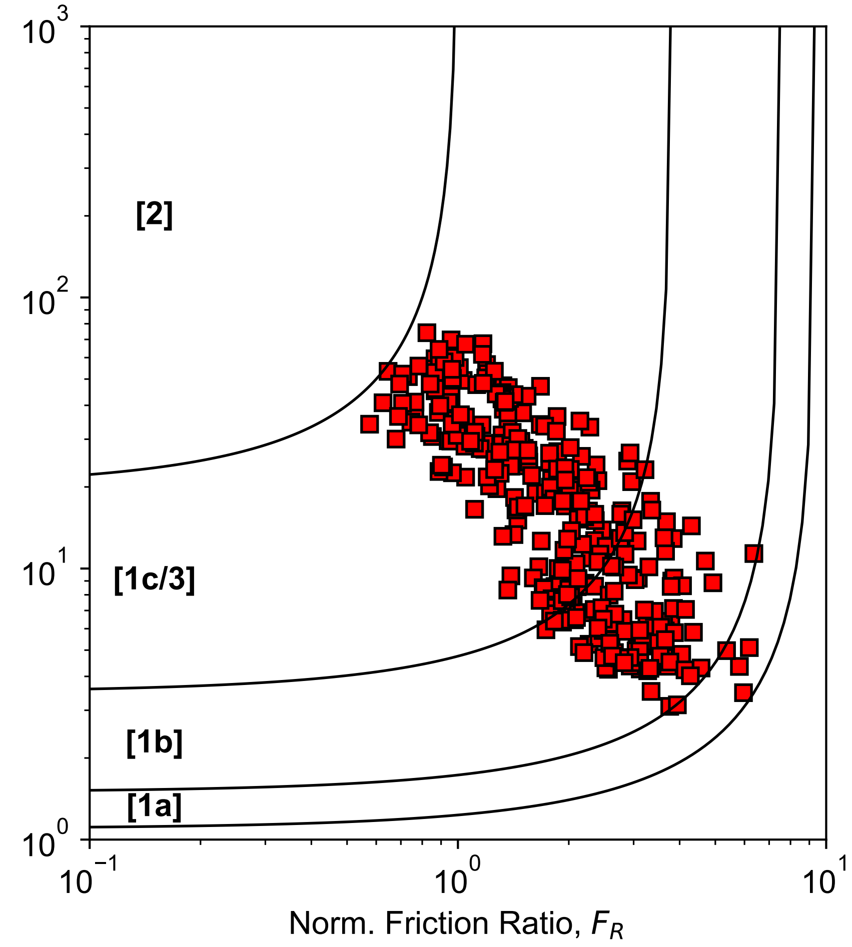

Robertson (2016) SBTn Zone:
SD = Sand-like - Dilative
SC = Sand-like - Contractive
TD = Transitional - Dilative
TC = Transitional - Contractive
CD = Clay-like - Dilative
CC = Clay-like - Contractive
CCS = Clay-like Contractive Sensitive

Typical USCS (Saye et al. 2017):
[1] $\Delta_Q > 90$ = SP, SW (FC $\leq$ 5%)
[2] $70 \leq \Delta_Q < 90$ = SP-SM, SP-SC (FC $\approx$ 5-12%)
[3] $31 \leq \Delta_Q < 70$ = SM, SC, GM, GC (FC $\approx$ 12-50%)
[4] $19 \leq \Delta_Q < 31$ = ML, CL (FC > 50%, $D_{50} = 75\mu$m)
[5] $15 \leq \Delta_Q < 19$ = MH, CH (Liquid Limit, $w_L > 50$)
[6] $\Delta_Q < 15$ = OL, OH, Pt (Highly Organic Soil)

Classification Zone Schneider et al. 2012:
Zone-[1a] = Low-I_R clays (I_R = G/S_u)
Zone-[1b] = Clays
Zone-[1c] = Sensitive clays
Zone-[3] = Silts and transitional soils
Zone-[2] = Essentially drained sands

PDX Fuel Tank SVA
Portland, OR

Soil Classification Chart
Layer-2: 17 ft to 68 ft
SCPT-6 : (45.597485 , -122.612872)

0204679-001 July 2023

HALEY ALDRICH

Figure
B-37

\\haleyaldrich.com\share\pdx_data\Notebooks\0204679-001_PDX_Fuel_Project_Tank_Design\Analysis and Calcs\5 2D FLAC NDA\CPTBased Assessment\SCPT-6.pdf

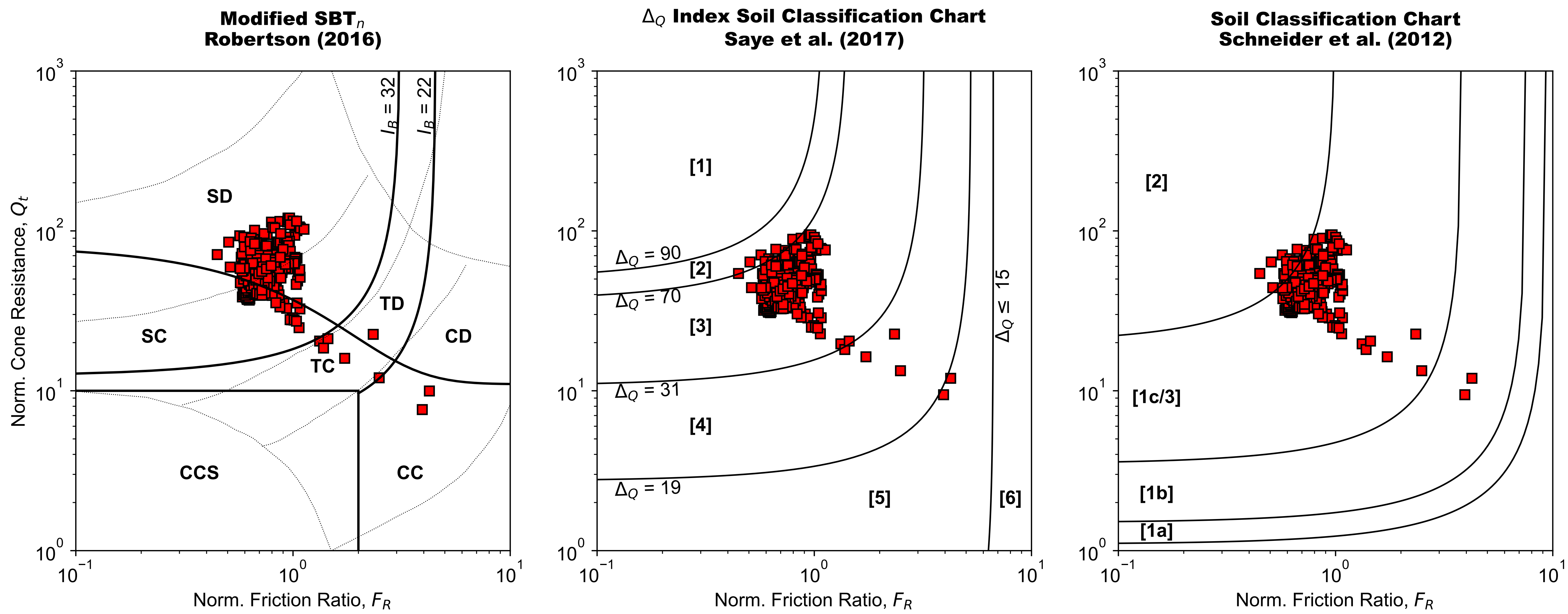

Robertson (2016) SBTn Zone:
SD = Sand-like - Dilative
SC = Sand-like - Contractive
TD = Transitional - Dilative
TC = Transitional - Contractive
CD = Clay-like - Dilative
CC = Clay-like - Contractive
CCS = Clay-like Contractive Sensitive

Typical USCS (Saye et al. 2017):
[1] $\Delta_Q > 90$ = SP, SW (FC $\leq$ 5%)
[2] $70 \leq \Delta_Q < 90$ = SP-SM, SP-SC (FC $\approx$ 5-12%)
[3] $31 \leq \Delta_Q < 70$ = SM, SC, GM, GC (FC $\approx$ 12-50%)
[4] $19 \leq \Delta_Q < 31$ = ML, CL (FC > 50%, $D_{50} = 75\mu$m)
[5] $15 \leq \Delta_Q < 19$ = MH, CH (Liquid Limit, $w_L > 50$)
[6] $\Delta_Q < 15$ = OL, OH, Pt (Highly Organic Soil)

Classification Zone Schneider et al. 2012:
Zone-[1a] = Low-I_R clays ($I_R = G/S_u$)
Zone-[1b] = Clays
Zone-[1c] = Sensitive clays
Zone-[3] = Silts and transitional soils
Zone-[2] = Essentially drained sands

PDX Fuel Tank SVA
Portland, OR

Soil Classification Chart
Layer-3: 68 ft to 122 ft
SCPT-6 : (45.597485 , -122.612872)

0204679-001 July 2023

HALEY ALDRICH

Figure
B-38

APPENDIX C
Summary of Interpreted Laboratory Testing Results

A. Constant Rate Strain Consolidation Results
B. Direct Simple Shear Test Results
C. Cyclic Direct Simple Shear Test Results
D. Index Testing

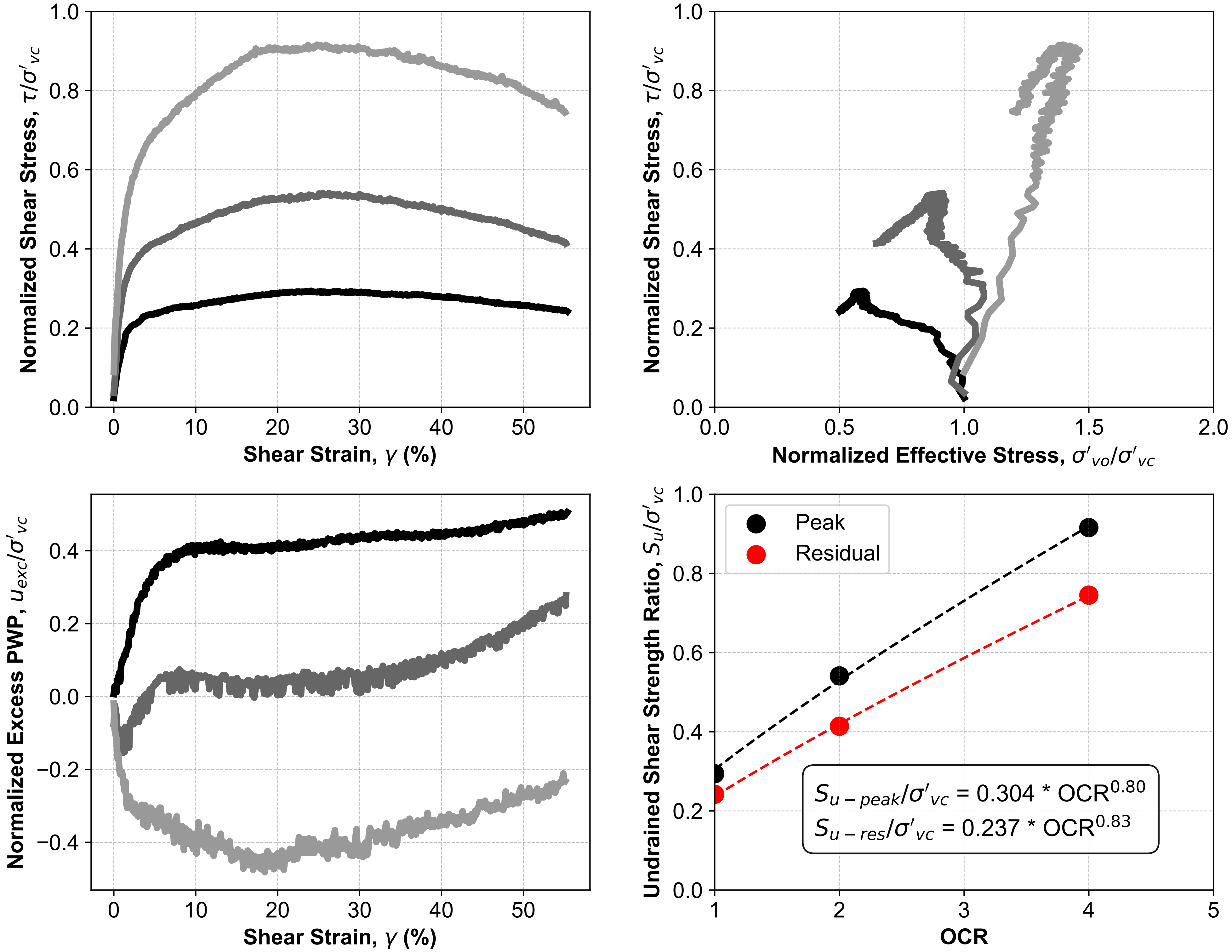

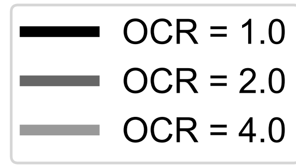

Test Date = 5/12/2023

Depth = 30 feet
σ'_{vc-1} = 5957 psf
σ'_{vc-2} = 3243 psf
σ'_{vc-3} = 1534 psf
$\sigma'_{vo-field}$ = 2100 psf
σ'_{pc} = 4500 - 5200 psf
Plasticity Index = TBD

Notes:

1. Specimen-1 was consolidated up to 6000 psf (OCR = 1), then shearing was performed
2. Specimen-2 was consolidated up to 6500 psf, unload to 3250 psf (OCR = 2), then shearing was performed
3. Specimen-3 was consolidated up to 6000 psf, unload to 1500 psf (OCR = 4), then shearing was performed
4. Based on ASTM D6528-17 Standard Test Metod for Consolidated Undrained DSS Testing
5. The normalized undrained shear strength vs OCR is determined using power-law regression

PDX Fuel Tank SVA
Portland, OR

Summary of Test Results
Monotonic Direct Simple Shear
Sample B2-U8 (Depth : 30 ft)

0204679-001 July 2023

HALEY ALDRICH

Figure
C-1

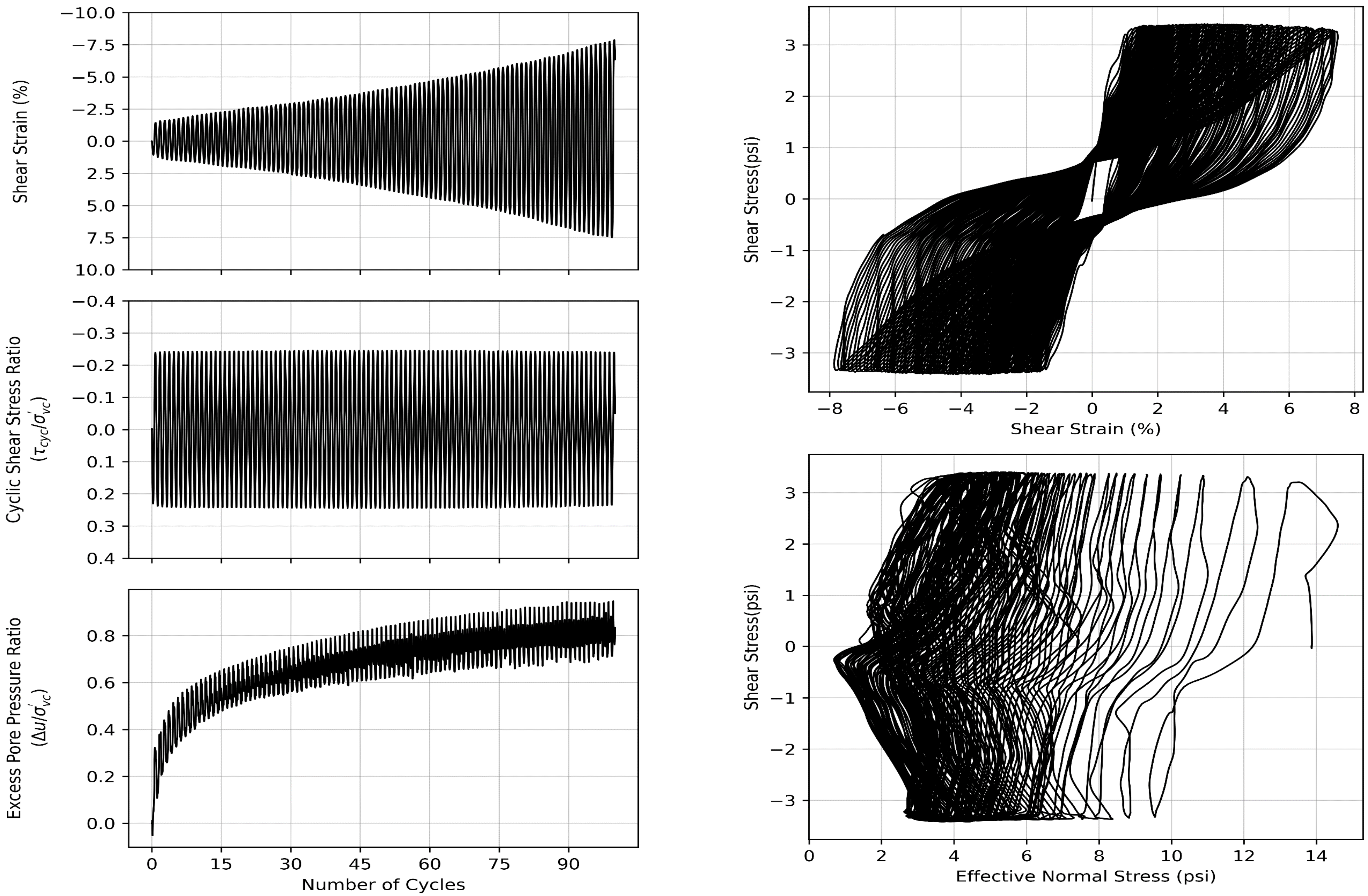

Depth	W.C. (%)		Atterberg Limits			Description	USCS
(ft)	Before	After	LL	PL	PI		
31.6	48	47	51	35	16	ELASTIC SILT	MH

Partical-size Distribution		
% Gravel	% Sand	% Fines
0	1.2	98.8

Initial Specimen Properties	
Height (inches)	1.00
Diameter (inches)	2.50
Weight (ounces)	4.78
Total Unit Weight (pcf)	105.57
Degree of Saturation (%)	96.31
Void Ratio (e_0)	1.315

PDX Fuel Tanks SVA
Portland, OR

Summary of Cyclic Direct Simple Shear Test: Sample B2-U8 (CSR = 0.25)

0204679-001 07 - 2023

HALEY ALDRICH

Fig. C-2

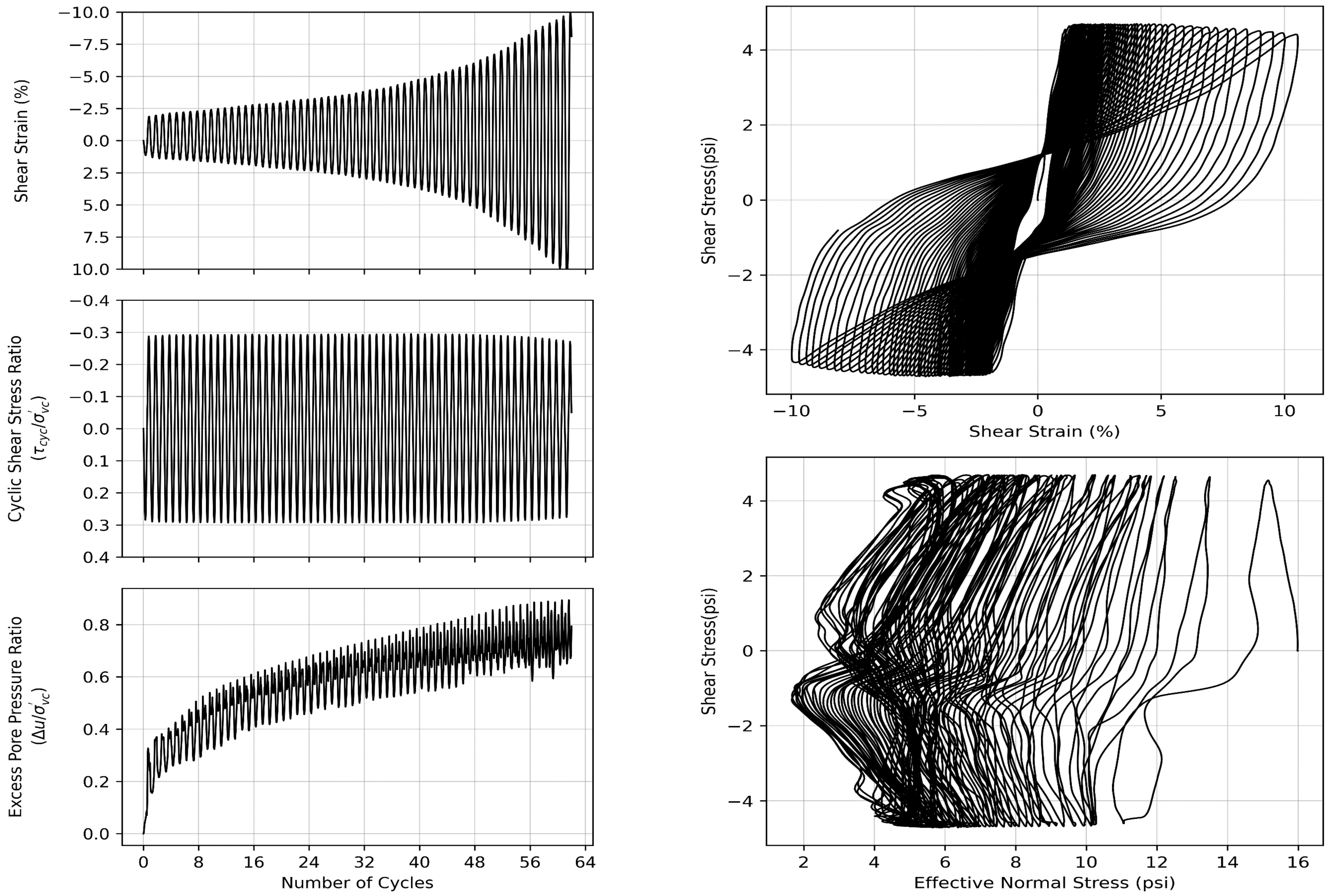

Depth	W.C. (%)		Atterberg Limits			Description	USCS
(ft)	Before	After	LL	PL	PI		
36.1	49	51	42	23	19	LEAN CLAY	CL

Partical-size Distribution		
% Gravel	% Sand	% Fines
0	0.25	99.75

Initial Specimen Properties	
Height (inches)	1.00
Diameter (inches)	2.50
Weight (ounces)	4.84
Total Unit Weight (pcf)	106.72
Degree of Saturation (%)	99.24
Void Ratio (e_0)	1.309

PDX Fuel Tanks SVA
Portland, OR

Summary of Cyclic Direct Simple Shear Test: Sample B2-U9 (CSR = 0.3)

0204679-001 07 - 2023

HALEY ALDRICH

Fig. C-3

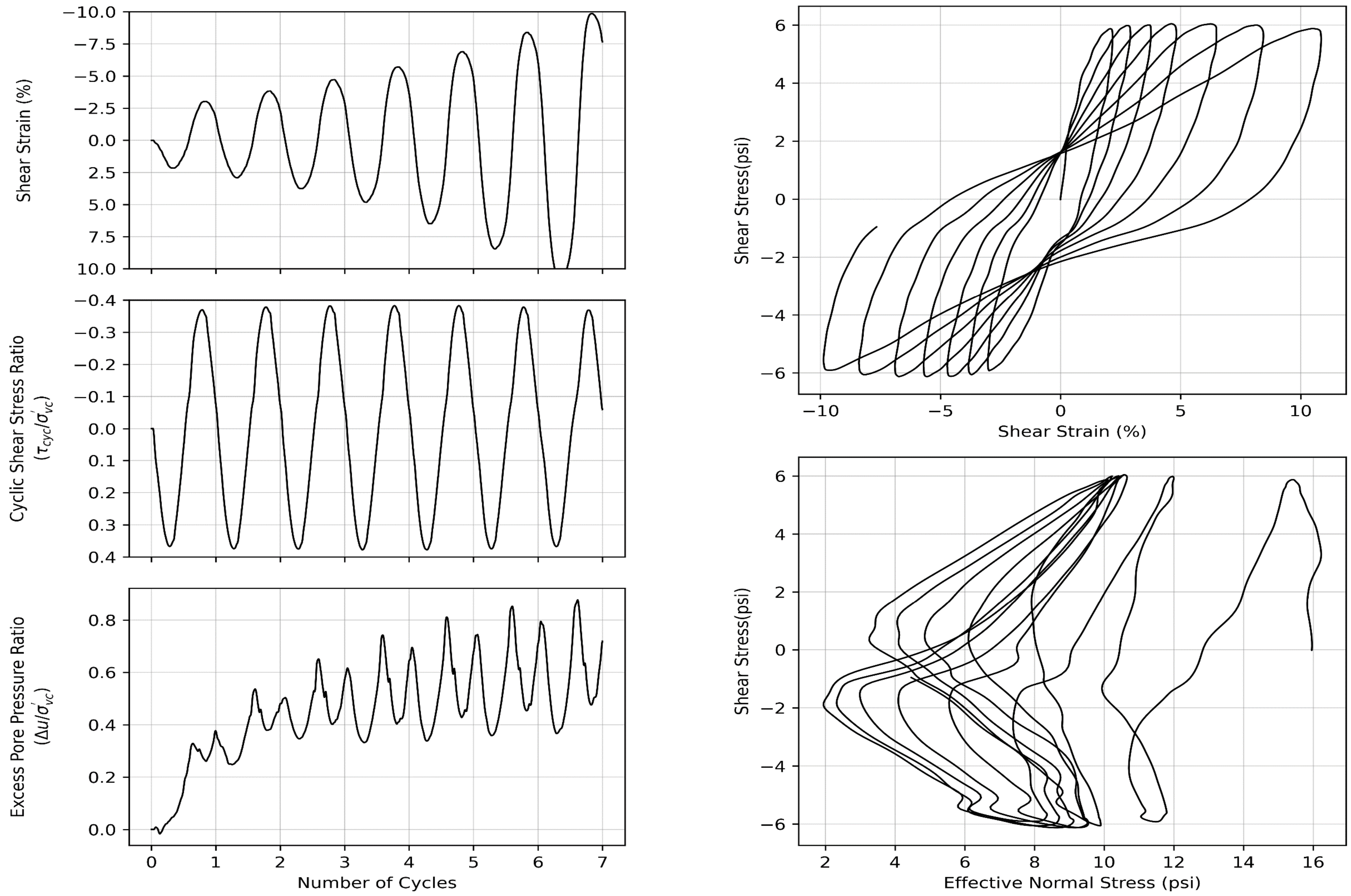

Depth	W.C. (%)		Atterberg Limits				
(ft)	Before	After	LL	PL	PI	Description	USCS
36.1	49	51	42	23	19	LEAN CLAY	CL

Partical-size Distribution		
% Gravel	% Sand	% Fines
0	0.25	99.75

Initial Specimen Properties	
Height (inches)	1.00
Diameter (inches)	2.50
Weight (ounces)	4.84
Total Unit Weight (pcf)	106.72
Degree of Saturation (%)	99.24
Void Ratio (e_0)	1.309

PDX Fuel Tanks SVA
Portland, OR

Summary of Cyclic Direct Simple Shear Test: Sample B2-U9 (CSR = 0.35)

0204679-001 07 - 2023

HALEY ALDRICH

Fig. C-4

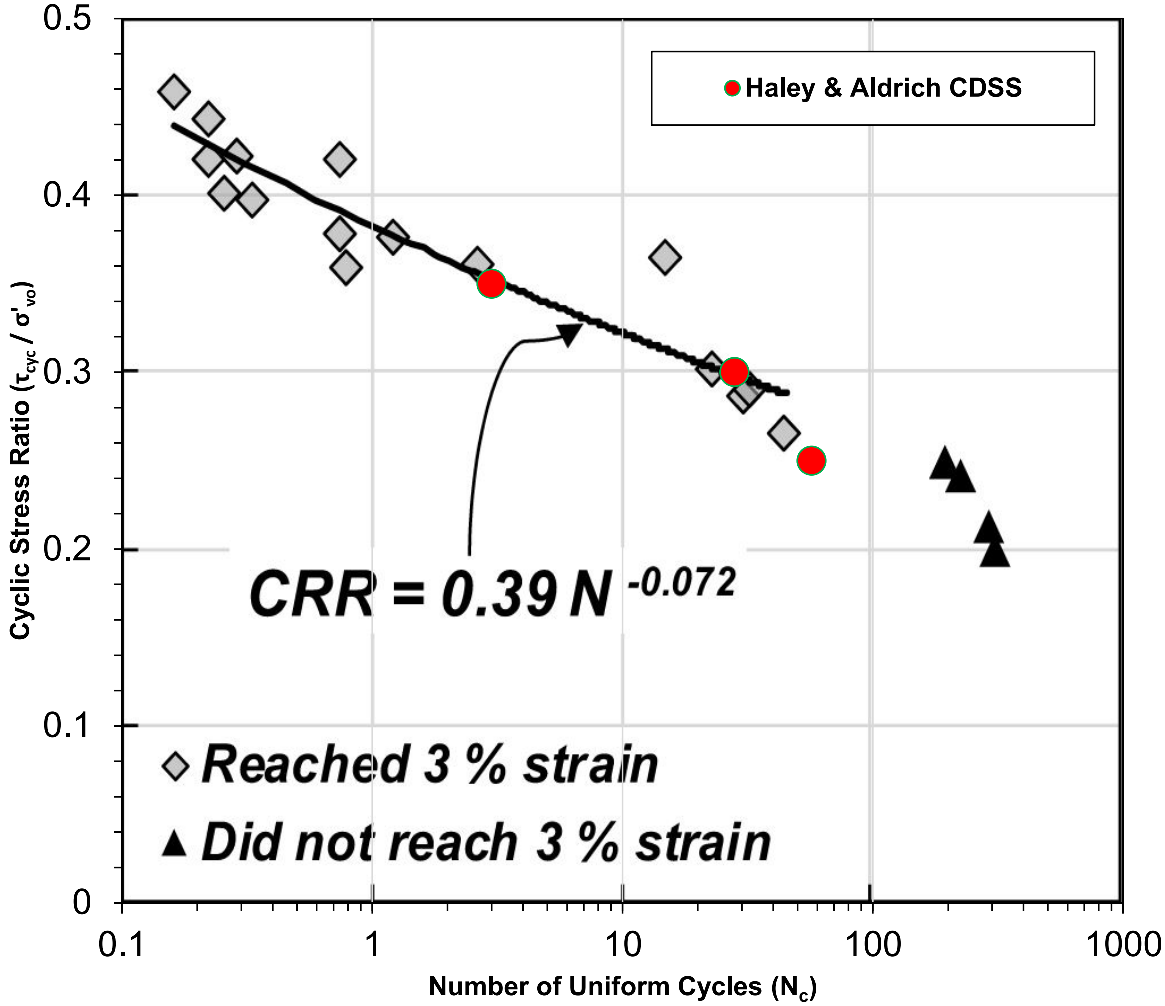

Notes:

1. Background figure was taken from Figure 2.17 of *Studlein & Jana (2020). Evaluation of Deep, Insitu, Blast-Induced Dynamic Response of Natural Silt and Sand: Dynamic Response of Soils at the Port of Portlan. Cascadia Lifeline Program (CLiP). OSU*

PDX Fuel Tank
Seismic Vulnerability Assessment
Portland, Oregon

Comparison of CSR vs N_c Results with Oregon State University Laboratory Testing Results

0204679-001 July 2023

HALEY ALDRICH

Fig. C-5

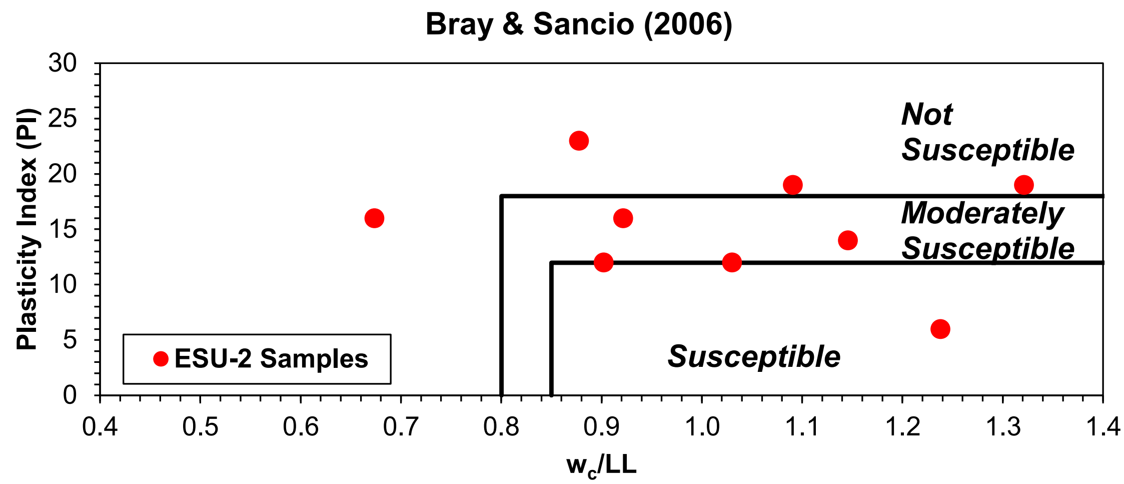

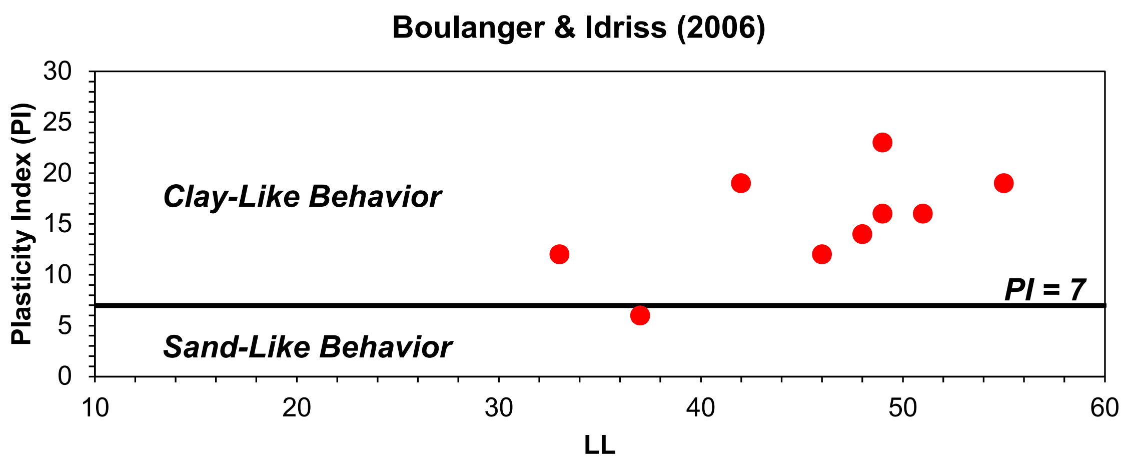

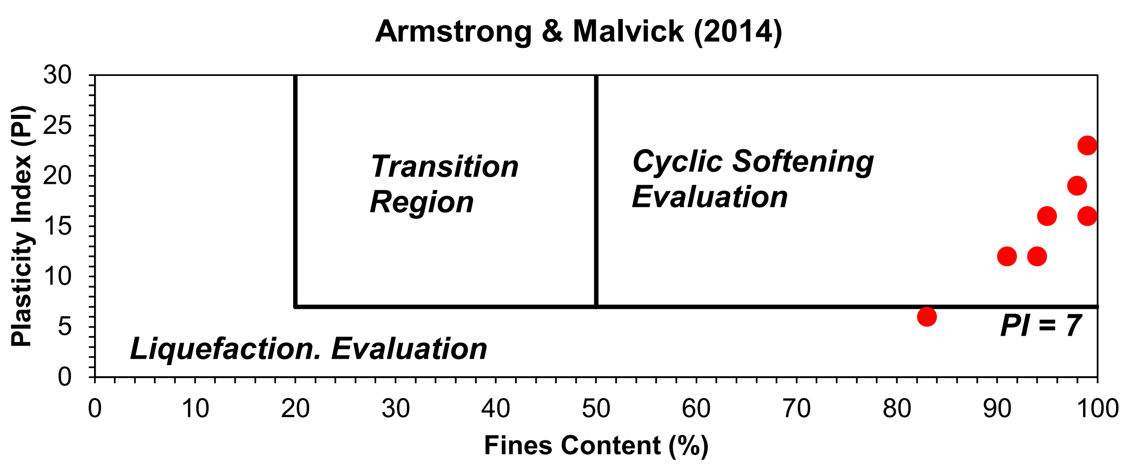

Notes:

1. All criteria were developed for different classification purposes and are complementary to each other.

PDX Fuel Tank
Seismic Vulnerability Assessment
Portland, Oregon

Liquefaction Susceptibility Assessment for ESU-2 (ML-CL)

0204679-001 July 2023

HALEY ALDRICH

Fig. C-6

C:\Script\HAGTL_CPT_LevelGround\Validation\[Engineering Properties.xlsx]Fig C-5

APPENDIX D
Probabilistic and Deterministic Seismic Hazard Analysis and Design Ground Motion Characterization

A. Total Mean Seismic Hazard Curve
B. Source Specific Hazard Curves:
Impulsive Period (0.2 seconds) and Convective Period (7.5 seconds)
C. Disaggregation Results:
Impulsive Period (0.2 seconds) and Convective g Period (7.5 seconds)
D. 84th-Percentiles Deterministic Spectrum Results:
Portland Hills Fault, CSZ Intraslab, and CSZ Interface
E. Deterministic Spectrum: All sources
F. Input Motions: Impulsive Period Suite
G. Input Motions: Convective Period Suite

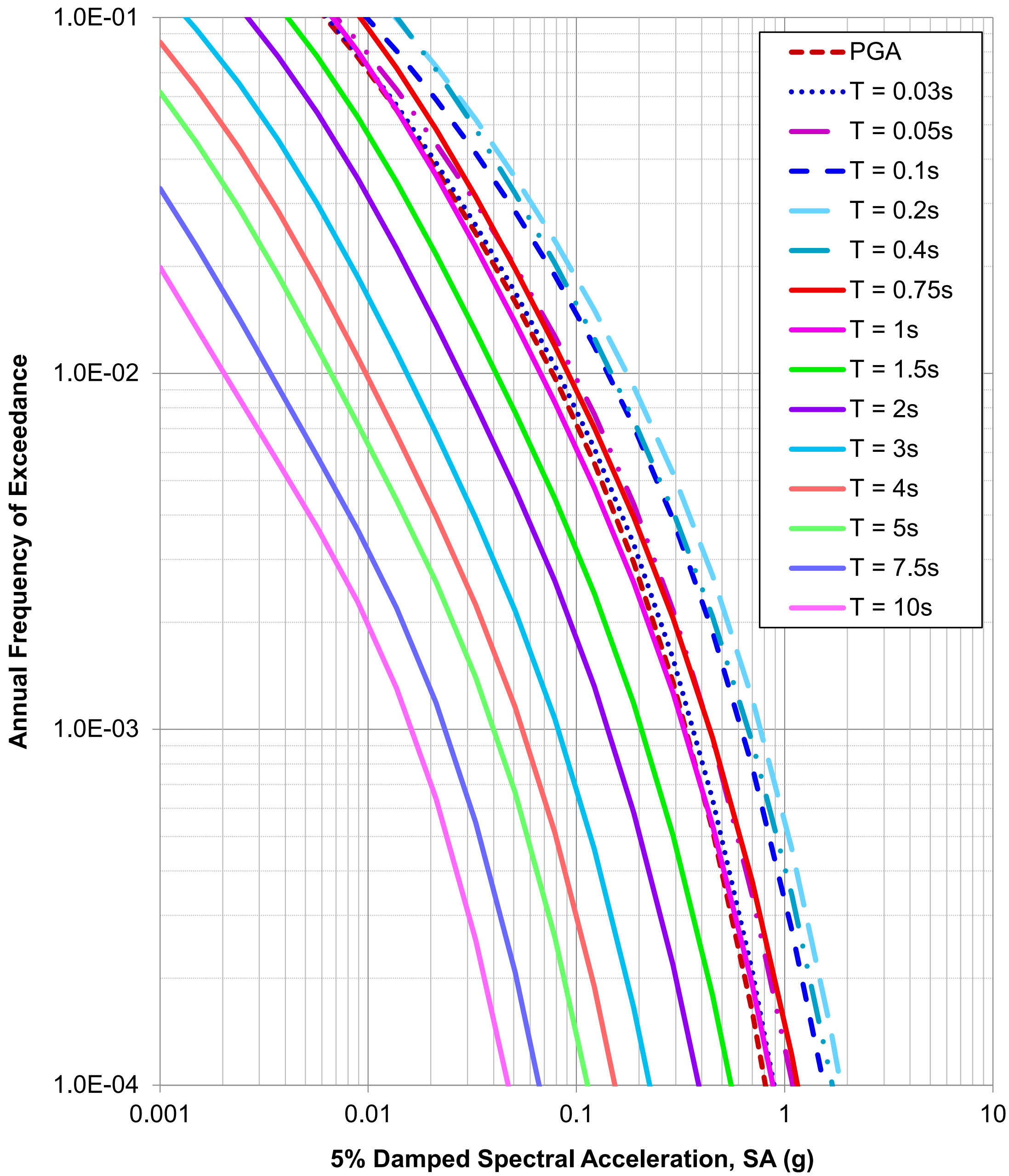

PDX Fuel Tank
Seismic Vulnerability Assessment
Portland, Oregon

Total Mean Seismic Hazard Curves

0204679-001 July 2023

HALEY ALDRICH

Fig. D-1

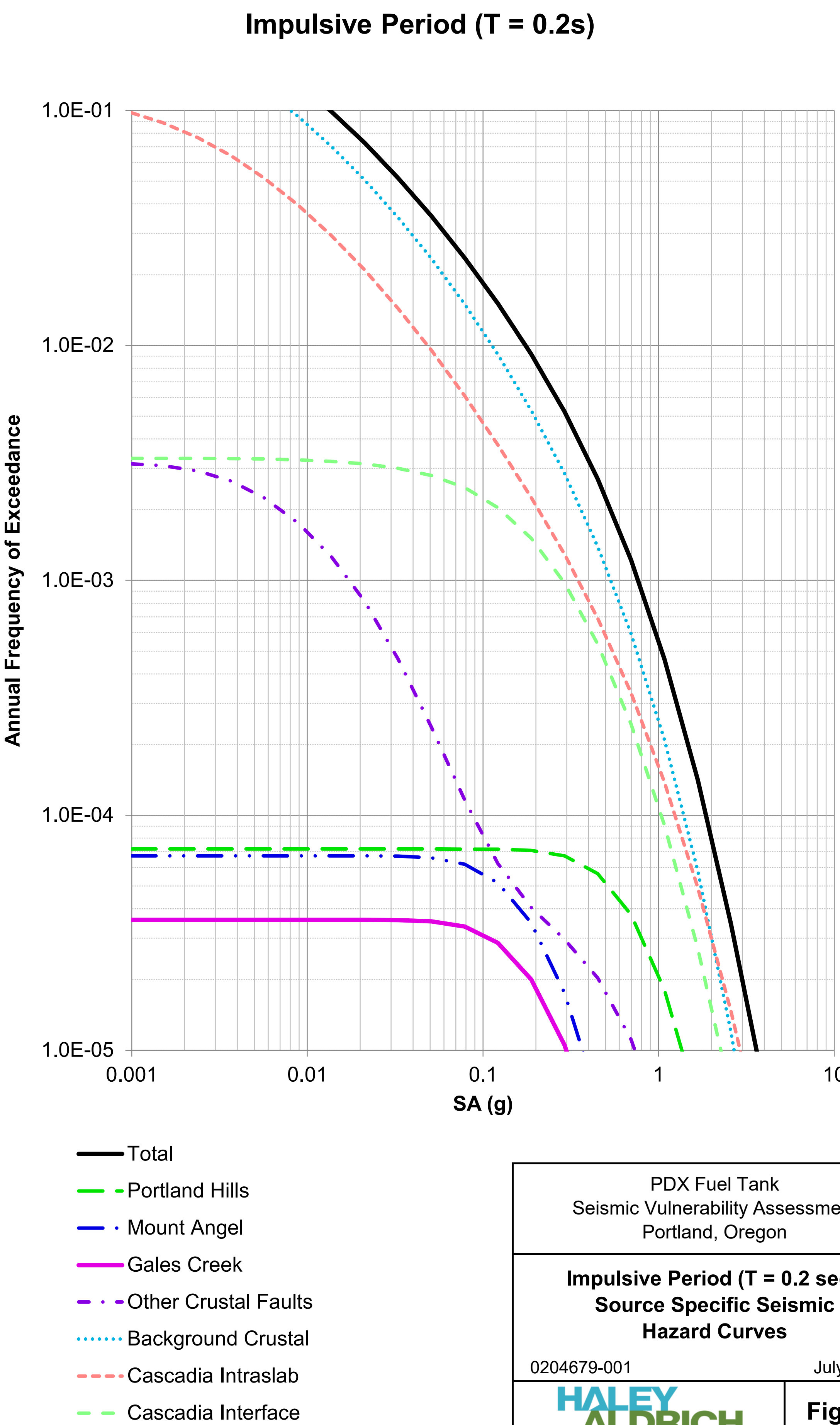

PDX Fuel Tank Seismic Vulnerability Assessment Portland, Oregon	
Impulsive Period (T = 0.2 sec) Source Specific Seismic Hazard Curves	
0204679-001	July 2023
HALEY ALDRICH	**Fig. D-2**

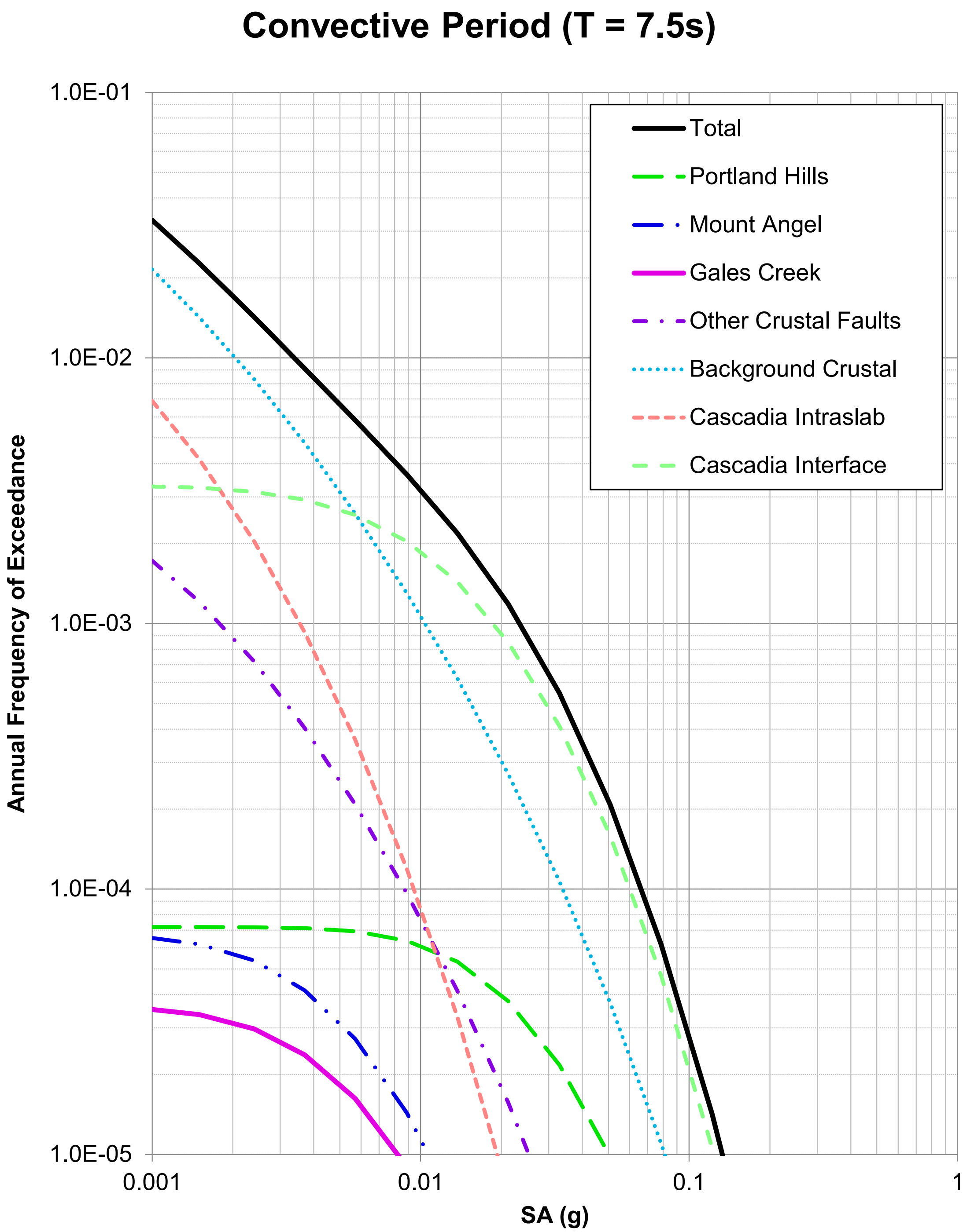

PDX Fuel Tank
Seismic Vulnerability Assessment
Portland, Oregon

Convective Period (T = 7.5 sec)
Source Specific Seismic
Hazard Curves

0204679-001 July 2023

HALEY ALDRICH

Fig. D-3

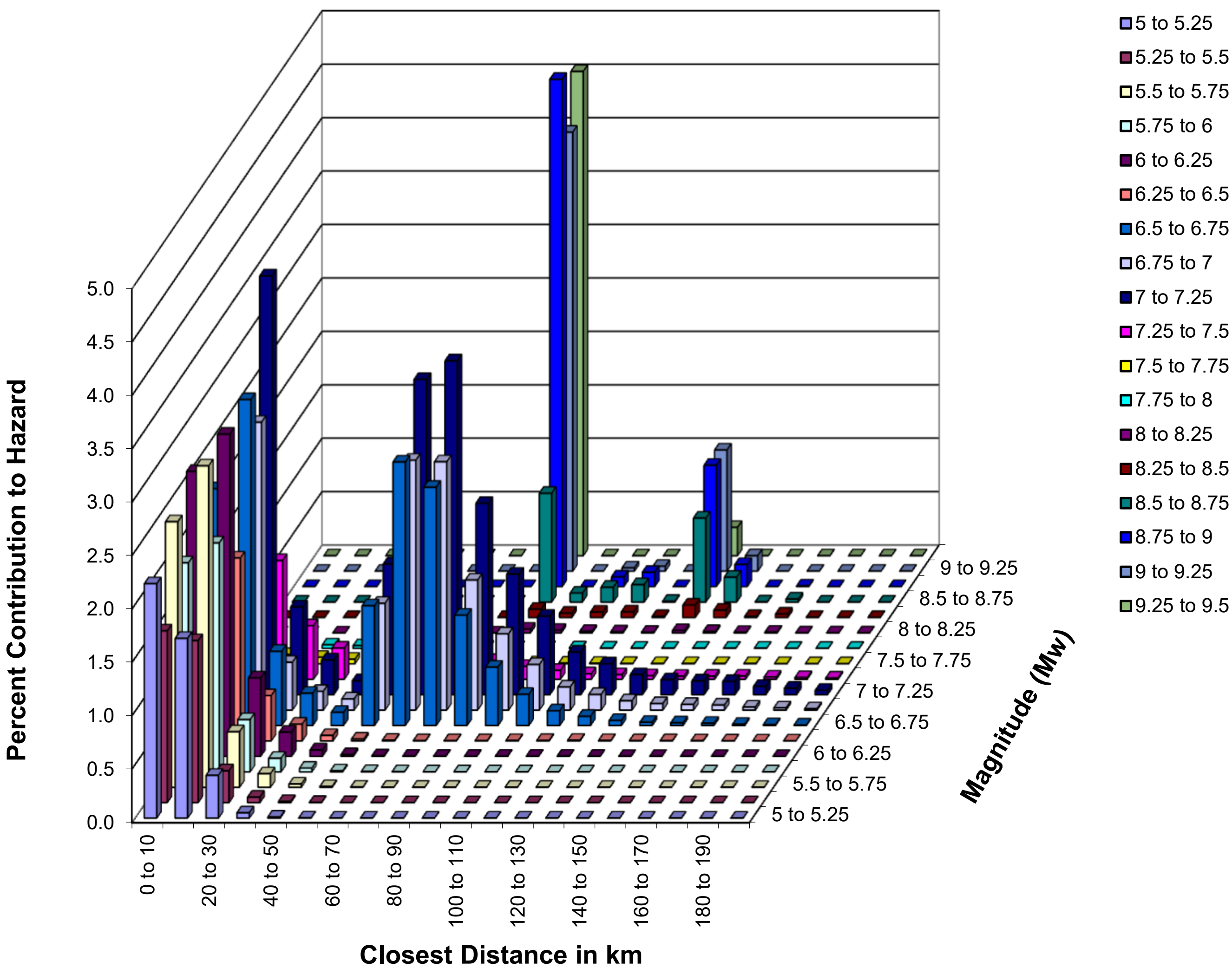

Source	Percent Contribution
Cascadia Interface	19.6%
Portland Hills	4.0%
Other Fault Sources	1.0%
Gridded Crustal Seismicity	45.0%
Deep Intraslab	30.4%

Site and Hazard Information	
Latitude	45.597485
Longitude	-122.6129
Return Period	2,475 years
V_{S30}	1,271 ft/sec
Sa Period	0.2 s
Amplitude	1.13 g

Summary Over All Sources		
Parameter	Mean	Modal
Magnitude	7.0	8.75 to 9
Distance (km)	50.0	80 to 90
Epsilon	1.22	-

Mean Parameters for Each Source Type		
Source Type	Mw	Rrup
Interface	9.0	93.8
Intraslab	6.9	81.1
Crustal	6.3	13.6

PDX Fuel Tank
Seismic Vulnerability Assessment
Portland, Oregon

2,475 Years Disaggregated Results at T = 0.2 sec (Impulsive Periods)

0204679-001 July 2023

HALEY ALDRICH

Fig. D-4

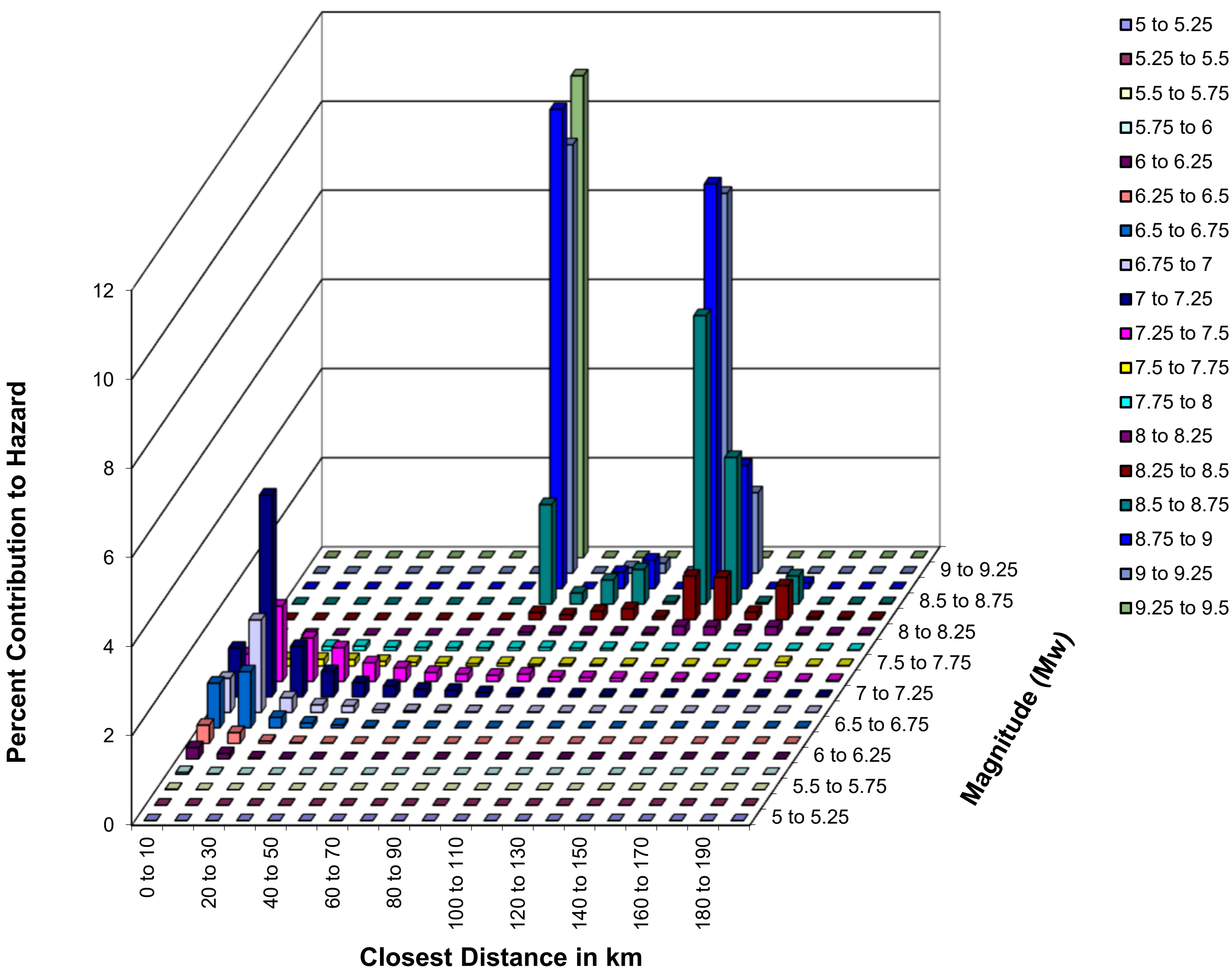

Source	Percent Contribution
Cascadia Interface	75.8%
Portland Hills	4.2%
Other Crustal sources	0.8%
Gridded Crustal Seismicity	18.9%
Deep Intraslab	0.2%

Site and Hazard Information	
Latitude	45.597485
Longitude	-122.6129
Return Period	2,475 years
Vs30	1,271 ft/sec
Sa Period	7.5
Amplitude	0.04 g

Summary Over All Sources		
Parameter	Mean	Modal
Magnitude	8.5	9.25 to 9.5
Distance (km)	93.4	80 to 90
Epsilon	0.89	-

Mean Parameters for Each Source Type		
Source Type	Mw	Rrup
Interface	8.9	112.5
Intraslab	7.2	75.6
Crustal	7.1	31.7

PDX Fuel Tank
Seismic Vulnerability Assessment
Portland, Oregon

2,475 Years Disaggregated Results at T = 7.5 sec (Convective Periods)

0204679-001 July 2023

HALEY ALDRICH

Fig. D-5

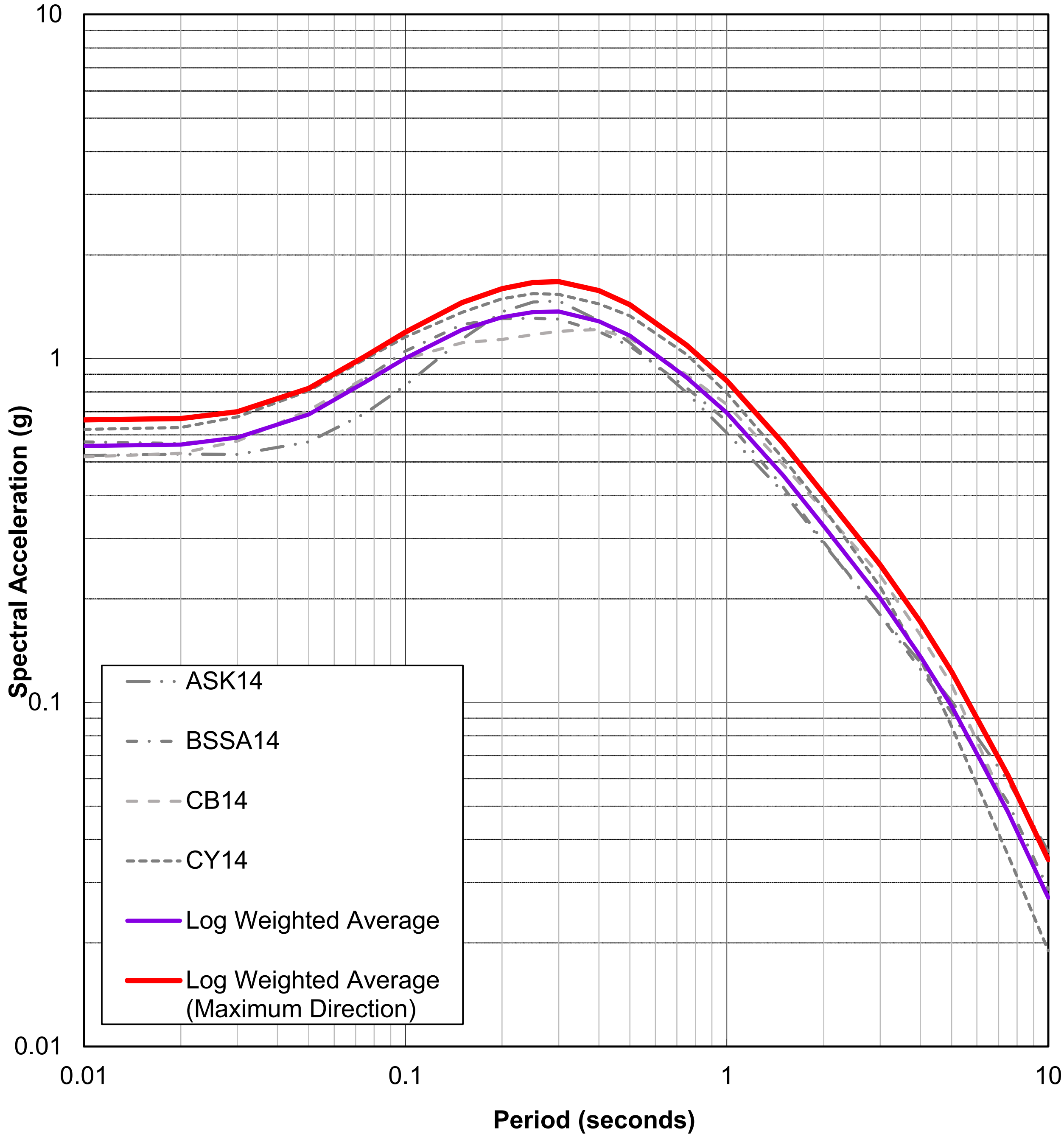

Notes:

1. Mw = 7.1, R_{rup} = 10.4 km, V_{S30} = 388 m/s
   Z_{TOR} = 0 km, $Z_{1.0}$ = 0.45 km, $Z_{2.5}$ = 1.8 km
   F_{RV} = 1, F_{HW} = 0, Dip = 70°
   Measured V_{S30}
   Region Global
   Others Parameter set to Default
   Calculated using NGAW2 GMPE Spreadsheet
2. Maximum Direction Factor
   (Shahi & Baker, 2014)

PDX Fuel Tank
Seismic Vulnerability Assessment
Portland, Oregon

Portland Hills (Crustal)
Deterministic 84-th Percentile
Response Spectrum

0204679-001 July 2023

HALEY ALDRICH

Fig. D-6

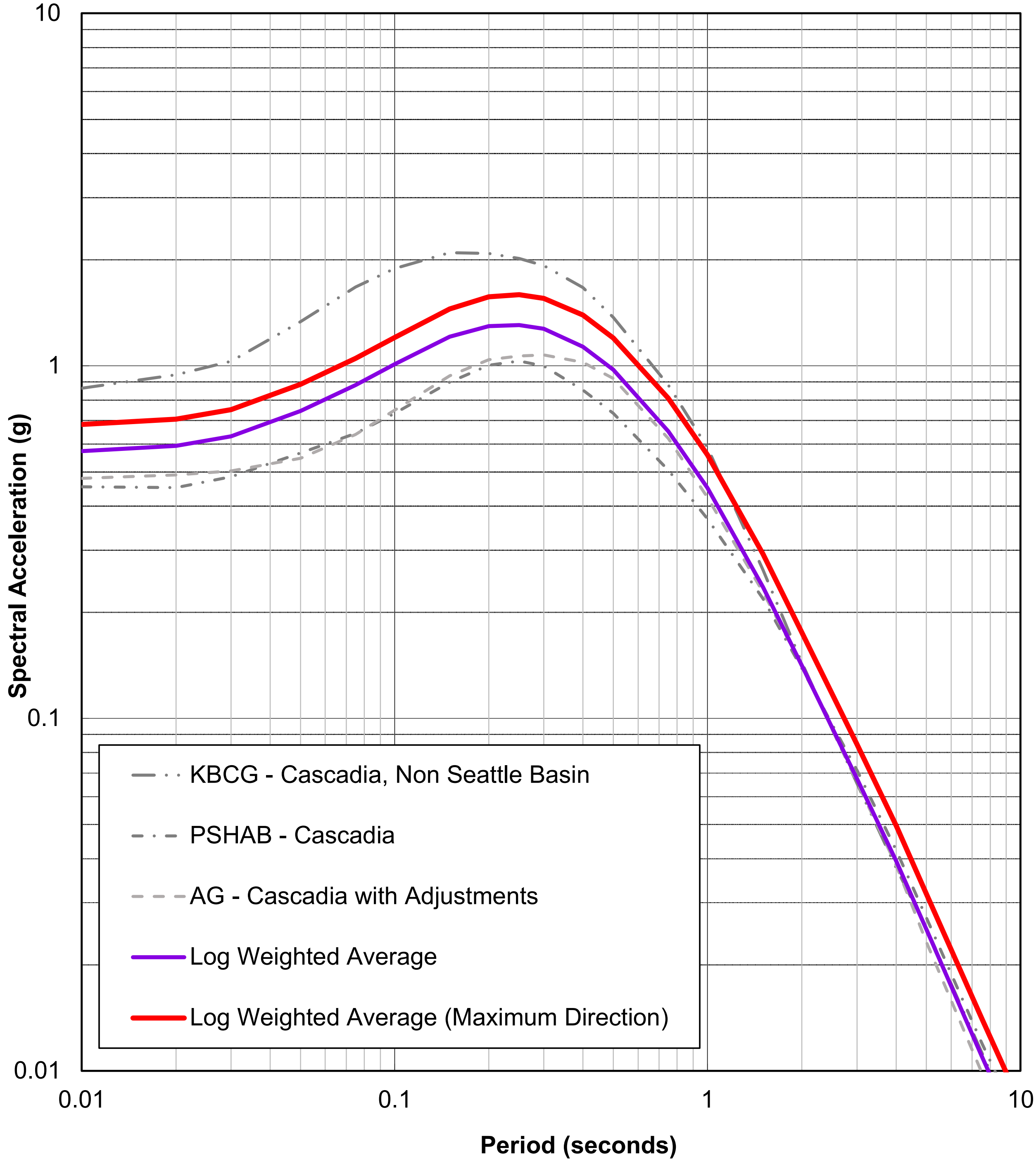

Notes:

1. Mw = 7.2, R_{rup} = 75 km, V_{S30} = 388 m/s
   Z_{TOR} = 50 km, Hypocentral Depth = 65 km
   $Z_{1.0}$ = 0.405 km, $Z_{2.5}$ = 1.8 km

PDX Fuel Tank
Seismic Vulnerability Assessment
Portland, Oregon

CSZ Intraslab Deterministic 84-th Percentile Response Spectrum

0204679-001 July 2023

HALEY ALDRICH

Fig. D-7

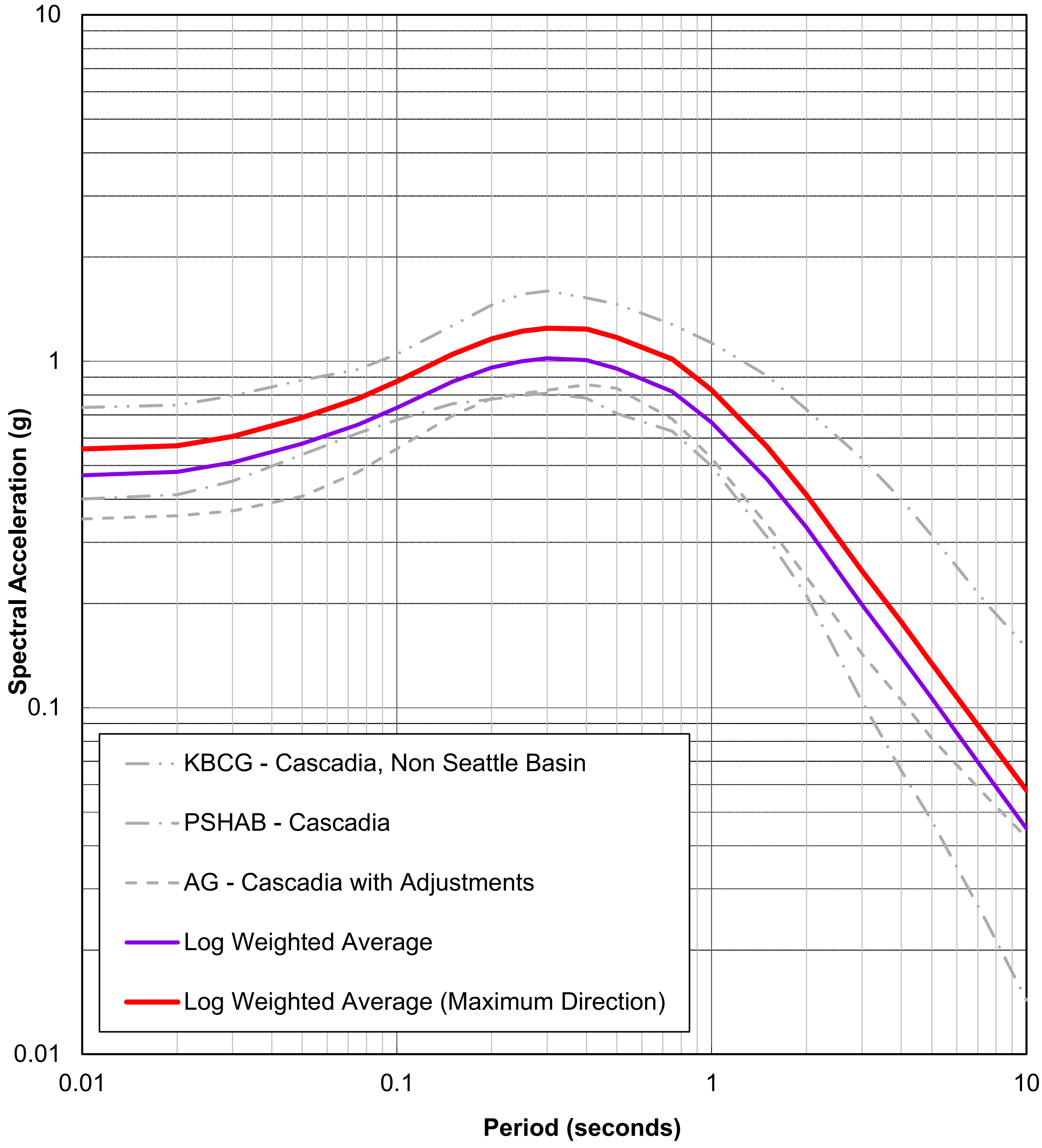

Notes:

1. M_w = 9.0, R_{rup} = 94 km, V_{S30} = 388 m/s
   Z_{TOR} = 5 km, $Z_{1.0}$ = 0.405 km, $Z_{2.5}$ = 1.8 km

PDX Fuel Tank
Seismic Vulnerability Assessment
Portland, Oregon

CSZ Interface Deterministic 84-th Percentile Response Spectrum

0204679-001 July 2023

HALEY ALDRICH

Fig. D-8

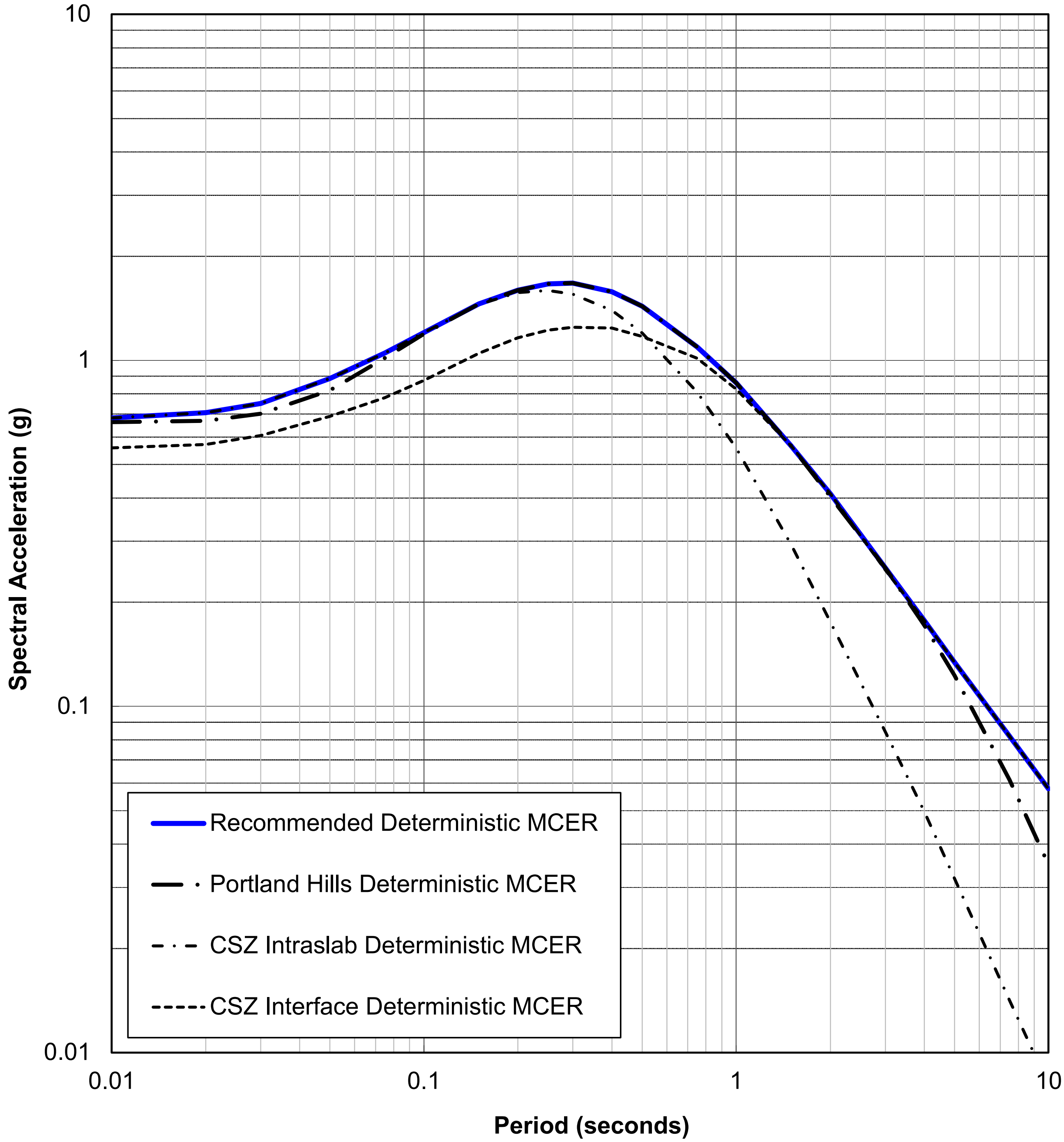

PDX Fuel Tank
Seismic Vulnerability Assessment
Portland, Oregon

Calculated Response Spectrum
Deterministic MCE_R: All Sources

0204679-001 July 2023

HALEY ALDRICH

Fig. D-9

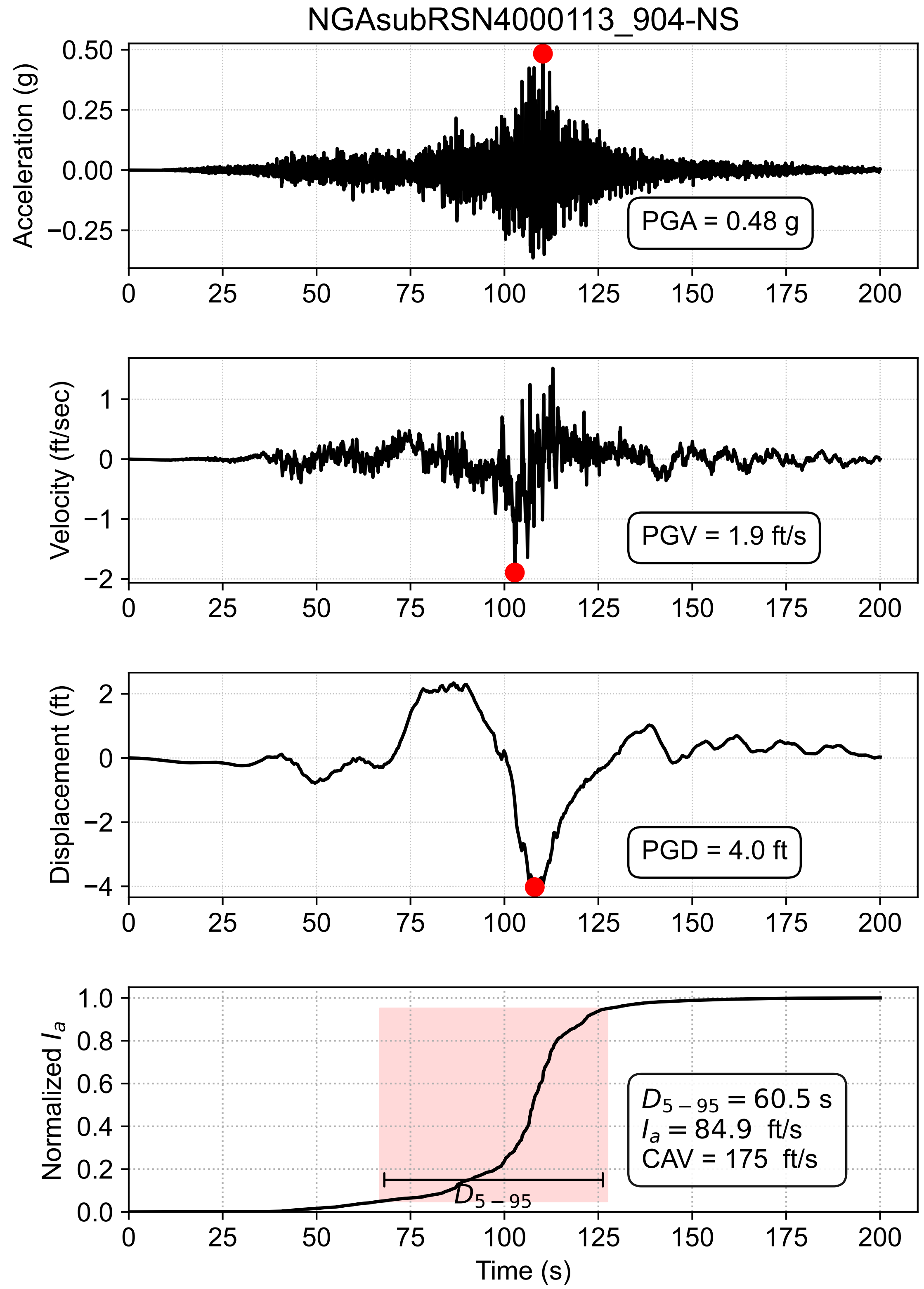

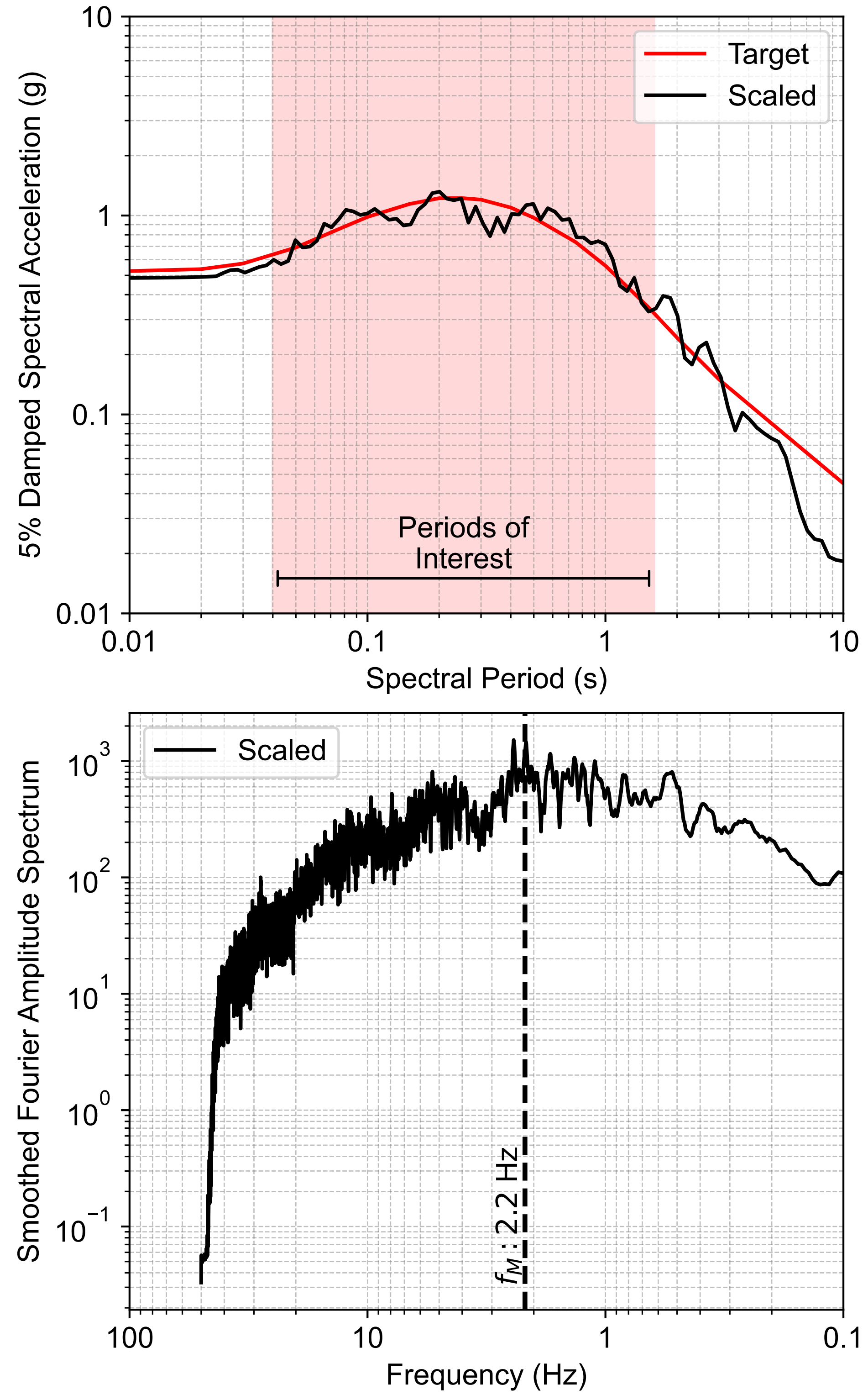

Event = Tohoku_Japan 2011
M_w = 9.1
R_{rup} = 91.8 km
V_{S30} = 411 m/s
Scale Factor = 2.22
Station = 42308
Mechanism = Interface
Pulse Tp = nan s
HW Index = N/A

Notes:

1. PGA, PGV, PGD = Peak Ground Acceleration, Velocity, Displacement
2. The quiet motion (head and tail) of original recording are truncated & baseline corrected
3. D_{5-95} = Significant duration from 5% to 95% Normalized Arias Intensity
4. I_a = Arias Intensity
5. CAV = Cumulative Absolute Velocity
6. f_M = Mean frequency based on Rathje et al. (1998)
7. Pulse Tp = Period of Pulse (seconds), if nan, not classified as a pulse-like record
8. HW Index = Hanging wall index, HW: Hanging Wall, FW: Foot Wall, NU: Neutral, N/A: not applicable

PDX Fuel Tank SVA
Portland, OR

Amplitude Scaled, One-Component Ground Motion Parameters RSN4000113_904-NS

0204679-001 July 2023

HALEY ALDRICH

Figure D-10

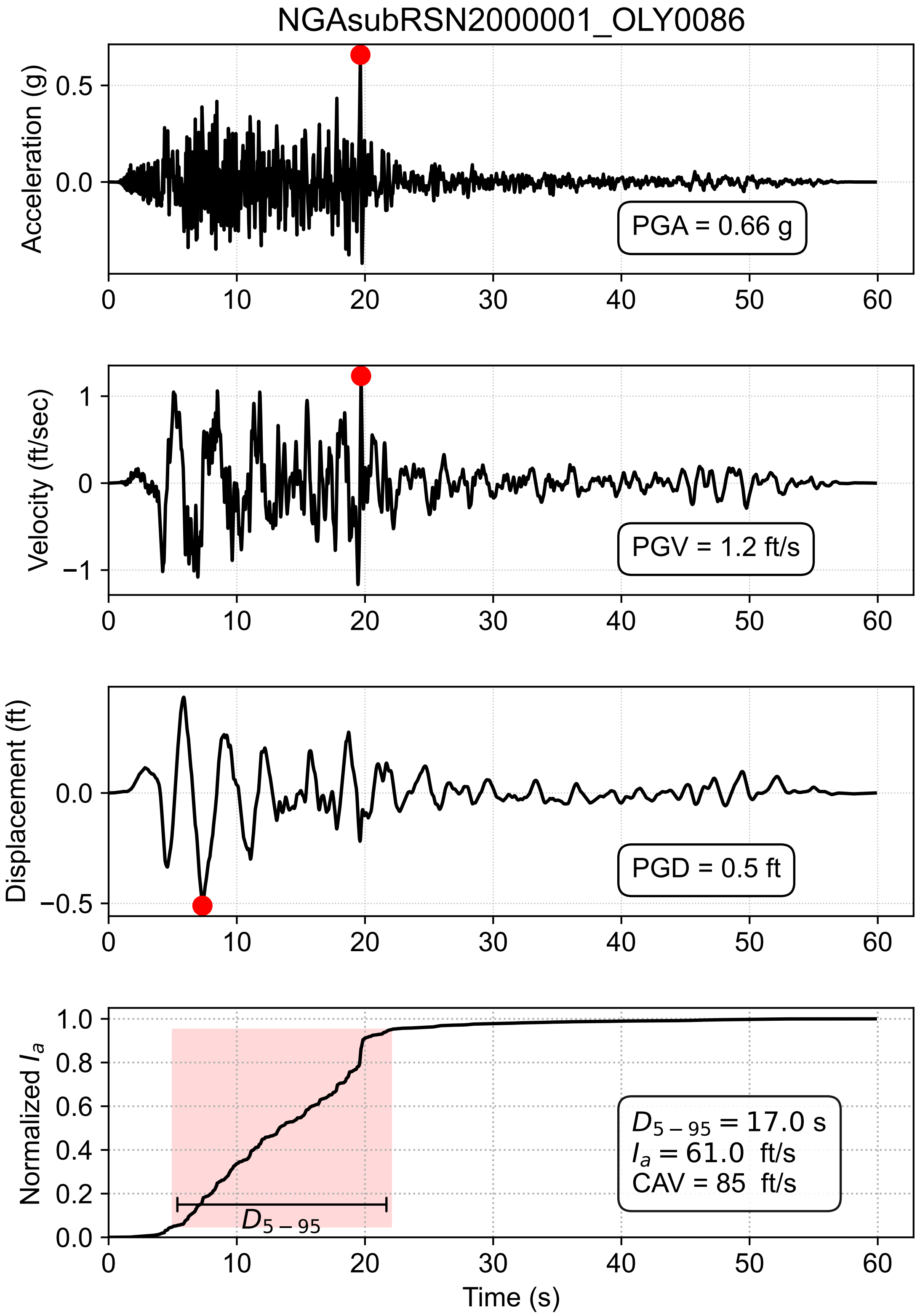

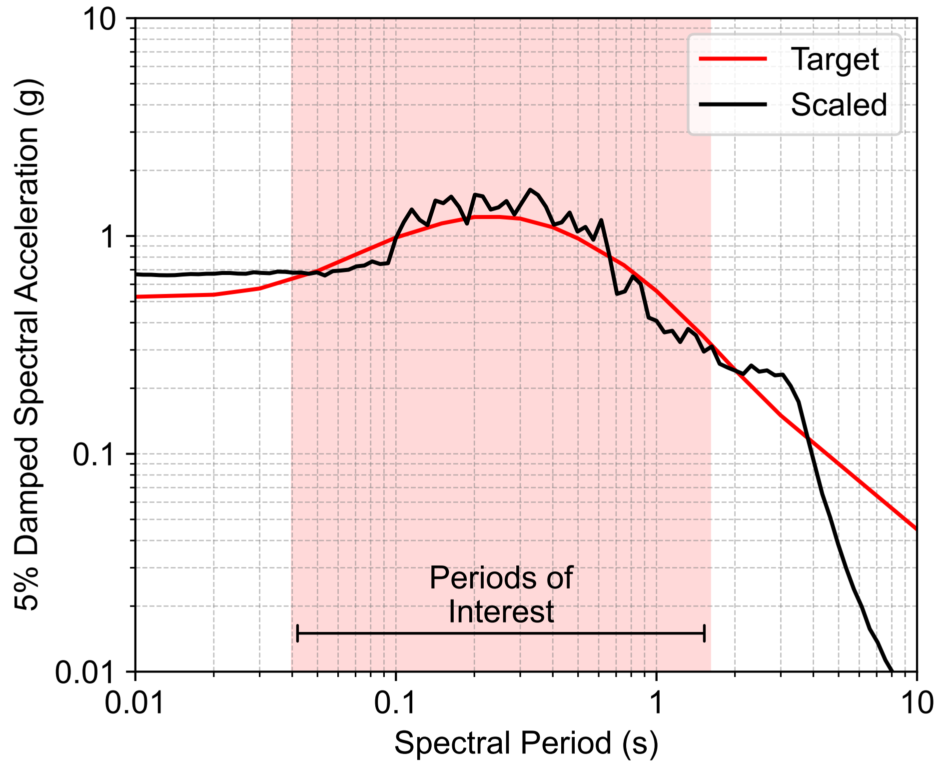

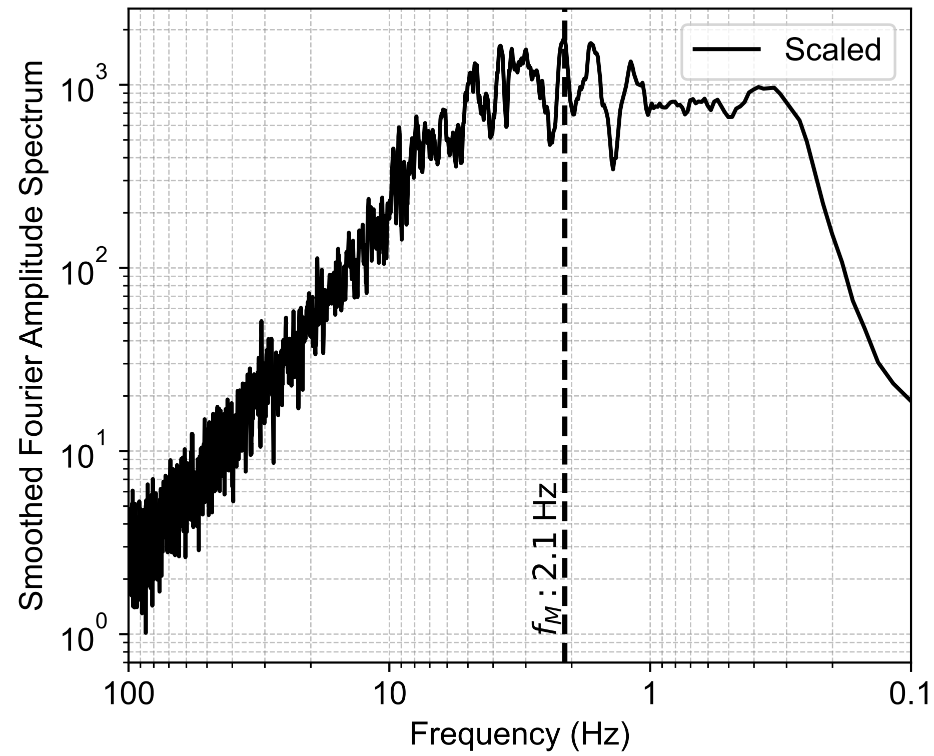

Event = Olympia_WA 1949
M_w = 6.7
R_{rup} = 47.6 km
V_{S30} = 399 m/s
Scale Factor = 2.20
Station = OLY0
Mechanism = Intraslab
Pulse Tp = nan s
HW Index = N/A

Notes:

1. PGA, PGV, PGD = Peak Ground Acceleration, Velocity, Displacement
2. The quiet motion (head and tail) of original recording are truncated & baseline corrected
3. D_{5-95} = Significant duration from 5% to 95% Normalized Arias Intensity
4. I_a = Arias Intensity
5. CAV = Cumulative Absolute Velocity
6. f_M = Mean frequency based on Rathje et al. (1998)
7. Pulse Tp = Period of Pulse (seconds), if nan, not classified as a pulse-like record
8. HW Index = Hanging wall index, HW: Hanging Wall, FW: Foot Wall, NU: Neutral, N/A: not applicable

PDX Fuel Tank SVA
Portland, OR

Amplitude Scaled, One-Component Ground Motion Parameters RSN2000001_OLY0086

0204679-001 July 2023

HALEY ALDRICH

Figure D-11

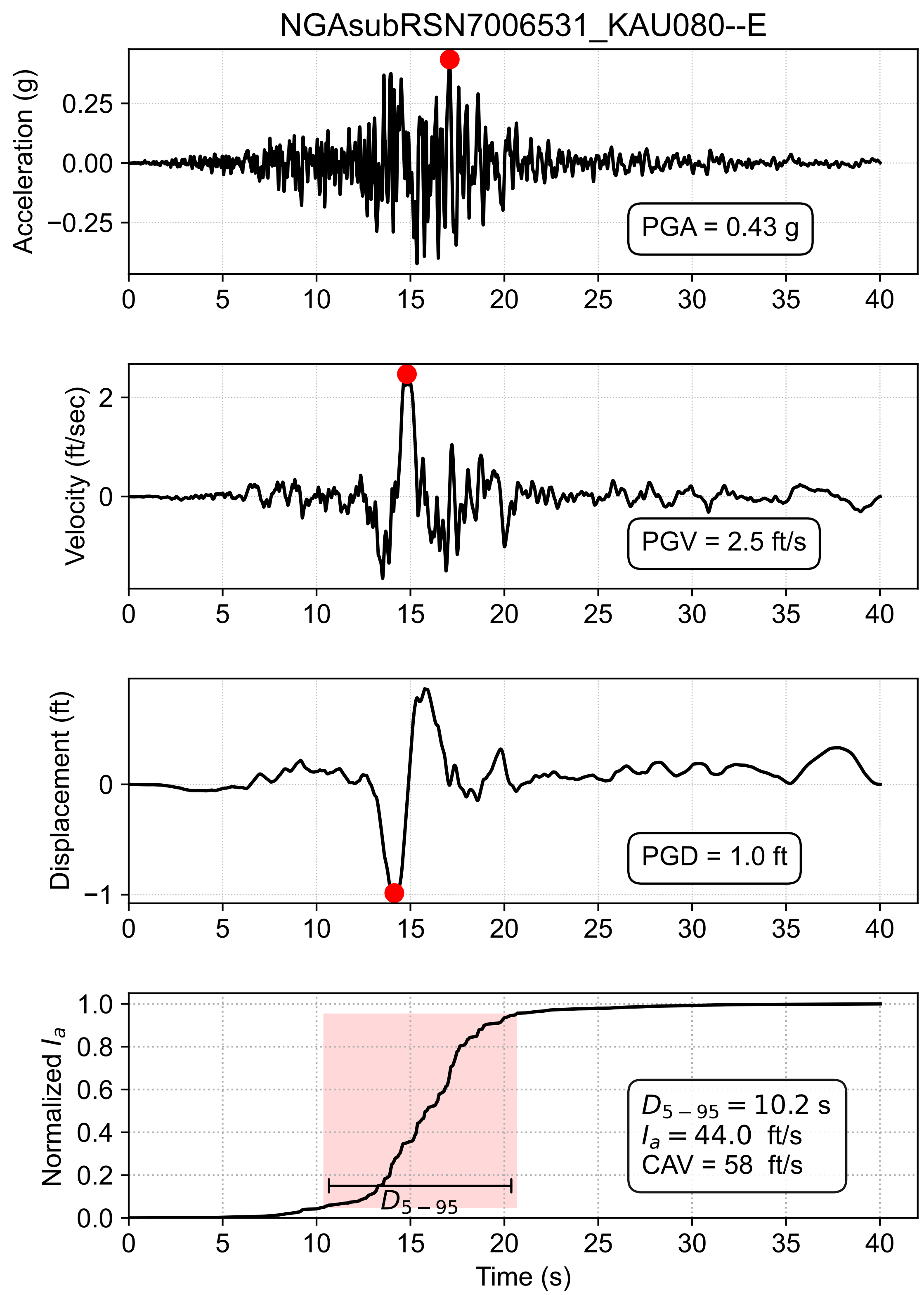

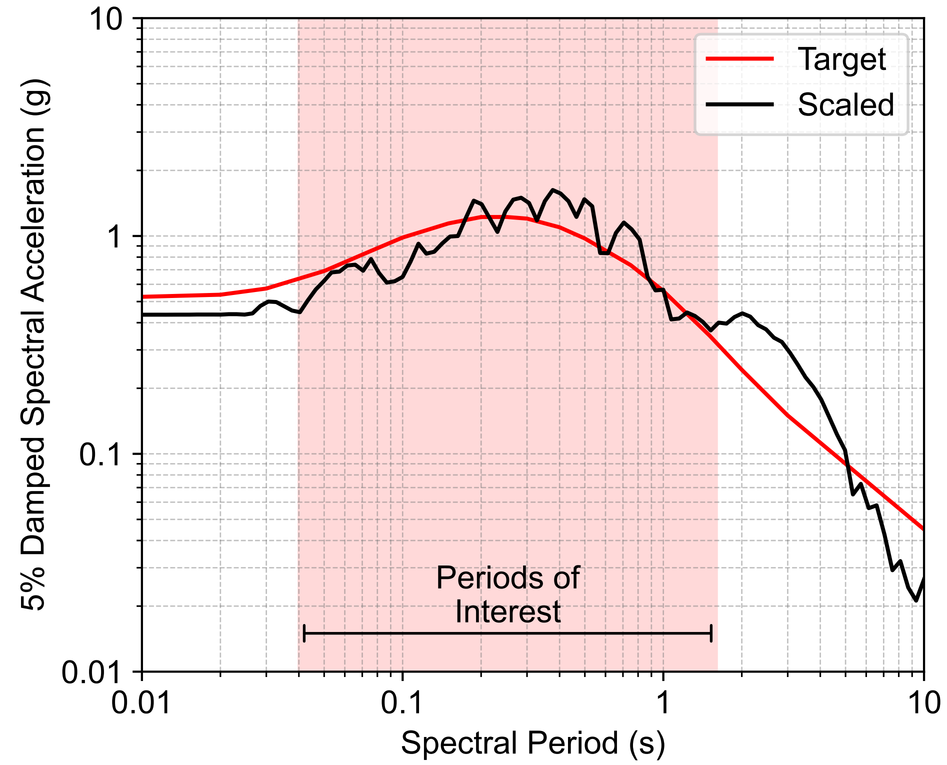

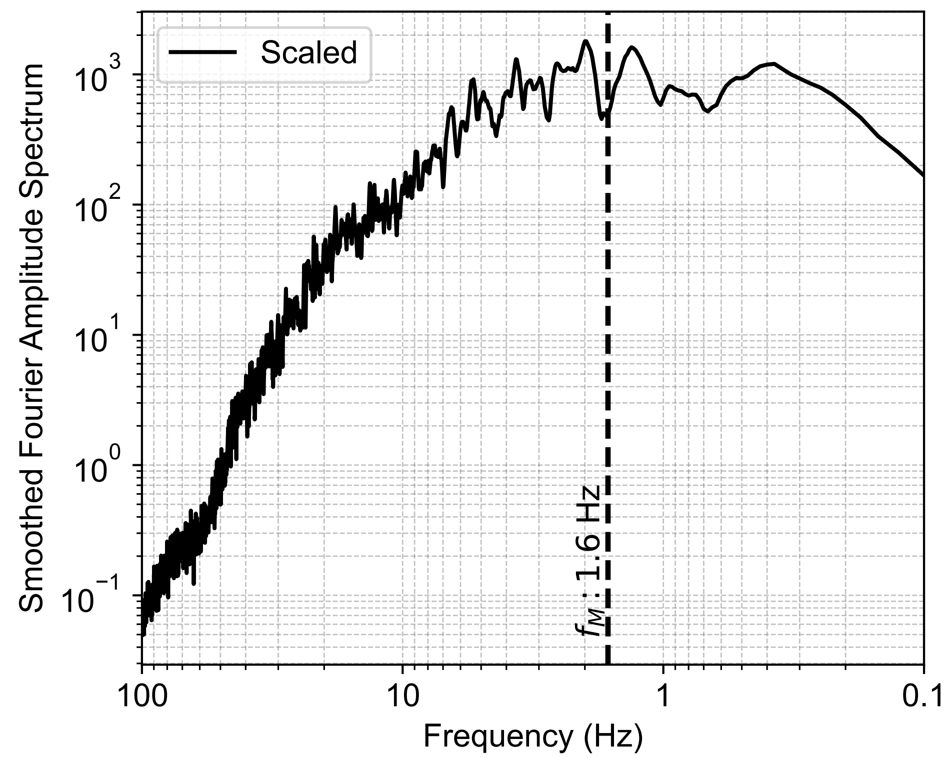

Event = Pingtung_Taiwan 2006
M_w = 6.94
R_{rup} = 34.7 km
V_{S30} = 400 m/s
Scale Factor = 2.21
Station = KAU080
Mechanism = Intraslab
Pulse Tp = nan s
HW Index = N/A

Notes:

1. PGA, PGV, PGD = Peak Ground Acceleration, Velocity, Displacement
2. The quiet motion (head and tail) of original recording are truncated & baseline corrected
3. D_{5-95} = Significant duration from 5% to 95% Normalized Arias Intensity
4. I_a = Arias Intensity
5. CAV = Cumulative Absolute Velocity
6. f_M = Mean frequency based on Rathje et al. (1998)
7. Pulse Tp = Period of Pulse (seconds), if nan, not classified as a pulse-like record
8. HW Index = Hanging wall index, HW: Hanging Wall, FW: Foot Wall, NU: Neutral, N/A: not applicable

PDX Fuel Tank SVA
Portland, OR

Amplitude Scaled, One-Component Ground Motion Parameters RSN7006531_KAU080--E

0204679-001 July 2023

HALEY ALDRICH

Figure
D-12

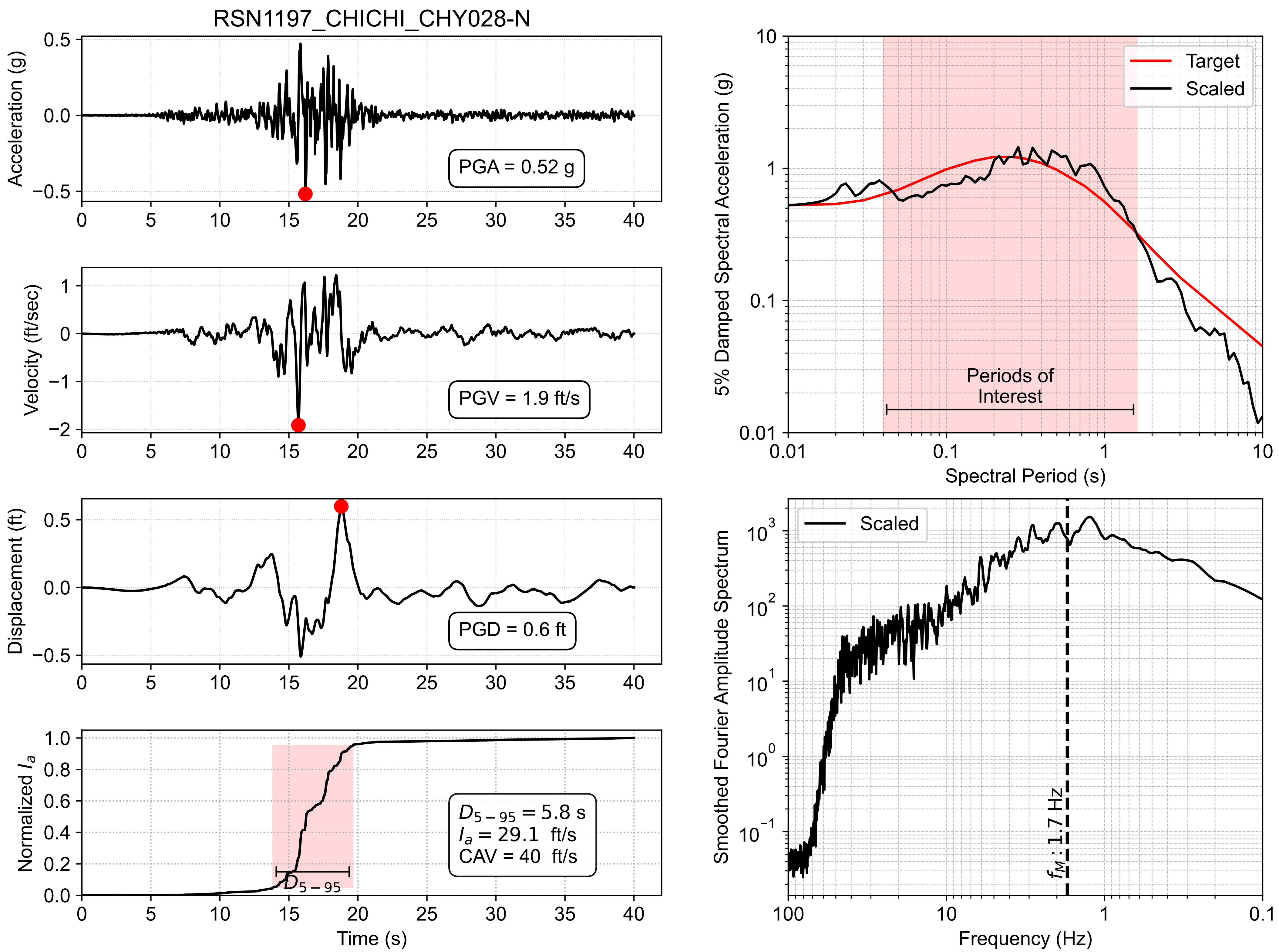

Event = Chi-Chi_ Taiwan 1999
M_w = 7.62
R_{rup} = 3.12 km
V_{S30} = 543 m/s
Scale Factor = 0.68
Station = 1197
Mechanism = Reverse-Oblique
Pulse Tp = nan s
HW Index = FW

Notes:

1. PGA, PGV, PGD = Peak Ground Acceleration, Velocity, Displacement
2. The quiet motion (head and tail) of original recording are truncated & baseline corrected
3. D_{5-95} = Significant duration from 5% to 95% Normalized Arias Intensity
4. I_a = Arias Intensity
5. CAV = Cumulative Absolute Velocity
6. f_M = Mean frequency based on Rathje et al. (1998)
7. Pulse Tp = Period of Pulse (seconds), if nan, not classified as a pulse-like record
8. HW Index = Hanging wall index, HW: Hanging Wall, FW: Foot Wall, NU: Neutral, N/A: not applicable

PDX Fuel Tank SVA
Portland, OR

Amplitude Scaled, One-Component Ground Motion Parameters RSN1197_CHICHI_CHY028-N

0204679-001 July 2023

HALEY ALDRICH

Figure D-13

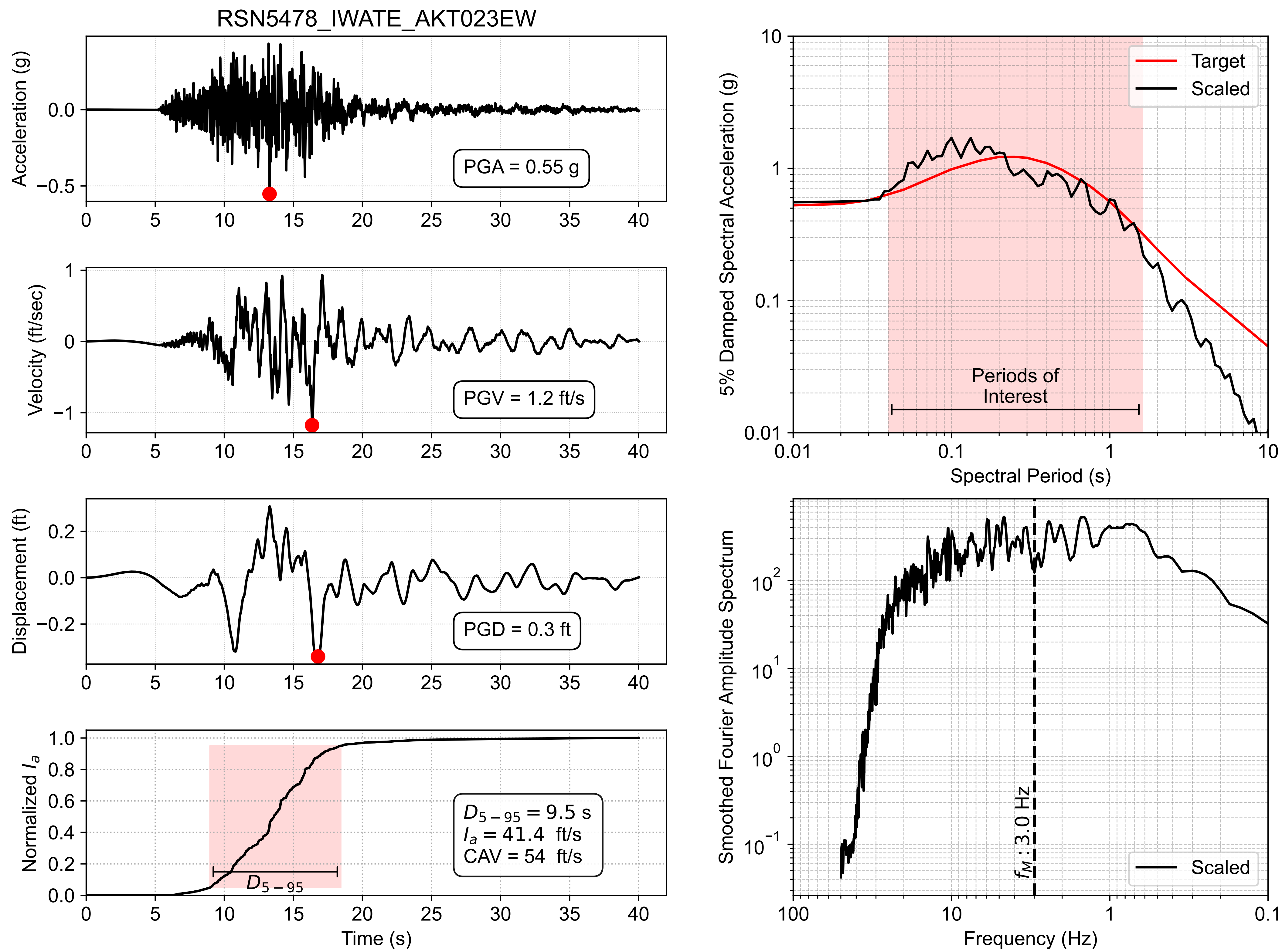

Event = Iwate_ Japan 2008
M_w = 6.9
R_{rup} = 16.96 km
V_{S30} = 556 m/s
Scale Factor = 1.51
Station = 5478
Mechanism = Reverse
Pulse Tp = nan s
HW Index = HW

Notes:

1. PGA, PGV, PGD = Peak Ground Acceleration, Velocity, Displacement
2. The quiet motion (head and tail) of original recording are truncated & baseline corrected
3. D_{5-95} = Significant duration from 5% to 95% Normalized Arias Intensity
4. I_a = Arias Intensity
5. CAV = Cumulative Absolute Velocity
6. f_M = Mean frequency based on Rathje et al. (1998)
7. Pulse Tp = Period of Pulse (seconds), if nan, not classified as a pulse-like record
8. HW Index = Hanging wall index, HW: Hanging Wall, FW: Foot Wall, NU: Neutral, N/A: not applicable

PDX Fuel Tank SVA
Portland, OR

Amplitude Scaled, One-Component Ground Motion Parameters RSN5478_IWATE_AKT023EW

0204679-001 July 2023

HALEY ALDRICH

Figure D-14

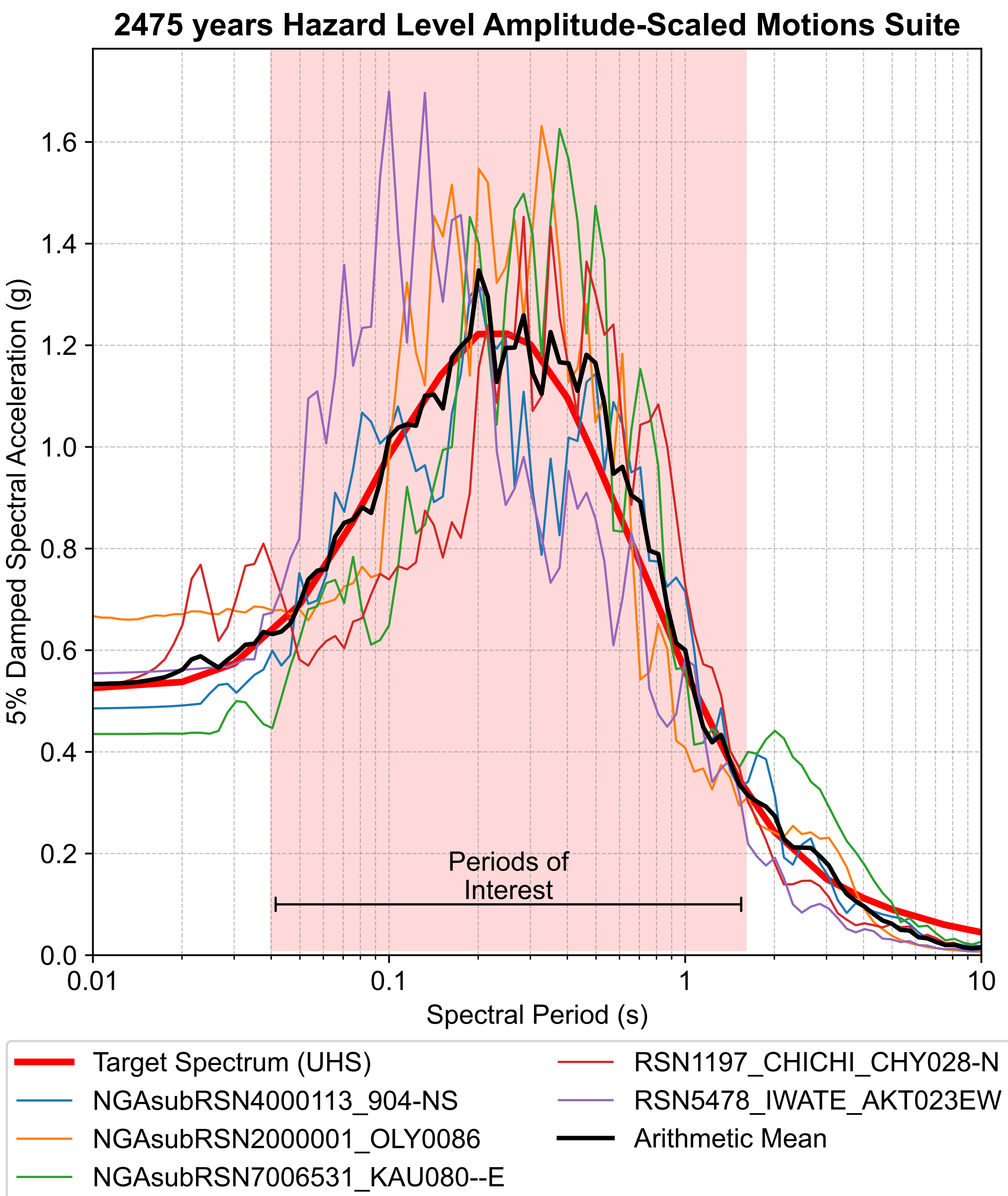

Notes:

1. Target spectrum is at halfspace elevation (1271 ft/s) and based on MCER per ASCE 7-16

HALEY ALDRICH

PDX Fuel Tank SVA
Portland, OR

Amplitude-Scaled Response Spectra Summary Impulsive Period (T = 0.2 sec)

July 2023

0204679-001

FIG. D-15

C:\Alyson Pyrch\Task 1 PDX Fuel Tanks\Ground Motion\Short Period (0.2s)\5Selected Motion\Scaled Input Motion\Results.pdf

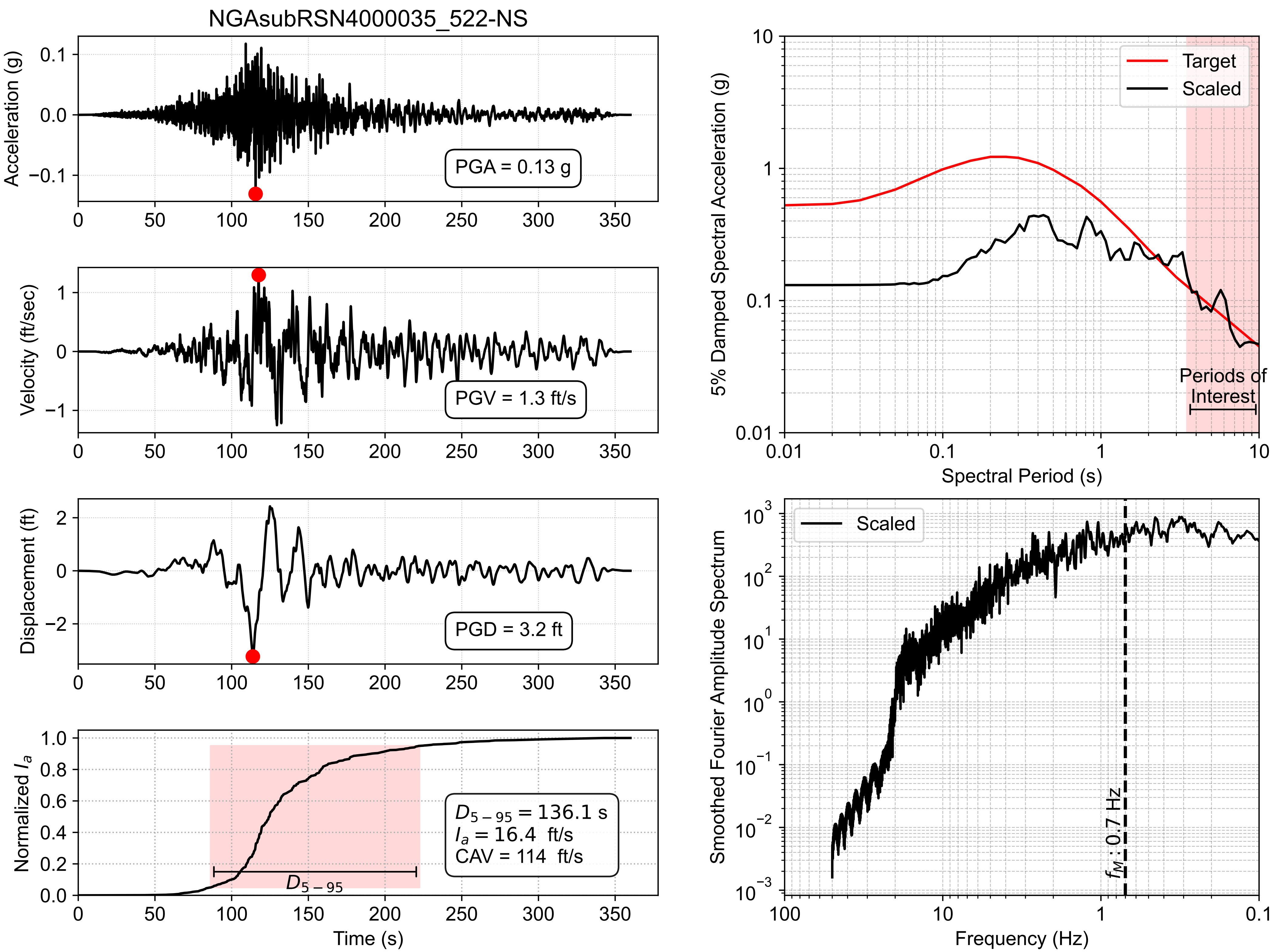

Event = Tohoku_Japan 2011
M_w = 9.12
R_{rup} = 107.7902495 km
V_{S30} = 257 m/s
Scale Factor = 2.03
Station = 41314
Mechanism = Interface
Pulse Tp = nan s
HW Index = N/A

Notes:

1. PGA, PGV, PGD = Peak Ground Acceleration, Velocity, Displacement
2. The quiet motion (head and tail) of original recording are truncated & baseline corrected
3. D_{5-95} = Significant duration from 5% to 95% Normalized Arias Intensity
4. I_a = Arias Intensity
5. CAV = Cumulative Absolute Velocity
6. f_M = Mean frequency based on Rathje et al. (1998)
7. Pulse Tp = Period of Pulse (seconds), if nan, not classified as a pulse-like record
8. HW Index = Hanging wall index, HW: Hanging Wall, FW: Foot Wall, NU: Neutral, N/A: not applicable

PDX Fuel Tank SVA
Portland, OR

Amplitude Scaled, One-Component Ground Motion Parameters RSN4000035_522-NS

0204679-001 July 2023

HALEY ALDRICH

Figure **D-16**

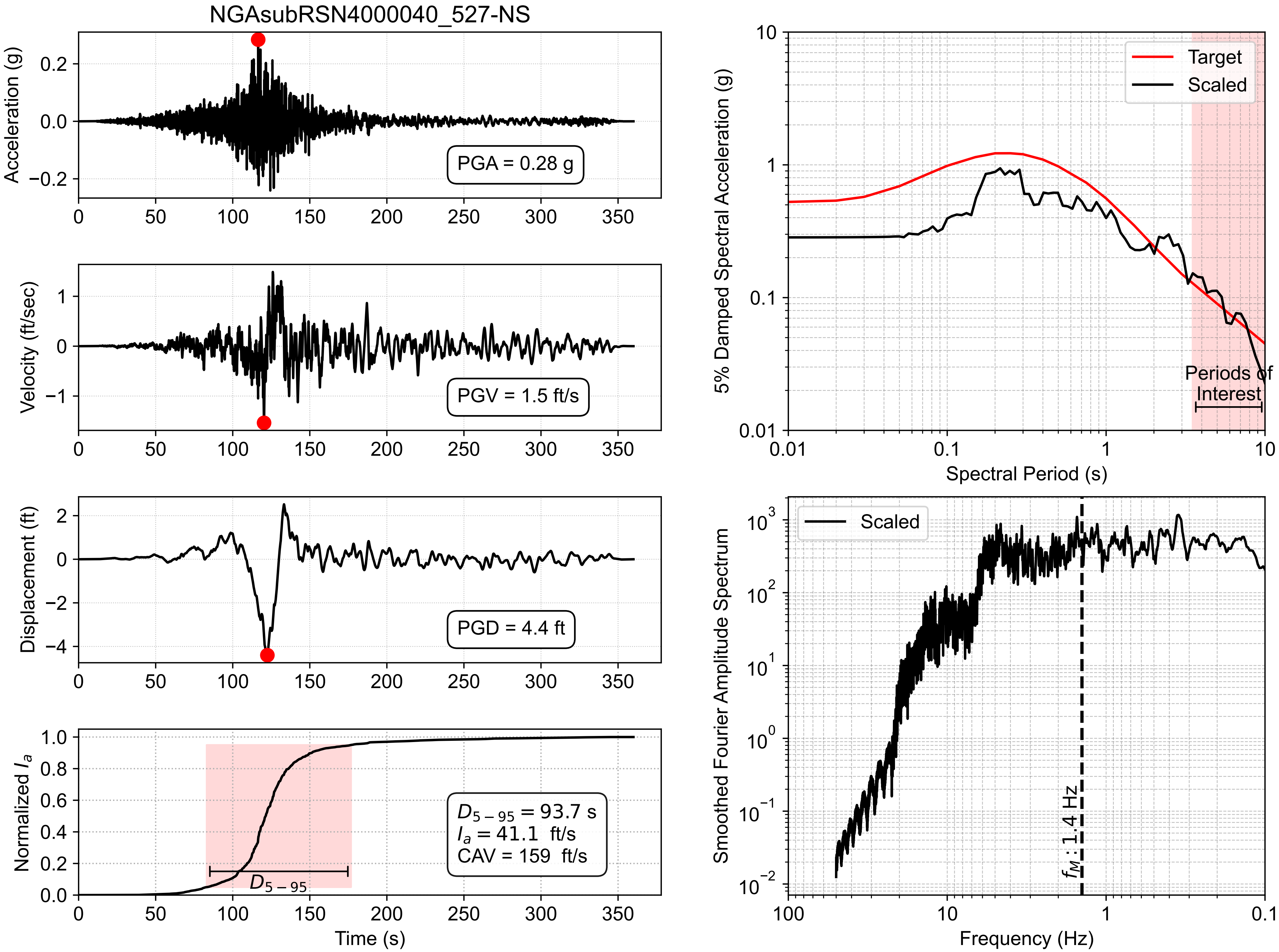

Event = Tohoku_Japan 2011
M_w = 9.12
R_{rup} = 124.5198836 km
V_{S30} = 270 m/s
Scale Factor = 2.44
Station = 41319
Mechanism = Interface
Pulse Tp = nan s
HW Index = N/A

Notes:

1. PGA, PGV, PGD = Peak Ground Acceleration, Velocity, Displacement
2. The quiet motion (head and tail) of original recording are truncated & baseline corrected
3. D_{5-95} = Significant duration from 5% to 95% Normalized Arias Intensity
4. I_a = Arias Intensity
5. CAV = Cumulative Absolute Velocity
6. f_M = Mean frequency based on Rathje et al. (1998)
7. Pulse Tp = Period of Pulse (seconds), if nan, not classified as a pulse-like record
8. HW Index = Hanging wall index, HW: Hanging Wall, FW: Foot Wall, NU: Neutral, N/A: not applicable

PDX Fuel Tank SVA
Portland, OR

Amplitude Scaled, One-Component Ground Motion Parameters RSN4000040_527-NS

0204679-001 July 2023

HALEY ALDRICH

Figure D-17

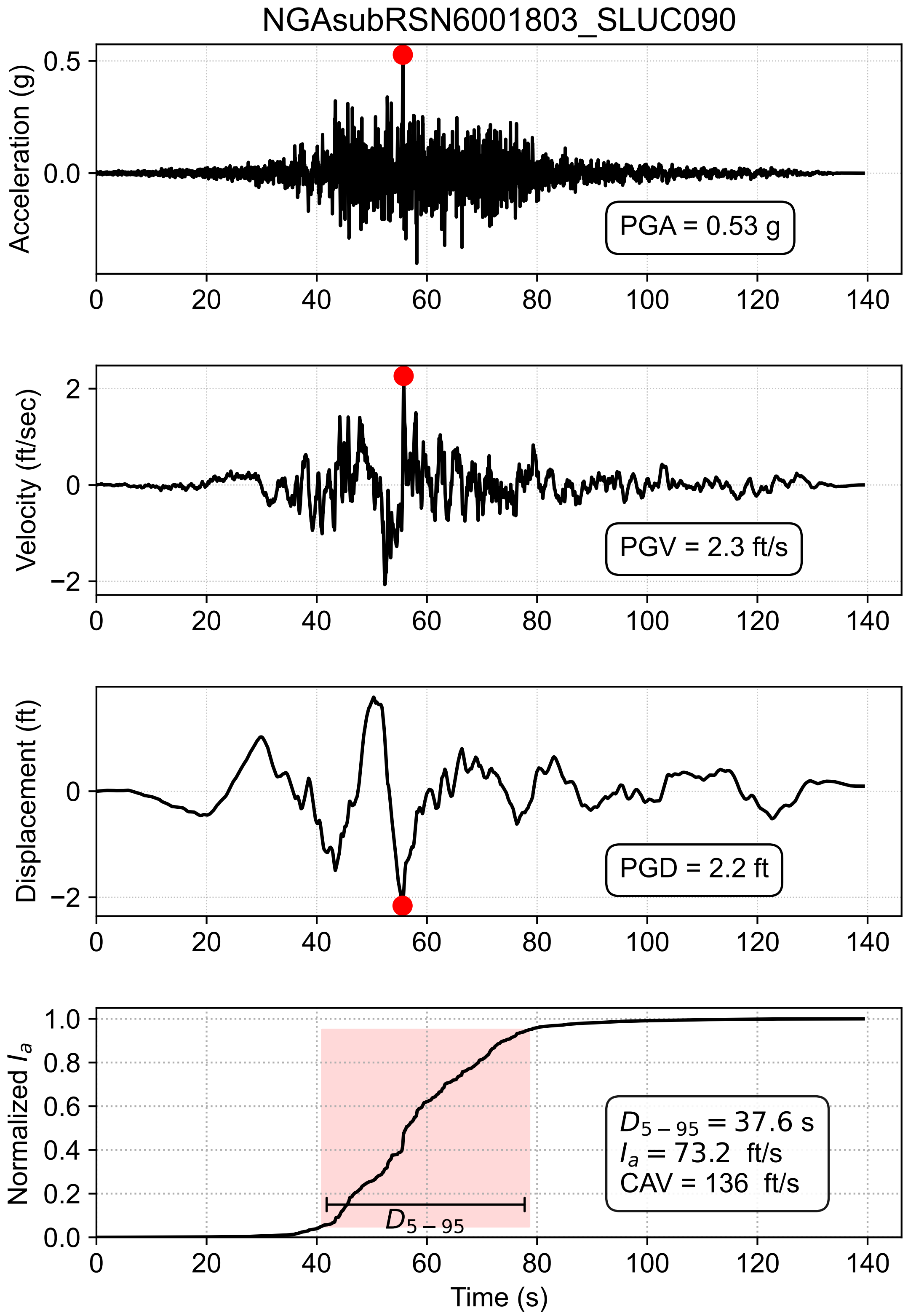

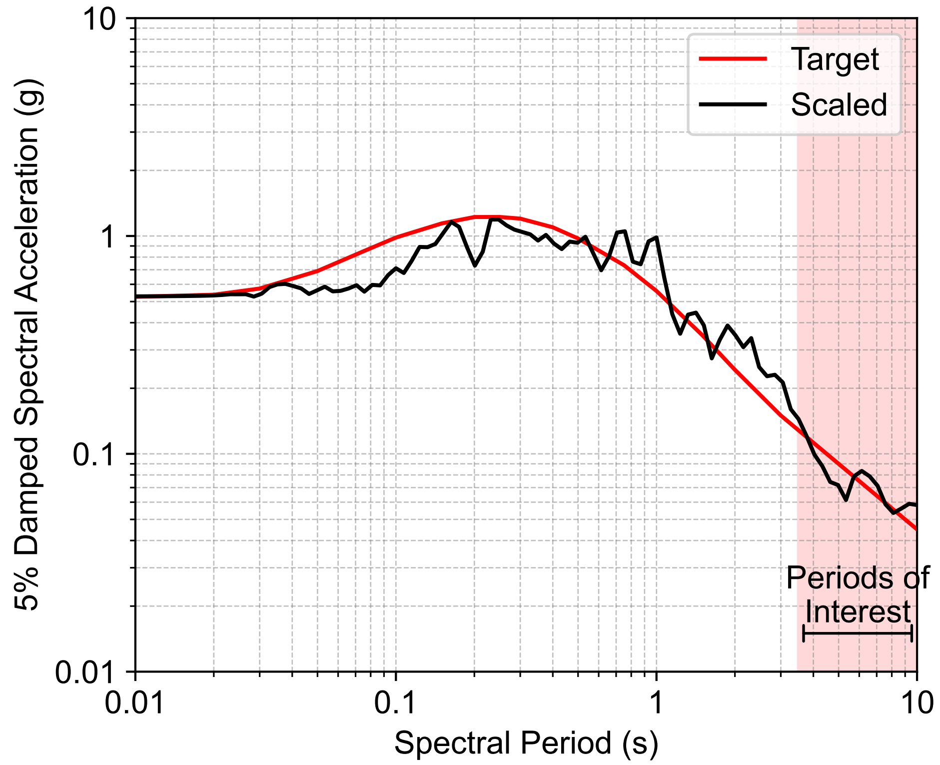

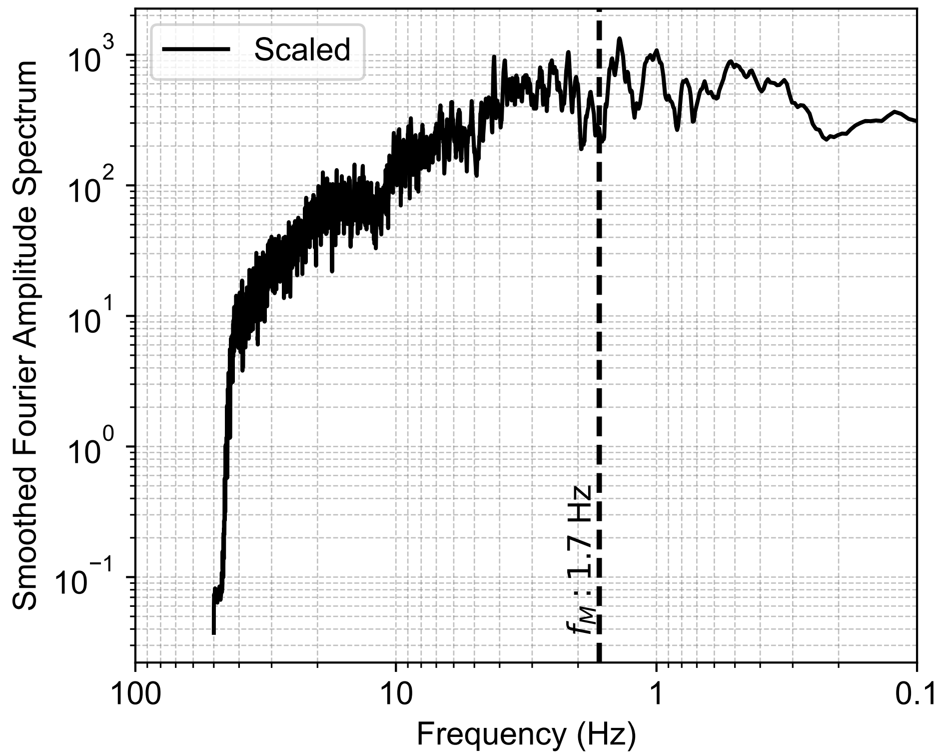

Event = 2010 Chile
M_w = 8.81
R_{rup} = 123.7126781 km
V_{S30} = 1411 m/s
Scale Factor = 1.56
Station = STL
Mechanism = Interface
Pulse Tp = nan s
HW Index = N/A

Notes:

1. PGA, PGV, PGD = Peak Ground Acceleration, Velocity, Displacement
2. The quiet motion (head and tail) of original recording are truncated & baseline corrected
3. D_{5-95} = Significant duration from 5% to 95% Normalized Arias Intensity
4. I_a = Arias Intensity
5. CAV = Cumulative Absolute Velocity
6. f_M = Mean frequency based on Rathje et al. (1998)
7. Pulse Tp = Period of Pulse (seconds), if nan, not classified as a pulse-like record
8. HW Index = Hanging wall index, HW: Hanging Wall, FW: Foot Wall, NU: Neutral, N/A: not applicable

PDX Fuel Tank SVA
Portland, OR

Amplitude Scaled, One-Component Ground Motion Parameters RSN6001803_SLUC090

0204679-001 July 2023

HALEY ALDRICH

Figure D-18

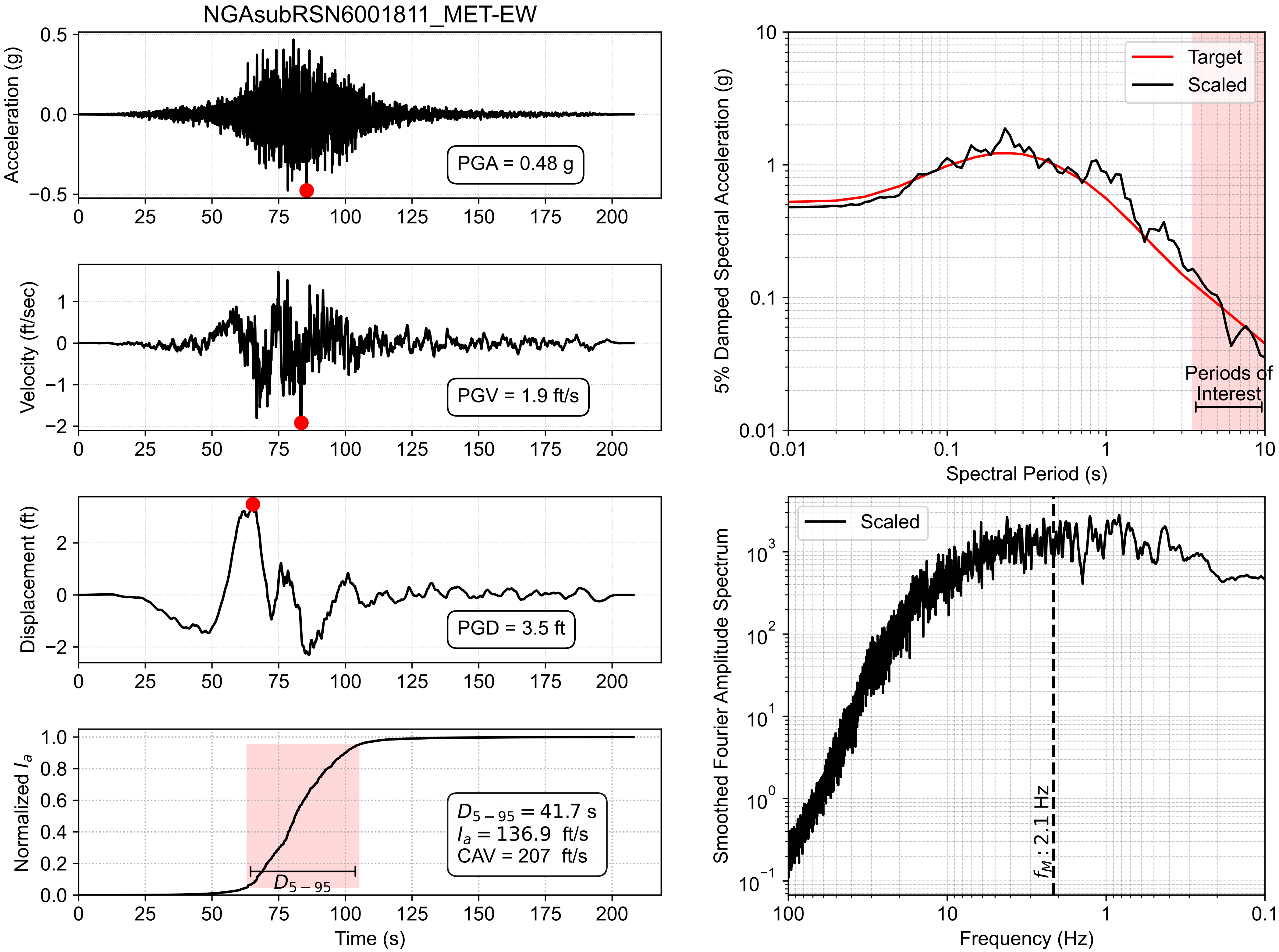

Event = 2010 Chile
M_w = 8.81
R_{rup} = 121.9390621 km
V_{S30} = 598 m/s
Scale Factor = 2.89
Station = MET
Mechanism = Interface
Pulse Tp = nan s
HW Index = N/A

Notes:

1. PGA, PGV, PGD = Peak Ground Acceleration, Velocity, Displacement
2. The quiet motion (head and tail) of original recording are truncated & baseline corrected
3. D_{5-95} = Significant duration from 5% to 95% Normalized Arias Intensity
4. I_a = Arias Intensity
5. CAV = Cumulative Absolute Velocity
6. f_M = Mean frequency based on Rathje et al. (1998)
7. Pulse Tp = Period of Pulse (seconds), if nan, not classified as a pulse-like record
8. HW Index = Hanging wall index, HW: Hanging Wall, FW: Foot Wall, NU: Neutral, N/A: not applicable

PDX Fuel Tank SVA
Portland, OR

Amplitude Scaled, One-Component Ground Motion Parameters RSN6001811_MET-EW

0204679-001 July 2023

HALEY ALDRICH

Figure D-19

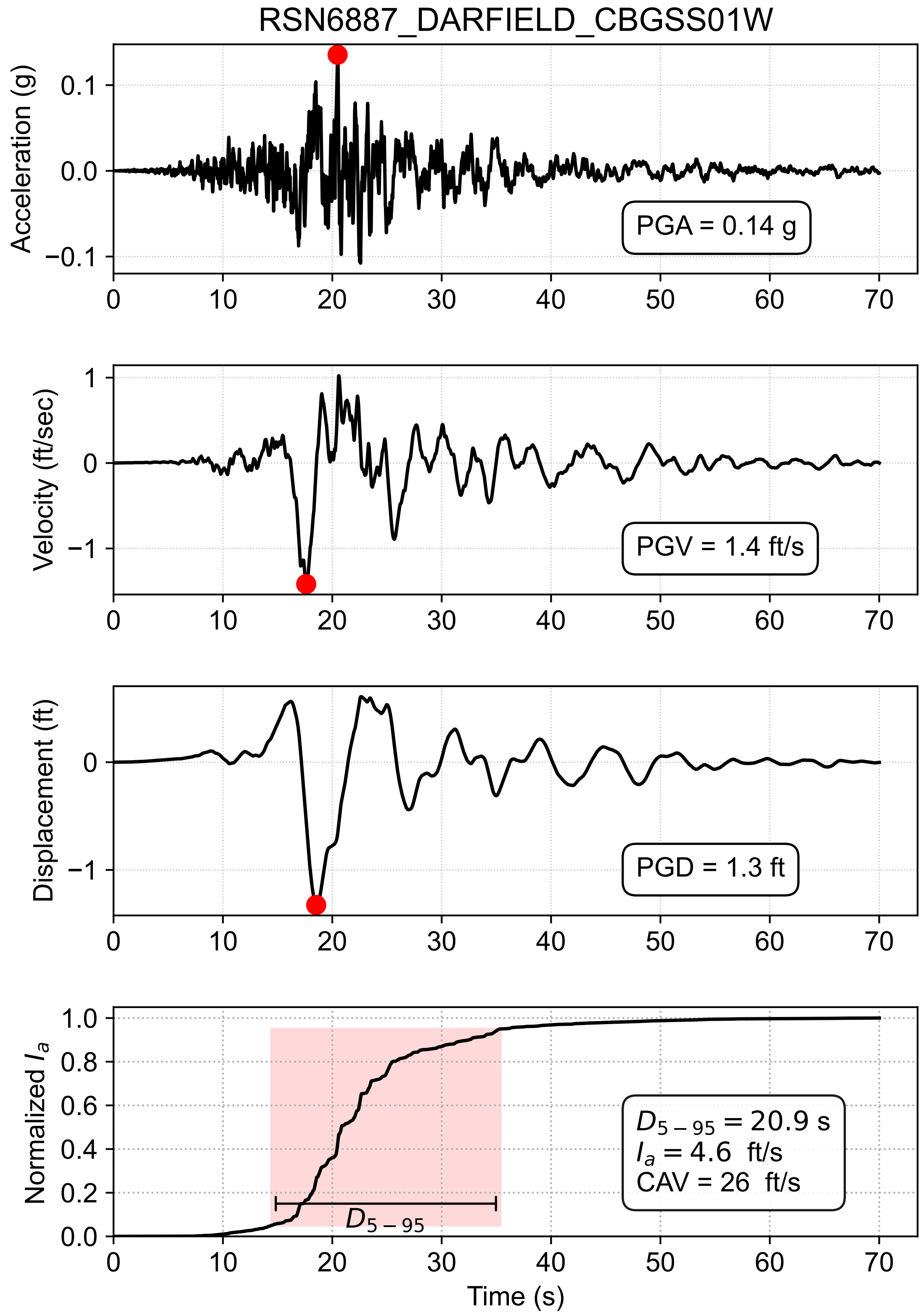

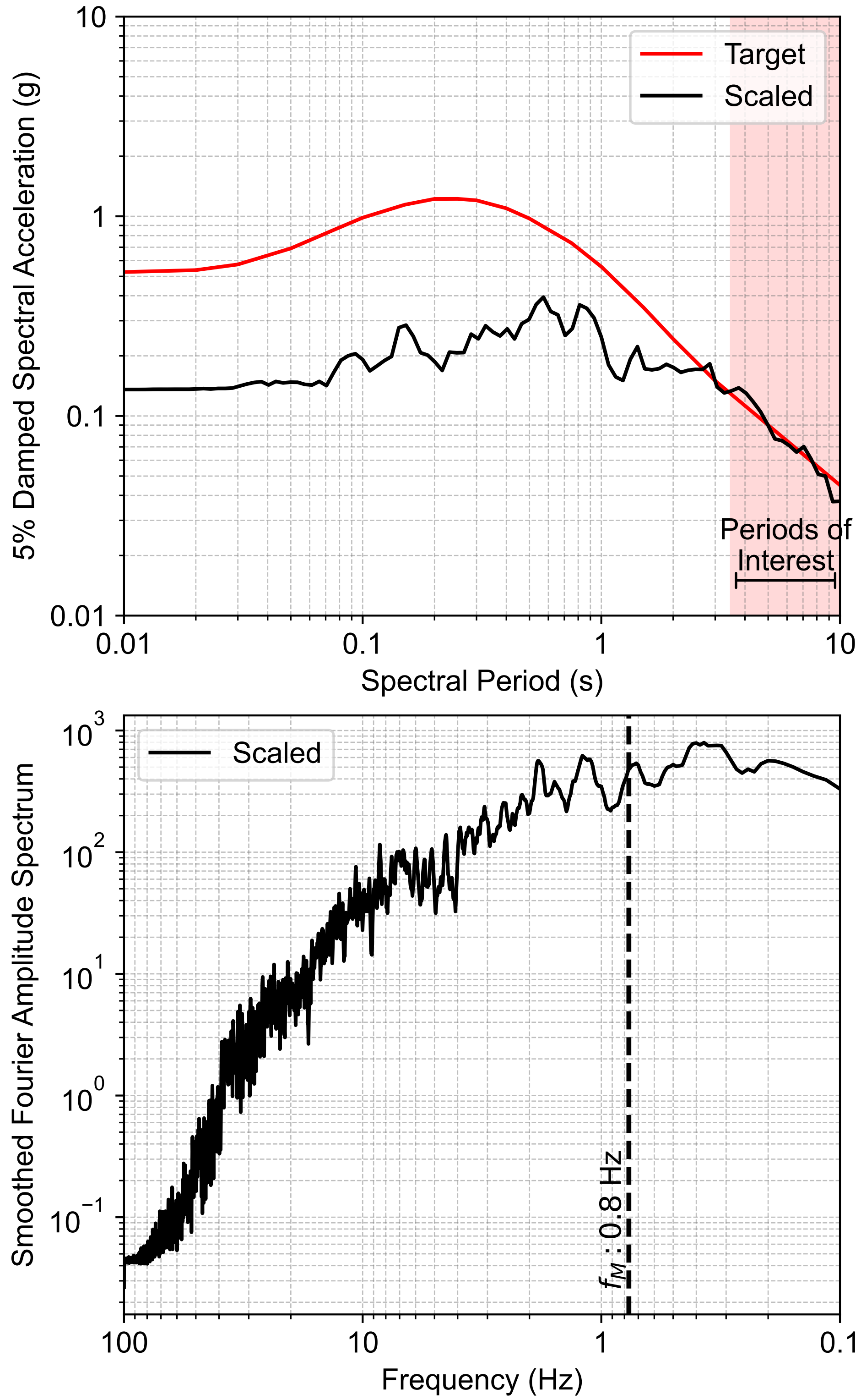

Event = Darfield_NZ 2010
M_w = 7.0
R_{rup} = 18.0 km
V_{S30} = 187 m/s
Scale Factor = 0.71
Station = CBGS
Mechanism = Strike-Slip
Pulse Tp = 12.6 s
HW Index = N/A

Notes:

1. PGA, PGV, PGD = Peak Ground Acceleration, Velocity, Displacement
2. The quiet motion (head and tail) of original recording are truncated & baseline corrected
3. D_{5-95} = Significant duration from 5% to 95% Normalized Arias Intensity
4. I_a = Arias Intensity
5. CAV = Cumulative Absolute Velocity
6. f_M = Mean frequency based on Rathje et al. (1998)
7. Pulse Tp = Period of Pulse (seconds), if nan, not classified as a pulse-like record
8. HW Index = Hanging wall index, HW: Hanging Wall, FW: Foot Wall, NU: Neutral, N/A: not applicable

PDX Fuel Tank SVA
Portland, OR

Amplitude Scaled, One-Component Ground Motion Parameters RSN6887_DARFIELD_CBGSS01W

0204679-001 July 2023

HALEY ALDRICH

Figure D-20

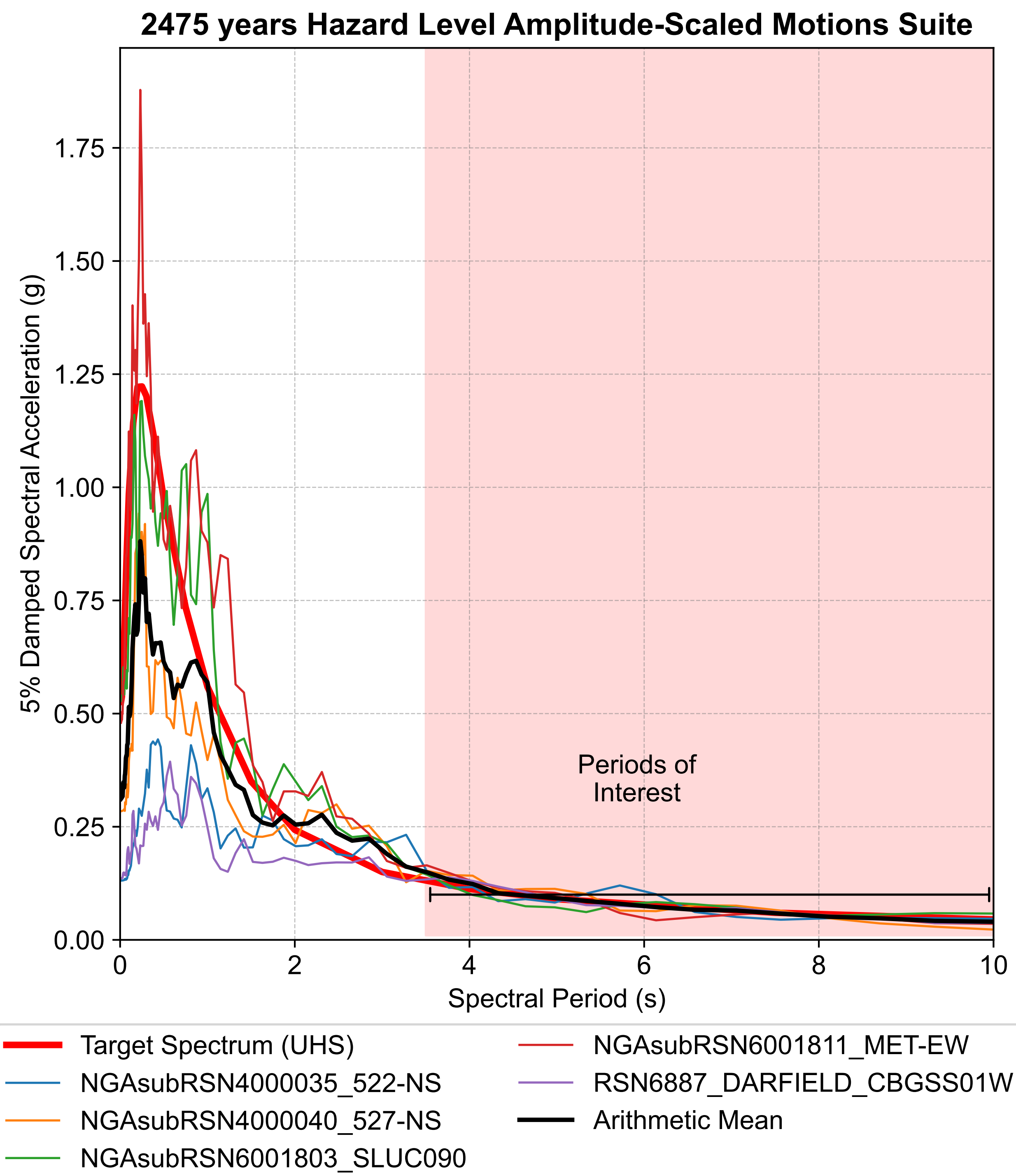

Notes:

1. Target spectrum is at halfspace elevation (1271 ft/s) and based on MCER per ASCE 7-16

HALEY ALDRICH

PDX Fuel Tank SVA
Portland, OR

Amplitude-Scaled Response Spectra Summary Convective Period (T=7.5 sec)

July 2023

0204679-001

FIG. D-21

APPENDIX E
2D-NDA (FLAC) and 1D-SRA (DEEPSOIL) Calculation Results

A. Model Geometry
B. Lateral Displacement Contour Map
C. Shear Strain Increment Contour Map
D. Excess Pore-Pressure Ratio (Ru) Contour Map
E. Maximum Shear Strain Profile (Left, Middle, Right)
F. Maximum Excess Pore Pressure Ratio Profile (Left, Middle, Right)
G. 1D-SRA Results: Profiles of Calculated Response

Material Name	Color	Unit Weight (lbs/ ft3)	Strength Type	Cohesion (psf)	Phi (deg)	Allow Sliding	Vertical Strength Ratio	Minimum Shear Strength (psf)	Water Surface	Hu Type	Hu	Shansep A (psf)	Shansep S	Shansep m	Stress History Type	Definition Method	Material Dependent Vertical Stress
ESU-1 (Top Soil)		120	Mohr-Coulomb	500	30				Water Surface	Custom	1						
ESU-2 (ML-MH)		115	SHANSEP						Water Surface	Custom	1	0	0.237	0.83	Overconsolidation Ratio	By depth from upper material boundary	No
ESU 3a (CRS)		120	Vertical Stress Ratio				0.08	0	Water Surface	Custom	1						
ESU 3b (CRS)		120	Vertical Stress Ratio				0.1	0	Water Surface	Custom	1						
ESU 3c (CRS)		120	Vertical Stress Ratio				0.12	0	Water Surface	Custom	1						
Halfspace		135	Infinite strength			No			Water Surface	Custom	0						

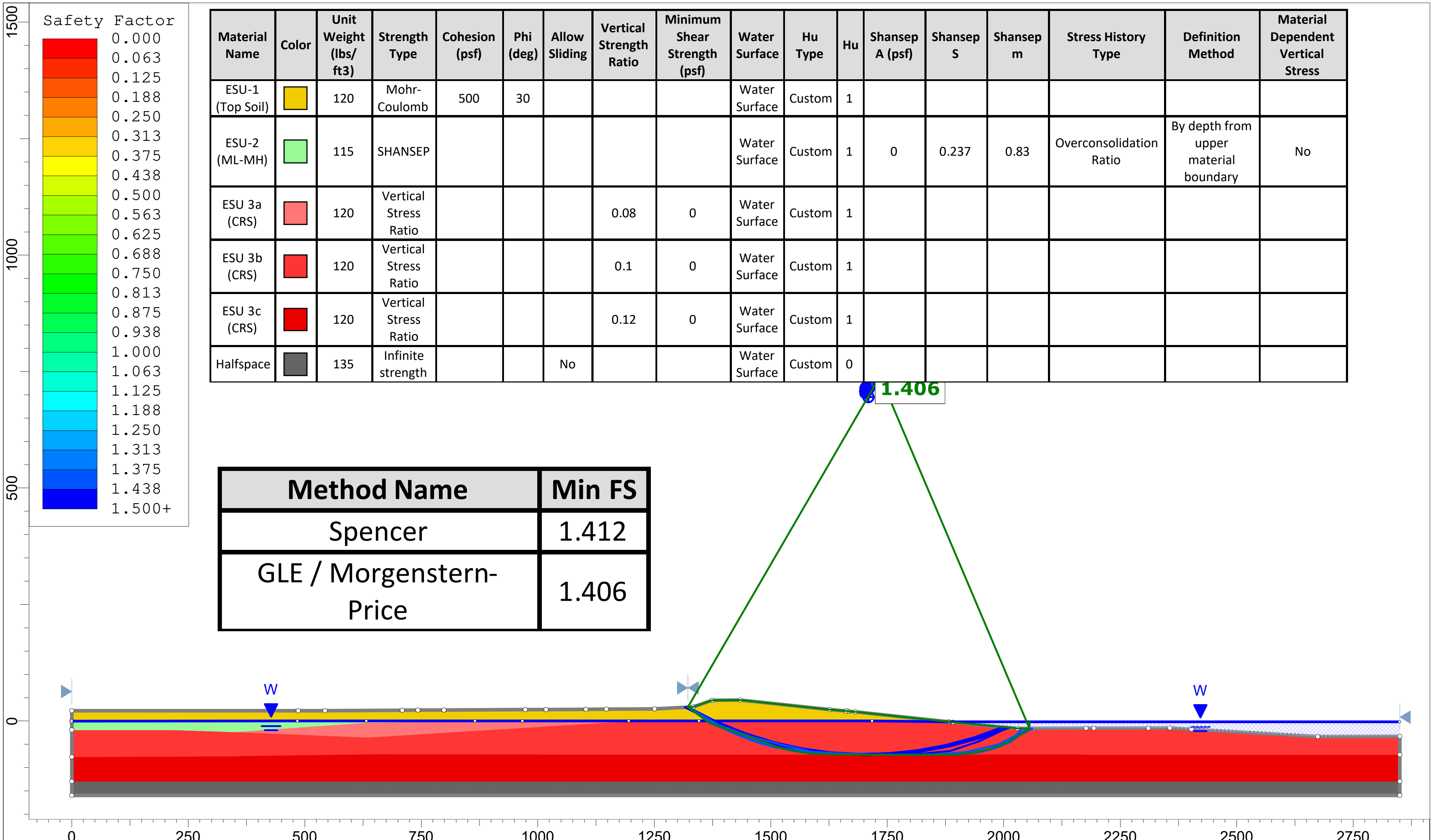

Method Name	Min FS
Spencer	1.412
GLE / Morgenstern-Price	1.406

PDX Fuel Tank SVA
Portland, OR

Post-Liquefied Stability Analysis Considering Void-Redistribution Mechanism

0204679-001 Scale 1:3500 7/14/2023

HALEY ALDRICH

Figure
E-1

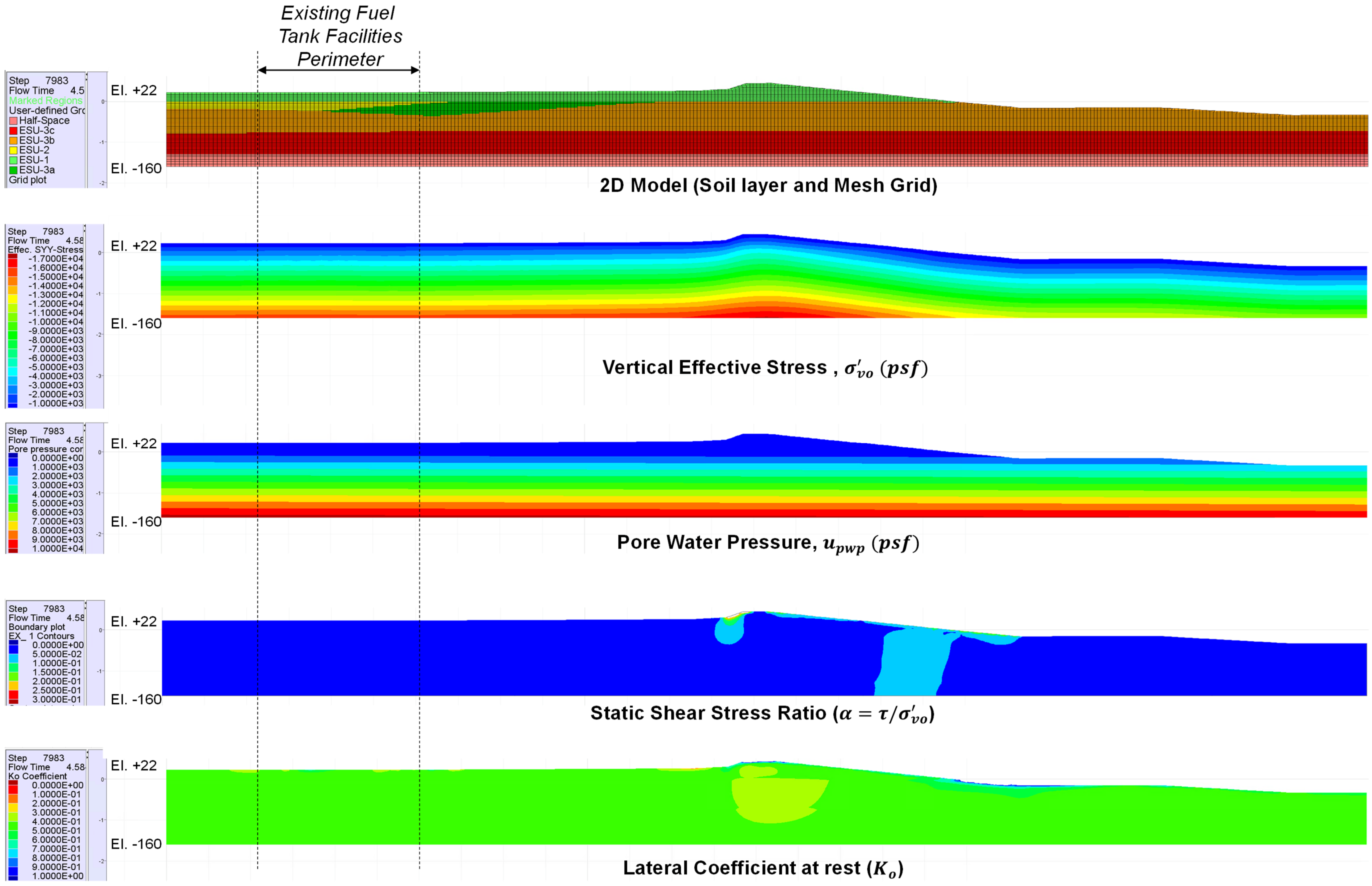

Notes:

1. The figure vertical and horizontal scale are 1V : 1H
2. The left boundary is at 0 feet and the right boundary is 2,850 feet

PDX Fuel Tanks SVA
Portland, OR

2D FLAC Numerical Model (Section B-B'): Initial State

0204679-001 07 - 2023

HALEY ALDRICH

Fig. **E-2**

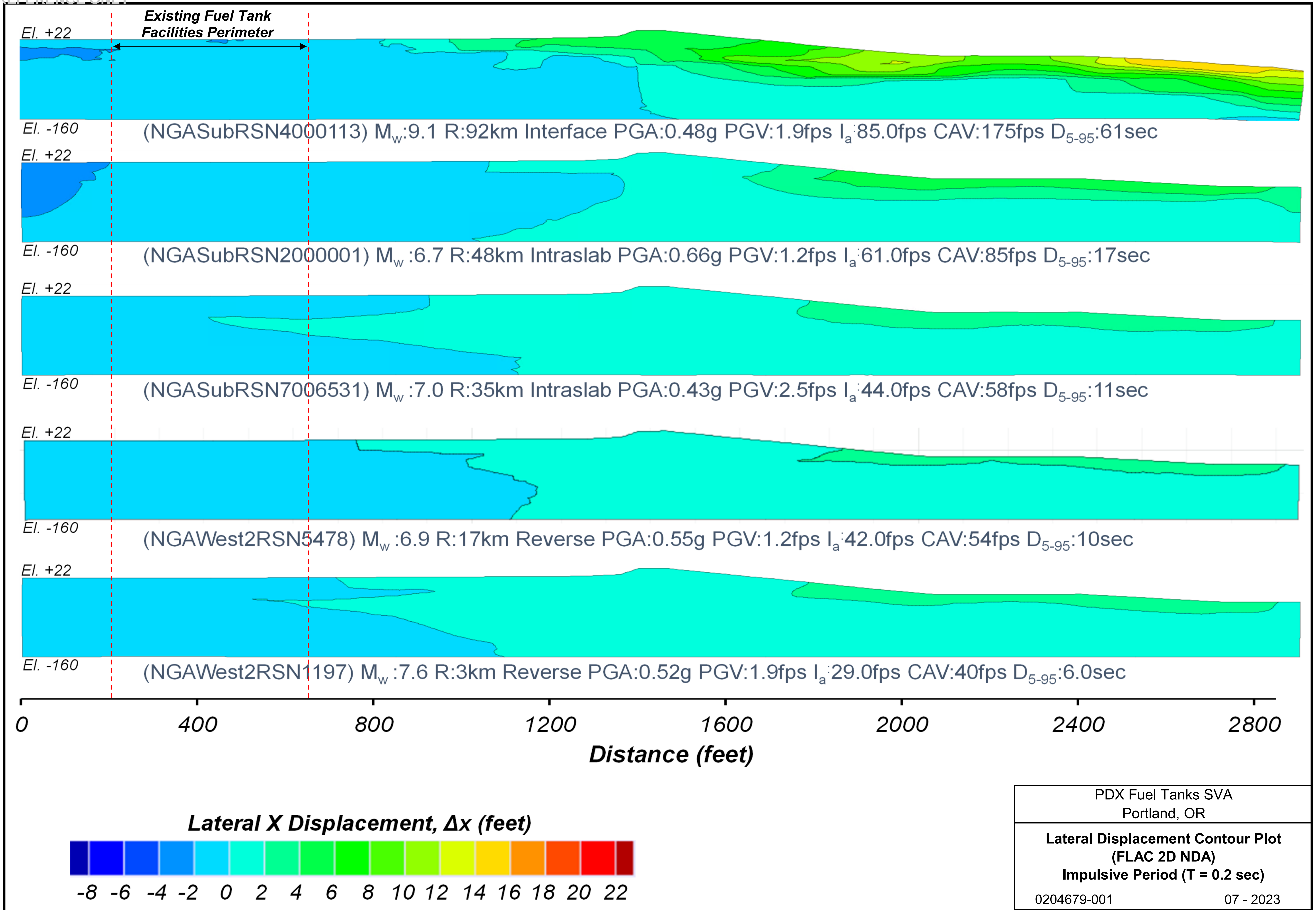

PDX Fuel Tanks SVA
Portland, OR

Lateral Displacement Contour Plot
(FLAC 2D NDA)
Impulsive Period (T = 0.2 sec)

0204679-001 07 - 2023

HALEY ALDRICH

Fig.
E-3

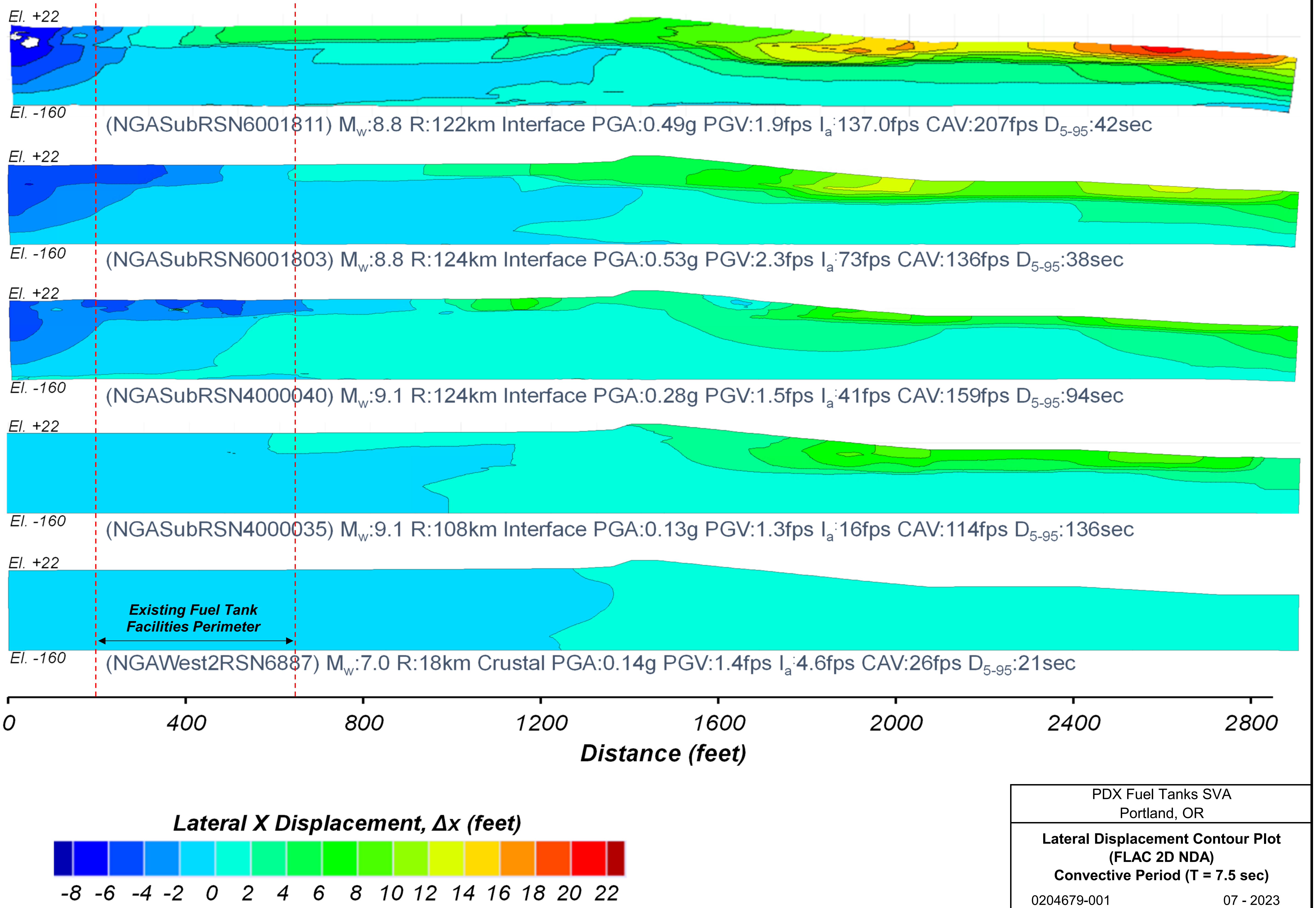

PDX Fuel Tanks SVA
Portland, OR

Lateral Displacement Contour Plot
(FLAC 2D NDA)
Convective Period (T = 7.5 sec)

0204679-001 07 - 2023

HALEY ALDRICH

Fig. E-4

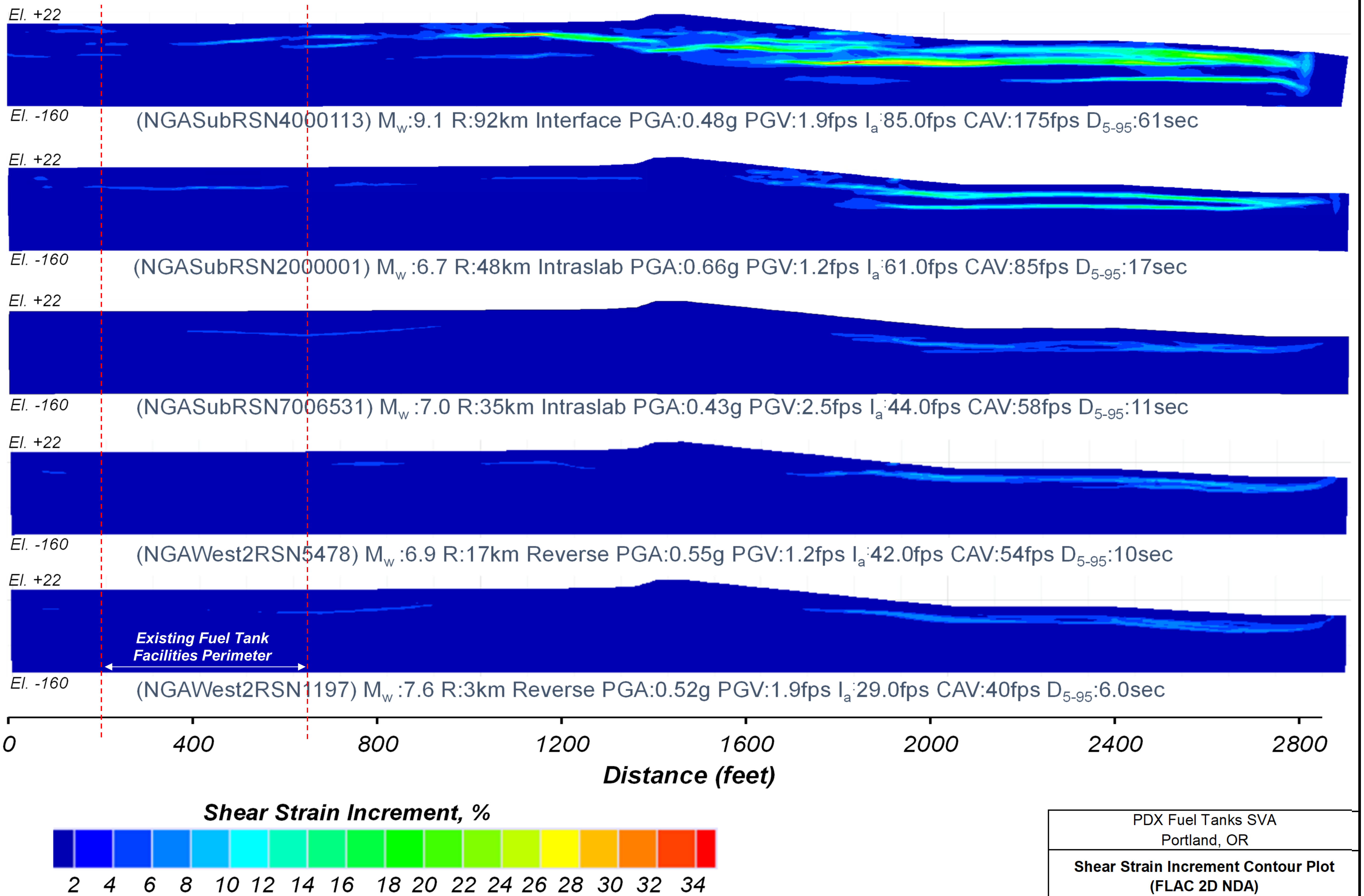

Notes:

1. Maximum (engineering) shear strain is approximately twice of shear strain increment plotted in this figure

PDX Fuel Tanks SVA
Portland, OR

Shear Strain Increment Contour Plot (FLAC 2D NDA) Impulsive Period (T = 0.2 sec)

0204679-001 07 - 2023

HALEY ALDRICH

Fig. **E-5**

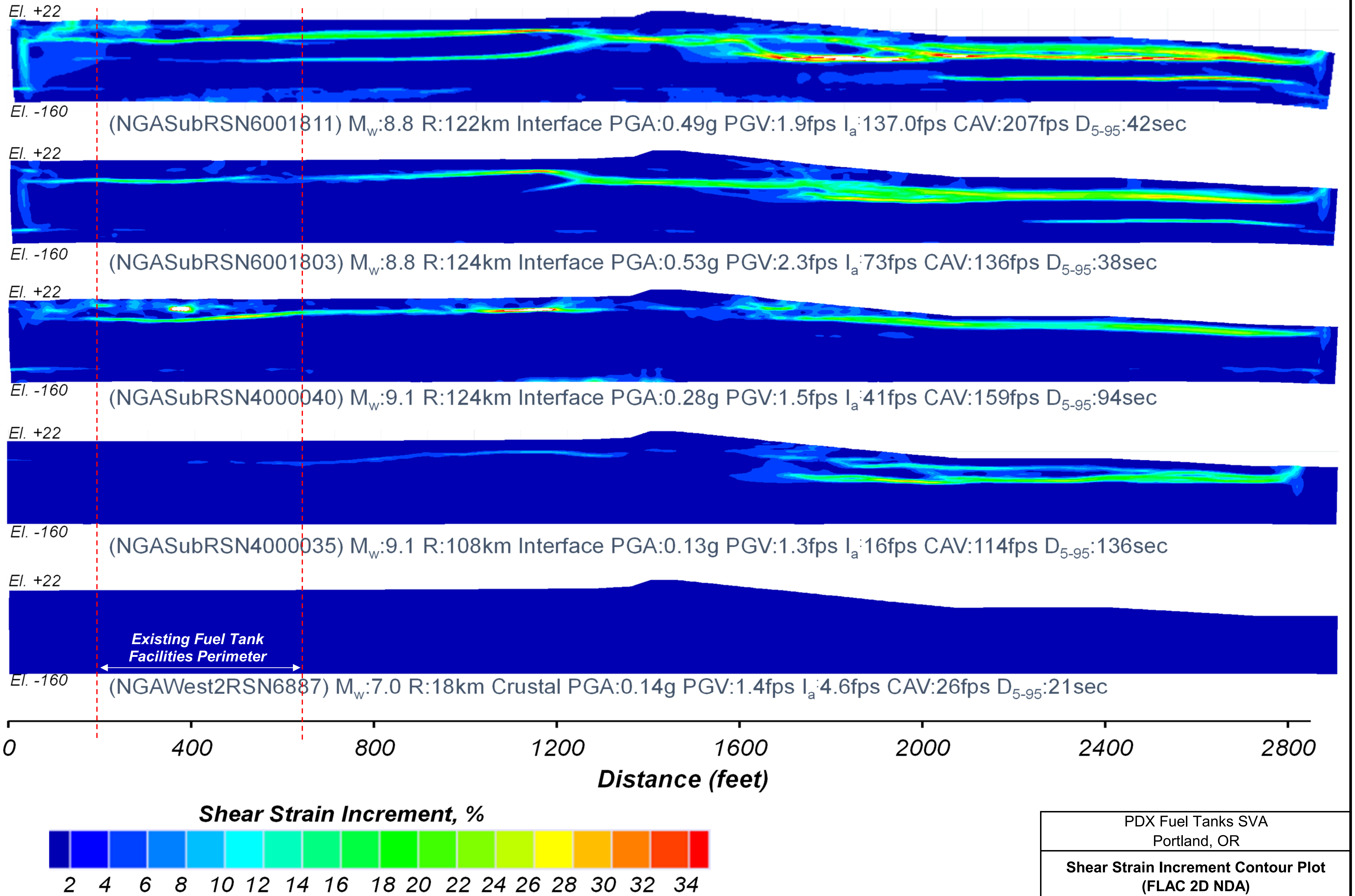

Notes:

1. Maximum (engineering) shear strain is approximately twice of shear strain increment plotted in this figure
2. Horizontal : Vertical Scale = 1 : 1

PDX Fuel Tanks SVA
Portland, OR

Shear Strain Increment Contour Plot
(FLAC 2D NDA)
Convective Period (T = 7.5 sec)

0204679-001 07 - 2023

HALEY ALDRICH

Fig. **E-6**

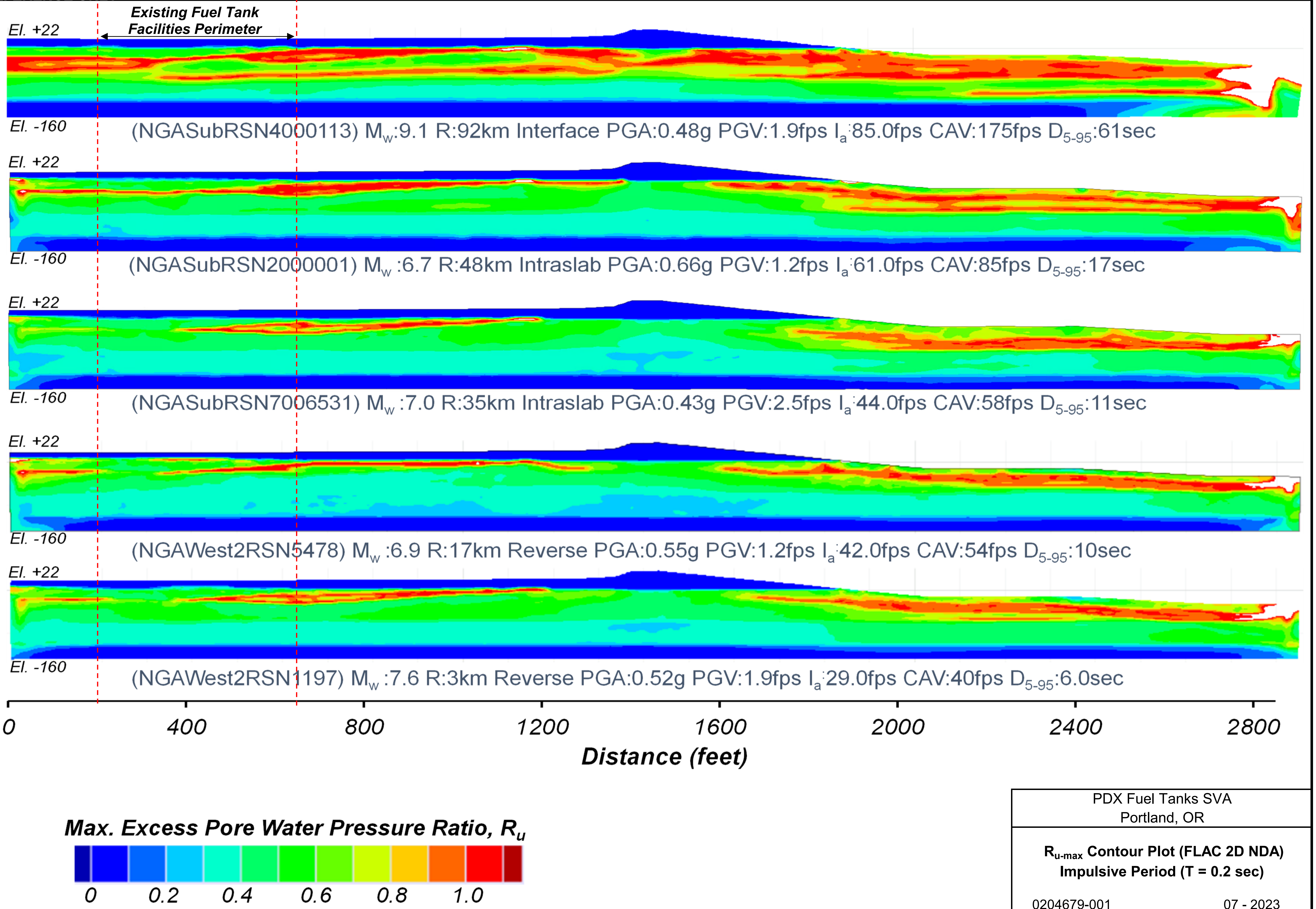

PDX Fuel Tanks SVA
Portland, OR

$R_{u\text{-}max}$ Contour Plot (FLAC 2D NDA)
Impulsive Period (T = 0.2 sec)

0204679-001 07 - 2023

HALEY ALDRICH

Fig. E-7

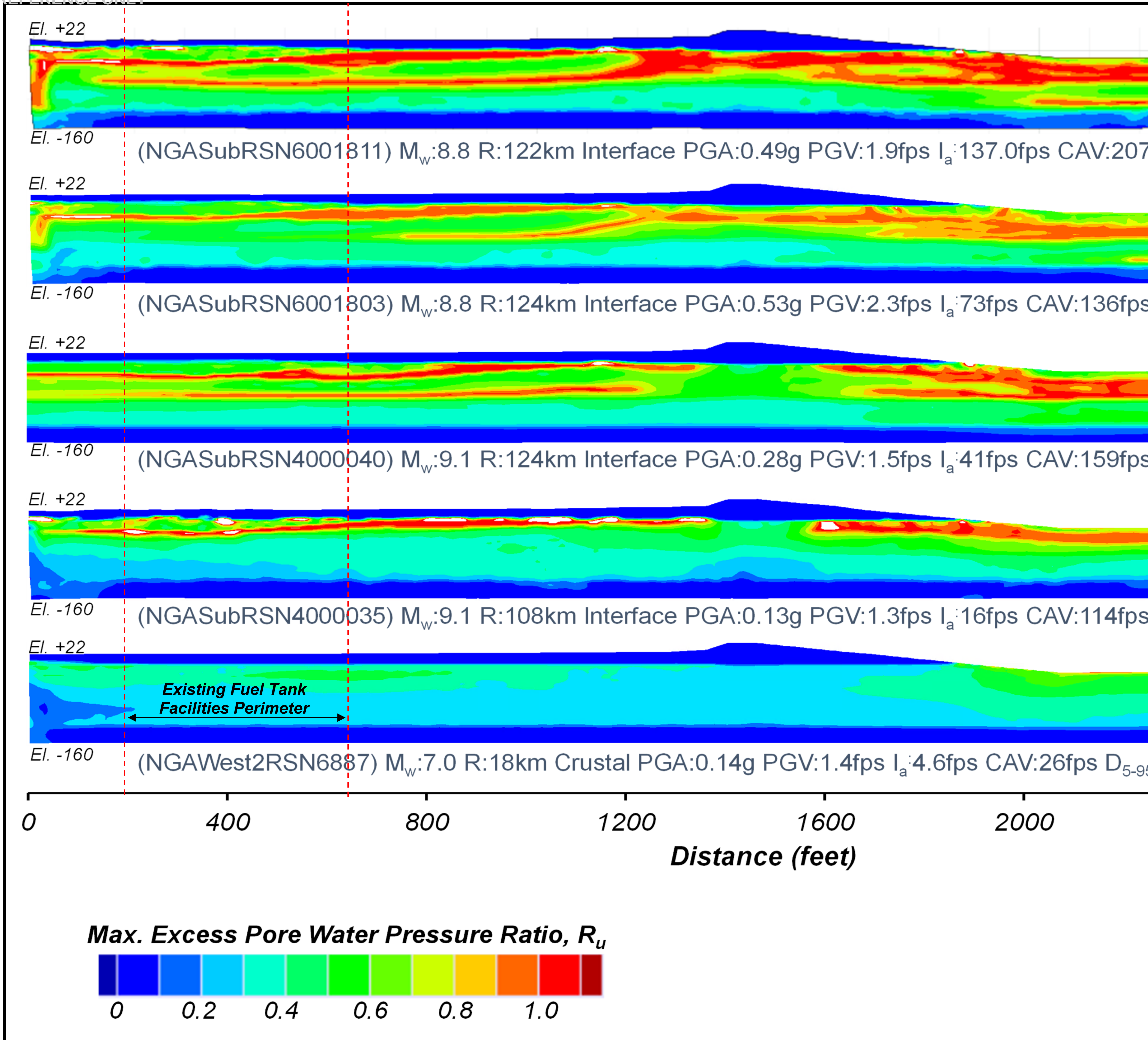

PDX Fuel Tanks SVA
Portland, OR

$R_{u\text{-}max}$ Contour Plot (FLAC 2D NDA)
Convective Period (T = 7.5 sec)

0204679-001 07 - 2023

HALEY ALDRICH

Fig. **E-8**

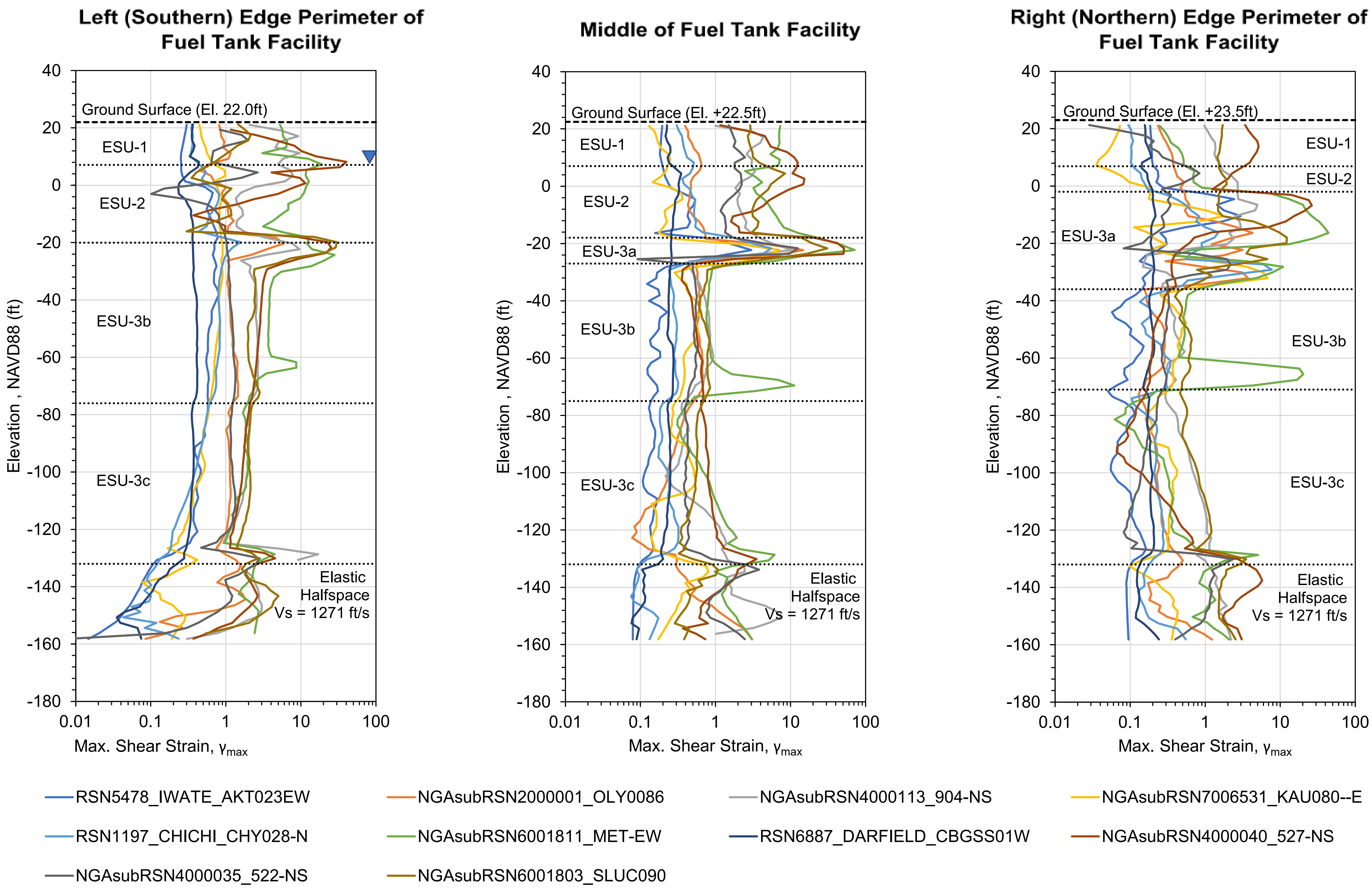

PDX Fuel Tanks SVA
Portland, OR

Max Shear Strain Profile (FLAC 2D NDA Results)

0204679-001 07 - 2023

HALEY ALDRICH

Fig. E-9

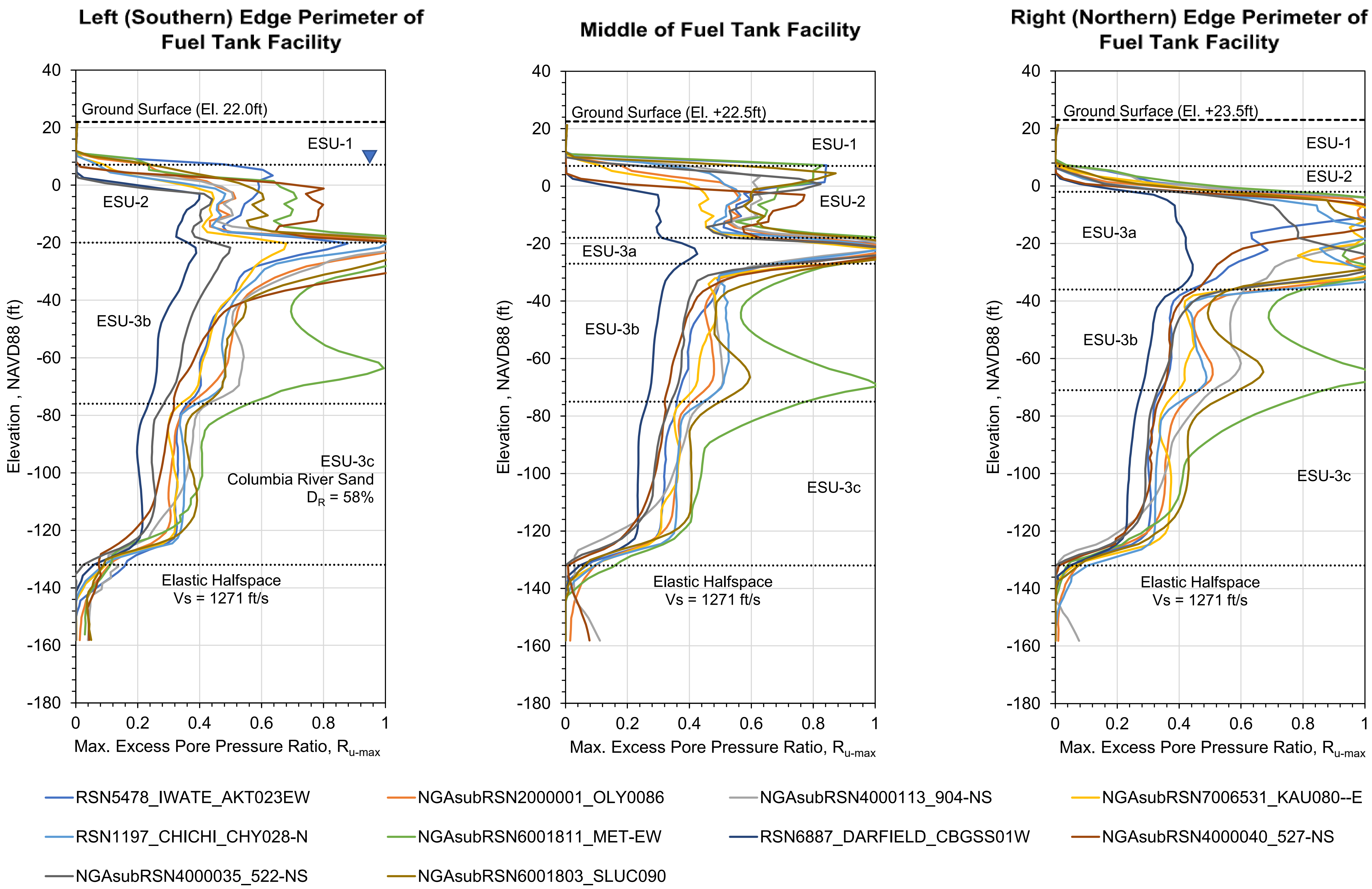

Notes:
1. The R_{u-max} value of ESU-2 layer were used to estimate the post-liquefaction settlement presented in Figure 10.

PDX Fuel Tanks SVA
Portland, OR

R_{u-max} Profile (FLAC 2D NDA Results)

0204679-001 07 - 2023

HALEY ALDRICH

Fig.
E-10

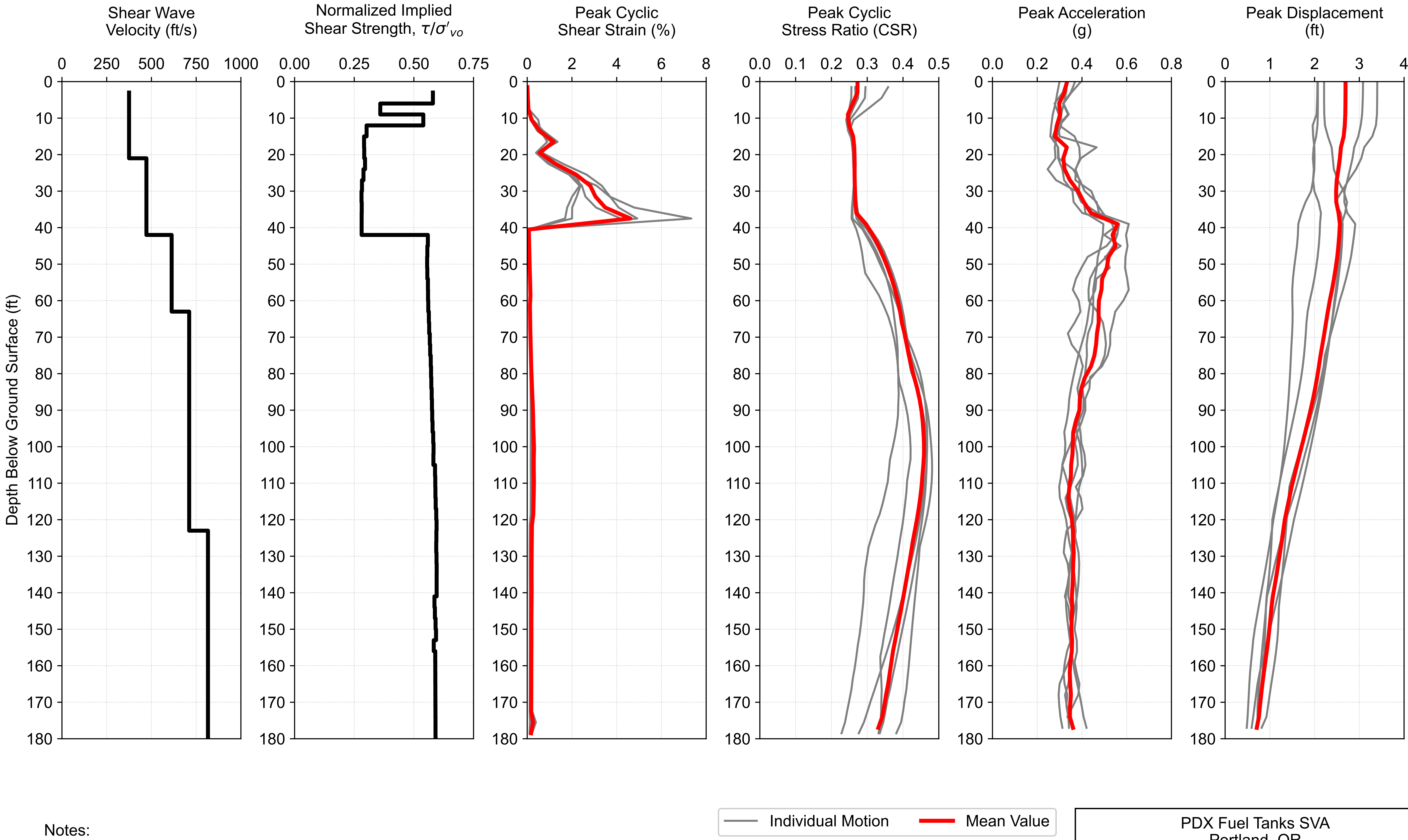

Notes:

1. Calculated using Deepsoil 7.0 - Time-Domain Nonlinear Total Stress Analysis
2. Soil layers are discretized to propagate maximum frequency of 25 Hz
3. Soil model: General Quadratic/Hyperbolic Model (GQ/H)
4. Hysteretic Re/Unloading Formulation: Non-Masing Rule

PDX Fuel Tanks SVA
Portland, OR

Calculated Site Response
1D Profiles Summary
Short Period (0.2 sec)

0204679-002 July 2023

HALEY ALDRICH

Figure
E-11

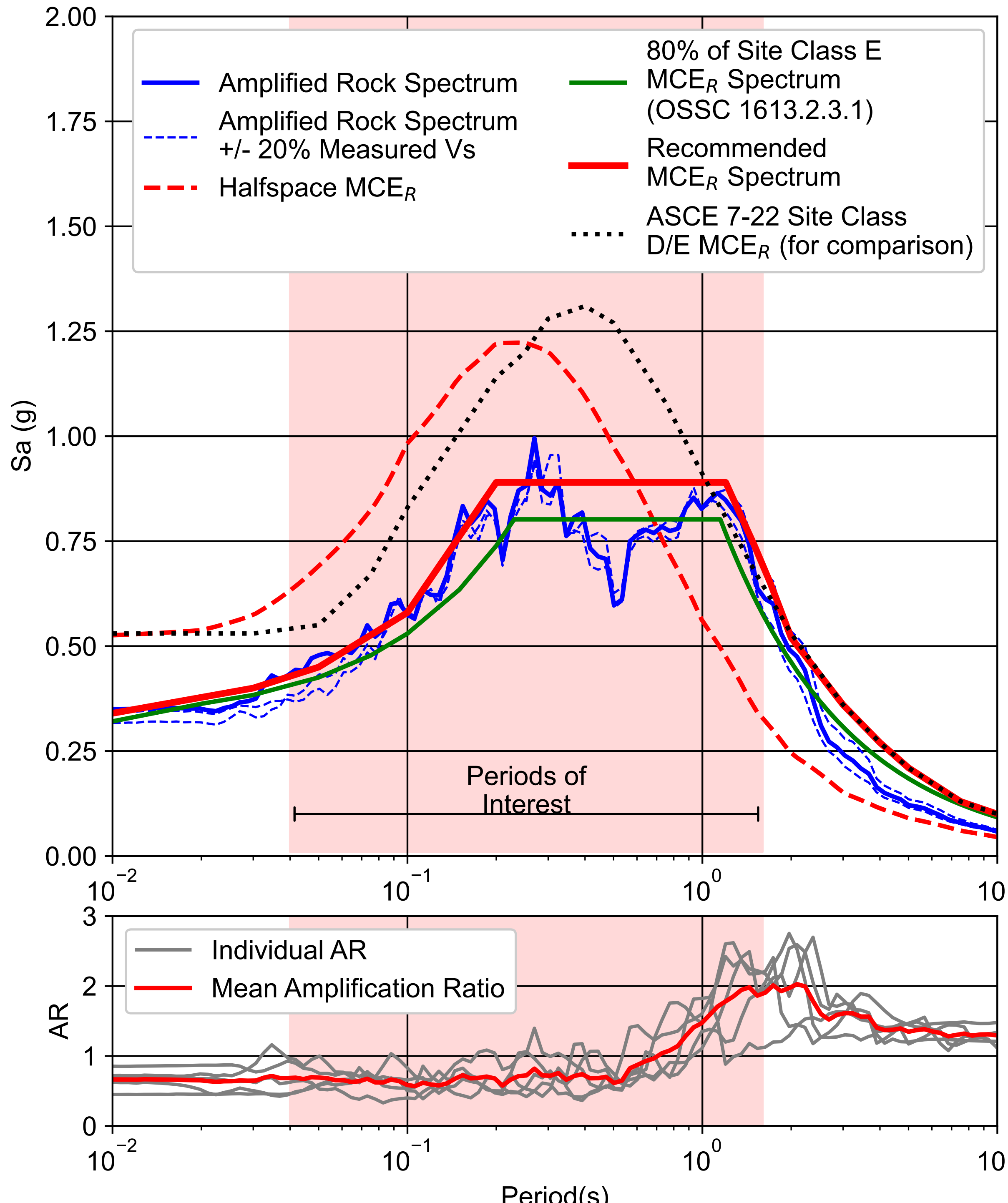

Notes:
1. Amplified Rock Spectrum = Halfspace MCE$_R$ x Mean Amplification Ratio
2. Site-specific Design Parameters are S_{DS} = 0.59g, S_{D1} = 0.74g
3. Half-space Vs = 1271 ft/s

HALEY ALDRICH

PDX Fuel Tanks SVA
Portland, OR

Calculated Surface MCE$_R$ Spectrum From 1D Site Response Analysis
July 2023

0204679-002	**FIG. E-12**

APPENDIX F
Geophysical Survey Report

Report on Seismic Velocity Study
PDX Fuel Facility
Portland, Oregon

Report Date: May 16, 2023

Prepared for:

Haley & Aldrich, Inc
6420 S. Macadam Ave.
Portland, OR 97239

Prepared by:

EARTH DYNAMICS LLC
2284 N.W. Thurman St.
Portland, OR 97210
(503) 227-7659
Project No. 23212

1.0 INTRODUCTION

Haley & Aldrich, Inc. engaged Earth Dynamics LLC to conduct geophysical explorations near the Portland International Airport (PDX) Fuel Facility in Portland, Oregon. The geophysical field work was completed under the supervision of Mr. Daniel Lauer of Earth Dynamics LLC on April 28, 2023. This report describes the methodology and results of the geophysical investigation.

2.0 SCOPE OF WORK

The purpose of this study is to characterize the subsurface shear wave and compressional wave velocities at the site. These data are needed to help determine the seismic response of the site to earthquake loading. The exploration methods consist of passive source refraction micro-tremor (ReMi), and active source Multichannel Analysis of Surface Waves (MASW). ReMi and active source MASW are used to help determine the shear-wave velocities of the underlying soil. ReMi provides average shear wave velocity for the site and MASW can be used to develop a 2-Dimensional profile of the shear wave velocity with depth. Data were acquired at four ReMi arrays and one MASW array. The locations of the arrays are shown in Figure 2-1.

The 2D MASW array was acquired using a 24-channel geophone array deployed on a seismic "land streamer" with a geophone spacing of 10 feet. MASW data were acquired along a 630-foot-long North/South profile within the PDX property. Three ReMi profiles were acquired using various geophone spacings and distances along the same profile. Data for a fourth ReMi array were acquired north of the site between Marine Drive and the Columbia River. The configuration details of the ReMi arrays are summarized in Table 2-1.

Table 2-1. Summary of ReMi Array Configuration.

ReMi Array	Geophone Spacing (ft)	Number of Geophones	Total Array Length (ft)
ReMi Array 1	10	24	230
ReMi Array 2	30	24	690
ReMi Array 3	15	24	345
ReMi Array 4	15	24	345

Figure 2-1. Site layout showing locations of geophysical arrays.

3.0 METHOD

3.1 Passive source ReMi

The ReMi technique provides a simplified characterization of relatively large volumes of the subsurface. The method can be used to estimate one-dimensional shear wave velocity profiles and provide site-specific soil classification data as described in ASCE/SEI 7-16 (2017). In a ReMi survey, geophones are deployed at designated intervals along a linear array. The resolution and depth of investigation depends upon the geophone cut-off frequency, spacing of the geophones, the total array length and the frequency characteristics of the Rayleigh waves at the site. For “rule of thumb” survey planning, the nominal depth of investigation is assumed to be approximately one-third of the geophone array length.

The theoretical basis of the ReMi method is the same as Spectral Analysis of Surface Waves (SASW) and Multi-channel Analysis of Surface Waves (MASW) as first described to the earthquake engineering community by Nazarian and Stokoe (1984). However, ReMi does not require a frequency-controlled source and the field equipment is much more compact and economical. A complete description of the theoretical basis for ReMi is described by Louie (2001). In ReMi analysis all interpretation is done in the frequency domain, and the method assumes that the most energetic arrivals recorded are Rayleigh waves. By applying a time-domain velocity analysis, Rayleigh waves can be separated from body waves, air waves, and other coherent noise. Transforming the time-domain velocity results into the frequency domain allows combination of many arrivals over a long time period, and yields easy recognition of dispersive surface waves.

Data reduction is completed in two steps. First, the time versus amplitude seismic records are transformed into spectral energy shear wave frequency versus shear wave velocity (or slowness). The data are graphically presented in what is commonly termed a p-f plot. The interpreter determines a dispersion curve from the p-f plot by selecting the lower bound of the spectral energy shear wave velocity versus frequency trend. The second phase of the analysis consists of fitting the measured dispersion curve with a theoretical dispersion curve that is based upon a model of multiple layers with various shear wave velocities. The model velocities and layer thicknesses are adjusted until a ‘best fit’ to the measured data is obtained. This type of interpretation does not provide a unique model. Interpreter experience and knowledge of the existing geology is important to provide a realistic solution. The data are presented as one-dimensional velocity profiles that represent the average shear wave velocities of the subsurface layers over the length of the geophone array.

For this project, data were acquired using a Seismic Source 24 channel DaqLink 4 seismograph equipped with twenty-four 4.5 Hz vertical geophones mounted on the ground surface. ReMi Array 1 was deployed with a ten-foot geophone spacing for a total array length of 230 feet. Array 2 was deployed with a 30-foot geophone spacing for a total array length of 690 feet. Arrays 3 and 4 were deployed using a 15-foot geophone spacing for an array length of 345 feet. Many 30-second-long seismic records of ambient seismic noise were recorded for each array. Data were also acquired when vehicles, airplanes, and people were moving on and near the site.

3.2 Active source MASW

Active source data were acquired over a 630 foot long profile. The geophone land streamer was configured with a 10 foot geophone spacing and data gathers were acquired with a shot point situated 50 feet south of the last geophone in the array. The entire array was moved 10 feet south for each data gather. Data were acquired at fourty-one locations for the Array. A 20-pound sledgehammer was used as a seismic energy source. The MASW data were analyzed using ParkSeis Software. The software allows for analysis of each shot to develop a fundamental mode dispersion curve. The dispersion curves from each shotpoint are combined to create a 2-D shear wave profile for the array.

4.0 RESULTS

The approximate locations of the geophysical arrays are shown on the Google Earth image contained in Figure 2-1. The ReMi analysis and results for ReMi Arrays 1 through 4 are contained in Figures 4-1 through 4-4 respectively. Figures 4-1 through 4-4 contain the p-f plot, the dispersion curve, the derived velocity versus depth model that best fits the geology of the site and a table containing the shear wave velocity with depth for the array.

The active source 2-D MASW analysis results are contained in Figure 4-5. Figure 4-5 contains the modelled two-dimensional shear wave velocity cross section and a map showing the estimated confidence levels of the shear wave velocity profile.

The ReMi dispersion curve data quality is good for all ReMi arrays acquired during this study. The model fit to the data for each array appears to be good to very good. The RMS error of the model fit for these data is less than 20 ft/s.

The MASW data correlate moderately well with the ReMi data. However the confidence level for the 2D MASW profile is very low deeper than approximately fifty feet below the ground surface (bgs). This low confidence level is most likely related to insufficient transmission of low frequency energy from the active source. The long data gathers of the ReMi method produce dispersion curves that are coherent into lower frequencies.

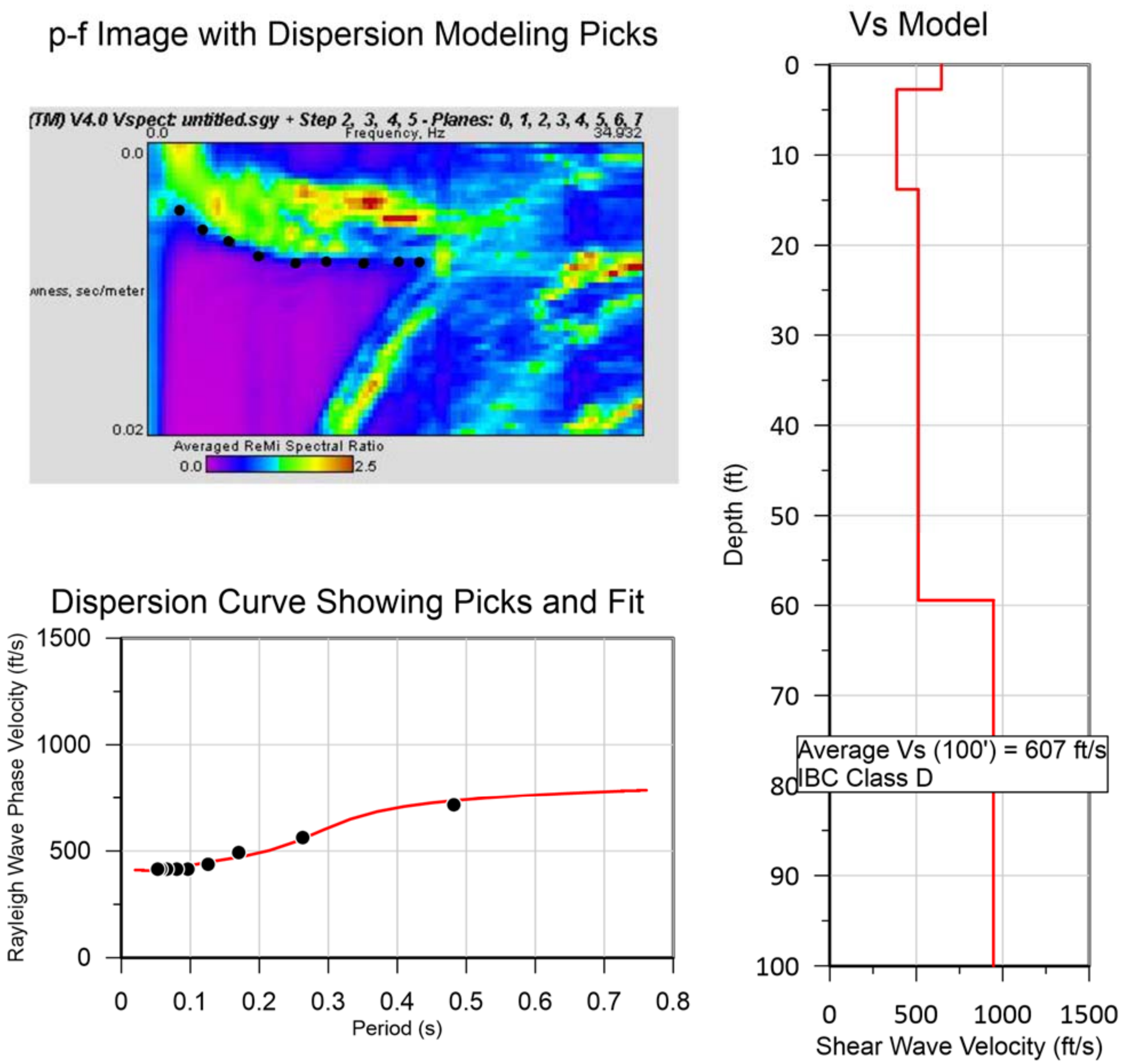

Depth Interval (ft)	Shear-wave velocity (ft/s)
0 – 2.75	645
2.75 – 13.8	387
13.8 –59.4	512
59.4 - 100	948

Figure 4-1. Array 1 ReMi Results

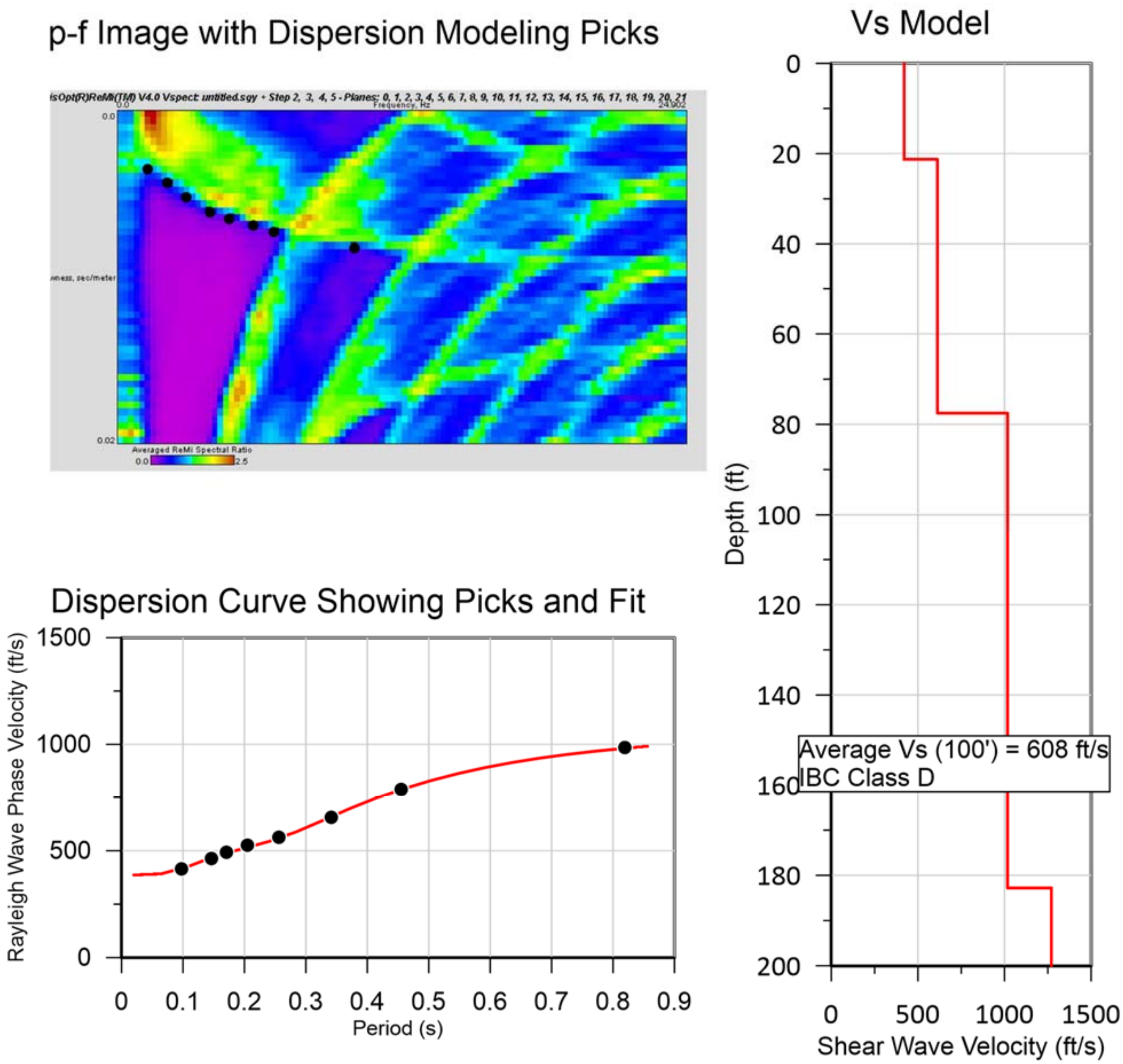

Depth Interval (ft)	Shear-wave velocity (ft/s)
0 – 21.3	420
21.3 – 77.5	613
77.5 – 182.8	1,017
182.8 – 200	1,271

Figure 4-2. Array 2 ReMi Results

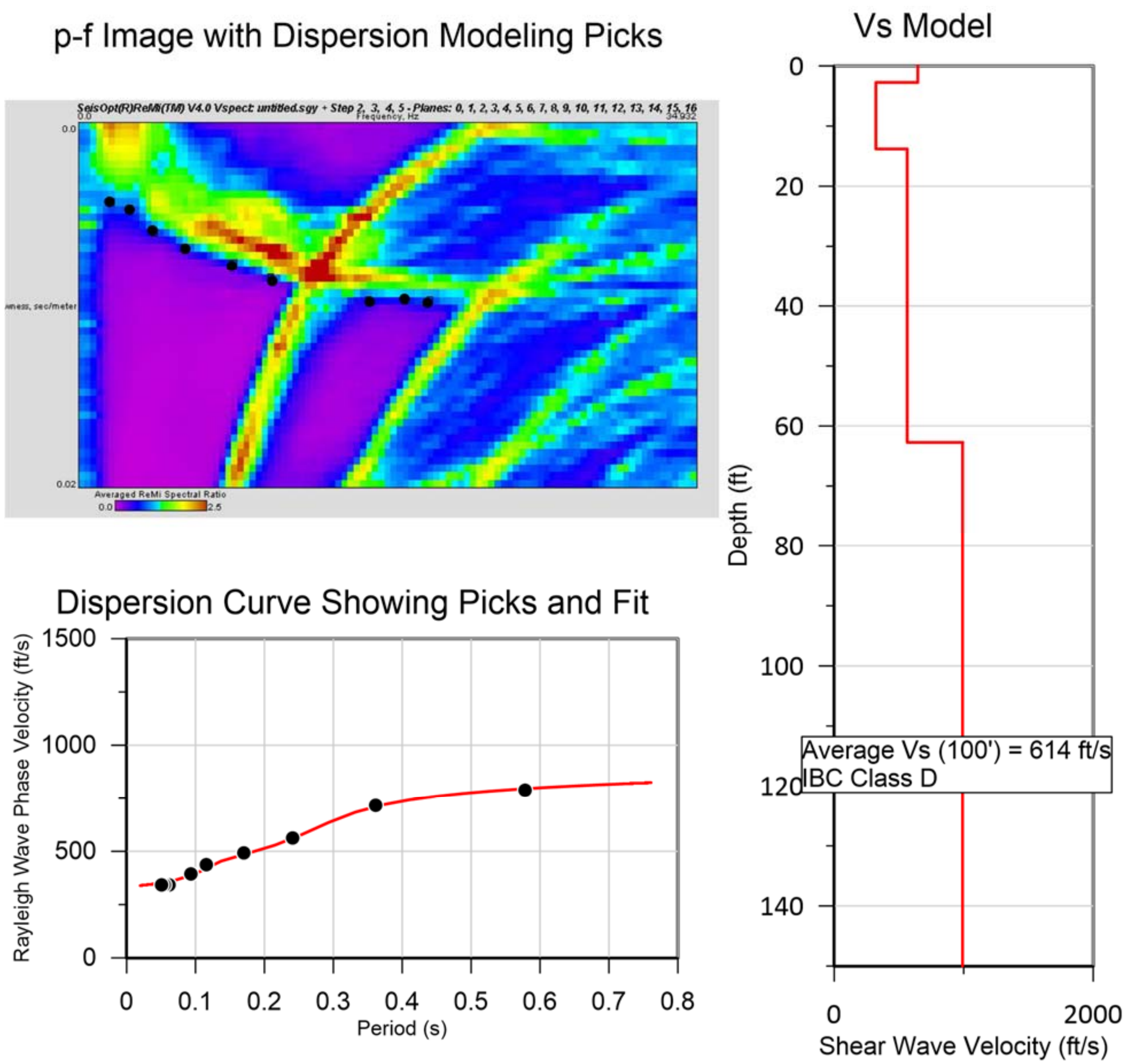

Depth Interval (ft)	Shear-wave velocity (ft/s)
0 – 2.75	644
2.75 – 13.8	322
13.8 – 62.7	564
62.7 - 150	993

Figure 4-3. Array 3 ReMi Results

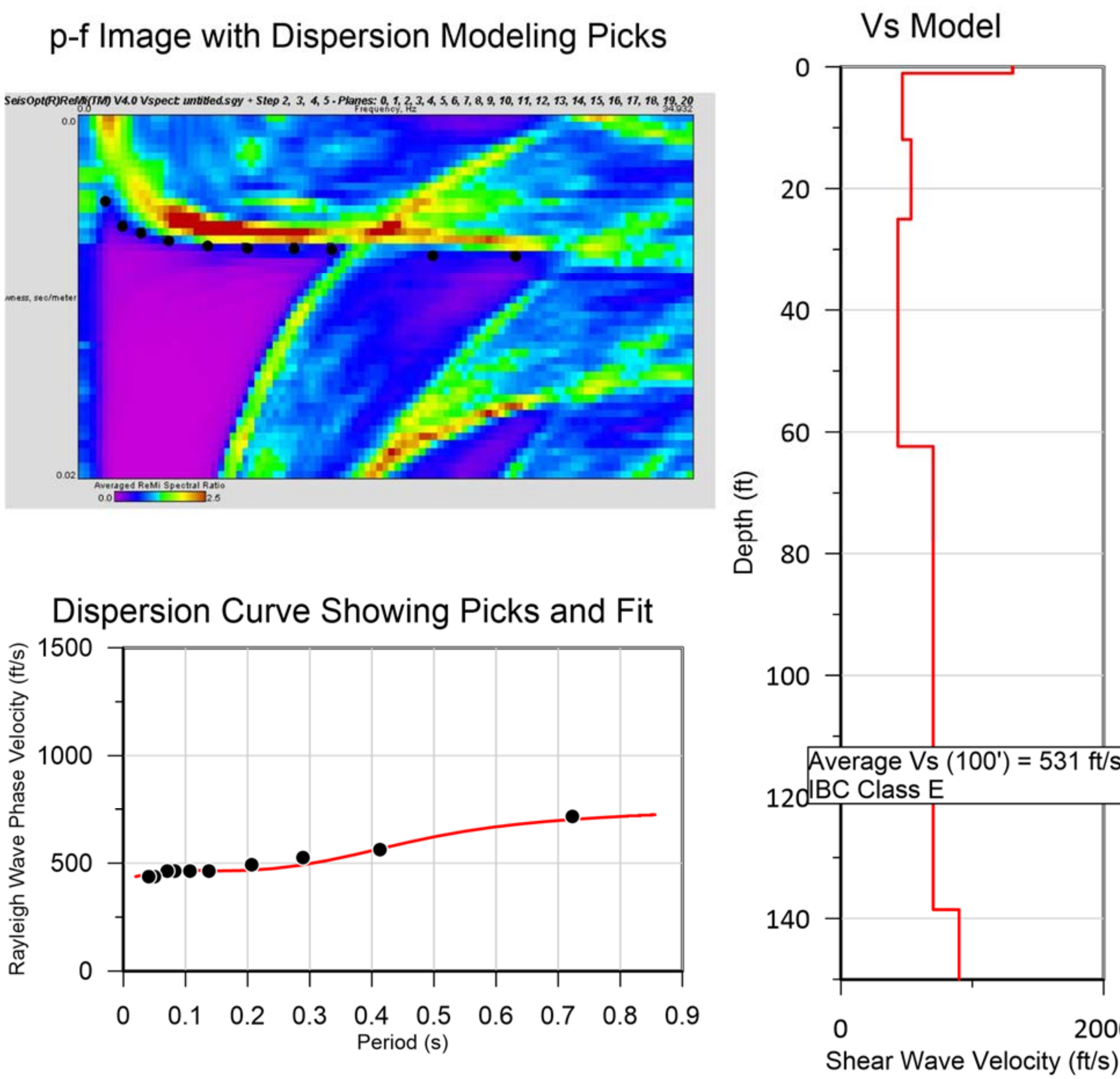

Depth Interval (ft)	Shear-wave velocity (ft/s)
0 – 1.1	1,307
1.1 – 11.9	468
11.9 – 25.0	534
25.0 – 62.4	434
62.4 – 138.6	702
138.6 – 150	900

Figure 4-4. Array 4 ReMi Results

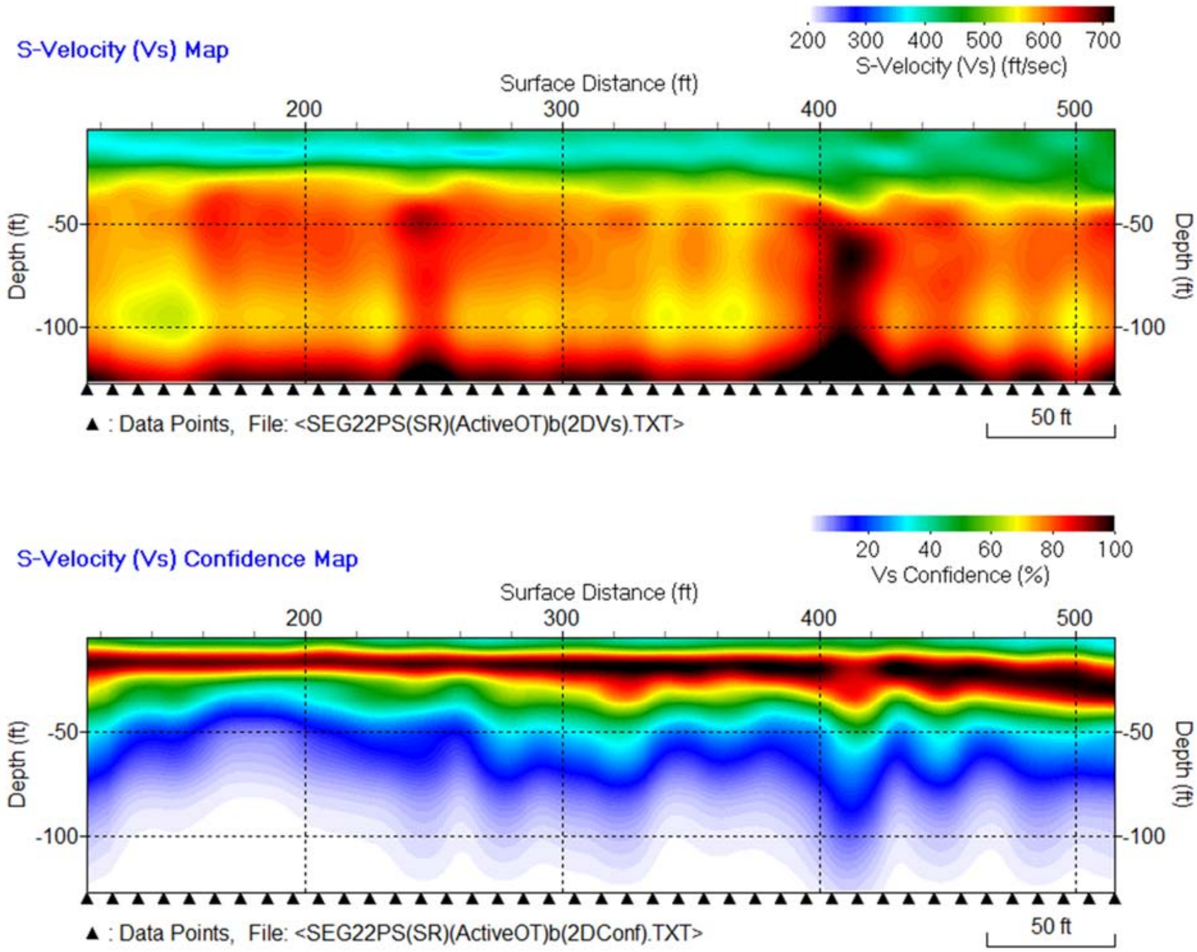

Figure 4-5. 2-D (top) Vs models and Confidence plot (bottom) from active source MASW Array.

5.0 <u>DISCUSSION</u>

There is good correlation of modeled velocity values for both methods. Generally the shear wave velocities at the site are laterally homogeneous with slightly increasing velocity towards the south.

ASCE/SEI 7-16 (2017) defines five site classes based upon the average shear-wave velocity of the soil to a depth of 30 Meters (100 feet). The ASCE classification is summarized in Table 5-1. The classifications in Table 5-1 are incorporated into the International Building Code (IBC 2018) Earthquake shaking is expected to be stronger where shear-wave velocity is lower. Average shear wave velocity to a depth of 100 ft (V_{s100}) is calculated using Equation 5-1.

$$Vs(100) = \frac{100}{\sum_{i=1}^{i=n}\left(\frac{d_i}{Vs_i}\right)} \qquad \text{Equation 5-1}$$

Where:

n = the number of intervals
i = the interval number
d_i = the thickness of the i^{th} interval in feet
Vs_i = the velocity of the i^{th} interval

Using Equation 5-1 and the data in Figures 4-1 through 4-4, the average shear wave velocity to a depth of 100 ft for ReMi Arrays 1 through 3 is slightly greater than 600 ft/s. These velocities are near the lower boundary of Site Class D. However, given the 20 ft/s uncertainty in the modeled results it is recommended that Site Class E be assigned to these models. The average shear wave velocity to a depth of 100 ft of ReMi Array 4 is calculated to be 531 ft/s. This velocity corresponds to Site ClassE. In summary, it is recommended that future seismic design for this site comply with requirements for Site Class E.

Table 5-1. Summary of ASCE soil classification.

Class	Average S-wave Velocity (ft/sec)	Description
A	> 5,000	Hard rock
B	2,500 – 5,000	Rock
C	1,200 – 2,500	Very dense soil and soft rock
D	600 – 1,200	Stiff soil
E	<600	Soil

6.0 LIMITATIONS

The geophysical methods used in this study involve the inversion of measured data. Theoretically, the inversion process yields an infinite number of models which will fit the data. Further, many geologic materials have the same seismic velocity. We have presented models and interpretations which we believe to be the best fit given the geology and known conditions at the site. However, no warranty is made or intended by this report or by oral or written presentation of this work. Earth Dynamics accepts no responsibility for damages because of decisions made or actions taken based upon this report.

7.0 REFERENCES

ASCE/SEI 7-16 (2017), Minimum Design Loads for Buildings and other Structures, American Society of Civil Engineers, Structural Engineering Institute, Reston, VA.

Louie, J.N. (2001). "Faster, better: shear-wave velocity to 100 meters depth from refraction microtremor arrays", Bull. Seism. Soc. Am., 91, 347-364.

Nazarian, S., and Stokoe II, K.H., (1984), "In situ shear-wave velocities from spectral analysis of surface waves", Proceedings for the World Conference on Earthquake Engineering Vol. 8, San Francisco, Calif., July 21-28, v.3, 31-38.

PARK ??

IBC (2012) 2012 International Building Code , International Code Council, Washington D.C.

RESPECTFULLY SUBMITTED
EARTH DYNAMICS LLC

Daniel Lauer
Partner - Senior Geophysicist